Investigating Inflammatory Pathways in Alcohol-Associated Liver Disease

Petagine, Lucy

https://doi.org/10.34737/wq305

INVESTIGATING INFLAMMATORY PATHWAYS IN ALCOHOL-ASSOCIATED LIVER DISEASE

Lucy Petagine

April 2024

A thesis submitted to the

University of Westminster

in partial fulfilment of the requirements for the degree of

Doctor of Philosophy

ABSTRACT

Alcohol-associated liver disease (ALD) is a global health issue, with limited treatment options. The pathogenic mechanisms involve many biochemical pathways and processes. Some of the key factors include iron overload, reactive oxygen species (ROS) production and mitochondrial dysregulation. This project aimed to investigate the role of alcohol and iron in inducing liver damage and toxicity.

HepG2 (VL-17A) cells were treated with alcohol (200 mM, 300 mM, and 350 mM) with/without iron (50 μM) over 72 hrs and markers of oxidative damage, cell death and mitochondrial function were assessed. The protective effects of antioxidants and nanoformulations were also measured. Subsequent studies also investigated the association between frequency of drinking, liver iron and liver fat in a UK BioBank cohort.

Results show 350 mM ethanol led to a 50% decrease ($p<0.0001$) in cell viability at 72 hrs and a significant increase in ROS at 30 mins ($p=0.0027$). At 72 hrs a substantial number of cells were late apoptosis (44%) ($p=0.0153$) as well as a 47% reduction ($p=0.0160$) in mitochondrial membrane potential after 350 mM ethanol treatment. Treatment with iron produced similar effects, whereby, 350 mM ethanol + 50 μM iron decreased cell viability by 63% at 72 hrs ($p=0.0448$) and increased ROS by 125% ($p=0.0014$) at 2 hrs. Pre-treatment with 10 μM curcumin nanoformulations increased viability by 78% ($p=0.0405$), as well as reducing ROS by up 51% ($p=0.0013$). In the UK BioBank cohort, increased frequency of drinking showed significant associations with liver iron and liver fat ($p<0.0001$).

In summary, alcohol alone or in combination with iron is associated with significant liver injury, which can be ameliorated with antioxidants and nanoformulations. In addition, UK BioBank data showed that frequency of drinking was associated with higher levels of liver iron. Future studies can target antioxidant-based formulations in the prevention of mitochondrial damage due to ethanol and iron.

ACKNOWLEDGEMENTS

To my beloved late mother, who did not witness this journey. Your memory continues to inspire me, and I know you are proud of me. This journey would not have been possible without the support of my family, friends, and all the incredible people who supported and surrounded me. With my deepest gratitude, I dedicate this thesis to them.

Firstly, I would like to express my appreciation to my supervisors, Professor Vinood Patel and Professor M. Gulrez Zariwala, for all their invaluable supervision, advice, and encouragement throughout my PhD and professional development. I would also like to thank my collaborators Dr Satyanarayana Somavarapu and Stefanie Chan for their assistance with the preparation and characterisation of the nanoformulations. I would like to extend my sincere thanks to Professor Jimmy Bell, Professor Louise Thomas, and Dr Marjola Thanaj for their invaluable help with UK BioBank data.

Finally, thank you to my friends, fellow PhD students and colleagues, specifically, Kurtis Edwards, Isabella Cooper, Dr Yvoni Kyriakidou and Dr Rhys Mould, who have provided me with endless moral support and understanding throughout this challenging journey.

AUTHORS DECLARATION

I declare that the present work was carried out in accordance with the Guidelines and Regulations of the University of Westminster.

I confirm that this is my own original work and any assistance or collaborations have been properly and fully acknowledged.

TABLE OF CONTENTS

LIST OF TABLES

LIST OF FIGURES

LIST OF ABBREVIATIONS

ADH	alcohol dehydrogenase
AKT	alpha serine/threonine-protein kinase
ALD	alcohol-associated liver disease
ALDH2	aldehyde dehydrogenase
ALT	alanine aminotransferase
ASC	apoptosis-associated speck like CARD-domain containing protein
AST	aspartate aminotransferase
ATP	adenosine triphosphate
CYP2E1	cytochrome P450 2E1
DAMPs	damage associated molecular patterns
DCFDA	2, 7-dichlorofluoresceindiacetate
DIABLO	direct IAP-binding protein with low PI
DISC	death-inducing signalling complex
DMEM	Dulbecco's Modified Eagle Medium
DMT1	divalent metal transporter 1
DSPE-PEG	1,2-distearoyl-sn-glycero-3-phosphoethanolamine polyethylene glycol
EtOH	Ethanol
FADD	Fas-associated protein with death domain
FADH2	reduced flavine-adenine dinucleotide
FCS	foetal calf serum
Fe	iron
FFA	free fatty acids

FNP1	ferroportin 1
IAP	inhibitor of apoptosis protein
IFN-γ	interferon-gamma
IFR3	interferon regulatory factor 3
Ig	immunoglobulin
IL	interleukin
LRR	leucine-rich repeat
MAIT	mucosa-associated invariant T cells
MASLD	metabolic dysfunction-associated steatotic liver disease
Mfn	mitochondrial fusion
MRI	Magnetic resonance imaging
mtDNA	mitochondrial DNA
MTT	mitochondrial 3-(4,5-Dimethylthiazol-2-yl)-2,5-diphenyltetrazolium bromide
NADH	nicotinamide adenine dinucleotide
NADPH	reduced nicotinamide adenine dinucleotide phosphate
NF-κB	nuclear factor kappa B
NLR	NOD, LRR-containing proteins
NLR	nucleotide-binding oligomerization domain-like receptor
NLRP3	NOD, LRR and pyrin domain-containing protein 3
NOD	nucleotide-binding oligomerization domain
NPBs	nucleoplasmic bridges
OH·	hydroxyl radical
Opa1	optic atrophy protein 1
PAMP	pathogen-associated molecular patterns

PDFF	proton density fat fraction
PGC-1α	peroxisome proliferator-activated receptor-gamma coactivator - 1 alpha
PPAR	peroxisome proliferator-activated receptor
PRR	pattern recognition receptor
RIP	receptor-interacting protein kinase
ROS	reactive oxygen species
SEM	standard error of the mean
SIRT	sirtuin
Smac	second mitochondria-derived activator of caspases
SREBP	sterol response element-binding protein
TGFβ	transforming growth factor beta
TLR	toll like receptor
TNF- α	tumour necrosis factor-alpha
TNFR	tumour necrosis factor receptor
TRADD	tumour necrosis factor receptor-associated death domain
TRAF2	tumour necrosis factor receptor-associated factor 2
TRAIL	tumour necrosis factor-related apoptosis-inducing ligand
TRIF	TIR-domain-containing adapter-inducing interferon-beta

CHAPTER 1 INTRODUCTION

Chronic liver disease is one of the most common liver diseases, grouped into two main categories: alcohol-associated liver disease (ALD), which occurs due to excessive alcohol consumption (Gao and Bataller, 2011) and metabolic dysfunction-associated steatotic liver disease (MASLD), which is related to high dietary fat and carbohydrate consumption (Brunt, 2001). MASLD also occurs as a consequence of metabolic syndromes such as obesity, insulin resistance, or type II diabetes (Gyamfi et al., 2012).

ALD is a major complication of alcohol abuse. Excessive alcohol consumption is a global healthcare problem causing significant mortality worldwide. ALD encompasses a spectrum of injury, ranging from simple steatosis to cirrhosis. The first stage in the pathogenesis of ALD is simple liver steatosis followed by steatohepatitis, which in turn, develops to cirrhosis/fibrosis then hepatocellular cancer (Mathurin et al., 2012). However, the pathogenesis of liver disease is still poorly understood (Adams, 2005; Gentile and Pagliassotti, 2008; Mantena et al., 2008; Gyamfi and Wan, 2010; L Li et al., 2017; Nicoletti et al., 2019).

Excessive drinking causes damage to multiple organs of the body, however, as the liver is the primary site for ethanol metabolism it sustains an extensive amount of injury (**Figure 1.1**). Ethanol is metabolised in the liver to acetaldehyde via alcohol dehydrogenase (ADH), catalase and cytochrome P450 of the microsomal ethanol-oxidizing system (Teschke, 2018). This results in modifications of liver parenchymal cells as well as Kupffer cells, hepatic stellate cells, and liver sinusoidal endothelial cells (Teschke, 2018). In response to alcohol consumption, Kupffer cells can produce reactive oxygen

species (ROS), pro-inflammatory cytokines, and chemokines as well as induction of other inflammatory cells promoting liver injury (Lucey, Mathurin and Morgan, 2009). Hepatic stellate cells are responsible for the synthesis of collagen leading to disease progression (Friedman, 2008). These resident cells become activated by acetaldehyde, ROS, and endotoxins (Teschke, 2018). ALD is a multifactorial disease involving mitochondrial dysfunction, oxidative stress, altered methionine metabolism, iron dysregulation and activation of a range of pathways including the immune system (Nagy, 2015).

Currently, the mechanisms by which alcohol interacts with pro-inflammatory cytokines resulting in cell death requires further research (Kawaratani et al., 2013; Nagy, 2015). The toxic effects of endotoxin and alcohol in inducing ROS and cell death, as well as signalling inflammatory mediators, is also poorly understood in relation to the pathogenesis of ALD. There is currently no reliable treatment for ALD, therefore, further research is required to reveal the pathogenic mechanisms responsible.

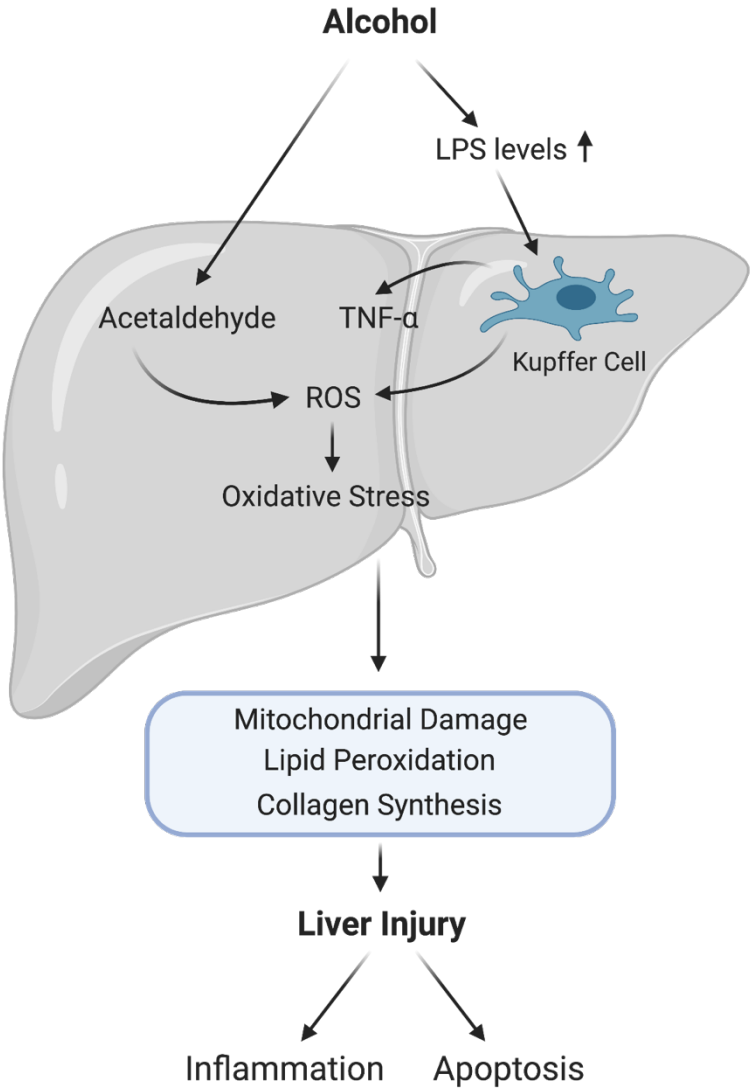

Figure 1.1 Overview of alcohol, oxidative stress, and liver injury. Alcohol abuse leads to lipopolysaccharide (LPS) translocation due to increases in gut permeability. Lipopolysaccharide then activates toll-like receptor (TLR) 4 on Kupffer cells. Activation of Kupffer cells, in turn, leads to reactive oxygen species (ROS) production and pro-inflammatory cytokines release including tumour necrosis factor-α (TNF-α). ROS Alcohol metabolism and acetaldehyde generation also causes ROS production. Excessive ROS eventually leads to apoptosis and inflammation. KC: Kupffer cell, LPS: Lipopolysaccharide, ROS: Reactive oxygen species, TLR4: toll-like receptor 4, TNF-α: Tumour necrosis factor-α. Source: Petagine, Zariwala and Patel (2021).

1.1 Epidemiology

Approximately 3 million deaths per year worldwide result from the harmful use of alcohol (WHO, 2018). Alcohol is a leading cause of liver disease globally, including cirrhosis and hepatocellular cancer (O'Shea, Dasarathy and McCullough, 2010). ALD is a major cause of alcohol-related morbidity and mortality. Over the last decade, an increase in alcohol-related cirrhosis has been observed. In 2016, 3 million deaths (5.3% of all deaths) worldwide were caused by the damaging effects of alcohol (WHO, 2018). In 2016, of all deaths attributable to alcohol consumption worldwide, 28.7% were due to injuries, 21.3% due to digestive diseases, 19.0% due to cardiovascular diseases, 12.9% due to infectious diseases and 12.6% due to cancers (WHO, 2018). Alcohol consumption was also responsible for 7.2% of all premature (those below 69 years old) mortality worldwide in 2016 (WHO, 2018). The excessive consumption of alcohol causes death and disability in younger age groups. In those aged 20–39 approximately 13.5% of the total deaths are alcohol-attributable (WHO, 2018). Alcohol is the leading risk factor for premature mortality and disability among those aged 15 to 49 years, accounting for 10% of all deaths in this age group (WHO, 2018).

In the US, chronic liver disease and cirrhosis is the 12th leading cause of death, with the proportion of ALD with stage 3 fibrosis increasing from 2.2% in 2001 to 6.6% in 2016 (Dang et al., 2020). The number of deaths due to alcohol-related liver disease has also been projected to increase from 2019-2040 by 84% (Julien et al., 2020). Globally, Europe has the largest burden of liver disease (Pimpin et al., 2018) and has the highest per capita alcohol

consumption and alcohol-related loss of disability-adjusted life years of any of the global WHO regions. Overall 5.1% of the global burden of disease and injury is attributable to alcohol, as measured in disability-adjusted life years (WHO, 2018). The high prevalence of alcoholic liver disease in Europe can also be evidenced by the large proportion of liver transplants. Approximately one-third of liver transplantations are due to alcohol-related liver cirrhosis (Parker and Holt, 2018). In England and Wales, the number of deaths due to ALD in 2020 was 5964 deaths rising by 20% from 4954 deaths in 2019 (ONS, 2021). A 72% increase in number of deaths due to ALD has been observed from 2001-2020 (ONS, 2021) (**Figure 1.2**).

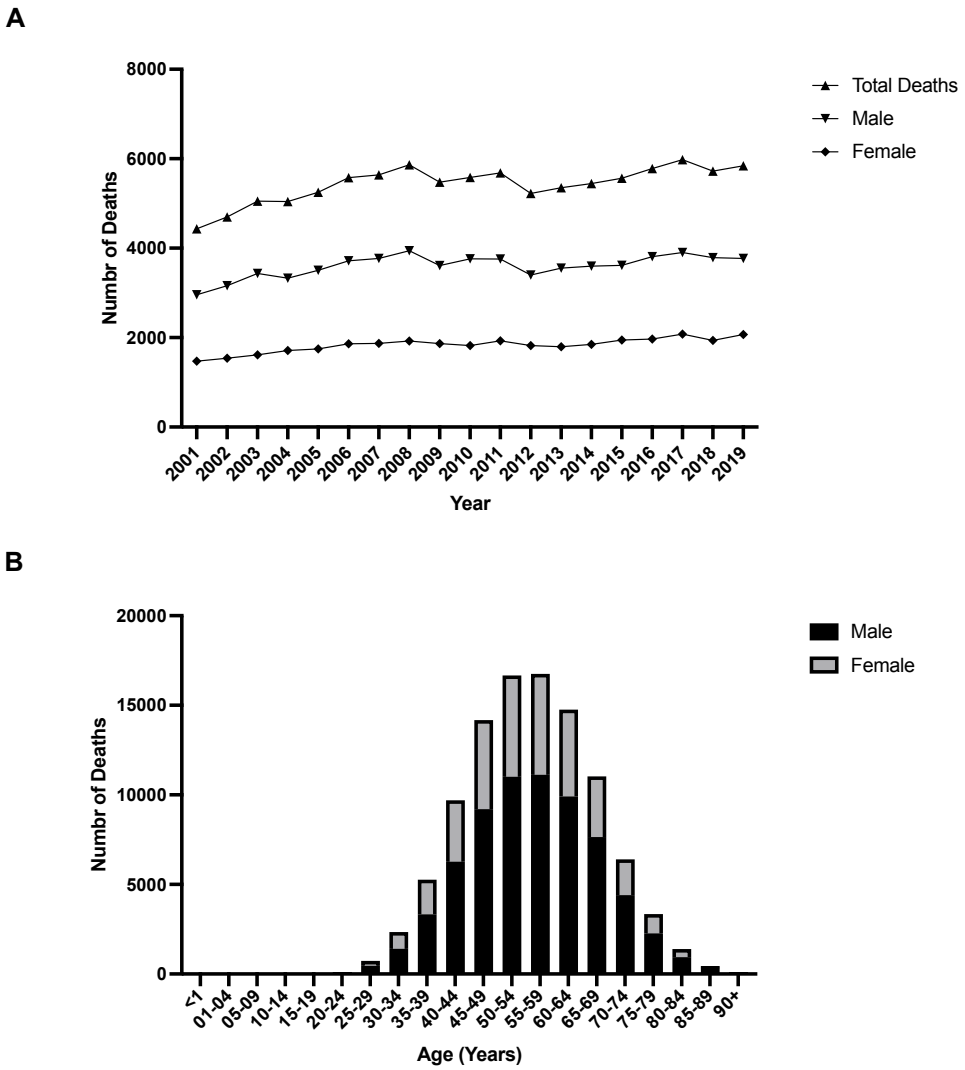

Figure 1.2 Total number of deaths due to alcoholic liver disease in the UK from 2001-2019. A) The total number of deaths in the UK from alcoholic liver disease from 2001 to 2019 showing the ratio between male and female deaths. B) Total number of deaths from alcoholic liver disease in the UK distributed by age groups in years. (Data collected from the Office for National Statistics).

1.2 Disease Spectrum

ALD comprises a broad spectrum of alcohol-related liver injury ranging from simple alcoholic fatty liver/steatosis to fibrosis/cirrhosis and hepatocellular cancer (**Figure 1.3**) (Mathurin et al., 2012). The stages of liver injury are classified based on the histology of the liver (Celli and Zhang, 2014). These stages are not necessarily distinct evolution of the disease, and frequently, multiple stages may be present simultaneously in a given individual (O'Shea, Dasarathy and McCullough, 2010). Simple liver steatosis is considered the first stage in the pathogenesis of liver disease. This is followed by hepatitis, which develops into cirrhosis or fibrosis and in some cases to hepatocellular cancer.

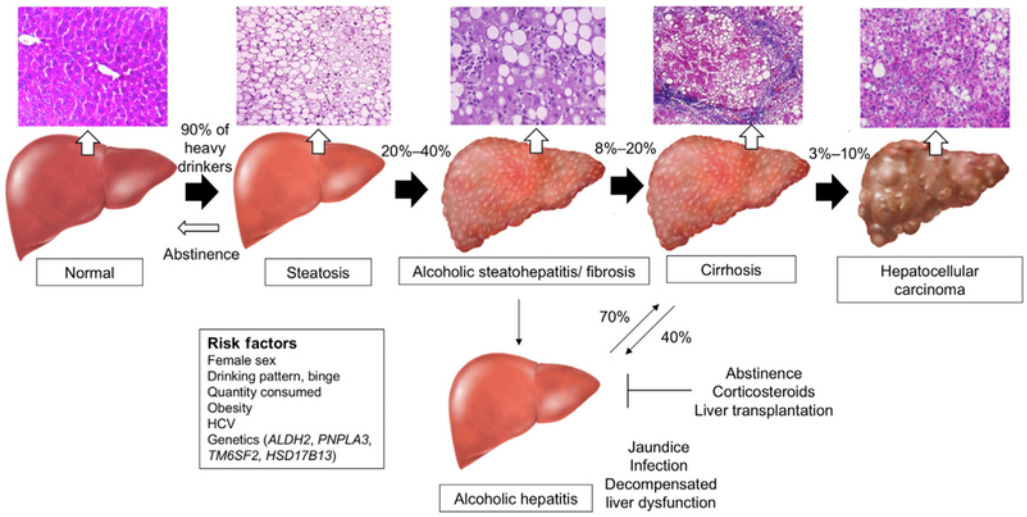

Figure 1.3 Stages of alcoholic liver disease. This figure outlines the disease spectrum of alcoholic liver disease. More than 95% of chronic alcohol abusers develop fatty liver of steatosis, however, only 35% of this population develop more severe forms of liver disease such as hepatitis, fibrosis/cirrhosis, and hepatocellular carcinoma. Source: Ohashi, Pimienta and Seki (2018).

1.2.1 Steatosis

The earliest response to alcohol abuse is fatty liver/steatosis. Generally, steatosis can be completely reversed by abstinence of drinking, however, it can also be maintained by the moderation of alcohol consumption (Singh, Osna and Kharbanda, 2017). Alcoholic fatty liver/steatosis is characterised by the deposition of fat observed microscopically as lipid droplets (Mavrelis et al., 2007). Steatosis progresses from microvesicular (small-droplet) to macrovesicular (large-droplet) forms (Celli and Zhang, 2014; Tiniakos, Anstee and Burt, 2018). Microvesicular steatosis is less prevalent and is characterised by central nuclei and small fat droplets around the nucleus. Macrovesicular steatosis is characterised by nuclei displaced to one side of the cell due to large fat droplets (Tandra et al., 2011). Hypertrophy or enlargement of mitochondria, (also known as megamitochondria) may occur during steatosis (Manzo-Avalos and Saavedra-Molina, 2010). Megamitochondria can be observed in association with steatosis, with or without other changes related to ALD (Theise, 2013), demonstrating alcohol has the potential to cause mitochondrial defects.

Abnormal accumulation of fatty acids and glycerides in hepatocytes causes the formation of lipid droplets (Celli and Zhang, 2014). During normal lipid metabolism in the liver, the free fatty acids (FFA) can be either oxidised for fuel in the hepatocyte mitochondria or stored in the liver as triglycerides (Celli and Zhang, 2014). Triglycerides can then be exported as very-low-density lipoprotein particles or organised into lipid droplets (Celli and Zhang, 2014). An abundance of lipid droplets can directly cause damage to the liver (Celli and Zhang, 2014). Increases in plasma FFA concentration are observed in both

non-alcohol and alcohol-induced steatosis, and therefore, is proposed to contribute to pathologic liver fat accumulation (Celli and Zhang, 2014). Furthermore, steatosis induced by alcohol consumption also stimulates a variety of pathophysiological pathways. The oxidation of ethanol, for example, reduces nicotinamide adenine dinucleotide (NADH), suppressing the oxidative mechanism of the mitochondria (Hoek, Cahill and Pastorino, 2002). Research on both cell culture and animal models has shown that ethanol stimulates hepatic lipogenesis via activation of transcription factors such as sterol response element-binding proteins (SREBP's), which regulate the expression of genes involved in lipid biosynthesis (Ji, Chan and Kaplowitz, 2006; Walker et al., 2011).

1.2.2 Hepatitis

Alcoholic steatohepatitis is characterised by hepatic injury and degeneration, independent of associated inflammation, which may present at different stages of severity. One of the most frequent injuries associated with alcoholic steatohepatitis is hepatocyte ballooning (Tiniakos, Anstee and Burt, 2018) but may also include rarefaction of the cytoplasm and disruption of the cytoskeleton, often with the formation of Mallory-Denk bodies (Celli and Zhang, 2014). Steatohepatitis is a histologic pattern that can be seen in chronic alcohol users. Diagnostic features of steatohepatitis are parenchymal inflammation, hepatocyte damage, and fibrosis (Celli and Zhang, 2014). Generally, in the early stages of disease, these changes are seen in a perivenular distribution but during the progression of disease, they extend throughout the lobules (Celli and Zhang, 2014).

The extent of inflammation can be variable. Inflammation seen in alcoholic steatohepatitis includes mononuclear infiltration of the portal tracts and hepatic parenchyma (Crawford, 2012; Celli and Zhang, 2014). Inflammation in alcoholic steatohepatitis is typically neutrophil-rich and occasionally include lymphocytes (An International Group, 1981; Lefkowitch, 2005). During inflammation satellitosis may occur as inflammatory cells circulate damaged hepatocytes (Lefkowitch, 2005). The infiltration of neutrophils has been linked to increases in the chemokines, interleukin (IL)-8, IL-17 and IL-1 (Lemmers et al., 2009; An, Wang and Cederbaum, 2012; Tilg, Moschen and Szabo, 2016; Gao et al., 2019).

Hepatocyte damage in alcoholic steatohepatitis produces many morphological changes. Mallory-Denk bodies are another characteristic finding of alcoholic steatohepatitis and the presence of Mallory-Denk bodies in the liver are an indication of oxidative stress, which can lead to other pathological conditions of the liver (Celli and Zhang, 2014). Mallory-Denk bodies are intracellular protein aggregates found in the cytoplasm of liver cells (Lackner et al., 2008). They are composed of cytokeratins 8 and 18 (Dancygier, 2010), which can bind to the TNF receptor 2 (TNFR2), thus influencing tumour necrosis factor-alpha (TNF-α)–induced activation of apoptosis and neutrophilic inflammation through nuclear factor kappa b (NF-κB) activation (Caulin et al., 2000). Therefore, Mallory-Denk bodies may also contribute to the advancement of disease and inflammation (Crawford, 2012).

Hepatic stellate cells are liver-specific mesenchymal cells which are important for physiology and fibrogenesis (Yin et al., 2013). Hepatic stellate cells are

found in the perisinusoidal space of the liver, also known as the space of Disse, whereby they maintain nearby interactions with sinusoidal endothelial cells and hepatic epithelial cells (Senoo, 2004). In a normal liver, stellate cells are defined as quiescent and contain lipid droplets. They function to store vitamin A and lipids as well being responsible for the production of intercellular collagen (Senoo, 2004; Yin et al., 2013). During liver injury, hepatic stellate cells receive damage signals causing them to transdifferentiate into activated myofibroblast-like cells (Friedman, 2008) (**Figure 1.4**). This can lead to an increase in cell size and proliferation. Hepatic stellate cells are the primary extracellular matrix–producing cells in the liver (Yin et al., 2013). Hepatic stellate cells also gain the ability to destroy normal intercellular matrix with the replacement of dense basement membrane-like collagen (Celli and Zhang, 2014). In addition, activated stellate cells generate a temporary scar at the site of injury to protect the liver from further damage as well as secreting cytokines and growth factors promoting regeneration of hepatic epithelial cells (Yin et al., 2013).

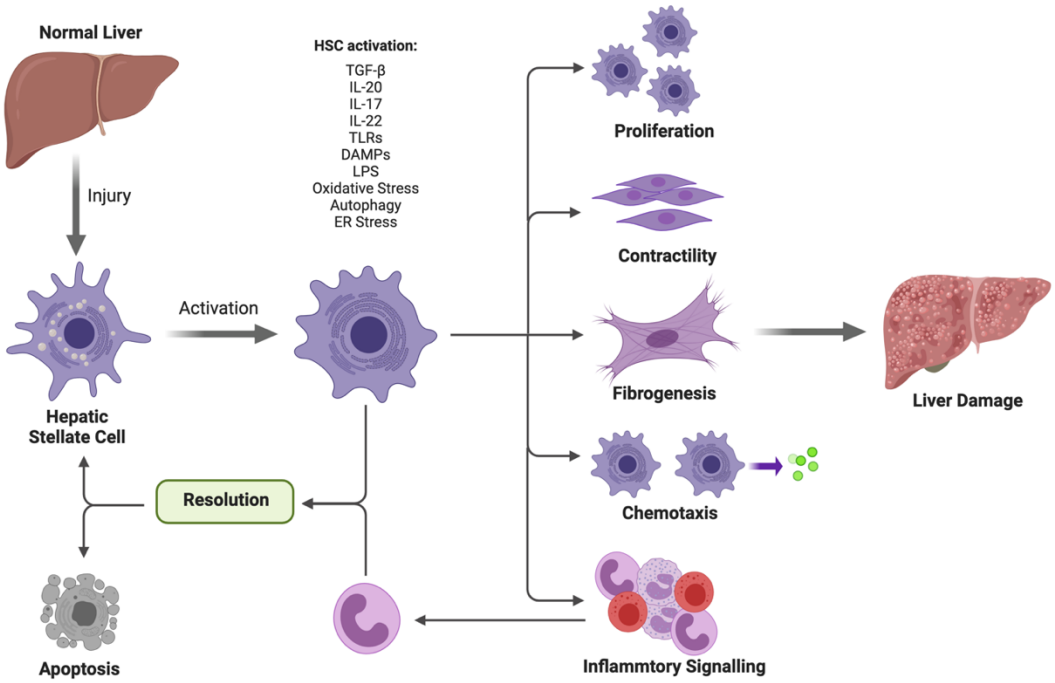

Figure 1.4 Activation of hepatic stellate cells during alcohol-associated liver disease. The excessive consumption of alcohol causes injury to the liver which begins the differentiation and activation of quiescent hepatic stellate cells. Activation of hepatic stellate cells leads to specific phenotypic changes including proliferation, contractility, fibrogenesis such as synthesis of collagen, chemotaxis and inflammatory signalling (Celli and Zhang, 2014). There are many key pathways which contribute to the activation of hepatic stellate cells including transforming growth factor-β (TGF-β), immune signalling, especially that mediated by Toll-like receptors (TLRs) and cytokines, as well as oxidative stress (Celli and Zhang, 2014; Tsuchida and Friedman, 2017). Hepatic stellate cells can be cleared by apoptosis or the activated phenotypes may be reserved or resolved (Tsuchida and Friedman, 2017). DAMPS: damage associated molecular patterns, HSC: hepatic stellate cell, IL: interleukin, LPS: lipopolysaccharide, TGF-β: transforming growth factor-β, TLR: toll-like receptors. Adapted from: Tsuchida and Friedman (2017).

1.2.3 Fibrosis/Cirrhosis

Fibrosis occurs due to heavy alcohol consumption. There are multiple interplaying factors which contribute to the development of fibrosis/cirrhosis in ALD. Oxidation of ethanol produces acetaldehyde, which is highly toxic (Seitz and Stickel, 2010). Acetaldehyde can destroy the microtubule structure of hepatocytes, which in turn causes microtubule dysfunction affecting nutrient transport (Manzo-Avalos and Saavedra-Molina, 2010; Groebner and Tuma, 2015). Liver fibrosis and cirrhosis also occur when acetaldehyde protein adducts cause inactivation of hepatocytes, abnormal DNA repair, damage to the mitochondrial structure, oxygen utilisation disorders, stimulation of collagen synthesis, and accumulation of extracellular matrix proteins (Kong et al., 2019). A key stage in the pathogenesis of disease is the activation of the hepatic stellate cells (**Figure 1.3**) (Kong et al., 2019).

As discussed previously, activated hepatic stellate cells can destroy normal intercellular matrix and replace it with dense basement membrane-like collagen (Celli and Zhang, 2014). A characteristic of this disease stage is the thick collagen strands located around the central vein in addition to throughout the hepatic lobules (Celli and Zhang, 2014; Lackner and Tiniakos, 2019). The collagen inhibits the diffusion of nutrients which in turn leads to cellular starvation and focal atrophy of hepatocytes (Celli and Zhang, 2014), thus, leading to an increase in scarring. In response to hepatic injury areas of hepatic regeneration will occur (Celli and Zhang, 2014). The finding of cirrhotic nodules provides evidence of the interplay between fibrosis, atrophy and regeneration (Celli and Zhang, 2014).

Generally, fibrosis will develop from alcoholic steatohepatitis, however, fibrosis may also develop from steatotic livers (Celli and Zhang, 2014). In this instance, fibrosis occurs as a direct response to the injury caused by alcohol (Celli and Zhang, 2014).

1.3 Alcohol Metabolism

1.3.1 Pathways of Alcohol Metabolism

The liver has various important functions involving both metabolism and detoxification. Primarily, alcohol is metabolised in the parenchymal cells of the liver, i.e. hepatocytes, and constitute approximately 70% of the liver mass (Seo and Jeong, 2016). Parenchymal cells express the highest levels of major ethanol-oxidising enzymes (Osna, Donohue and Kharbanda, 2017). These enzymes are ADH, located in the cytosol and cytochrome P450 2E1 (CYP2E1), located in the smooth endoplasmic reticulum and catalase, situated in peroxisomes (**Figure 1.5**).

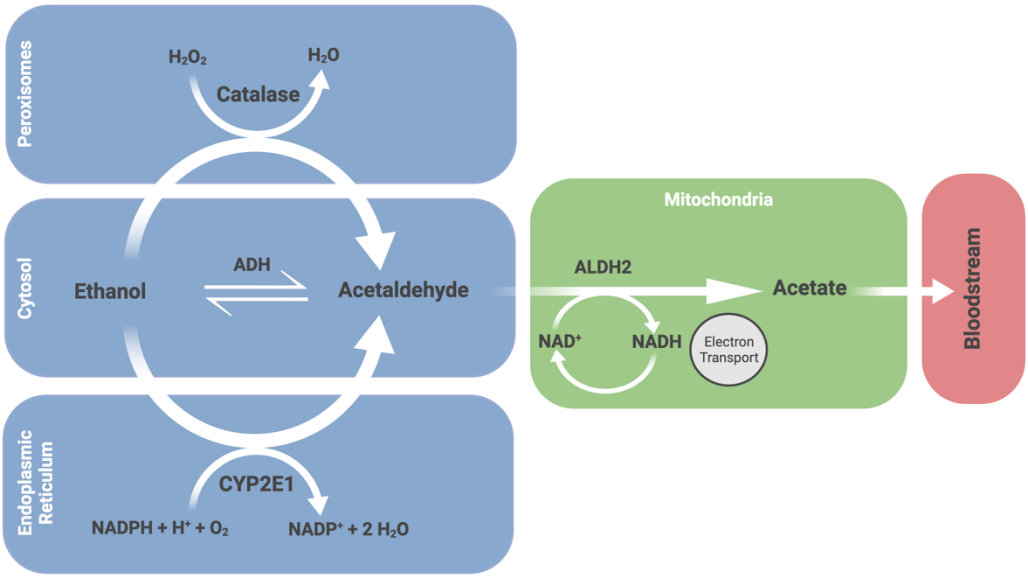

Figure 1.5 Pathways of alcohol metabolism. The enzymes alcohol dehydrogenase (ADH), cytochrome P450 2E1 (CYP2E1), and catalase, are involved in the metabolism of alcohol (Cederbaum, 2012). In the cytosol, ADH converts ethanol to acetaldehyde. Aldehyde dehydrogenase 2 (ALDH2) in the mitochondria then metabolises acetaldehyde forming acetate and nicotinamide adenine dinucleotide (NADH) (Tiniakos, Anstee and Burt, 2018). In the endoplasmic reticulum, CYP2E1 requires oxygen (O_2) to oxidise ethanol to acetaldehyde, in the process producing reduced NAD (NADPH). In this process reactive oxygen species (ROS) are formed (Lu and Cederbaum, 2008). In peroxisomes, hydrogen peroxide (H_2O_2) is required for the enzyme catalase to oxidise alcohol. ADH: alcohol dehydrogenase, ALDH2: aldehyde dehydrogenase 2, CYP2E1: cytochrome P450 2E1, H_2O_2: hydrogen peroxide, NADH: nicotinamide adenine dinucleotide, NADPH: reduced NAD, ROS: reactive oxygen species.

Catalase, an enzyme located in peroxisomes, is also expressed at high levels by hepatocytes. Usually, catalase acts in the decomposition of hydrogen peroxide (H_2O_2) to water and oxygen (Chelikani, Fita and Loewen, 2004). However, in the presence of ethanol, catalase is involved in ethanol metabolism by using H_2O_2 to oxidise ethanol to acetaldehyde (Aragon, Rogan and Amit, 1992). The pathway of ethanol metabolism by catalase is a minor pathway in the liver, however, it is a very important enzyme in protecting the cell from oxidative damage by ROS (Cederbaum, 2012).

The most catalytically efficient ethanol-metabolising enzyme in the liver is ADH. ADH-catalysed ethanol oxidation requires nicotinamide adenine dinucleotide (NAD^+) as a cofactor, creating reduced NAD^+ (NADH) and acetaldehyde (CH_3CHO) (Cederbaum, 2012). Acetaldehyde is highly toxic and a known carcinogen (Seitz and Stickel, 2010), and can bind to proteins (Donohue, Tuma and Sorrell, 1983), lipids (Kenney, 1982) and nucleic acids (Brooks and Zakhari, 2014), forming acetaldehyde adducts. These adducts can, in turn, disrupt the function and structure of these molecules (Mauch et al., 1986). To minimise the toxicity, acetaldehyde generated by the metabolism of ethanol is further oxidised to create acetate, where the enzyme mitochondrial aldehyde dehydrogenase (ALDH2) facilitates this step (Cederbaum, 2012). The ALDH2 reaction is also an oxidation-reduction reaction, producing NADH and acetate. Acetate can be excreted by the liver and diffuse into the bloodstream, which can then be utilised in other metabolic pathways. The elevated generation of NADH decreases the normal intrahepatocyte NAD^+/NADH ratio, called the cellular redox potential (Osna, Donohue and Kharbanda, 2017). This contributes to fatty liver development

due to the formation of fatty acids (Donohue, 2007). A decrease in β-oxidation of long-chain fatty acids occurs by the inhibition of long-chain 3-hydroxyacyl-CoA dehydrogenase activity (Tiniakos, Anstee and Burt, 2018).

The microsomal ethanol-oxidizing system is a cytochrome P-450-dependent pathway which includes the ethanol-inducible CYP2E1. CYP2E1 is the other major hepatic enzyme that catalyses ethanol oxidation to acetaldehyde (Cederbaum, 2012). CYP2E1 is an inducible enzyme, and during chronic alcohol consumption the hepatocellular content increases (Lieber and DeCarli, 1968; Dilger et al., 1997). Ethanol directly interacts with the CYP2E1 protein causing a conformational change which is resistant to degradation by the ubiquitin-proteasome system, resulting in the accumulation of CYP2E1 molecules (Roberts, 1995).

The metabolism of ethanol can also cause lactic acidosis producing secondary hyperuricaemia (Tiniakos, Anstee and Burt, 2018). An imbalance in carbohydrate metabolism may occur with reduced gluconeogenesis, which in turn leads to hypoglycaemia (Tiniakos, Anstee and Burt, 2018). Impaired fat metabolism is also documented in the development of steatosis due to hydrogen ions depressing the citric acid cycle (Tiniakos, Anstee and Burt, 2018). This leads to decreased fatty acid oxidation, an increase in α-glycerophosphate, an increase in the trapping of fatty acids, and increased synthesis of triglycerides (Tiniakos, Anstee and Burt, 2018). In chronic alcohol consumption, the synthesis of proteins is depleted as well as the impairment of liver cell secretory functions, which in turn causes retention of lipoproteins and fat accumulation in hepatocytes (Tiniakos, Anstee and Burt, 2018).

In addition to the pathways of alcohol metabolism mentioned, a small proportion of ethanol can be metabolised by non-oxidative pathways. Ethanol has the ability to interact with fatty acid, generating fatty acid ethyl ester via fatty acid ethyl ester synthase (Zelner et al., 2013). Research has shown that metabolism via fatty acid ethyl ester exacerbates injury caused by alcohol in tissues including liver (Wu et al., 2006), pancreas and heart (Beckemeier and Bora, 1998; Werner et al., 2002; Wu et al., 2007). Fatty acid ethyl ester has been shown to cause mitochondrial damage by its ability to bind to the mitochondrial membrane and uncoupling oxidative phosphorylation (Lange and Sobel, 1983).

1.3.2 Effects of Alcohol Metabolism

As discussed previously, in hepatocytes, the primary pathway of ethanol metabolism is through acetaldehyde by ADH and ALDH. Due to the highly reactive nature of acetaldehyde, it can form complexes with protein or DNA known as adducts (Heymann, Gardner and Gross, 2018; Tiniakos, Anstee and Burt, 2018). A relative deficiency of the ALDH2 isozyme causes the accumulation of acetaldehyde (Goedde et al., 1983). The microsomal ethanol-oxidizing system involving CYP2E1 has profound effects on the pathogenesis of liver disease. Accumulation of CYP2E1 molecules occurs due to resistance to degradation by the ubiquitin-proteasome system. Due to an increase in CYP2E1 oxidation a ‘metabolic tolerance’ can develop (Osna, Donohue and Kharbanda, 2017). Also, accelerated alcohol metabolism by an increase in CYP2E1 places liver cells in metabolic peril (Osna, Donohue and Kharbanda, 2017). This is due to an increase in acetaldehyde and a higher generation of ROS. This continuous generation of reactive molecules causes a condition

referred to as oxidative stress (Schieber and Chandel, 2014). During oxidative stress, the rate of ROS generated is greater than the livers capacity to neutralise them with natural antioxidants such as glutathione and vitamins E, A, and C (Lobo et al., 2010). Oxidative stress is exacerbated when ROS undergo secondary reactions with proteins and unsaturated lipids, resulting in the formation of lipid peroxides which can form adducts, and have the potential to cause an immune response (Ayala, Muñoz and Argüelles, 2014).

Additionally, during liver disease, ROS-induced oxidative stress can inhibit the expression of energy metabolism signalling pathway-related proteins including 5' adenosine monophosphate-activated protein kinase, Sirtuin 1 (SIRT1), and the transcription factor signal transducer and activator of transcription 3 (STAT3) (Seitz et al., 2018). Downregulation of adiponectin and zinc also occur which activates peroxisome proliferator-activated receptor (PPAR)-α, producing lipid free radicals, and promoting the expression of early growth response protein 1, TNF-α, adiponectin and acetyl-CoA carboxylase, which causes accumulation of fat in the liver (Gao and Bataller, 2011).

Furthermore, research has indicated that the consumption of alcohol can regulate transcription factors involved in lipid metabolism. Alcohol stimulates lipogenesis by upregulation of SREBP-1c (Ji, Chan and Kaplowitz, 2006). SREBPs are membrane-bound transcription factors that activate genes involved in cholesterol synthesis (Bayly, 2014). Alcohol can upregulate SREBP-1c directly via acetaldehyde, and indirectly by many different mechanisms including lipopolysaccharide signalling (Dunn and Shah, 2016). As SREBPs are involved in pathological processes, such as endoplasmic reticulum stress (Dara, Ji and Kaplowitz, 2011), the upregulation of SREBP-1c

could contribute to ALD pathogenesis, ultimately leading to inflammation and cell death.

It has been documented patients with ALD have an increase in FFAs, consisting of both saturated fatty acids and unsaturated fatty acids (Mavrelis et al., 2007). Saturated fatty acids have the potential to both, directly and indirectly, induce an inflammatory response by activation of toll like receptor-4 (TLR4) on macrophages, inducing NF-κB activation and Cox-2 expression (Lee et al., 2001; Shi et al., 2006; Wang et al., 2012). Saturated fatty acids have also been shown to directly activate inflammasomes and stimulate hepatocytes to produce chemokines (Wang et al., 2012). High levels of free unsaturated fatty acids may also induce an inflammatory response. In animals models, high-fat diets consisting of free unsaturated fatty acids or esterified unsaturated fatty acids increase lipid peroxidation and oxidative stress, promoting the development of ALD (Wang et al., 2012), inducing inflammation by activating NF-κB (Nanji and French, 1989). It has also been shown unsaturated fatty acids induce oxidative stress and activate TNF-α production in Kupffer cells (Cubero and Nieto, 2008), thus, leading to inflammation, proliferation, and apoptosis.

1.4 Apoptosis and Autophagy

Various mechanisms of cell injury have been implicated with hepatocyte death in the progression of ALD. One of the major types of cell injury in ALD is apoptosis, also known as programmed cell death. Apoptosis is a caspase-dependent and occurs via two distinct pathways; the extrinsic (death-receptor-mediated) or the intrinsic (mitochondria-mediated) pathway (Barnes,

Roychowdhury and Nagy, 2014; Hancock, 2016) (**Figure 1.6**). Apoptosis is characterised by nuclear fragmentation, chromatin condensation, and cellular shrinkage (Wang et al., 2016). Apoptotic cells can break apart into apoptotic bodies which are phagocytosed by immune cells such as macrophages and Kupffer cells, without eliciting an inflammatory response (Guicciardi, 2005).

1.4.1 Intrinsic Pathway

The intrinsic pathway, also known as the mitochondrial apoptotic pathway is activated by exogenous and endogenous stressors including DNA damage and oxidative stress (Yin and Ding, 2003; Wang, 2014). During apoptosis, the mitochondria become permeable and release proteins, or apoptotic factors into the cytoplasm such as cytochrome c, second mitochondria-derived activator of caspases (Smac)/direct IAP-binding protein with low PI (DIABLO), apoptosis-inducing factor, and endonuclease G (Guicciardi, 2005; Barnes, Roychowdhury and Nagy, 2014). This permeabilisation involves proteins from the B-cell lymphoma 2 (Bcl-2) family (Hancock, 2016). Cytochrome c has a redox function, shuttling electrons through the electron transport chain. Once released in the cytoplasm, cytochrome c binds to apoptotic protease activating factor-1 (Apaf-1) and caspase-9 forming the apoptosome, triggering caspase-9 activation when adenosine triphosphate (ATP) is present (Li et al., 1997). Downstream caspases such as caspase-3, -6 and -7 are activated via caspase-9. When Smac/DIABLO are released into the cytoplasm, binding of inhibitor of apoptosis proteins (IAPs) halts the inhibitory effect of caspases (Guicciardi, 2005). This allows cleavage of cellular substrates, leading to apoptosis characterised by morphological changes such as DNA

fragmentation, chromatin condensation and formation of apoptotic bodies (Barnes, Roychowdhury and Nagy, 2014).

1.4.2 Extrinsic Pathway

The extrinsic pathway, also known as the death receptor pathway, is usually initiated by binding of death receptor ligands to receptors (Ashkenazi and Dixit, 1998; Locksley, Killeen and Lenardo, 2001). These receptors are cell-surface cytokine receptors mainly belonging to the TNF family (Ashkenazi and Dixit, 1998). In the intracellular death domain, these receptors also share sequence homology (Ashkenazi and Dixit, 1998). These receptors include TNF-receptor 1 (TNFR1), Fas, TNF-related apoptosis-inducing ligand (TRAIL)-receptor 1 (DR-4), and TRAIL receptor 2 (DR5) (Guicciardi, 2005). The ligands of these receptors are TNF-α, FasL and TRAIL, respectively (Yin and Ding, 2003; Guicciardi, 2005).

In the Fas pathway, when FasL binding occurs the Fas-associated protein with death domain (FADD) and caspase-8 form the death-inducing signalling complex (DISC) (Guicciardi, 2005), inducing caspase-8 activation (Kischkel et al., 1995; Wajant, 2002; Wang, 2014). Activated caspase-8 can then activates other downstream effector caspases, i.e. caspase-3, which triggers apoptosis (Yin and Ding, 2003). Activated caspase-8 also cleaves Bid, the proapoptotic Bcl-2 family protein, which can translocate to the mitochondria and induce the release of apoptotic factors including cytochrome c and Smac/DIABLO (Yin et al., 1999; Adrain, Creagh and Martin, 2001).

In the TNF-α pathway, TNF-α binds to TNFR1 forming a TNFR complex, which in turn, activates downstream factors which include TNFR-associated death

domain (TRADD), receptor-interacting protein kinase (RIP) 1, TNFR-associated factor 2 (TRAF2), and cellular IAPs 1 and 2 (Vucic, Dixit and Wertz, 2011; Zhou, Han and Han, 2012). Cylindromatosis, a deubiquitinating enzyme, de-ubiquitinates RIP1 which induces the recruitment of factors such as TRADD, FADD and caspase-8 forming the pro-death complex (Kischkel et al., 1995; Wajant, 2002). The pro-death complex along with activated caspase-8 cleaves Bid and activates the mitochondrial-apoptotic pathway (Ding and Yin, 2004).

An increase in FasL-mediated apoptosis has been reported in response to alcohol, although zinc treatment could inhibit this process (Lambert, Zhou and Kang, 2003). As well as Fas-mediated apoptosis, there is evidence suggesting TNF-α-mediated cell death is crucial to the pathogenesis of ALD (Yin et al., 1999; Nagy et al., 2016). As mentioned previously, alcohol consumption increases intestinal permeability and elevated levels of gut-derived endotoxins such as lipopolysaccharide (Hartmann, Seebauer and Schnabl, 2015). Lipopolysaccharide activates Kupffer cells which induces production of TNF-α (Osna, Donohue and Kharbanda, 2017), leading to TNF-α-mediated apoptosis. Although, it is clear apoptosis via both intrinsic and extrinsic mechanisms plays an important role in alcohol-induced liver damage, other pathways of cell death are also involved in the pathogenesis of disease.

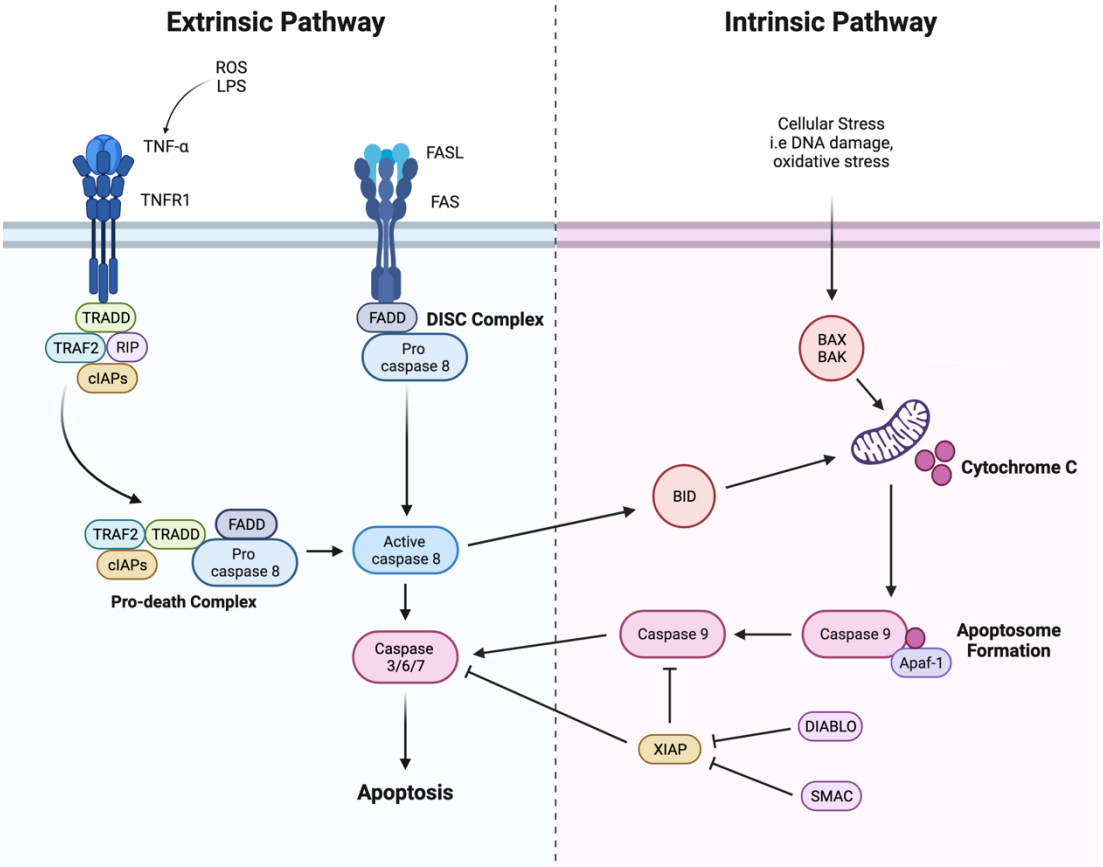

Figure 1.6 The extrinsic and intrinsic pathways of apoptosis. The two main pathways of apoptosis are the extrinsic and intrinsic pathway. The excessive consumption of alcohol causes increases in reactive oxygen species (ROS) and lipopolysaccharide (LPS) which induce the production of TNF-α (Pani et al., 2004), as well as causing Fas ligand-dependent apoptosis by recruitment of neutrophils (Abdelmegeed et al., 2013). The extrinsic pathway is activated by the binding of FasL to Fas receptor. This in turn recruits FADD and caspase-8 to form the death-inducing signalling complex (DISC) (Guicciardi, 2005) which then activates caspase-8 (Wang, 2014) and other downstream executing caspases. The extrinsic pathway is also activated via the binding of tumour necrosis factor (TNF)-α to TNFR1. This initiates the recruitment of TRADD, RIP, TRAF2/5 and cellular inhibitor of apoptosis proteins 1 and 2 (cIAPs) (Vucic, Dixit and Wertz, 2011; Zhou, Han and Han, 2012). The pro-death complex is then formed when TRADD and RIP then associate with FADD and caspase-8 (Kischkel et al., 1995; Wajant, 2002). This continuous generation of ROS causes oxidative stress which activated the intrinsic pathway (Yin and Ding, 2003; Wang, 2014). Oxidative stress leads to activation of Bax/BAK causing release of cytochrome c. The apoptosome is then formed when

cytochrome c associates with Apaf-1 and caspase-9. Smac/DIABLO have the ability to regulate apoptosis via inhibiting the inhibitor of apoptosis proteins (IAPs) (Guicciardi, 2005; Barnes, Roychowdhury and Nagy, 2014). Apaf-1: apoptotic protease activating factor-1, BID: BH3-interacting domain death agonist, cIAPs: cellular inhibitor of apoptosis proteins, DIABLO: direct IAP Binding protein with low PI, DISC: death-inducing signalling complex, FADD: Fas associated death domain, cIAP: cellular inhibitor of apoptosis, LPS: lipopolysaccharide, RIP: receptor interacting protein, ROS: Reactive oxygen species, SMAC: second mitochondrial-derived activator of caspase, TNF-α: tumour necrosis factor-α, TNFR: TNF receptor, TRADD: TNFR1 associated death domain.

1.4.3 Autophagy

Autophagy is a self-degrative process occurring by the action of lysosomes (Chen et al., 2012). Research has found that during ALD, autophagy has inhibitory effects on steatosis, inflammation and apoptosis (Lu and Cederbaum, 2015; Song et al., 2015).

Damaged mitochondria are removed through the process of autophagy known as mitophagy (**Figure 1.7**). There are 3 types of mitophagy with distinct variations. Type 1 mitophagy, is induced by nutrient deprivation (Lemasters, 2014; Lemasters and Zhong, 2018). Activation of beclin-1/phosphoinositide 3-kinases (PI3K) leads to the formation of phagophores which sequester individual mitochondria into mitophagosomes (Lemasters, 2014; Lemasters and Zhong, 2018). This process often occurs in coordination with mitochondrial fission (Lemasters and Zhong, 2018). Mitochondrial depolarisation then takes place, and the entrapped mitochondrion becomes fused with lysosomes. Type 2 mitophagy is induced by mitochondrial injury or sustained mitochondrial depolarisation (Lemasters, 2014). The mitophagosome forms independent of beclin-1/PI3K and is characterised by coalescence of autophagic microtubule-associated protein 1A/1B-light chain (LC) 3-containing structures on mitochondrial surfaces (Lemasters, 2014; Lemasters and Zhong, 2018). After induction, the process then follows as in type 1 mitophagy (Lemasters, 2014). Type 3 mitophagy, also known as micromitophagy, is induced when mitochondria-derived vesicles containing oxidised proteins bud off from mitochondria and become internalised into multivesicular bodies which fuse to lysosomes causing degradation (Lemasters, 2014; Lemasters and Zhong, 2018).

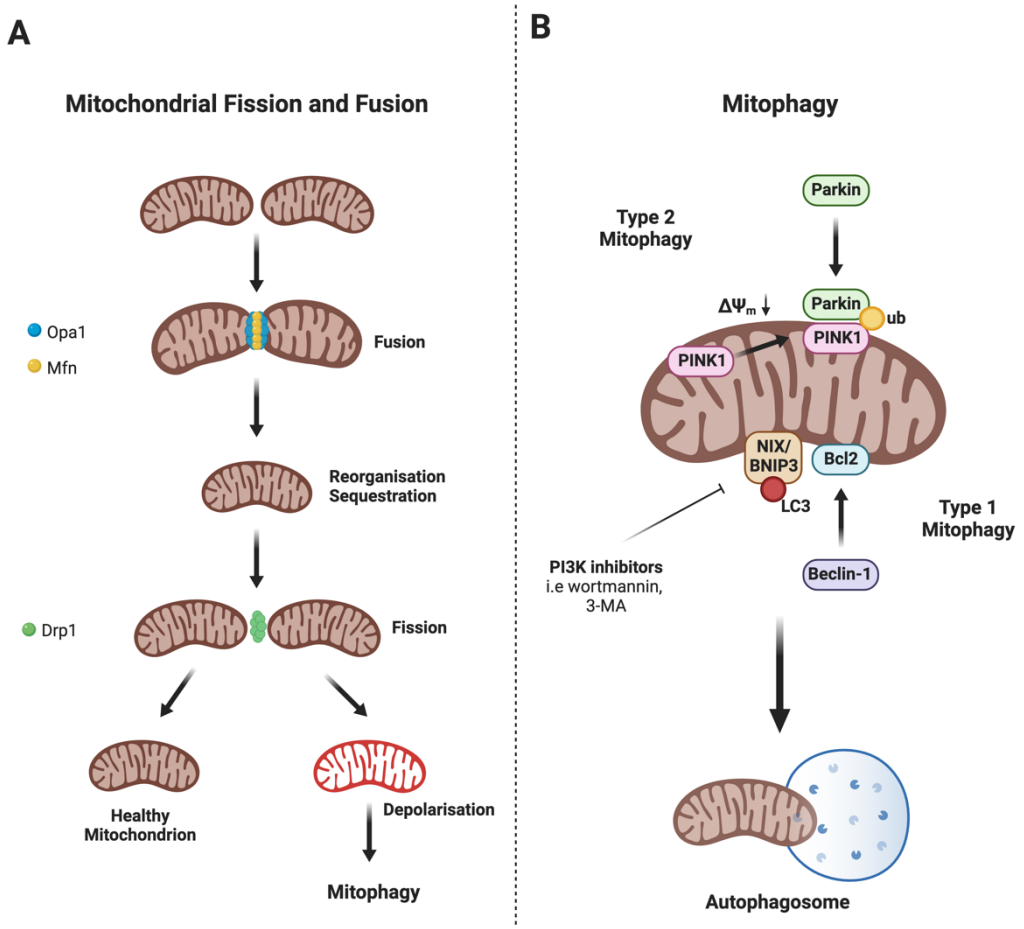

Figure 1.7 Pathways of mitochondrial fission, fusion and mitophagy. A) Mitochondrial fusion is driven by mitochondrial fusion (Mfn) proteins located on the mitochondrial outer membranes as well as optic atrophy protein 1 (Opa1) which drives fusion of the inner membrane (Van Der Bliek, Shen and Kawajiri, 2013; Tilokani et al., 2018). Mitochondrial fission is mediated by Drp1 which resides predominantly in the cytosol (Youle and Van Der Bliek, 2012; Tilokani et al., 2018). B) In type 2 mitophagy, or Parkin-dependent mitophagy the loss of mitochondrial membrane potential (Δψm) causes accumulation of PINK on the outer membrane (Lemasters, 2014; Ma et al., 2020). Parkin that localises to the mitochondria induces mitophagy and promotes ubiquitination (Narendra et al., 2008; Williams et al., 2015; Ma et al., 2020). In type 1 mitophagy, or Parkin-independent mitophagy, activation of beclin-1/PI3K induces formation of the mitophagosome (Lemasters, 2014). In this process NIX/BNIP3 localises to the mitochondria and binds to the autophagy protein LC3 (Ma et al., 2020). Bcl-2- also promotes type 1 mitophagy (Ma et al., 2020). Bcl2: B cell lymphoma 2, Drdp1: dynamin-related protein 1, Mfn: mitochondrial fusion, Opa1: optic atrophy protein 1, Ub: Ubiquitin.

Mitophagy has been shown to become induced as a protective effect in response to cellular stress such as the loss of mitochondrial membrane potential and accumulation ROS (Ding and Yin, 2012; Shefa et al., 2019), stressors which have been implicated in the pathogenesis of ALD, and it is possible they lead to alcohol-induced mitophagy in the liver. After chronic excessive alcohol consumption, mitophagy has been shown to serve as a protective mechanism via the elimination of dysfunctional mitochondria (Ding, Li and Yin, 2011; Eid et al., 2013). These results provide scope for the target of mitophagy as a therapeutic approach in ALD. In a rat model, after an acute alcohol binge, mitophagy was shown to increase (Ma et al., 2014; Eid et al., 2016). However, the mechanisms by which mitophagy is induced in the liver in response to alcohol warrants further research (Ma et al., 2020). It is of importance that future research should validate pathways and markers involved in human livers at different disease states.

As well as mitophagy, mitochondrial spheroid formation may serve as another pathway for the removal of damaged mitochondria (Ding et al., 2012; Yin and Ding, 2013; Ni, Williams and Ding, 2015), and may provide some protection against liver injury caused by alcohol (Yin and Ding, 2013; Ni, Williams and Ding, 2015). Mitochondrial spheroids are mitochondria which become shaped with a ring or cup-like morphology (Williams and Ding, 2015a). The formation of mitochondrial spheroids is dependent on the presence of ROS as well as mitochondrial fusion proteins (Williams and Ding, 2015a). Mitochondrial spheroid formation can be inhibited by Parkin which can initiate degradation of mitochondrial fusion proteins (Yin and Ding, 2013; Ni, Williams and Ding, 2015). Targeting removal of damaged mitochondria via the mitophagy

pathways, as well as through induction of mitochondrial spheroids, may provide scope for further research and future treatment.

1.4.4 Mitochondrial Alterations

Studies have shown that chronic ethanol exposure in both mice and humans leads to changes in mitochondrial morphology and function, including enlargement and structural changes (Gordon, 1984; Nassir, 2014). Mitochondrial DNA (mtDNA) encodes for subunits of the electron transport chain and ATP synthase. Damage to mtDNA impairs metabolism and enhances ROS production. A previous study has shown a single dose of ethanol was able to damage mtDNA and induce cell toxicity (Mansouri et al., 1999). It is possible that the combination of impaired oxidative phosphorylation and damaged mtDNA may reflect the alterations in mitochondrial architecture, for example, cristae organisation and matrix swelling (García-Ruiz, Kaplowitz and Fernandez-Checa, 2013). Damage to mtDNA caused by alcohol impairs mitochondrial function leading to additional oxidative stress, thus, it is a vicious cycle of cell damage associated with ageing (Hoek, Cahill and Pastorino, 2002). These alterations to mitochondria may also promote apoptosis and necrosis, contributing to the pathogenesis of ALD (Hoek, Cahill and Pastorino, 2002).

Acetylation is one of the major post-translational protein modifications in the cell that regulates proteins. Recently, a family of NAD^+ dependent deacetylases have been recognised, named sirtuins. They are able to regulate functions including energy metabolism and stress responses, as well as influencing ageing (Moniot, You and Steegborn, 2018). In mammals, there are

7 proteins (SIRT1-7) which have been identified as key players in longevity, DNA repair and the control of metabolic enzymes. SIRT3, SIRT4 and SIRT5 are localised within the mitochondrial matrix (Hirschey et al., 2011). Studies have identified that SIRT3-deficient mice show increased mitochondrial protein hyperacetylation which suggests SIRT3 is a major mitochondrial deacetylase (Lombard et al., 2007; Nassir, 2014). Chronic alcohol consumption induces acetylation of mitochondrial proteins, therefore, sirtuins have been implicated in the pathogenesis of ALD. SIRT3 is responsible for the deacetylation and activation of enzymes which can modulate ROS levels (Nassir, 2014). Excessive alcohol consumption also impairs lipid metabolism by modulation of SIRT1, leading to fatty liver (You et al., 2015). In a rodent model, alcohol has been shown to decrease hepatic SIRT1 (Nassir, 2014). SIRT1 can regulate lipid metabolism by the deacetylation of SREB-1c and PPARγ coactivator 1α (PGC-1α) (Nassir, 2014). This, in turn, increases fatty acid synthesis and decreases fatty acid β-oxidation (Nassir, 2014). Evidence suggests ethanol mediated reduced deacetylation of PGC-1α may inhibit mitochondrial biogenesis (Yin et al., 2012). Studies have shown that sirtuins can also modulate the levels of ROS (Merksamer et al., 2013; Singh et al., 2018). As previously discussed, mitochondria are involved in the generation of ROS, as well as ROS defence (Nassir, 2014). In embryonic stem cells, SIRT1 is essential for ROS-mediated apoptosis via facilitation of p53 mitochondrial localisation (Han et al., 2008). SIRT1 is also capable of inactivating the p65 subunit of NF-κB through direct acetylation (Lee et al., 2009; Nassir, 2014). Inhibition of NF-κB suppresses the inducible nitric oxide synthase and nitrous acid production, therefore it is suggested this may lower cellular ROS levels

(Lee et al., 2009). SIRT1 contributes to the regulation of lipid metabolism, hepatic oxidative stress and inflammation in the liver (Ding, Bao and Deng, 2017), therefore, SIRT1 activators and their downstream signalling may serve as promising treatments for fatty liver diseases.

There is substantial evidence showing that the metabolism of alcohol can cause mitochondrial dysfunction inducing the release of apoptotic factors including cytochrome c and Smac/DIABLO. Previous research has shown that in cultured rat hepatocytes, treatment with ethanol triggers cytochrome c release, which can be inhibited by mitochondrial permeability transition inhibitors such as cyclosporin A (Higuchi, 2001). Other studies have shown *in vivo* that alcohol can cause reversible hepatic mitochondrial depolarisation and mitochondrial permeability transition, which is dependent on alcohol metabolism in mouse models (Zhong et al., 2014). There are mechanisms in place in the liver that become activated in response to alcohol-induced mitochondrial damage and metabolic stress. These damaged mitochondria can be removed by Parkin-mediated mitophagy (Williams and Ding, 2015b; Williams et al., 2015). On the other hand, chronic alcohol exposure also enhances PGC-1α-mediated mitochondrial biogenesis, which in mouse models has been found to increase fusion and respiration (Han et al., 2012). These findings may suggest that there is a balance between the damage to mitochondria induced by alcohol and repair and biogenesis. Therefore, a disruption to this balance could induce apoptosis and liver injury.

1.4.5 Cell Death Pathways: ROS Accumulation and Apoptosis

The metabolism of alcohol is central to inducing the mitochondrial apoptotic pathway. When alcohol is metabolised by ADH, there is an increase in the conversion of NAD^+ to NADH, resulting in alterations of cellular redox status and decreased NAD^+-dependent enzyme activities. This increase in conversion results in accumulation and leakage of electrons, producing ROS. Furthermore, chronic alcohol exposure decreases mitochondrial maximal oxygen consumption rate and in turn increases the susceptibility of hepatocytes to alcohol-induced hypoxia and liver injury (Zelickson et al., 2011). When alcohol is metabolised by CYP2E1, ROS can also be generated (Lu and Cederbaum, 2008). In rats, chronic alcohol exposure leads to a reduction in antioxidant enzymes and also damages mitochondria, inducing mitochondrial depolarisation and mitochondrial permeability transition (Hoek, Cahill and Pastorino, 2002). This creates a vicious cycle as the induction of mitochondrial permeability transition in turn, leads to depolarisation and ROS production (Zorov et al., 2000), further exacerbating pathogenesis of disease.

ROS accumulation in response to alcohol metabolism plays an important role in mitochondrial-dependent apoptosis, inhibiting the phosphorylation of alpha serine/threonine-protein kinase (AKT) (Abdelmegeed et al., 2013), which downregulates G1 protein cyclin D1 through the inhibition of glycogen synthase kinase 3 beta (GSK3β)/Wnt/β-catenin signalling pathway activation in hepatocytes (Huang et al., 2015). This causes cell cycle arrest and activation of mitochondria-dependent apoptosis (Kong et al., 2019). ROS also induces mitochondrial-dependent apoptosis via directly activating apoptosis signal-regulating kinase 1 (Ibusuki et al., 2017), NF-κB, and c-Jun N-terminal

kinases (JNK)/P38 (Lee and Shukla, 2007). As discussed previously, alcohol consumption causes production of lipopolysaccharide due to increased gut permeability. ROS and lipopolysaccharide induce the production of TNF-α, inducing apoptosis and activation of JNK/STAT3 and p53 (Pani et al., 2004), as well as causing Fas ligand-dependent apoptosis by recruitment of neutrophils (Abdelmegeed et al., 2013). TNF-α can also induce liver injury via necrosis and apoptosis occurring via activation of two signalling pathways TNFR1 and TNFR2 (Nace et al., 2013; Nagy, 2015; Yang and Seki, 2015).

The oxidation of FFA's also occurs in the mitochondria. FFA's become oxidised into acetyl-CoA, which then undergoes the citric acid cycle generating reduced NADH and reduced flavine-adenine dinucleotide (FADH2). NADH and FADH2 serve as electron donors in mitochondrial respiration. Excessive flow of electrons results in accumulation and leakage of electrons leading to the production ROS (Zhao et al., 2019). Mitochondria, therefore, have an important role in ROS homeostasis, however, they can also be a target for excessive ROS exposure, consequently causing cell damage (including damage to lipids, proteins and nucleic acids), in turn causing oxidative stress and apoptosis (Nassir, 2014).

Alcohol-Induced Necrosis

As well as apoptosis, alcohol-induced liver injury also activates other cell death pathways including necrosis, however, currently little is known about the molecular mechanisms of alcohol-induced necrosis (Malhi, Guicciardi and Gores, 2010). As well as increasing the levels of ROS, alcohol can reduce the levels/activities of antioxidants, which may contribute to necrosis in the liver

(Nanji and Hiller-Sturmhöfel, 1997). Therefore, there is rationale for a therapeutic approach using antioxidants as a treatment for ALD.

Necroptosis is another cell death pathway which has recently been identified in multiple cell types, but has also been implicated in the development of ALD in mouse models (Roychowdhury et al., 2013). Similarly to apoptosis, necroptosis is a regulated pathway which resembles morphological features of both apoptosis and necrosis (Degterev et al., 2005). Necroptosis is inhibited by Necrostatin-1 which inhibits the activity of receptor-interacting protein kinase 1 (RIPK1) (Dhuriya and Sharma, 2018). Research has also shown that during necroptosis the secretion of cytokines and chemokines results in inflammation (Degterev et al., 2008). Necroptosis is initiated by TNF receptors, TLR3 and TLR4, and interferon receptors (Dhuriya and Sharma, 2018). The release of damage associated molecular patterns (DAMPs), activation of NOD-, LRR- and pyrin domain-containing protein 3 (NLRP3) inflammasome and an increase in cellular leakage is associated with necroptosis (Schwabe and Luedde, 2018), therefore, this may contribute to inflammation in ALD.

1.5 Innate and Adaptive Immunity

Despite extensive research, the pathogenesis of fatty liver disease remains unclear (Adams, 2005; Gentile and Pagliassotti, 2008; Gyamfi and Wan, 2010). Understanding the disease progression from fatty liver to hepatitis is also an area that is poorly understood (Mantena et al., 2008). Liver toxicity and alcohol metabolism induce oxidative stress and inflammation via the generation of ROS, bacterial over-growth and an increase in gut permeability

(Gao and Bataller, 2011). This ultimately leads to apoptosis, accelerating the progression of ALD.

The innate immune system is stimulated in the early stages of ALD, particularly due to endoplasmic reticulum. Interferon regulatory factor 3 (IRF3) becomes activated under endoplasmic reticulum initiating apoptotic signalling in hepatocytes. Data shows ethanol causes endoplasmic reticulum, activating IFR3, leading to subsequent phosphorylation (Petrasek et al., 2013). IRF3 is expressed in hepatocytes and recent research has shown it to be involved in hepatocyte apoptosis in ethanol-treated mice (Petrasek et al., 2013; Dunn and Shah, 2016) (**Figure 1.8**).

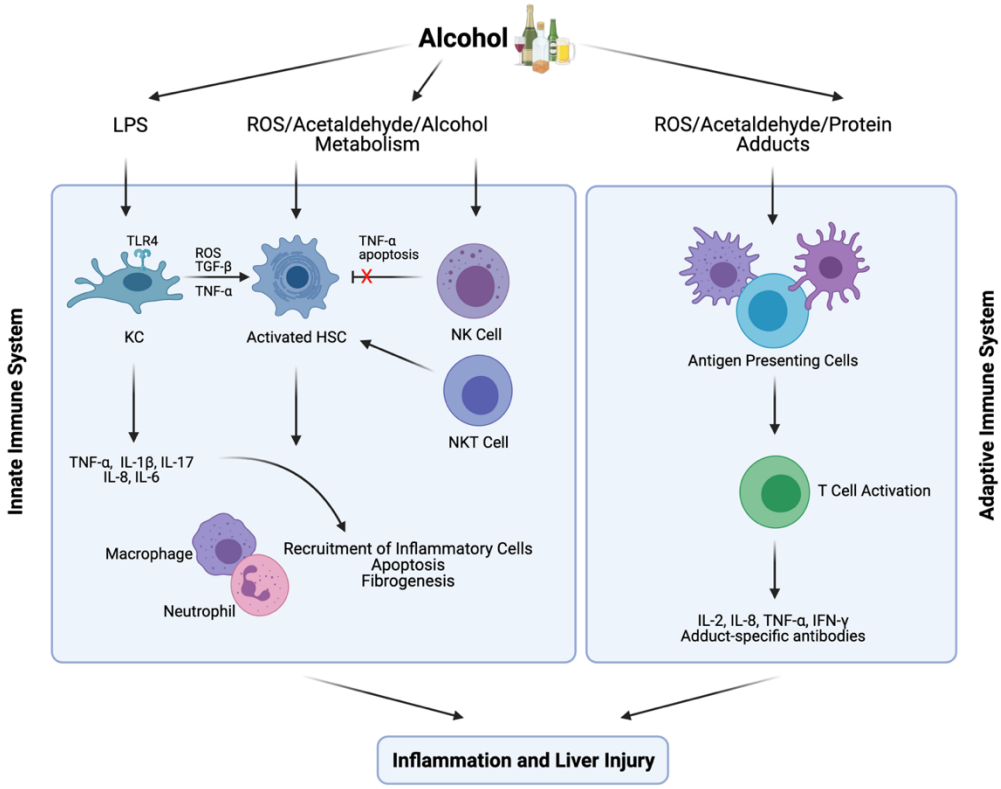

Figure 1.8 Innate and adaptive immune response to alcohol exposure. The innate immune system comprises of Kupffer cells (KC), hepatic stellate cells (HSCs) and natural killer (NK) cells. These cells can become activated after excessive alcohol consumption which causes inflammatory cytokine release and recruitment of other inflammatory cells. The adaptive immune system also becomes activated via reactive oxygen species (ROS), ethanol metabolites such as acetaldehyde and protein adducts, for example malondialdehyde-acetaldehyde adducts. HSC: hepatic stellate cell, IFN-γ: interferon-γ, IL: interleukin, KC: Kupffer cell, LPS: lipopolysaccharide, NK: natural killer, NKT: natural killer T, ROS: reactive oxygen species, TGF-β: transforming growth factor β, TLR4: toll-like receptor 4, TNF-α: tumour necrosis factor-α. Source: Petagine, Zariwala and Patel (2021).

1.5.1 Gut Permeability

The gut barrier is a multi-layer system which provides both physical and immunological defence mechanisms able to restrict toxins, antigens, and enteric flora from entering the circulation. Another key feature of the intestinal epithelium is that it can selectively permit absorption of nutrients across the tight junctions (Groschwitz and Hogan, 2009). The gut also contains commensal bacteria, referred to as the intestinal microbiota. Research has shown that alcohol affects the gut mucus layer and immune cells, as well as primarily affecting epithelial junction permeability (Groschwitz and Hogan, 2009). Excessive consumption of alcohol is known to cause increased gut permeability which facilitates the translocation of gut microbiota into the portal circulation (Neuman et al., 2015). Endotoxins, such as lipopolysaccharide, interact with TLR4 on Kupffer cells, leading to an increase tight junction permeability (Guo et al., 2013; Dunn and Shah, 2016) (**Figure 1.9**). Downstream signalling via the TIR-domain-containing adapter-inducing interferon-β (TRIF) and IRF-3 occurs, which leads to the production of proinflammatory cytokines. Elevated levels of lipopolysaccharide can affect immune cells as well as parenchymal cells which produce inflammatory cytokines and recruitment of inflammatory cells (Neuman et al., 2015). This, in turn, can cause hepatic inflammation and injury as well as further recruitment of immune cells, contributing to disease pathogenesis (Arrese et al., 2016). Gut permeability in repose to alcohol consumption has been documented both clinically and experimentally (Keshavarzian et al., 2009; Ding and Yin, 2012; Riva et al., 2018).

1.5.2 Inflammasomes

It is recognised that the metabolism of alcohol leads to oxidative stress and hepatocyte death. Inflammation occurs due to the damaged hepatocytes releasing endogenous DAMPs which activate cellular pattern recognition receptors (PRRs) (Gao et al., 2019). This inflammatory response includes proinflammatory cytokines, immune cell localisation and inflammasome activation (Luan and Ju, 2018) (**Figure 1.9**). Inflammasomes are critical innate immune sensors of the host immune system in defence to stress signals.

Inflammasomes are multi-protein complexes containing a nucleotide-binding oligomerization domain-like receptor (NLR), and the activation of inflammasomes is thought of as a two-step process. The assembly of inflammasomes is triggered by sensor molecules, including NLR molecules such as NLRP3 (NOD-, LRR- and pyrin domain-containing 3) (Kelley et al., 2019). Pathogen-associated molecular patterns (PAMP)/DAMP signalling causes NLR to form complexes with pro-caspase 1 and may also contain an adaptor molecule such as apoptosis-associated speck like CARD-domain containing protein (ASC) (Kelley et al., 2019). Upon stimulation, inflammasome assembly activates cleavage of procaspase-1 to its active form, caspase-1, which promotes the secretion and activation of pro-inflammatory cytokines interleukin-1β (IL-1β) and interleukin-18 (IL-18), and initiates pyroptotic cell death (pyroptosis) (Luan and Ju, 2018). IL-1β contributes to the infiltration of immune cells including recruitment of invariant natural killer T cells, promoting neutrophil recruitment. IL-18 is important for the production interferon-gamma (IFN-γ) and causes pleiotropic effects on hepatic natural killer cells.

Bacterial toxins such as lipopolysaccharide, mitochondrial dysfunction and production of ROS can stimulate the activation of NLRP3. Although inflammasomes are central to protecting the liver from infection, oxidative stress and cancer, excessive inflammasome responses may contribute to the pathogenesis of liver disease (Tilg, Moschen and Szabo, 2016). IL-1β, ASC and NLRP3 have been reported to be increased in the livers of ethanol fed mice and mRNA expression of IL-1β, IL-18 and caspase-1 is reported to be elevated in the liver of ALD patients, which correlated with liver lesions (Voican et al., 2015) and liver fibrosis. Caspase-1 knockout mice show protection from fibrosis, and treatment with IL-1 receptor antagonist 2 weeks after ethanol feeding is capable of attenuating steatosis and liver injury (Tilg, Moschen and Szabo, 2016; Petagine, Zariwala and Patel, 2021). Also, NLRP3 deficiency has been shown to decrease inflammation, steatosis and IL-1β expression as well as provide protection against ethanol-induced inflammation (Petagine, Zariwala and Patel, 2021). NLRP3 and ASC are present in hepatic stellate cells, and are important in the development of liver fibrosis via upregulation of transforming growth factor (TGF)-β and collagen (Petagine, Zariwala and Patel, 2021).

1.5.3 Complement System

Alcohol also activates the complement system and hepatocytes are the primary cells responsible for the biosynthesis of most complement components as well as some complement regulatory proteins found in plasma (Nagura et al., 1985; Morgan and Gasque, 1997; Qin and Gao, 2006). The complement system provides crucial protection against pathogens, however, research has shown activation of complements in chronic inflammatory

diseases, such as ALD (Qin and Gao, 2006; Pritchard et al., 2007; Wang et al., 2012). Proinflammatory cytokines are released due to the interaction of Kupffer cells and complement proteins. The production of these proinflammatory cytokines such as TNF-α and IL-17 causes hepatocytes to produce chemokines for neutrophil recruitment (**Figure 1.9**).

1.5.4 Neutrophils

Neutrophils have an important role in the liver as they clear dying hepatocytes by phagocytosis. However, research has shown in alcoholic patients the baseline function of neutrophils in the liver is decreased (Celli and Zhang, 2014), and therefore, may provide an explanation for infection in alcoholic patients. On the other hand, it is thought that neutrophils promote the pathogenesis of ALD by inducing hepatocyte injury. This injury occurs via the release of ROS, proteases, and proinflammatory mediators (Ramaiah and Jaeschke, 2007; Gao and Tsukamoto, 2016) (**Figure 1.9**). In mouse models it has been shown blockade of inflammatory mediators involved in neutrophil infiltration ameliorates ALD (Chang et al., 2015; Gao and Tsukamoto, 2016), thus, supporting the premise that neutrophils play a role in disease progression.

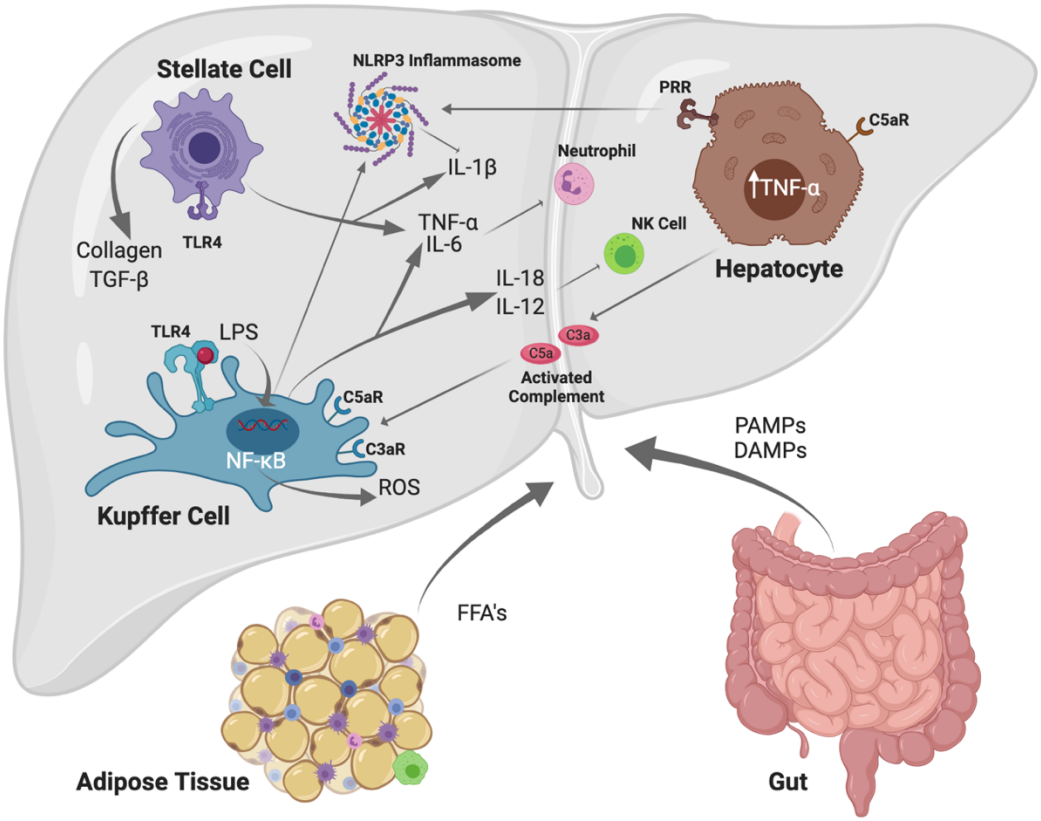

Figure 1.9 The role of the innate immune system during alcohol-associated liver disease. Heavy alcohol consumption causes the release of lipopolysaccharide (LPS) from the gut which leads to activation of toll-like receptor (TLR)4 downstream signalling. PAMPs and DAMPs released from the gut activate pattern recognition receptors (PRRs) inducing the secretion of proinflammatory cytokines and inflammasome activation. The production of IL-18 causes activation of natural killer (NK) cells (Luan and Ju, 2018). Activation of the complement system contributes to the pathogenesis of ALD. Activated C3a and C5a interact with receptors on Kupffer cells producing TNF-α which in turn promotes liver injury (Qin and Gao, 2006; Lin et al., 2018). TLR stimulation in hepatic stellate cells results in the expression of IL-6, TGF-β1 and TNF-α (Nagy, 2015; Li et al., 2019). DAMPs: damage-associated molecular patterns, FFA: free fatty acids, PAMPs: pathogen-associated molecular patterns, IL: interleukin, LPS: lipopolysaccharide, NF-κB: nuclear factor-κB, NK: natural killer, NLRP3: NOD, LRR and pyrin domain-containing protein 3, PRR: pattern recognition receptor, ROS: reactive oxygen species, TGF-β: transforming growth factor β, TLR4: toll-like receptor 4, TNF-α: tumour necrosis factor-α. Adapted from: Petagine, Zariwala and Patel (2021).

1.5.5 Adaptive Immunity

To date, the mechanisms by which the adaptive immune system contributes to inflammation in ALD lacks research. Although the pathogenesis of ALD remains unclear, acetaldehyde and ROS are mediators of disease. Acetaldehyde binds with DNA, RNA and proteins forming adducts, which triggers an immune response, further contributing to liver injury through the formation of neoantigens (McCullough, O'Shea and Dasarathy, 2011), activating adaptive immunity (Dunn and Shah, 2016).

Excessive alcohol consumption has been shown to reduce the numbers of peripheral T cells as well as disrupt the balance between T cell phenotypes and impair their function, promoting apoptosis (Petagine, Zariwala and Patel, 2021). Experimentally and clinically, alcohol consumption has been shown to cause a shift between T cell populations from naïve to memory cells (Pasala, Barr and Messaoudi, 2015), as well as causing lymphopenia (Petagine, Zariwala and Patel, 2021). Research on animal models has also shown chronic ethanol consumption decreases the frequency of naïve T-cells and increased the percentage of memory T-cells (Song et al., 2002; Zhang and Meadows, 2005). This shift in phenotype may lead to an insufficient immune response to common antigens (Song et al., 2002).

A reduction in cytotoxic CD8+ T cells has been reported in ALD and this also correlated with stage of fibrosis and Child-Pugh score (Petagine, Zariwala and Patel, 2021). In alcoholic hepatitis, immune activation and inflammatory cytokine production has been linked to a decreased number of regulatory T cells (Petagine, Zariwala and Patel, 2021). On the other hand, the chemokine

ligand CCL5 has been reported to be upregulated in the liver (Petagine, Zariwala and Patel, 2021).

As mentioned previously, protein adducts derived from alcohol metabolism and lipid peroxidation act as neoantigens, triggering an immune response. These antigens are presented to CD4+ T cells by antigen presenting cells and occurs via antigen-specific activation (Gao et al., 2019). In the absence of antigens, bystander activation of T cells occurs (Gao et al., 2019) and has been reported to correlate with both inflammation and necrosis in ALD as well as regeneration. Therefore, antigen-specific and bystander activation may be involved in the pathogenesis of ALD as well as providing a beneficial role.

Differences in regulatory cell populations may also play a role in the pathogenesis of disease. Oxidative stress and injury are known to lower regulatory T cell populations in the liver (Petagine, Zariwala and Patel, 2021). A subset of CD4 T cells, Th17 cells, which produce IL-17 and promote neutrophil infiltration, have been identified in the livers of ALD patients. Although Th17 cells have a pro-inflammatory bias, studies have demonstrated a critical role for Th17 cells in the immune system's defence of bacterial infections (Li et al., 2019). Mucosa-associated invariant T cells (MAIT) are also an innate-like subset of T cells which are involved in the defence against bacterial infection and have also been found to be reduced in ALD patients, which in turn increases bacterial infection. The differentiation of MAIT cells is controlled by transcription factors RORC/RORγt, ZBTB16/PLZF and Eomes and have been reported to be lower in patients with alcoholic hepatitis compared to heathy controls (Gao, Ma and Xiang, 2018).

A loss of peripheral B cells has been documented in ALD, as well as increased circulating immunoglobulin (Pasala, Barr and Messaoudi, 2015). In heavy drinkers (90 to 249 drinks per month), B cell numbers are documented to be lower when compared to both moderate (30 to 89 drinks per month) and light drinkers (<9 drinks per month) (Petagine, Zariwala and Patel, 2021). A loss or circulating B cells in ALD patients who consume 164.9 g to 400 g of alcohol per day on average was also reported (Petagine, Zariwala and Patel, 2021). Ethanol may also affect the differentiation of progenitor B cells via down-regulation of transcription factors (early B cell factor and Pax5) and cytokine receptors (IL-7R α) (Wang et al., 2011). This means that excessive alcohol consumption can affect the subpopulations of B cells (B-1a, B-1b, B2-B) (Pasala, Barr and Messaoudi, 2015). Impaired B cell differentiation due to transcription factor blockade has been reported after exposure to 100 mM of alcohol (Wang et al., 2011). The reduction of high-affinity antibody-producing B-2B subset may provide an explanation as to why patients with ALD cannot respond adequately to antigens (Pasala, Barr and Messaoudi, 2015). There is also a link between decreased B-2B subsets and a decreased number of B-1a cells, as well as a relative increase in the percentage of B-1b cells, which are central for T cell independent responses (Pasala, Barr and Messaoudi, 2015). In cirrhosis, although a decrease in B cell numbers may be evident, the levels of circulating immunoglobulins such as IgA, IgG, and IgE, may be increased against liver antigens (Petagine, Zariwala and Patel, 2021). In alcohol fed rats and patients with severe ALD, IgG antibodies against CYP2E1 have been documented (Vidali et al., 2003).

1.5.6 Immune Paralysis

The leading cause of death in patients with alcoholic hepatitis is multiorgan failure, which occurs due to bacterial infection (Dunn and Shah, 2016). Susceptibility to bacterial infection is a feature of ALD (Markwick et al., 2015). Programmed cell death protein-1 and T-cell immunoglobulin and mucin protein-3 are inhibitory receptors which regulate the balance between protective immunity and host immune-mediated damage (Markwick et al., 2015). However, hyperexpression of these receptors can lead to chronic inflammation, as well as immune exhaustion and paralysis (Markwick et al., 2015). Research has shown that programmed cell death protein-1 and T-cell immunoglobulin and mucin protein-3 are overexpressed in alcoholic hepatitis patients and also lymphocytes produce less IFN-γ and increased IL-10 in response to chronic endotoxin exposure (Markwick et al., 2015). Blockade of programmed cell death protein-1 and T-cell immunoglobulin and mucin protein-3 has been shown to reverse these effects, thus, increasing antimicrobial activities (Markwick et al., 2015).

1.6 Iron Overload and Alcohol-Associated Liver Disease

In the human body, iron is necessary for enzyme function, oxygen transport and oxidative phosphorylation (Milic et al., 2016). The liver plays a significant role in iron metabolism and homeostasis due to its functions in iron storage, iron trafficking, hepcidin production and also protein synthesis (Anderson and Frazer, 2005). Iron overload has been linked to ALD and excessive iron can cause formation of free radicals and ROS causing oxidative stress, liver damage and apoptosis (Galaris, Barbouti and Pantopoulos, 2019).

1.6.1 Iron Homeostasis: Absorption, Regulation and Metabolism

Iron is an essential element for DNA synthesis, enzyme function, oxygen transport and oxidative phosphorylation (Milic et al., 2016). Iron levels in the body are controlled vastly by absorption. The two types of absorbable dietary iron exist as heme iron and nonheme iron (Li et al., 2020). Most iron is biologically unavailable ($Fe3^{+}$) and therefore, must undergo redox cycling prior to absorption. Dietary non-haem iron, must be reduced to $Fe2^{+}$ prior to its absorption (Piskin et al., 2022). $Fe3^{+}$ is reduced to $Fe2^{+}$ by duodenal enterocytes which include cytochrome b (Dcytb). $Fe2^{+}$ can then be transported via divalent metal transporter 1 (DMT1) (Wallace, 2016; Li et al., 2020). On the other hand, absorption of heme iron absorption occurs via heme carrier protein 1 which is then further degraded into iron, carbon monoxide, and biliverdin by heme oxygenase 1 or 2 (Shayeghi et al., 2005; Krishnamurthy, Xie and Schuetz, 2007; Gottlieb et al., 2012).

Ferroportin is encoded by the SLC40A1 gene and contains 12 transmembrane domains (Piskin et al., 2022). Intracellular iron can then be transported to the extracellular space through ferroportin 1 (FPN1) (Troadec et al., 2010; Li et al., 2020; Piskin et al., 2022), which is highly expressed in intestinal enterocytes as well as in macrophages and hepatocytes (Piskin et al., 2022). Ferroportin, is therefore important for iron export into systemic circulation. However, in the case of excess cellular iron, iron may be stored in ferritin and then transported into the bloodstream most commonly bound to transferrin, but can also be transported as non-transferrin bound iron (Li et al., 2020). During iron overload, toxicity can occur due to levels of non-transferrin bound iron, as transferrin

saturation is also increased which in turn can cause damage both intracellularly and extracellularly and generate free radicals leading to oxidative damage (**Figure 1.10**).

The levels of iron related proteins are regulated by the iron-responsive element/iron-responsive protein system (Wallace, 2016). Uptake and delivery of iron occurs via receptor-mediated endocytosis by transferrin receptor 1, which is ubiquitous to the cell surface (Wallace, 2016). Transferrin-bound iron becomes internalised into the cell though transferrin receptor 1, iron then becomes released from transferrin, which can recycle to the cell surface (Ohgami et al., 2005; Wallace, 2016). DMT1 is then able to transport and release iron from the endosome (Wallace, 2016). Iron delivery is dependent on cellular demands; it may be delivered to the mitochondria for metabolic function as mitochondria play a pivotal role in iron metabolism (Anderson and Frazer, 2017). Co-factor synthesis of enzymes in the mitochondria is dependent on cellular iron (Paul, D Manz, et al., 2017). If cellular demands for iron are met and iron is not further required, excessive iron is stored in ferritin, primarily in the liver and in hepatocytes (Li et al., 2020). Once it is stored in the liver, iron can be taken up by Kupffer cells. As hepatocytes produce ferritin, the liver plays a crucial role in iron mobilisation.

Iron regulation is critical for cell functioning to ensure iron overload or anaemia does not develop. Regulation of iron occurs via two main molecules, ferroportin and hepcidin. Ferroportin and hepcidin function together to regulate iron. Hepcidin is regulated by JAK2/STAT3 signalling pathways (Nemeth and Ganz, 2009) and its synthesis is dependent on levels of blood iron as well as iron

delivery via ferroportin. During iron overload, translation of ferritin mRNA is increased which results in promotion of iron storage (Anderson and Frazer, 2017). Iron uptake into cells also becomes limited due to degradation of transferrin receptor 1 mRNA.

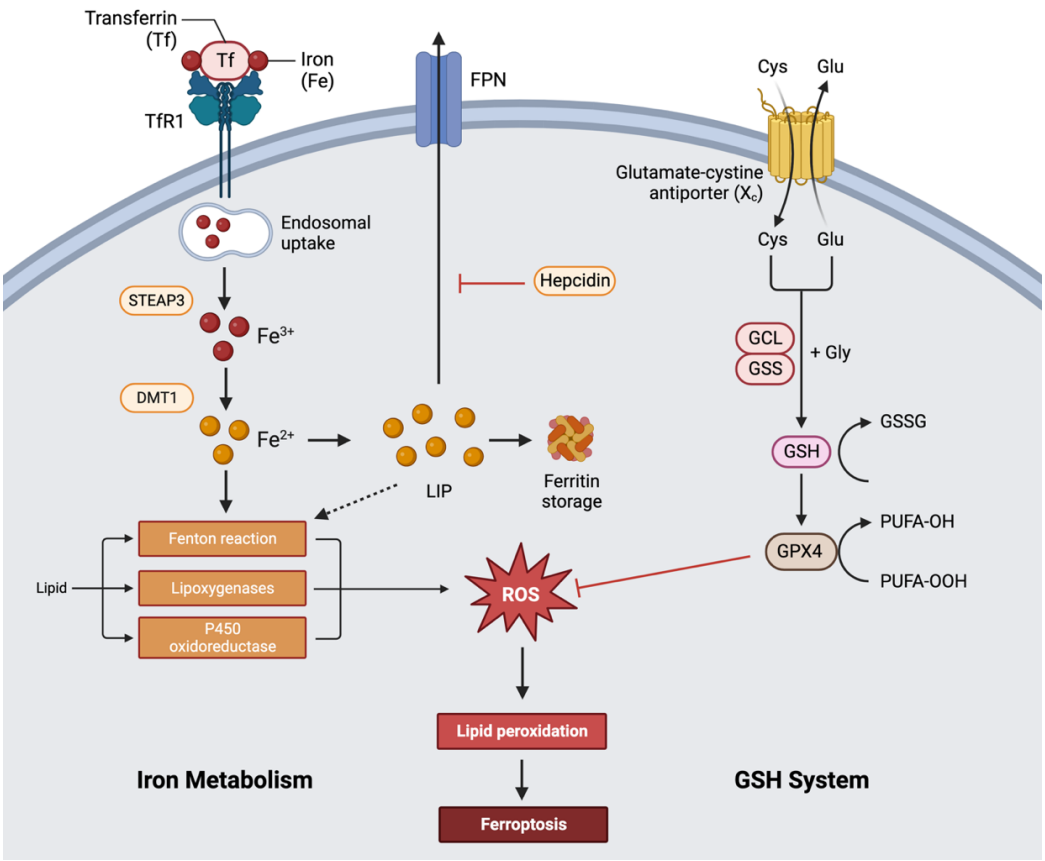

Figure 1.10 Signalling pathways in iron metabolism and ferroptosis. Most iron exists as transferrin (Tf) bound iron which binds to transferrin receptor 1 (TfF1) on the cell surface for intracellular trafficking by receptor mediated endocytosis. Following endosomal uptake, iron is released from Tf and reduced by STEAP3 and then is further transported and released by the divalent metal transporter 1 (DMT1) and can become part of the labile iron pool (LIP) in the cytosol. Iron may also be transported to the cell surface by ferroportin or stored in ferritin. During iron overload and dysregulated iron metabolism, reactive oxygen species (ROS) can form and contribute to oxidative damage and lead to lipid peroxidation and ferroptosis. Suppression from ferroptosis occurs though the glutathione (GSH) system. Cyc: cysteine, DMT1: divalent metal transporter 1, Fe: iron, FPN: ferroportin, GCL: glutamate-cysteine ligase, Glu: glutamate, Gly: glycine, GPX4: glutathione peroxidase 4, GSH: glutathione, GSS: glutathione synthetase, GSSG: Glutathione disulphide, LIP: labile iron pool, PUFA-OH: polyunsaturated fatty acid alcohols, PUFA-OOH: polyunsaturated fatty acid peroxides, ROS: reactive oxygen species, STEAP3: six-transmembrane epithelial antigens of the prostate 3, Tf: transferrin, TfR1: transferrin receptor 1.

1.6.2 Role of Iron in Liver Disease Pathogenesis

Hepcidin

In the liver, hepcidin expression and regulation can be influenced by alcohol. Research indicates hepcidin expression is decreased in both alcohol metabolising hepatoma cells and also in mice exposed to short-term alcohol consumption (Harrison-Findik et al., 2006). Other animal models have shown that hepcidin 1 mRNA expression is also reduced by alcohol, whereas, iron causes upregulation of hepcidin 1 gene expression (Lou et al., 2004; Harrison-Findik et al., 2006). Expression levels of iron transported proteins are also affected by alcohol. Alcohol reduced expression of hepcidin which in turn elevates expression of DMT1, ferroportin and ferritin (Harrison-Findik et al., 2006; L-X Li et al., 2022).

As described previously, both alcohol and iron can cause oxidative stress which can alter hepcidin transcription though inhibition of transcription factor C/EBPα. Antioxidants have the ability to scavenge ROS and reduce oxidative damage and antioxidant treatment such as vitamin E and N-acetylcysteine were able to reduce the suppression of hepcidin (L-X Li et al., 2022). In response to alcohol, the downregulation of hepcidin has potential to cause iron overload in ALD, and suggests a mechanism behind oxidative stress and hepcidin expression in the pathogenesis of ALD.

In cases of chronic liver disease, disruptions in iron regulation can occur due to the liver's crucial role in maintaining iron balance. People who chronically drink alcohol often exhibit elevated serum ferritin levels, leading to an increase in iron stored in the liver. In chronic liver diseases, a decrease in hepcidin

levels are observed (Nemeth and Ganz, 2009). Reduced hepcidin levels result in an excess of iron, which accumulates in the liver (Milic et al., 2016).

Hepcidin as well as surplus iron, when combined with ROS can cause an increase in hydroxyl radicals leading to phospholipid peroxidation as well as DNA strand breaks. Liver injury may also be increased due to elevated intestinal iron absorption which contributes to oxidative stress and lipid peroxidation, potentially exacerbating liver injury. Therefore, iron overload in patients with ALD may be a factor for disease progression (Milic et al., 2016).

Iron overload is a primary feature of ALD and research has demonstrated a link between even moderate alcohol consumption and elevated liver iron levels (Harrison-Findik, 2007). Notably, previous studies have established a negative correlation between liver iron content and survival in ALD (Ganne-Carrié et al., 2000). The excessive iron accumulation plays a role in driving the progression of alcohol-induced liver damage through diverse mechanisms, including oxidative stress, inflammation, ferroptosis, and DNA damage.

Ferroptosis

The Fenton reaction generates ROS when ferrous iron interacts with H_2O_2, converting it into the formation of highly reactive hydroxyl radicals. This iron-driven ROS production exacerbates oxidative stress due to ethanol, further damaging lipids, proteins, and DNA. Excess iron in the liver can initiate a controlled and regulated cellular death pathway referred to as ferroptosis (**Figure 1.10**).

Ferroptosis is distinct from other cell death pathways and is characterised by its iron-dependence high levels of lipid peroxidation (Chen et al., 2022). Although iron metabolism is known to contribute to ferroptosis, many other pathways such as the cyst(e)ine/glutathione/glutathione peroxidase 4 axis, the guanosine triphosphate cyclohydrolase 1/tetrahydrobiopterin (BH4)/dihydrofolate reductase axis, and the ferroptosis suppressor protein 1/coenzyme Q axis, have all recently been proposed to influence the induction of this pathway (Zheng and Conrad, 2020).

Ferroptosis is protected by antioxidant molecules such as glutathione and coenzyme Q10, however, a drop in NADPH levels can initiate the ferroptosis pathway (Wang et al., 2017), and therefore, NADPH levels have been utilised as a biomarker for ferroptosis (Dixon et al., 2012; Bersuker et al., 2019). Depleted levels of glutathione can also induce ferroptosis (Sun et al., 2018). Excessive ethanol consumption is known to lower levels of glutathione and glutathione peroxidase levels and has also been shown to increase iron accumulation and upregulate biomarkers of ferroptosis (L-X Li et al., 2022).

Inflammatory Response

An inflammatory response may become activated by ROS which can be generated by both iron and ethanol independently. Lipid peroxidation by products such as 4-hydroxy-2-nonenal may also cause inflammatory activation, causing downstream activation of Kupffer cells and hepatic stellate cells (Pietrangelo, 2003). In animal models of ALD, iron was shown to be elevated in Kupffer cells which in turn caused activation of NF-κB and TNF-α (She et al., 2002; Xiong et al., 2003; Harrison-Findik, 2007). Research has also

shown that when bone marrow-derived macrophages were treated with iron they polarised to an inflammatory phenotype (M1), therefore, causing inflammation (Handa et al., 2019). Iron overload can cause lipid peroxidation to cellular membranes, mitochondrial damage, and endoplasmic reticulum which can cause damage to the intestinal barrier and lead to leaky gut. Iron overload can therefore increase exposure to lipopolysaccharide (which is often translocated from the gut during ALD), inducing production of pro inflammatory cytokines such as IL-1β, IL-6, IL-12, IFN-β or IFN-γ, which may exacerbate inflammation (Malesza et al., 2022). Mitochondrial damage may in turn lead to mtROS and superoxide production (Hoeft et al., 2017; L-X Li et al., 2022). Progression of disease may also occur due to hepatic stellate cell activation which may increase expression of TGF-β1 as well as form collagen deposits, and fibrotic disease (Houglum, Bedossa and Chojkier, 1994). Hepatic stellate cells may also trigger fibrosis in iron overload, causing Kupffer cell activation and release of proinflammatory and profibrotic mediators such as TNF-α, IL-1, IL-6, IL-8, IL-10, IFN-γ, TGF-β1, platelet-derived growth factor, β-fibroblast growth factor, monocyte chemoattractant protein-1, and ROS.

1.7 Diagnosis

Generally, the diagnosis of ALD is based on a combination of factors such as history of alcohol intake and clinical and laboratory abnormalities. The diagnosis of ALD can be clinically challenging due to the fact there is no single study able to confirm a diagnosis. In some cases, patients may be completely asymptomatic, with liver enzymes at normal levels (Torruellas, French and

Medici, 2014). Diagnosis of ALD can rely on indirect evidence such as questionnaires to confirm clinical suspicion.

ALD is suspected when patients have a history of alcohol abuse along with abnormal serum transaminases, hepatomegaly, clinical signs of chronic liver disease, radiographic evidence of hepatic steatosis or fibrosis/cirrhosis, or who have had a liver biopsy showing macrovesicular steatosis or cirrhosis (Torruellas, French and Medici, 2014). However, not all patients will have elevated serum aminotransferases and the level of liver enzyme does not always correlate with the severity of ALD (Torruellas, French and Medici, 2014). The pattern of elevation in transaminases may help diagnose liver injury if the level of aspartate aminotransferase (AST) is greater than that of alanine aminotransferase (ALT) (Torruellas, French and Medici, 2014).

Physical examination of steatosis and alcoholic hepatitis can reveal hepatomegaly. Patients with more severe ALD may exhibit other symptoms such as splenomegaly, jaundice, and ascites (Frazier et al., 2011). In patients with compensated cirrhosis, symptoms of hepatomegaly and splenomegaly may present, whereas, in decompensated cirrhosis ascites, cachexia, palmar erythema and Dupuytren's contractures may occur (Frazier et al., 2011).

Liver biopsies in ALD are useful to clarify atypical disease and establish the stage and severity of ALD (Kobyliak, Dynnyk and Abenavoli, 2016). The typical histological features seen in patients with ALD include steatosis, hepatocellular damage (ballooning and/or Mallory-Denk bodies), giant mitochondria, lobular inflammation and lobular distortion (Kobyliak, Dynnyk and Abenavoli, 2016). Liver biopsies which reveal severe mixed micro- or

macrovesicular patterns, and/or giant mitochondria have an increased likelihood in developing fibrosis/cirrhosis (Teli et al., 1995; Frazier et al., 2011).

1.8 Clinical Staging of Disease

A variety of algorithms are currently used to assess the staging and severity of ALD as well as their use in predictive survival outcomes and treatment options. Initially the Child-Pugh score and the model for end-stage liver disease were developed. The Child-Pugh score categorises patients as class A, B or C defined by their levels of serum bilirubin and albumin, prothrombin time, ascites, and encephalopathy (Angermayr et al., 2003; Forrest et al., 2007). Each measure is scored between 1-3, with 3 defined as most severe. A final Child-Pugh score of 5-6 points (Class A) is associated with an 100% 1-year survival and 85% 2-year survival. A final score of 7-9 points (Class B) has an 80% 1-year survival and 60% 2-year survival, whereas, a score of 10-15 points (Class C) is associated with the highest severity and also correlates with lower survival (45% 1-year survival and a 35% 2-year survival) (Rahimi and Pan, 2015). The model for end-stage liver disease score also measures total bilirubin levels but also includes creatinine and international normalized ratio (INR) levels which has been identified as a useful tool for the evaluation of liver transplantation (Forrest et al., 2007). The formula for model for end-stage liver disease score calculation is $9.57 \times \log_e(\text{creatinine}) + 3.78 \times \log_e(\text{total bilirubin}) + 11.2 \times \log_e(\text{INR}) + 6.43$ (Rahimi and Pan, 2015). These algorithms are most useful for the predication of mortality and have less use in treatment selection and prognosis (Petagine, Zariwala and Patel, 2021). It has been shown that model for end-stage liver disease scores greater than 11 for 30-

day mortality predictions are 86% sensitive and 82% specific (Sheth, Riggs and Patel, 2002).

To determine disease severity and treatment options for patients with alcoholic hepatitis, The Maddrey Discriminant Function score and The Glasgow Alcoholic Hepatitis Score were created. Serum bilirubin and prothrombin time are assessed to generate the Maddrey Discriminant Function score via the equation DF = (4.6 x [prothrombin time (sec) - control prothrombin time (sec)]) + (serum bilirubin) (Rahimi and Pan, 2015). The scoring classifies the staging of disease as severe (Maddrey Discriminant Function > 32) or non-severe (Maddrey Discriminant Function < 32). Steroid treatment is most beneficial to those patients who fall in the severe category (Rahimi and Pan, 2015). The Maddrey Discriminant Function scoring system has been shown to be 86% sensitive and 48% specific when the score was above 32 (Sheth, Riggs and Patel, 2002). Another scoring system, the Glasgow Alcoholic Hepatitis Score, was developed to predict treatment outcomes in patients with alcoholic hepatitis. To generate a Glasgow Alcoholic Hepatitis Score, a patients age, white blood cell count, serum urea, bilirubin and prothrombin time are analysed. A final score between 5 and 12 is given with scores above 9 associated with a worse prognostic outcome. Treatment with steroids in patients with an Maddrey Discriminant Function score > 32 and a Glasgow Alcoholic Hepatitis Score > 9 have shown higher survival rates (59%) than those without treatment (38%) (Forrest et al., 2007). Another scoring system named the Lille model was developed to assess prognosis and response to corticosteroids in severe alcoholic hepatitis patients after 7 days of treatment (Louvet et al., 2007). The Lille model score is calculated via the equation (exp(-

R))/(1 + exp(-R)). Where R = 3.19 – 0.101*(age, years) + 0.147*(albumin day 0, g/L) + 0.0165* (evolution in bilirubin level, µmol/L) - 0.206*(renal insufficiency) - 0.0065*(bilirubin day 0, µmol/L) - 0.0096*(prothrombin time, seconds) (Rahimi and Pan, 2015). The Lille model is highly sensitive and specific and is therefore useful to predict short-term survival as well as identify patients who at high risk of death at 6 months (Louvet et al., 2007).

1.9 Treatment

The treatment of ALD is dependent on the stage of the disease and the aims of treatment (Lieber, 2004). Patients with ALD are most commonly treated with approaches to eliminate alcohol intake, as the continuation of alcohol consumption is the most important risk factor for disease progression. Regardless of disease severity, abstinence is the foundation of therapy and early management of alcohol abuse or dependence. Malnutrition is frequent and nutrition status should be evaluated (**Table 1.1**). Patients with symptomatic forms of alcoholic steatohepatitis often develop acute renal failure which negatively impacts survival.

Table 1.1 Therapeutic treatment options for patients with alcohol-associated liver disease. Adapted from: Petagine, Zariwala and Patel (2021).

Treatment	Target	Treatment Method	Treatment Effects
Abstinence	Abstain from drinking	Pharmacotherapy in combination with psychological interventions	The role of pharmacologic agents in maintaining abstinence is unclear. Improve histology of hepatic injury, to reduce portal pressure and decrease progression to cirrhosis, and to improve survival (Petagine, Zariwala and Patel, 2021).
Nutritional Therapy	Correct malnutrition	Protein intake of 1.5 g/kg of body weight and 35 to 49 kcal per kg body weight per day.	Vitamin A, thiamine, vitamin B_{12}, folic acid, pyridoxine, vitamin D, magnesium, selenium, and zinc may be administered (Petagine, Zariwala and Patel, 2021).
Corticosteroid	Decrease inflammation	40 mg daily for 28 days, followed by 20 mg daily for 7 days, and 10 mg daily for 7 days	Studies have demonstrated short-term histological improvement but have not improved long-term survival. Increase in the serum bilirubin and Lille score > 0.45 after 1 week of therapy are associated with worse outcome (Petagine, Zariwala and Patel, 2021).
Pentoxifylline	Reduction in cytokines	400 mg orally three times a day for 4 weeks	Show to reduce levels of cytokines including TNF-α. Protective effect against hepatorenal syndrome (Petagine, Zariwala and Patel, 2021).
Infliximab	Anti-TNF-α	Not confirmed	Further studies needed. Research has shown decreases in cytokines with combination therapy. Although, associated with a higher likelihood of severe infections and mortality (Petagine, Zariwala and Patel, 2021).
N-acetylcysteine	Antioxidant	Further studies required.	
Metadoxine	Antioxidant		
Silymarin	Antioxidant		
Liver transplantation	Surgical Procedure	Damaged liver is removed and replaced with a healthy ‘donor’ liver.	The standard practice for end-stage liver disease. A period of 6 months of abstinence is recommended prior to transplantation. Studies have demonstrated an improvement in quality of life (Singal et al., 2012; Singal, 2013). Post-transplant interventions are necessary to support patients to continue with abstinence (Donnadieu-Rigole et al., 2017).

1.9.1 Abstinence

Abstinence is the most important therapy for patients with ALD (Pessione et al., 2003). Abstinence from alcohol is considered the most effective and has been shown to improve the outcome and survival of cirrhotic patients as well as resolving alcoholic steatosis (Mathurin et al., 2012). Abstinence has been shown to improve the outcome and histological features of hepatic injury, to reduce portal pressure and decrease progression to cirrhosis, and to improve survival at all stages in patients with ALD (Brunt et al., 1974; Pessione et al., 2003).

1.9.2 Nutritional Therapy

A significant proportion of patients with ALD are malnourished and the degree of malnutrition correlated with the severity of disease (Frazier et al., 2011). Deficiencies in several vitamins and minerals, including vitamin A, vitamin D, thiamine, folate, pyridoxine, and zinc often occur in ALD, and in some cases, they are thought to be involved in the pathogenesis of disease (Halsted, 2004). For patients with ALD a protein intake of 1.5 g per kg body weight and 35 to 49 kcal per kg body weight per day is recommended (Frazier et al., 2011). If an individual develops deficiencies, then micronutrient supplements may be advised. Supplementation with zinc has been shown to be therapeutic in animal models by blocking mechanisms or liver injury including ‘leaky gut’, oxidative stress and apoptosis (Mohammad et al., 2012). Long-term aggressive nutritional therapy including oral/enteral nutritional supplements in patients with cirrhosis have shown improved nutritional status.

1.9.3 Steroids

Corticosteroids are the current main treatment for severe alcoholic hepatitis (Mathurin et al., 2011). The effect of corticosteroids is a reduction in pro-inflammatory cytokines (i.e. TNF-α) and an increase in anti-inflammatory cytokines (i.e. IL-10) (John et al., 1998; Gao, 2012). Research has shown glucocorticoids decrease pro-inflammatory cytokines as well as intracellular adhesion molecule 1 expression (Menachery and Duseja, 2011). They also inhibit neutrophil activation. The use of glucocorticoids in alcoholic hepatitis has demonstrated short-term histological improvement. Unfortunately, they do not improve long-term survival (Menachery and Duseja, 2011). The Lille model identifies the response to corticosteroids in severe alcoholic hepatitis patients following 7 days of treatment and is useful for predicting short-term survival (Louvet et al., 2007).

1.9.4 Anti-cytokine Therapy

Pentoxifylline

Research has shown that cytokines play a vital role in the pathogenesis of ALD. Therefore, several agents have been developed to target these cytokines, in particular TNF-α. One of the first anti-cytokine therapies to be studied was pentoxifylline, a phosphodiesterase inhibitor initially used in the treatment of peripheral vascular disease (McCullough, O'Shea and Dasarathy, 2011), but has been found to reduce levels of cytokines including TNF-α. A randomised placebo-controlled trial with 101 patients was conducted on patients with severe alcoholic hepatitis (O'Shea, Dasarathy and McCullough, 2010; McCullough, O'Shea and Dasarathy, 2011). In-hospital mortality in the

treated patients was 40% lower than in the patients receiving the placebo, reducing the likelihood of hepatorenal syndrome developing. Hepatorenal syndrome was responsible for 50% of the 12 deaths in the treatment group, compared to 91.7% of the 24 deaths in the placebo group. Another study found when compared to placebo, patients with severe alcoholic hepatitis treated with pentoxifylline exhibited a higher 6-month survival by the reduction in the incidence of hepatorenal syndrome (Lenz et al., 2015). A randomised controlled trial in cirrhotic patients also supported the reduction in hepatorenal syndrome (Lebrec et al., 2010). However, a recent randomised controlled trial of 270 patients with severe alcoholic hepatitis studying prednisolone and pentoxifylline found no benefit to patients compared to using only corticosteroids (Mathurin et al., 2013).

The STOPAH trial was a multicentred, double-blind, randomised trial with a 2-by-2 factorial design to evaluate the effect of treatment with prednisolone or pentoxifylline; drugs recommended for the treatment of severe alcoholic hepatitis (Forrest et al., 2013, 2018; Thursz et al., 2015). The primary endpoint of the STOPAH trial was mortality at 28 days and the secondary endpoints included death/liver transplantation at 90 days, then 1 year (Thursz et al., 2015). A total of 1103 patients underwent randomisation, and data from 1053 were available for the primary end-point analysis (Thursz et al., 2015). Mortality at 28 days was 17% in the placebo–placebo group, 14% in the prednisolone–placebo group, 19% in the pentoxifylline–placebo group, and 13% in the prednisolone–pentoxifylline group (Thursz et al., 2015). Pentoxifylline showed no improvement in the survival of patients (Thursz et al., 2015; Dao and Rangnekar, 2018). The comparison of patients with and without

steroid treatment recognised a trend toward reduced 28-day mortality in the steroid group but this did not show significance (Thursz et al., 2015). Also, serious infection was almost doubled for patients who received steroid treatment (Thursz et al., 2015; Dao and Rangnekar, 2018).

Infliximab

Infliximab is another cytokine inhibitor studied in ALD. Infliximab is a monoclonal chimeric anti-TNF antibody, and etanercept, a fusion protein containing the ligand-binding portion of the human TNF receptor fused to the Fc portion of human immunoglobulin G1 (Menon et al., 2004). The first trial using infliximab studied 20 patients with alcoholic hepatitis. Patients were randomised to either 5 mg/kg of infliximab as well as 40 mg/day of prednisone or prednisone alone (Spahr et al., 2002). Although no differences were found in overall mortality, decreases in cytokines were found in the patients on combination therapy (O'Shea, Dasarathy and McCullough, 2010). Another clinical trial of 36 patients in France studied prednisolone (40 mg/day for 4 weeks) to prednisolone with infliximab (10 mg/kg, at study entry, 2 weeks and 4 weeks after entry) (Naveau et al., 2004). However, the trial was stopped early due to 7 deaths in the infliximab group and 3 in the prednisolone group due to infection (O'Shea, Dasarathy and McCullough, 2010). The study has been criticised due to the dose of infliximab predisposing patients to infections (Mookerjee et al., 2004). This indicates that anti-TNF-α treatment has been associated with a higher likelihood of severe infections and mortality. It has been speculated the repeated and excessive use of TNF blockades may negatively impact liver regeneration. There has been no clinical evidence that

compares the use of anti-TNF therapy to the use of steroids or nutrition therapy.

1.9.5 Combination Therapy

There is currently little evidence that identifies the effects and benefits of sequential therapies or combined approaches. Several older studies have examined the use of steroids and nutritional therapy. For example, a pilot study evaluated the role of steroids and enteral nutritional therapy in 13 patients wither severe alcoholic hepatitis and found mortality was 15%, which was lower than expected (Alvarez et al., 2004).

1.9.6 Liver Transplantation

ALD is the second most common indication for liver transplantation for chronic liver disease in the Western world (Burra and Lucey, 2005). The procedure remains the standard practice for patients with end-stage liver disease. A period of 6 months of abstinence is recommended for the criteria for liver transplantation (Lucey et al., 1997). This allows dependency issues to be addressed and will allow for clinical improvement. Therefore, some patients with ALD are not listed for liver transplant due to continued alcohol consumption, improvement in liver function after abstinence, and a higher incidence of cancers of the upper airways and upper digestive tract. Therefore, patients who are listed for liver transplant must first undergo screening. Less than 20% of patients with end-stage liver disease and a history of alcohol abuse receive liver transplants (Lucey, 2014). However, those who receive transplants have an improvement in quality of life (Singal et al., 2012; Singal, 2013). Patients who undergo liver transplants due to excessive alcohol

consumption are highly likely to return to drinking after transplantation (Zetterman, 2005), therefore, post-transplant interventions are necessary to support patients to continue with abstinence (Donnadieu-Rigole et al., 2017). Generally speaking, only a small percentage of those who undergo a liver transplant revert to heavy drinking (O'Grady, 2006).

1.9.7 Antioxidants and Alternative Treatment

Due to contribution of oxidative stress and damage in the pathogenesis of liver disease antioxidant therapy has been considered for treatment of disease. Vitamins E and C, N-acetylcysteine as well as S-adenosyl methionine, and betaine have been shown to moderate ROS. Glutathione is the main cellular antioxidant, and S-adenosyl methionine is a main precursor of glutathione (Cederbaum, 2010; Lu and Mato, 2012). Decreased S-adenosyl methionine levels have been documented in patients with either alcoholic hepatitis or cirrhosis (Lee et al., 2004). Supplementation with S-adenosyl methionine has been shown to reverse liver injury and mitochondrial damage due to alcohol insult in animal models (Lieber, 2002), although this did not appear to show significant difference. A trial using S-adenosyl methionine and choline aims to assess the effect of treatment with a combined formulation. Half of the patients in the trial will receive the formulation once daily for 24 weeks and the other half will receive a placebo (trial number NCT03938662). As damaged livers cannot produce sufficient levels of S-adenosyl methionine it been hypothesised that administration of choline and S-adenosyl methionine can be beneficial in patients with ALD.

Betaine is also involved in formation and synthesis of glutathione and has been shown to ameliorate effects of oxidative stress in animal models after dietary supplementation (Kharbanda et al., 2005; Kim et al., 2008; Alirezaei et al., 2011; Petagine et al., 2021). N-acetylcysteine has been reported to reduce both ethanol intake by 70% as well as ethanol seeking behaviour by 77% in rats (Quintanilla et al., 2016; Lebourgeois et al., 2018).

Many patients with ALD often use alternative medicine such as natural and herbal remedies. A U.S. survey showed that 41% of patients with ALD used some form of alternative medicine for the treatment of liver disease, most commonly these were silymarin and garlic (Kim, Ong and Qu, 2016). Other alternative medicine includes ginseng, green tea, ginkgo, echinacea, and St. John's wort (Strader et al., 2002). A recent review (Kim, Ong and Qu, 2016) showed other alternative medicine, such as betaine, curcumin, fenugreek seed polyphenol, LIV-52, vitamin E, and vitamin C which had efficacy in experimental models of alcoholic liver injury.

1.9.8 Faecal Bacteria Transplants

It is known that excessive alcohol consumption causes bacterial overgrowth and gut dysbiosis. Bacteroidetes and Firmicutes phyla show decreased levels in cirrhotic patients (Schwenger, Clermont-Dejean and Allard, 2019), whereas, increases in Proteobacteria, Fusobacteria and Actinobacteria phyla have been observed (Schwenger, Clermont-Dejean and Allard, 2019). A reduction in beneficial autochthonous bacteria in cirrhosis has been reported, as well as increases in pathogenic bacteria (Bajaj et al., 2014). The transfer of gut microbiota from healthy patients decreased inflammation liver injury.

Improvement in liver function, including reduction of ALT, AST and bilirubin has been reported after administration of probiotics containing beneficial autochthonous bacteria (Li et al., 2016). A current trial is investigating modulation of the gut microbiota using Profermin Plus® and probiotics been hypothesised to reduce disease progression (trial number NCT03863730) (**Table 1.2**).

1.9.9 Nanomedicine

Numerous treatments of ALD have not been successful in clinical trials; including IFN-γ, angiotensin II antagonists and IL-10 (Bartneck, Warzecha and Tacke, 2014). A problem with these treatments may be due to the formulation's low specificity. Nanoformulations may overcome some of the difficulties faced with traditional drugs as they are able to deliver drugs to specific cell types based on surface receptor binding (Bartneck, Warzecha and Tacke, 2014). Specific drug delivery increases the concentration at the target cell which is an important feature of nanomedicine, as many drugs have limited efficacy due to the low concentration at the target site (Bartneck, Warzecha and Tacke, 2014). Nanomedicine may also inhibit the metabolism of the drug enabling a prolonged release (Bartneck, Warzecha and Tacke, 2014).

Table 1.2 Overview of the current and completed clinical trials for ALD treatment.

Intervention	Target	Condition	Clinical Trial Number	Phase	Status	Primary Endpoint
Livitol-70 (Herbal supplements)	Oxidative damage	ALD	NCT03503708	N/A	Not yet recruiting	Change from baseline in ALT, AST, ALP, GGT and bilirubin.
Profermin®	Gut microbiome	ALD Cirrhosis Fibrosis	NCT03863730	N/A	Active, not recruiting	Hepatic stellate cell activity defined by proportion of patients with 10% or more reduction by liver biopsy.
Candersartan	Angiotensin II inhibitor	ALD	NCT00990639	Phase I/II	Completed	Histological grading of hepatic fibrosis.
Guselkumab	Anti-IL23 monoclonal antibody	ALD	NCT04736966	Phase I	Recruiting	Safety and tolerability of Guselkumab including adverse events.
sgp130	IL-6 receptor signalling inhibitor	ALD Hepatitis C	NCT00770198	Observational	Completed	Measurement of plasma cytokine levels, PBMC cytokine release and liver IL-6 mRNA.
Fermented Protaetia brevitarsis seulensi	Gut microbiome	ALD	NCT04320199	N/A	Recruiting	Concentration of GGT.
HA35	TLR4 target	Alcoholic Hepatitis	NCT05018481	Phase I	Recruiting	Skeletal muscle mass percentage change from baseline to day 90.
DUR-928	Inflammation, cell survival, tissue regeneration	Alcoholic Hepatitis	NCT03917407	Phase II	Recruiting	Assessment of adverse events and pharmacodynamics of ALT, AST, bilirubin, albumin, CRP, IL-6, IL-8 and cytokeratins.
BATTLE Trial	Bacteriophages	Alcoholic Hepatitis	NCT05618418	Observational	Recruiting	Patient survival and E. faecalis in faecal sample at hospital admission.
Canakinumab	IL-1β antibody	Alcoholic Hepatitis	NCT03775109	Phase II	Recruiting	Histological improvements of alcoholic hepatitis at 28 days compared to baseline
Cellgram-LC	Bone marrow derived mesenchyme stem cells	Alcoholic Cirrhosis	NCT04689152	Phase III	Recruiting	Transplant free survival (3 years).

1.10 Further Research

Inflammatory conditions have been linked to the pathogenesis of ALD. Significant developments have been made identifying inducers of inflammation and their role in the development of ALD, which has directed further research.

The causes of alcohol-induced liver inflammation are complex. Multiple factors have been identified as inducers of liver inflammation including lipopolysaccharide, alcohol metabolites, enriched FFAs, necrotic cell products, and complements. Research has shown that these factors are highly interactive with common downstream intermediates, in particular, ROS (Cichoz-Lach and Michalak, 2014). These inflammatory factors have also been shown to cause injury, thus, the link between alcohol-induced inflammation and injury supports further research into the inflammatory process in ALD. Inflammation also produces pathological protective functions. Therefore, it is important to identify pathways and factors that are primarily pathogenic as well as preserving the protective functions of these components when developing effective treatment. A better understanding of cellular and molecular changes which occur in ALD is also necessary to develop treatments.

The excessive intake of alcohol also activates cell death and cell adaptive survival pathways in the liver and therefore may contribute to the pathogenesis of ALD. Although apoptosis in ALD has been studied emerging evidence supports RIP1-RIP3-mediated necroptosis also contributes to the pathogenesis of ALD. Therefore, an ideal development to treat ALD should

consider the pathways of cell death. However, future work is needed to determine whether the beneficial effects against alcohol-induced liver injury.

Nanomedicine is an emerging technology in the field of medicine providing new approaches for the treatment of liver diseases. Conventional approaches provide only symptomatic treatment. Nanoparticles have numerous advantages over conventional treatment based on their delivery at target sites, therefore, it may provide considerable scope for future treatment of liver disease.

1.11 Aim and Objectives

Aim

To investigate the role of alcohol and iron in inducing cell toxicity in HepG2 (VL-17A) cells, specifically focusing on oxidative stress and mitochondrial function and to investigate the association between frequency of drinking, liver iron content and percentage of liver fat in a UK BioBank cohort.

Objectives

1. To characterise the effects of ethanol on mechanisms of liver injury, oxidative stress, mitochondrial function, and cell death pathways.
2. To explore the mechanisms of liver injury, oxidative stress, mitochondrial function, and apoptosis in a combined model cell model of ethanol and iron overload.
3. To study the protective effects of free drug antioxidants such as curcumin and silibinin, as well as nanoformulated curcumin in a model of ALD and iron overload.

4. To investigate correlations between frequency of drinking and levels of iron in the liver in alcohol consumers.

Hypothesis

Ethanol and iron treatment causes liver injury such as oxidative stress, cell death and mitochondrial dysfunction, and treatment with antioxidant nanoformulations mitigate parameters of oxidative stress and liver injury.

CHAPTER 2 MATERIALS AND METHODS

Objectives 1 and 2

2.1 Cell Culture

Human hepatoma cell lines (HepG2) named as VL-17A cells, which overexpress both CYP2E1 and ADH were obtained from Dr Dahn Clemens, (University of Nebraska, USA) and stored in cryovials frozen in liquid nitrogen. Cells were thawed and cultured in a high-glucose (4.5 g/L) Dulbecco's Modified Eagle Medium (DMEM) supplemented with 10% (v/v) foetal calf serum (FCS), 1% penicillin/streptomycin (100 U/mL) and 1% L-glutamine (2 mM). Cells were cultured at 37°C in a 5% CO_2 atmosphere. VL-17A cells were also grown in the presence of Plasmocin Prophylatic 5 µg/mL, and Fungin 10 mg/mL for the initial four weeks prior to their culturing in a high glucose complete media. Cells were cultured to 70% confluence before passage. Cell monolayers were washed with sterile phosphate-buffered saline (PBS) and trypsin (1:250 1x 0.25% in DPBS) was added to the flask for 5 mins at 37°C to dissociate cells. Trypsin was neutralised by addition of complete DMEM, and the detached cells centrifuged at 400 g for 5 mins. Cells were then resuspended in media and seeded into 175 cm^2 flasks seeded with $1x10^6$ cells/mL.

2.2 Assay Optimisations

Optimum concentrations of alcohol were also determined to model cell toxicity and liver injury. Previous research has used concentrations between 10 mM to 800 mM to model alcohol toxicity and oxidative stress in VL-17A cells

(Madushani Herath et al., 2018; Khodja and Samuels, 2020). Cell viability was quantified using the mitochondrial 3-(4,5-Dimethylthiazol-2-yl)-2,5-diphenyltetrazolium bromide (MTT) reduction assay. Firstly, the optimum seeding density was determined. To optimise the assay cells were then seeded in 96-well plates at varying concentrations (5 x 10^3, 1 x 10^4, 1.5 x 10^4, and 2 x 10^4 cells/mL) were assayed for cell viability. Varying concentrations of alcohol were analysed (50 mM, 100 mM, 200 mM, 250 mM, 300 mM, 350 mM, 400 mM, 450 mM, and 500 mM). To enhance the MTT assay effectiveness, cells were treated with varying concentrations of MTT (0.125 mg/mL and 0.5 mg/mL). In the case of 1 x 10^4 and 0.125 mg/mL MTT the absorbance values showed a gradual decrease at higher concentrations of ethanol treatment. Alcohol concentrations were assessed as 100 mM, 200 mM, 250 mM, 300 mM, 350 mM, 400 mM, and final concentrations decided as 200 mM, 300 mM and 350 mM ethanol. Lower concentrations of alcohol (50 mM) did not show an effect on cell viability in comparison to the control and the highest concentrations (450 mM and 500 mM) were toxic to cells.

2.3 Treatment of Cells

Cells were seeded according to the appropriate protocol (as below) and treated with alcohol (as above) with or without iron (50 μM) or combinations of both in low glucose (1.0 g/L) DMEM supplemented with 1% (v/v) FCS, 1% penicillin/streptomycin (100 U/mL) and 1% L-Glutamine (2 mM). The varying treatments were studied on their ability to induce liver toxicity over 30 mins to 72 hrs. The effects of cell treatment were assessed by the methods below.

2.4 Measurement of Cell Viability

VL-17A cells were seeded in 96-well plates (1 x 10^4 cells/ 200 µL DMEM per well) and then treated with the corresponding concentrations of alcohol with or without iron over a 24 hr, 48 hr and 72 hr time periods. MTT (5 mg/ml) (Fisher Scientific, UK) was added to each well and incubated and 37ºC for 2 hrs. After the incubation, the reagent was removed, and cells were incubated with (100 µl/well) DMSO for 15 mins at room temperature. Cell viability was determined by assaying the ability of the dehydrogenase enzyme in the mitochondria to reduce the MTT to blue formazan crystal via measurement of the intensity calorimetrically at 550 nm using the VersaMax microplate reader (Molecular Devices, UK). Data is expressed as percentages from the control.

2.5 Measurement of ROS

The level of intracellular ROS was investigated using 2, 7-dichlorofluoresceindiacetate (DCFDA) (Sigma, UK). VL-17A cells were seeded at 1 x 10^4 cell/well in a 96-well plate at 37ºC and incubated overnight. Cells were then treated as described above and incubated for 30 mins, 1 hr and 2 hrs. Following the incubation, the cells were incubated with 10 µM DCFDA diluted in PBS for 45 mins at 37ºC. The intensity of fluorescence was determined by FLUOstar OPTIMA (Jencons-PLS, UK) at an excitation of 485 nm and an emission of 535 nm. The intracellular ROS level was indicated by the fluorescence level, and the results are expressed as percentage from the control.

2.6 Measurement of Mitochondrial Respiration

To analyse mitochondrial dysfunction, an XF Cell Mito Stress Test Kit (Agilent Technologies, UK) was used following the manufacturer's instructions and protocol adapted from Ghazali et al., 2020. Treated cells were analysed on the Seahorse extracellular flux analyser which measures oxygen consumption and mitochondrial respiration. For this assay cells were seeded at a density of 2 x 10^4 cells/100 µL in (10% FCS) DMEM and on SeaHorse 24-well cell culture microplates and were incubated at 37ºC, 5% CO_2. Following 2 hrs of adherence, 150 µL of DMEM (10% FCS) was added to the cultured cells and re-incubated overnight. Cells were then treated with 500 µL per well of alcohol with or without iron as above for varying time points. 24 hrs before running the assay 1 mL per well of XF Calibrant Solution was added into the 24-well SeaHorse Utility Plate topped with a SeaHorse Sensor Cartridge and incubated overnight at 37°C with 0% CO_2 atmosphere. Seahorse Assay Medium (pH 7.4) was prepared with 25 mM glucose and 1mM sodium pyruvate. Cells were then washed twice with 500 µL of Seahorse Assay Medium and incubated with 500 µL of Seahorse Assay Medium for 45 min at 37ºC without CO_2. MitoStress drugs oligomycin (4 µM) to inhibit ATP synthase; FCCP (4 µM), an uncoupling agent; and antimycin/Rotenone mixture (2.5 µM)—to inhibit oxidative phosphorylation and electron transfer will be added (**Table 2.1**). Following measurement, results were quantified and normalised to protein concentrations using the Bio-Rad protein assay kit (Bio-Rad Laboratories, UK). Graphical presentation of the SeaHorse MitoStress profile is shown in **Figure 2.1**.

Table 2.1 SeaHorse MitoStress assay parameters. Calculations of mitochondrial respiration parameters, performed by MitoStress Test Report Generator.

Parameter	Equation
Non-mitochondrial respiration	Minimum rate measurement following Rotenone/antimycin injection
Basal respiration	(Last rate measurement prior to injection of oligomycin) - (non-mitochondrial respiration rate)
Maximal respiration	(Maximum rate measurement following FCCP injection) - (non-mitochondrial respiration)
Proton Leak	(Minimum rate measurement following oligomycin injection) - (non-mitochondrial respiration)
ATP Production	(Last rate measurement prior to injection of oligomycin) - (Minimum rate measurement following oligomycin injection)
Spare Respiratory Capacity	(Maximal Respiration) - (Basal respiration)

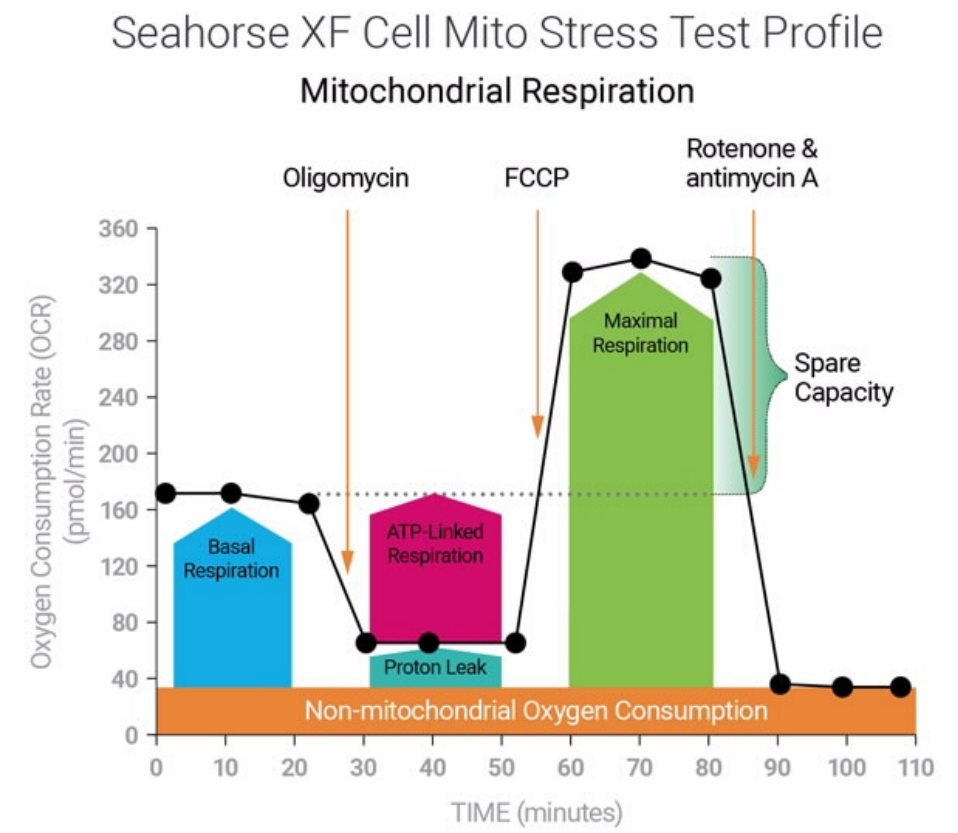

Figure 2.1 SeaHorse MitoStress Assay. Graphical presentation of a typical SeaHorse MitoStress Assay profile of oxygen consumption rate in response to injections of MitoStress drugs Oligomycin, FCCP, and Rotenone & antimycin A. Image available at: https://www.agilent.com/en/product/cell-analysis/real-time-cell-metabolic-analysis/xf-assay-kits-reagents-cell-assay-media/seahorse-xf-cell-mito-stress-test-kit-740885#howitworks

2.7 Total Protein Quantification

The Quick Start™ Bradford Protein Assay (Bio-Rad Laboratories, UK) is simple colorimetric assay for total protein quantification in solution and was utilised to quantify total protein in treated cells and is based on the Bradford dye-binding method (Bradford, 1976). Cells were washed twice with ice cold PBS prior to starting the Bradford assay. Cells were then lysed with 100 μL 1% Triton 100 X per 1 mL PBS and shaken until solution becomes clear, to extract protein from cells. If the assay was performed in a microplate, each well was then scraped using sterile cell scrapers, and its contents transferred to individual labelled Eppendorf tubes. 5 μL of each sample or standard (0.125-1.5 mg/mL) were then added in triplicate wells to a 96-well plate. 200 μL Bradford Reagent (Bio-Rad Laboratories, UK) was then added on top of the sample or standard induing a colour change. Protein concentration was measured by absorbance at 595 nm using the VersaMax microplate reader (Molecular Devices, UK). Protein standards were used to create a standard curve to allowing extrapolation of values to quantify unknown protein sample concentrations via linear regression.

2.8 Measurement of Apoptosis

To determine the quantity of apoptotic cells the Annexin VFITC/propidium iodide staining kit (BioLegend, UK) and measured by flow cytometry. Cells were stained with FITC labelled Annexin-V to detect extracellular expression of phospholipid phosphatidylserine and propidium iodide.

Annexin V is an intracellular protein which binds to phospholipid phosphatidylserine in a calcium-dependent manner. Usually, phospholipid phosphatidylserine is in the inner membrane but during apoptosis it translocated to the outer membrane. Propidium iodide is a fluorescent dye able to bind to DNA allowing for distinction of early and late apoptosis as well as necrosis. 3 x 10^5 cells were seeded in 12-well plates overnight and the following day treated with the varying concentrations of alcohol with or without iron as described above. Following treatment, supernatant of cells was kept, and cells were washed once with PBS and detached from the plate using 200 µL trypsin (incubated at 37°C for 5 mins). 800 µL of serum containing media was then added to the cell plate and mixed with the supernatant. Cells were then centrifuged at 400 g for 5 mins. Cells were then resuspended in 500 µL of 1X Annexin V Binding Buffer and then stained with 5 µl of Annexin V-FITC and 5 µL propidium Iodide. Cells were analysed on the BD LSRFortessa™ (Ex=488 nm, Em=530 nm) using the FACSDiva software. Data analyses were then performed using the FlowJo software. An unstained control was used to set voltages of fluorescence channel 1 (FL1, Annexin V-FITC) and fluorescence channel 2 (FL2, propidium iodide). Cell debris was characterised by low forward scatter and side scatter and were excluded from analysis. Single stained controls were also used to compensate for spectral overlap. The percentage of events in the each of the 4 quadrants were recorded for analysis (**Table 2.2**).

Table 2.2 Analysis of apoptosis measurements. Classification of events captured via flow cytometry based on positive staining of FITC and PI. The percentage of events were combined to produce total apoptotic events at each time point.

Annexin V-FITC	Propidium Iodide	Apoptotic Classification
-	-	Live cells
+	-	Early Apoptosis
+	+	Late Apoptosis
-	+	Necrosis

2.9 Mitochondrial Hydroxyl Radical Detection

The Mitochondrial Hydroxyl Radical Detection Assay Kit (ab219931) (Abcam, UK) was utilised to detect intracellular hydroxyl radical (OH·) in live cells. Cells were seeded in 96-well plates at 1 x 10^4 cells/90 µL per well and left to adhere for 24 hrs. After 24 hrs, cells were treated as per conditions above. Treatment was then removed and 100 µL/well of OH580 Stain Working Solution (25 µL of 250X OH580 Stain stock solution in 10 mL Assay Buffer) was added to each well and incubated at 37ºC for 1 hr in the dark. Cells were then washed 2-3 times with DPBS before the addition of 100 µL Assay Buffer to each well. Intracellular hydroxy radical was then measured using fluorescence at Ex/Em= 540/590 nm by FLUOstar OPTIMA (Jencons-PLS, UK). Data is presented as percentage change from the control.

2.10 Measurement of Mitochondrial Membrane Potential

The TMRE-Mitochondrial Membrane Potential Assay Kit (ab113852) (Abcam, UK) was used to quantifying changes in mitochondria membrane potential in live cells by flow cytometry. 3 x 10^5 cells were seeded in 12-well plates overnight and the following day treated as described above. Cells were then detached with trypsin and resuspended in media prior to staining. FCCP was added to appropriate control cell samples and incubate for 10 mins. Cells were then stained with TMRE working solution (200 nM) for 15 mins and analysed on the BD LSRFortessa™ (Ex=488 nm, Em=575 nm) using the FACSDiva software. Data analyses were then performed using the FlowJo software.

2.11 Measurement of Mitochondrial Superoxide

The MitoSOX™ Assay Kit (Invitrogen, UK) was used to quantifying changes in mitochondrial superoxide production. Cells were seeded in 96-well plates at 1 x 10^4 cells/200 µL per well and left to adhere for 24 hrs. After 24 hrs, cells were treated as per conditions above. Treatment was then removed and 100 µL/well of MitoSox Red Dye (5 µM) was added to each well and incubated at 37ºC for 15 mins in the dark. Mitochondrial superoxide production was then measured using fluorescence at Ex/Em= 396/610 nm by FLUOstar OPTIMA (Jencons-PLS, UK). Data is presented as percentage change from the control.

2.12 Measurement of Genome Damage

The cytokinesis-block micronucleus cytome assay was performed as described by Michael Fenech (Fenech, 2007) to analyse measures of genome damage and chromosomal instability. In this assay, 1 x 10^5 cells were seeded in T25 flasks and left to adhere overnight, and the following day treated with varying concentrations of ethanol as described above. Cells were then treated with Cytochalasin B for 24 hrs prior to their fixation. Following this, cells were then detached from flasks using trypsin and centrifuged at 400 g before the supernatant was discarded and replaced with 7 mL prewarmed 0.075 M potassium chloride and incubated at 37°C for 7 mins. Cells were then centrifuged and 5 mL fixative (methanol:acetic acid (3:1)) was added. For analysis, cells were centrifuged and resuspended in 500 µL cold fixative and dropped onto microscope slides and allowed to air dry. One dry, slides were stained with DAPI (4′,6-diamidino-2-phenylindole) and analysed at 100x under the fluorescence microscope (Olympus BX41). Slides were also stained with

5% Giemsa for 7 min and washed twice with distilled water then mounted with Distyrene Plasticizer Xylene. Giemsa-stained slides were imaged at 40x on a light microscope (Olympus) by Evrim Aslan Kaya. The number of micronuclei, nucleoplasmic bridges, and nuclear buds were scored from 100 binucleated cells.

Objective 3

To determine whether oxidative damage could be reversed or reduced, VL-17A cells were treated with antioxidant compounds and nanoformulations (Zupančič et al., 2014; Mursaleen, Somavarapu and Zariwala, 2020), at differing concentrations and time points as either a pre-treatment or, co-treatment. To evaluate the protective effects of these products, cells were assessed as described in **Objectives 1 and 2**.

2.13 Preparation of antioxidant nanoformulations

All nanoformulations were prepared using a modified thin-film hydration method at The School of Pharmacy, University College London by Dr Satyanarayana Somavarapu and Stefanie Chan. Nanocarrier polymers (100 mg) such as DSPE-PEG were dissolved in 10 mL of methanol as well as the appropriate antioxidant compounds (10 mg) (curcumin, ascorbyl palmitate (AP)). Nanoformulatioms were formulated as 100% curcumin DSPE-PEG and 90% curcimin DSPE-PEG, 10% AP. A rotary evaporator (Hei-VAP Advantage Rotary Evaporator, Germany) was then used to evaporate the methanol (200 rpm and 80°C), under vacuum. Once a thin film was achieved it was then hydrated with 10 mL of distilled Milli-Q water and mixed at 80°C for 1-2 min

then sonicated for a further 1 min. The solution was then filtered through a sterile 0.45 μm filter to remove any unloaded antioxidants.

2.14 Size and surface charge of nanoformulations

The size and surface charge of nanoformulations were measured by dynamic light scattering (DLS) as Z_{Ave} hydrodynamic diameter, polydispersity index (PDI) and zeta potential (§), using the Zetasizer Nano ZS (Malvern Instruments, UK) at The School of Pharmacy, University College London by Stefanie Chan. 1 mL of the nanoformulated sample was pipetted into the zeta potential DTS1070 folded capillary cell (Malvern Panalytical, UK). Zeta potential was calculated via electrophoretic mobility using Malvern data analysis software following the Helmholtz-Smoluchowski equation (Chan et al., 2023)

2.15 Determination of drug loading and encapsulation efficiency

Drug loading and encapsulation efficiency of nanoformulations was measured by UV-Visible spectroscopy using free drug calibration curves. A 1:1 ratio of methanol and water were added to dissolve the carrier, allowing drug release, and enabling measurement of a theoretical concentration of each drug. The percentage of drug loading and encapsulation efficiency were calculated using the following equations:

$$Drug\ loading\ (\%) = \frac{total\ weight\ of\ entrapped\ drug}{total\ weight\ of\ all\ raw\ materials} X\ 100$$

$$Encapsulation\ efficiency\ (\%)$$

$$= \frac{(total\ concentration\ of\ drug - concentration\ of\ untrapped\ drug)}{total\ concentration\ of\ drug}\ X\ 100$$

2.16 Assessing the therapeutic potential of nanoformulations

As described previously, VL-17A cells were used to create an *in vitro* model of ALD and iron overload. As in **Section 2.1** and **Section 2.3**, cells were grown in DMEM until 70% confluence then detached from the surface of the flasks via trypsinisation and seeded into 96-well plates at (1 x 10^4 cells/ 200 µL DMEM per well). Cells were pre-treated for 3 hrs with either free curcumin or nanoformulated curcumin, as well as the corresponding unloaded, blank formulations (DSPE-PEG carriers). After pre-treatment with formulations, cells were also treated with ethanol and iron as described in **Section 2.3** and the therapeutic potential of nanoformulations was assessed via MTT and DCFDA assays (previously described in **Section 2.4** and **Section 2.5**). DMEM only, ethanol only and iron only, without any pre-treatments of nanoformulations, were used as corresponding controls. Data is presented as percentage from control.

2.17 Statistical Analysis

Statistical analysis was completed using GraphPad Prism, Version 9.5.1 (San Diego, USA). Differences between treatment groups were analysed using one-way analysis of variance (ANOVA). Nanoformulation data, with two independent variables was analysed using two-way ANOVA. Statistical analysis was followed by Tukey's multiple comparisons post hoc test. Data is

expressed as mean + standard error of the mean (SEM) and P values ≤ 0.05 were considered statistically significant.

CHAPTER 3 THE EFFECT OF ETHANOL EXPOSURE ON LIVER INJURY, OXIDATIVE STRESS AND MITOCHONDRIAL FUNCTION

Description of Chapter

This chapter focuses on oxidative stress and mitochondrial function of HepG2 (VL-17A) cells treated with ethanol. Parameters of oxidative stress and mitochondrial function have not been well characterised in a cell model overexpressing both CYP2E1 and ADH, alcohol metabolising enzymes. Therefore, this chapter aims to establish an *in vitro* model of ALD to elucidate the mitochondrial and inflammatory mechanisms involved in ALD investigating parameters of oxidative stress and mitochondrial function.

3.1 Introduction

Oxidative stress is defined as an imbalance in production and elimination of ROS as well as a reduction in the production of antioxidants. As described previously in **Chapter 1**, oxidative stress and liver injury have widely been implicated in response to chronic ethanol exposure. The excessive generation of ROS plays a central role in the progression of ALD via mediation of the inflammatory response and direct liver damage.

A mechanism for the overproduction of ROS is due to alcohol metabolism by ADH and CYP2E1, and resultant acetaldehyde formation. During chronic ethanol consumption accumulation of CYP2E1 molecules occurs causing an increase in the generation of acetaldehyde and ROS. The role of CYP2E1 in progression of disease and liver injury has been extensively studied in HepG2 cells. Metabolism of alcohol via the ADH pathway causes elevated conversion

of NAD^+ to NADH which results in leakage of electrons, which in turn, causes overproduction of ROS (Petagine, Zariwala and Patel, 2021). ROS formed during alcohol metabolism can interreact with lipid molecules in cell membrane causing lipid peroxidation which can generate reactive metabolites such as malondialdehyde and 4-hydroxy-2-nonenal (Ayala, Muñoz and Argüelles, 2014; Tan et al., 2020). Due to their highly reactive nature, these metabolites can interact with other proteins and molecules forming adducts, thought to be a central step to the development of liver injury and can trigger an inflammatory response (Tuma, 2002).

Changes in mitochondrial architecture, morphology and function, including enlargement and structural changes have been documented as a hallmark in ALD (Gordon, 1984; Nassir, 2014). Mitochondria play an important role in energy generation, metabolism, and cell fate, therefore, understanding the changes to mitochondria caused by alcohol are important for the pathogenesis of disease and may also be important for potential future therapeutics.

Mitochondria play a critical role in energy metabolism and the formation of ROS. Research has shown alcohol can cause mitochondrial damage and dysfunction via oxidative damage, impaired mitochondrial biogenesis, mtDNA damage and apoptosis (Abdallah and Singal, 2020). Studies have also shown that chronic alcohol consumption impairs hepatic mitochondrial oxidative phosphorylation via the suppression of respiratory complex subunits such as NADH dehydrogenase (Complex I), cytochrome b–c1 (Complex III), and cytochrome oxidase (Complex IV), as well as the ATP synthase complex (Complex V) (Cunningham, Coleman and Spach, 1990; Venkatraman et al.,

2004). Alcohol can also increase the activation of the mitochondrial permeability transition pore due to dysregulated fatty acid metabolism caused by reactive lipid species such as 4-hydroxy-2-nonenal (García-Ruiz, Kaplowitz and Fernandez-Checa, 2013). Enhanced levels of Complex I, IV, V have also been reported to increase following chronic alcohol exposure (Han et al., 2012). In addition, excessive alcohol intake in chronic models has shown decreases in mitochondrial maximal oxygen consumption rate which can render hepatocytes susceptible to liver injury (Zelickson et al., 2011). Chronic alcohol exposure in rats has also shown damage to mitochondria leading to mitochondrial depolarisation and mitochondrial permeability transition which further exacerbates disease state (Hoek, Cahill and Pastorino, 2002).

Apoptosis and hepatocyte death have been documented in the progression of ALD. Alterations in mitochondria impairing their function may promote apoptosis, contributing to the pathogenesis of disease (Hoek, Cahill and Pastorino, 2002). Oxidative stress caused by consumption of alcohol causes hepatic apoptosis as well as inflammatory mediators such as ROS, lipopolysaccharide and TNF-α, activating both the intrinsic and extrinsic pathways. Although changes in hepatic apoptosis and alterations in mitochondrial respiration have been linked to the progression of ALD, further investigation is required to establish a comprehensive understanding of their involvement in the pathogenesis of disease.

Therefore, *in vitro* models of alcohol exposure are useful to gain wider understanding into the mechanisms behind liver injury. To study the chronic effects of alcohol consumption VL-17A cells, which overexpress both ADH and

CYP2E1, were utilised to research hepatic oxidative damage over a 72-hr period with the aim to first define a model of liver injury.

3.2 Aims and Objectives

The primary aim of this chapter was to investigate and characterise the effect of varying concentrations of ethanol on liver injury, oxidative stress, mitochondrial function, and apoptosis in VL-17A cells. Specific research objectives were to:

1. Characterise the effect of ethanol on liver injury by measurement of cell viability and oxidative stress.
2. Assess the effect of ethanol treatment on apoptosis.
3. Characterise the effect of ethanol on mitochondrial function measured by oxygen consumption, mitochondrial ROS, and mitochondrial membrane potential.
4. Investigate differences in genome damage after treatment with varying concentrations of ethanol.

3.3 Results

3.3.1 Effect of ethanol exposure on cell viability

To assess the role of ethanol in inducing cell toxicity VL-17A cells were exposed to varying concentrations of ethanol (100 mM to 400 mM) and cell viability was assessed using the MTT assay over a 72-hr period to model chronic liver injury. At 24 hrs there were no significant changes in cell viability after exposure with ethanol at all concentrations (**Figure 3.1**). On the other hand, at 48 hrs, significant changes in cell viability were observed. An 18% decrease in cell viability was observed after 300 mM ethanol exposure at 48 hrs. Also 48 hrs after ethanol exposure, 350 mM ethanol led to a significant 31% decrease in viability ($p=0.0005$) and 400 mM also led to a significant 37% reduction ($p<0.0001$) in viability (**Figure 3.1**). Amongst all time points, ethanol toxicity was most apparent after 72 hrs in comparison to both 24 and 48 hrs. Concentrations of alcohol treatment from 300 mM and above led to significant changes. The 300 mM ethanol treatment led to a 27% reduction in cell viability ($p= 0.0438$) and a significant 50% decrease ($p<0.0001$) in viability was observed after 350 mM ethanol exposure. The 400 mM ethanol treatment produced the most toxic effect, and a 63% decrease ($p<0.0001$) was observed after 72 hrs ethanol exposure (**Figure 3.1**).

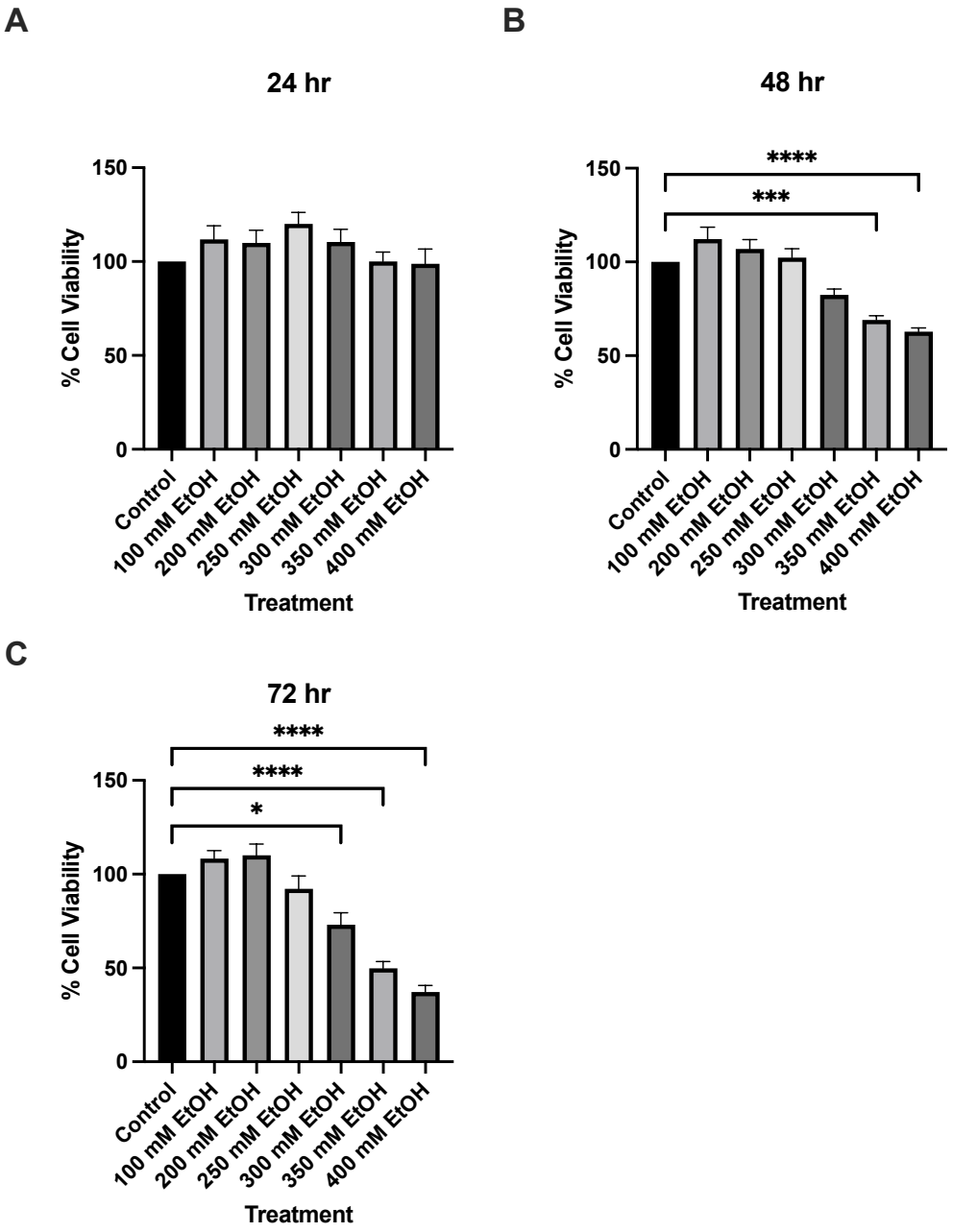

Figure 3.1 The effect of ethanol exposure on cell viability over a 72-hr period. A) percentage of cell viability at 24 hrs, B) percentage of cell viability at 48 hrs and C) percentage of cell viability at 72 hrs. Cells were seeded in 96-well plates and treated with 100 mM, 200 mM, 250 mM, 300 mM, 350 mM and 400 mM ethanol. Viability of cells was determined by the MTT assay and measured at 24, 48 and 72 hrs. Data is presented as percentage from the control. Results presented as mean ± SEM (n = 9) * $P \leq 0.05$, *** $P \leq 0.001$, **** $P \leq 0.0001$.

3.3.2 Effect of ethanol exposure on ROS production

Exposure at 30 mins led to a 13% decrease in ROS production with 200 mM ethanol administration, a 25% increase after treatment with 300 mM and a 53% increase ($p=0.0027$) after treatment with 350 mM ethanol. At 1 hr, decreases in ROS production were observed whereby 200 mM ethanol led to a 41% decrease, 300 mM led to a 14% decrease and 350 mM ethanol led to a 39% decrease. At 1.5 hrs, no statistical changes were observed, however, ROS increased by 26% when treated with 350 mM ethanol. Whereas, at 2 hrs a similar pattern occurs to 1 hr, whereby 200 mM ethanol led to a 26% decrease and 350 mM ethanol led to a 33% decrease in ROS. At 6 hrs, no changes were observed with 200 mM and 300 mM ethanol treatment, however, 350 mM ethanol led to a 39% decrease ($p=0.0220$) in ROS (**Figure 3.2**)

At 24 hrs, no significant changes were observed, although, ROS accumulation increased by 37% after 300 mM ethanol exposure (**Figure 3.3**). At 48 hrs ROS production decreased dose-dependently, at 200mM ethanol ROS decreased by 16% ($p=0.0416$), at 300 mM alcohol ROS production significantly decreased by 37% ($p<0.0001$) and at 350 mM, ROS accumulation also significantly decreased by 54% ($p<0.0001$), respectively (**Figure 3.3**). At 72 hrs, a different pattern occurred whereby ROS increased significantly. After 200 mM ethanol exposure ROS increased by 42% and at 300 mM ROS increased by 96% ($p=0.0005$) (**Figure 3.3**).

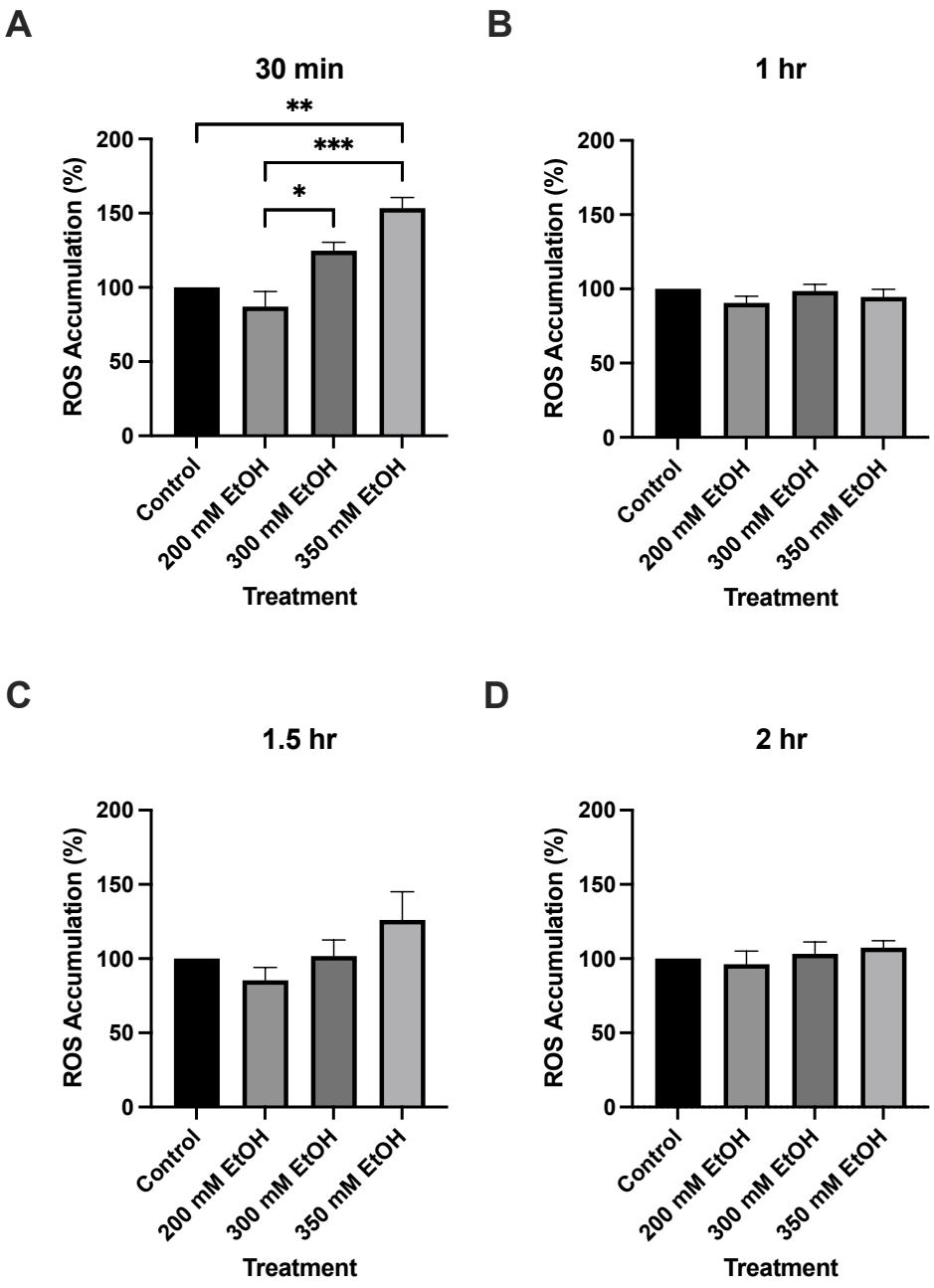

Figure 3.2 The effect of alcohol exposure on ROS accumulation over a 6-hr period. A) percentage of ROS accumulation at 30 mins, B) percentage of ROS accumulation at 1 hr, C) percentage of ROS accumulation at 2 hrs and D) percentage of ROS accumulation at 6 hrs. Cells were seeded in 96-well plates and treated with 200 mM, 300 mM, and 350 mM ethanol. ROS accumulation was determined by the DCFDA assay and measured using fluorescence at 30 mins, 1 hr, 2 hrs and 6 hrs. Data is presented as percentage from the control. Values are the mean ± SEM (n = 3-6). * $P \leq 0.05$, ** $P \leq 0.01$ *** $P \leq 0.001$.

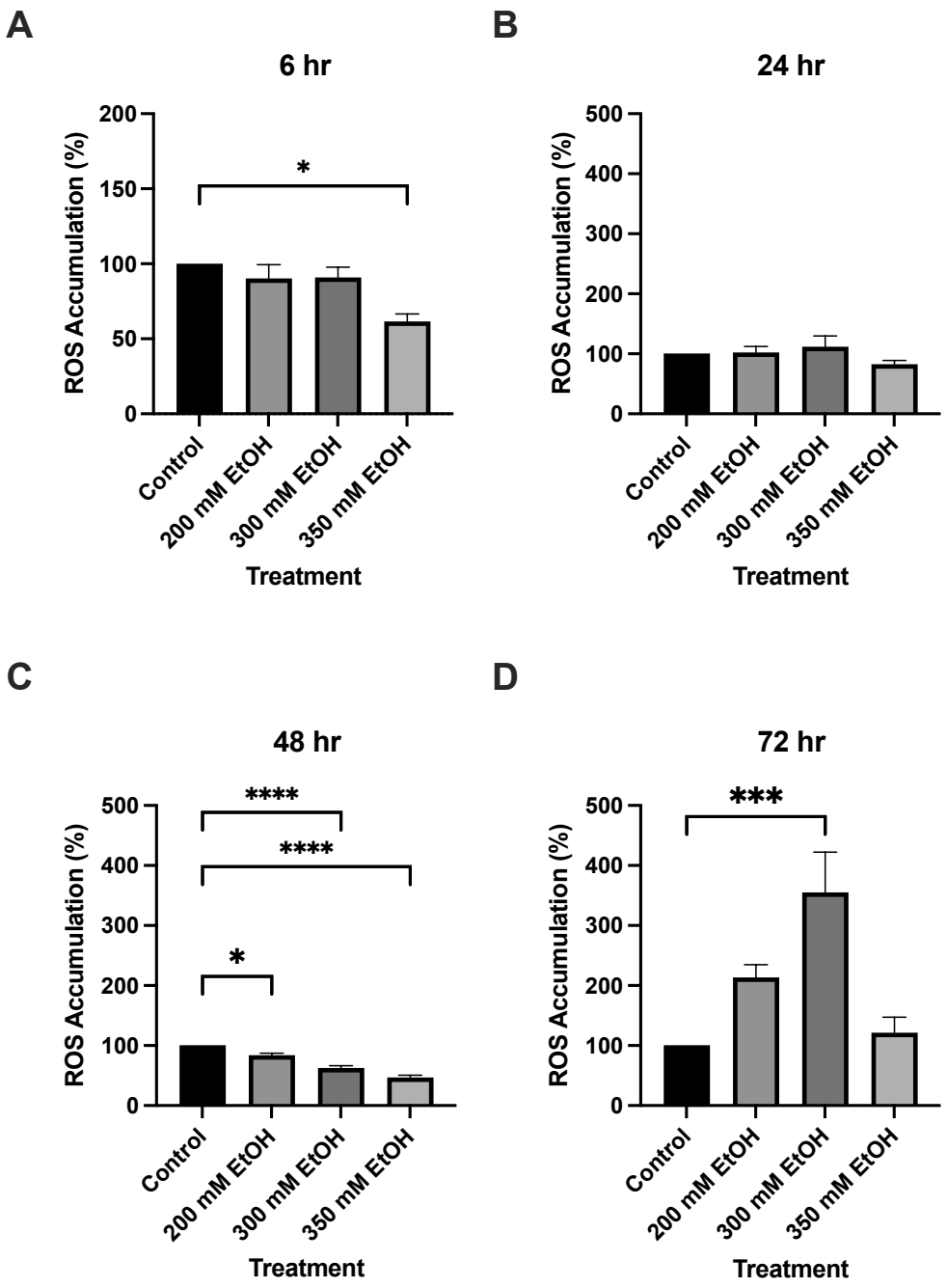

Figure 3.3 The effect of alcohol exposure on ROS accumulation over a 72-hr period. A) percentage of ROS accumulation at 24 hrs, B) percentage of ROS accumulation at 48 hrs and C) percentage of ROS accumulation at 72 hrs. Cells were seeded in 96-well plates and treated with 200 mM, 300 mM, and 350 mM and ethanol. ROS accumulation was determined by the DCFDA assay and measured using fluorescence at 24, 48 and 72 hrs. Data is presented as percentage from the control. Values are the mean ± SEM (n = 6). * P ≤ 0.05, ** P ≤ 0.01 *** P ≤ 0.001, **** ≤ 0.0001.

3.3.3 Effect of ethanol exposure on apoptosis

Oxidative stress due to excessive alcohol consumption as well as mitochondrial alterations may promote apoptosis and contribute to the pathogenesis of ALD. To assess the quantity of apoptotic cells, VL-17A cells were stained with FITC and PI and apoptosis was measured using flow cytometry. Cells in early apoptosis were defined as FITC positive and PI negative. The late stage of apoptosis was defined as both FITC and PI positive. At 24 hrs across exposure to all ethanol concentrations the percentage of cells in early and late apoptosis remained low with no significant differences (**Figure 3.4**). At 48 hrs, the percentage of cells in early apoptosis increased significantly. The percentage of cells in early apoptosis after 350 mM ethanol reached 20% ($p=0.0313$). No significant changes were observed in late apoptosis at 48 hrs. At 72 hrs, overall, the percentage of cells in apoptosis was highest, and 200 mM ethanol caused early apoptosis in 50% of cells, 48% at 300 mM ethanol and 36% at 350 mM ethanol. Late apoptosis reached significance in the 350 mM ethanol treated group whereby 44% of cells were in late apoptosis ($p=0.0153$) (**Figure 3.4**).

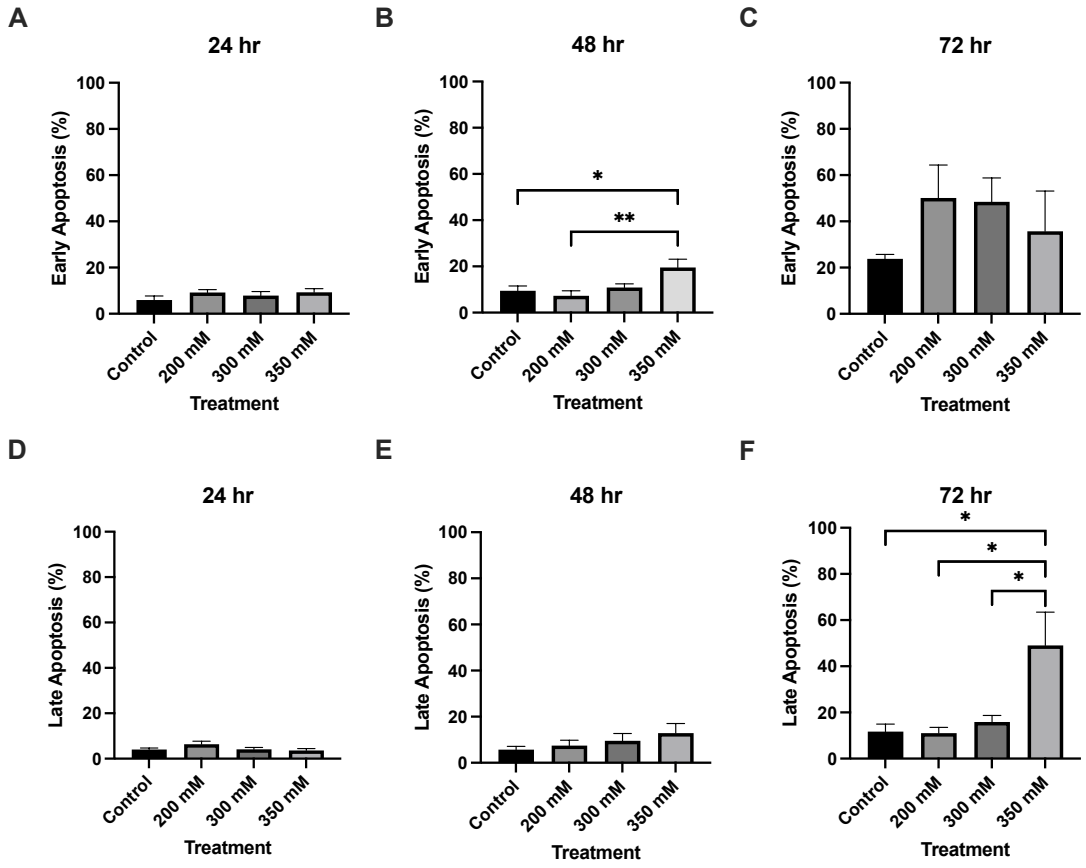

Figure 3.4 The effect of ethanol exposure on apoptosis over a 72-hr period. A) percentage of cells in early apoptosis at 24 hrs, B) percentage of cells in early apoptosis at 48 hrs, C) percentage of cells in early apoptosis at 72 hrs, D) percentage of cells in late apoptosis at 24 hrs, D) percentage of cells in late apoptosis at 48 hrs and E) percentage of cells in late apoptosis at 72 hrs. Cells were seeded in 12-well plates and treated with 200 mM, 300 mM and 350 mM ethanol. Apoptosis was assessed at 24 hrs, 48 hrs and 72 hrs using the Annexin VI kit and measured using flow cytometry. Data is presented as percentage of positive cells. Results presented as mean ± SEM (n = 3-10). * $P \leq 0.05$, ** $P \leq 0.01$.

3.3.4 Effect of ethanol exposure on mitochondrial hydroxyl radical production

The hydroxy radical (HO·) is a highly reactive ROS and a by-product of oxidative metabolism. Ethanol metabolism via CYP2E1 leads to ROS generation hydroxyl radicals which can lead to oxidative damage and cell death. The mitochondrial HO· detection assay was used to detect intracellular hydroxyl radicals. This data shows that there is an increase in mitochondrial HO· radicals across the 72-hr period which increases by up to 26% after ethanol exposure (**Figure 3.5**). At 48 hrs, significant differences were observed between control cells and 300 mM ethanol treatment ($p=0.0264$).

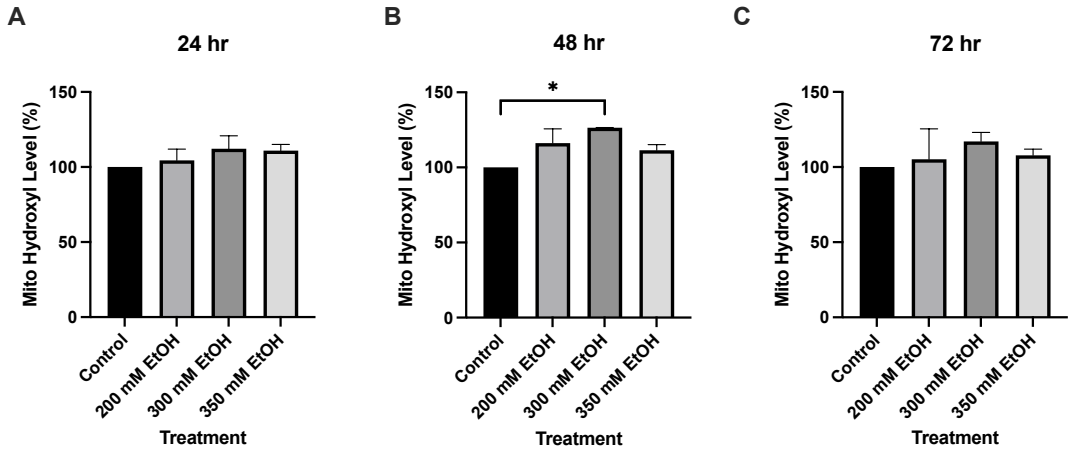

Figure 3.5 The effect of ethanol exposure on mitochondrial hydroxy radical formation over a 72-hr period. A) mitochondrial hydroxyl levels at 24 hrs, B) mitochondrial hydroxyl levels at 48 hrs and C) mitochondrial hydroxyl levels at 72 hrs. Cells were seeded in 96-well plates and treated with 200 mM, 300 mM, and 350 mM ethanol. Mitochondrial hydroxyl levels were assessed at 24 hrs, 48 hrs and 72 hrs using the Mitochondrial Hydroxyl Radical Detection Assay Kit (ab219931). Data is presented as percentage from control. Results presented as mean ± SEM (n = 3). * $P \leq 0.05$, ** $P \leq 0.01$.

3.3.5 Effect of ethanol exposure on mitochondrial oxygen consumption rate

Mitochondria are central to the formation of ROS and energy metabolism within the cell. Recent studies have found that alcohol consumption can alter mitochondrial morphology and function which is caused by changes or impairment of mitochondrial biogenesis, mtDNA damage, lipid accumulation, oxidative damage, and cell death (Abdallah and Singal, 2020). Therefore, pinpointing changes in mitochondrial function are essential to the understanding of ALD pathogenesis. The respiratory function of mitochondria was evaluated by measuring the oxygen consumption rate (**Figure 3.6**). No significant changes were observed in oxygen consumption rate at both 24 hrs and 48 hrs when compared to the control. Although it is evident that 350 mM ethanol caused the largest reductions in oxygen consumption rate, however, this did not reach statistical significance when compared against the control.

At 24 hrs, basal respiration was decreased by 26% at 200 mM ethanol and 62% at 350 mM ethanol when compared to control DMEM. Proton leak and maximal respiration were decreased by 56% and 59% respectively, by 350 mM ethanol. Non-mitochondrial oxygen consumption also decreased dose dependently, 13% by 200 mM ethanol, 51% by 300 mM ethanol, and 59% by 350 mM ethanol. ATP was also decreased by 64% when treated with 350 mM ethanol (**Figure 3.7**) Although no significant differences were observed between ethanol treatment and control cells, significance was observed between 300 mM ethanol and 350 mM ethanol in basal respiration ($p=0.0379$) and maximal respiration ($p=0.0286$).

At 48 hrs, basal respiration was decreased by 24% at 200 mM ethanol, and 2% at 350 mM ethanol when compared to control DMEM. Basal respiration increased by 20% when treated with 300 mM ethanol. Proton leak and maximal respiration were decreased by 42% and 26% respectively, by 200 mM ethanol. They were also decreased by 350 mM ethanol which caused a 6% decrease in proton leak and 15% decrease in maximal respiration. Spare respiratory capacity was also decreased by 23% and 16% respectively when treated by 300 mM and 350 mM ethanol. Non-mitochondrial oxygen consumption increased at 48 hrs, by 10% by 200 mM ethanol, 37% by 300 mM ethanol, and 10% by 350 mM ethanol. ATP was also decreased by 31% when treated with 200 mM ethanol and 64% when treated with 350 mM ethanol (**Figure 3.8**).

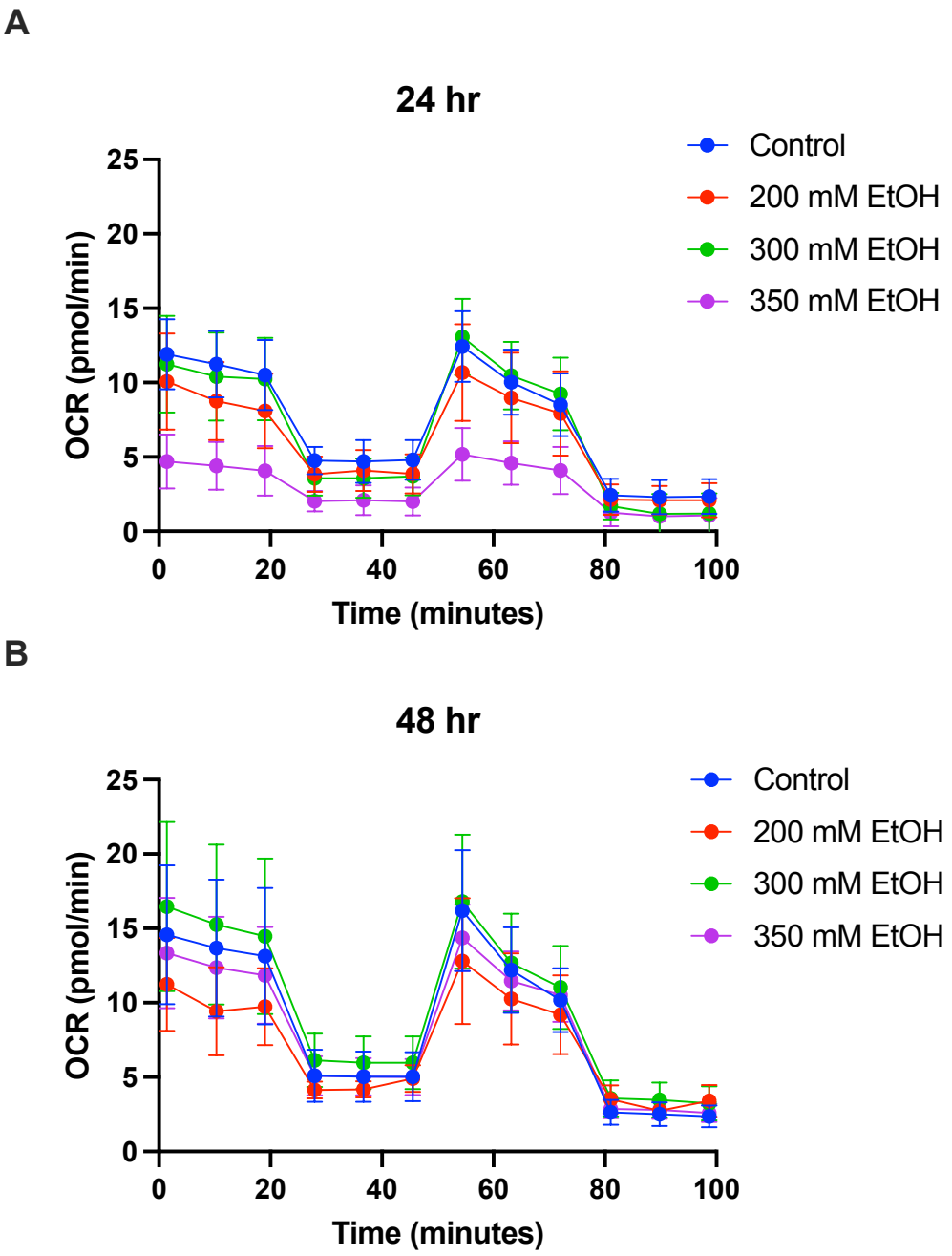

Figure 3.6 Mitochondrial oxygen consumption rate and ethanol exposure at 24 hrs and 48 hrs. A) oxygen consumption rate at 24 hrs and B) oxygen consumption rate at 48 hrs. Cells were seeded in 24-well plates and treated with 200 mM, 300 mM, and 350 mM ethanol. Oxygen consumption rate was assessed over 48 hrs using the Seahorse XF24 analyser. Results presented as mean of replicates ± SEM (n = 3). OCR: oxygen consumption rate.

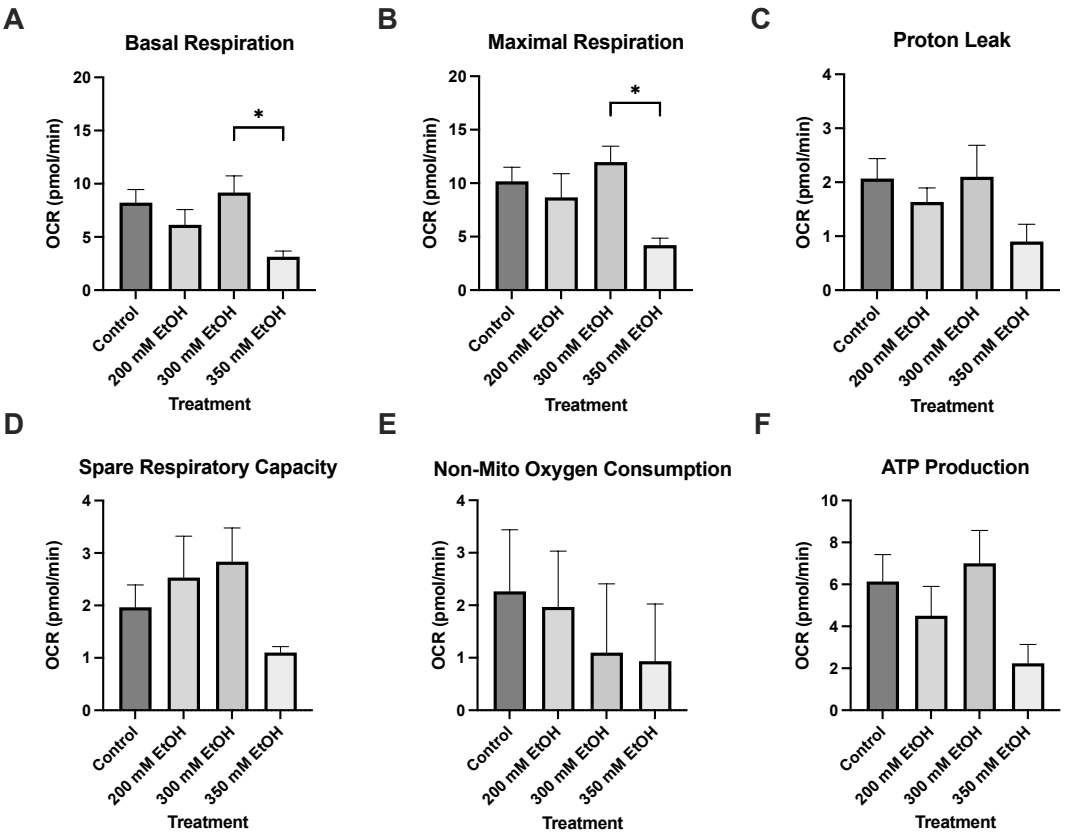

Figure 3.7 The effect of ethanol on mitochondrial oxidative phosphorylation parameters at 24 hrs. A) Basal respiration, B) maximal respiration, C) proton leakage, D) spare respiratory capacity, E) non-mitochondrial oxygen consumption and F) ATP production. Cells were seeded in 24-well plates and treated with 200 mM, 300 mM, 300 mM, and 350 mM. Oxygen consumption rate was assessed at 24-hrs using the Seahorse XF24 analyser. Results presented as mean of replicates ± SEM (n = 3). OCR: oxygen consumption rate. * $P \leq 0.05$.

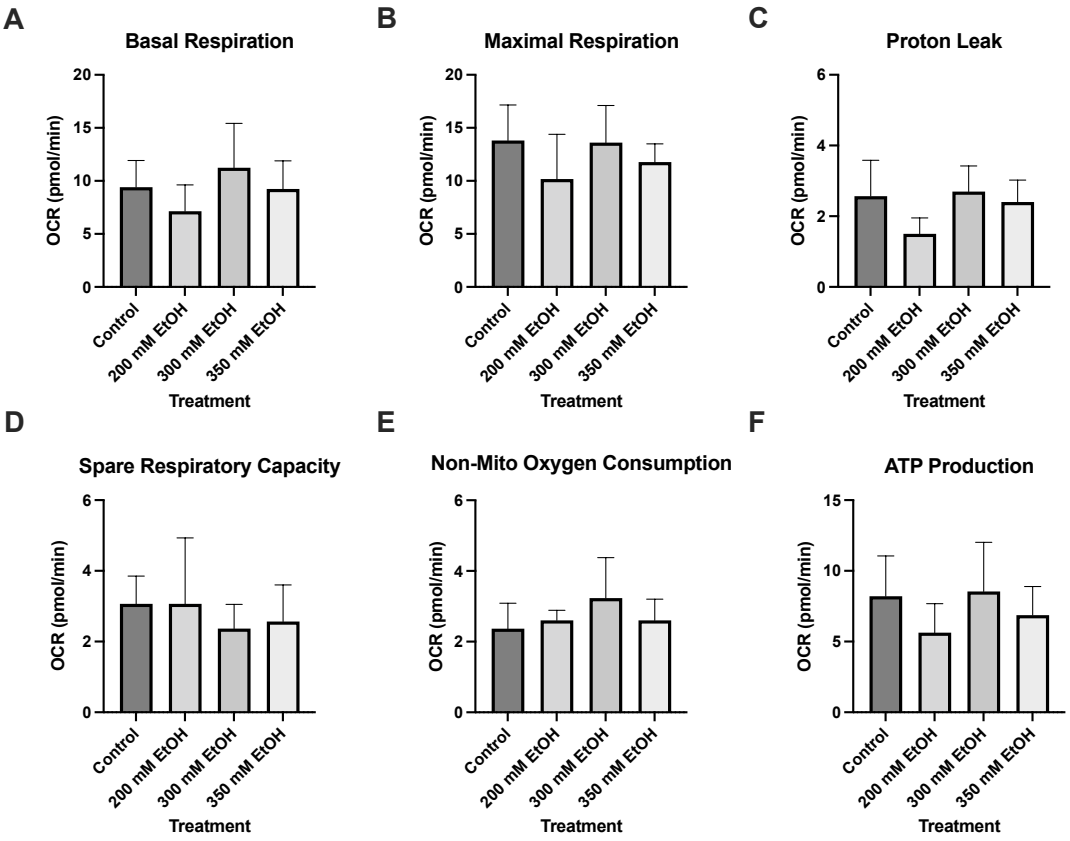

Figure 3.8 The effect of ethanol on mitochondrial oxidative phosphorylation parameters at 48 hrs. A) Basal respiration, B) maximal respiration, C) proton leakage, D) spare respiratory capacity, E) non-mitochondrial oxygen consumption and F) ATP production. Cells were seeded in 24-well plates and treated with 200 mM, 300 mM, 300 mM, and 350 mM. Oxygen consumption rate was assessed at 48 hrs using the Seahorse XF24 analyser. Results presented as mean of replicates ± SEM (n = 3). OCR: oxygen consumption rate.

3.3.6 Effect of ethanol exposure on mitochondrial membrane potential

The data across all time points shows ethanol treatment causes a dose dependent decrease in mitochondrial membrane potential. At 24 hrs, treatment with 300 mM ethanol caused a 12% decrease and 350 mM ethanol cause a 59% reduction in mitochondrial membrane potential. At 48 hrs, mitochondrial membrane potential continued to decrease, 200 mM ethanol cause a 30% reduction, 300 mM caused a 38% reduction and 350 mM caused a 40% reduction in TMRE mean fluorescence. At 72 hrs a similar pattern occurred whereby 200 mM ethanol caused a 28% decrease; 300 mM caused a 38% decrease ($p=0.0467$), and 350 mM caused a 47% decrease ($p=0.0160$) in TMRE mean fluorescence (**Figure 3.9**).

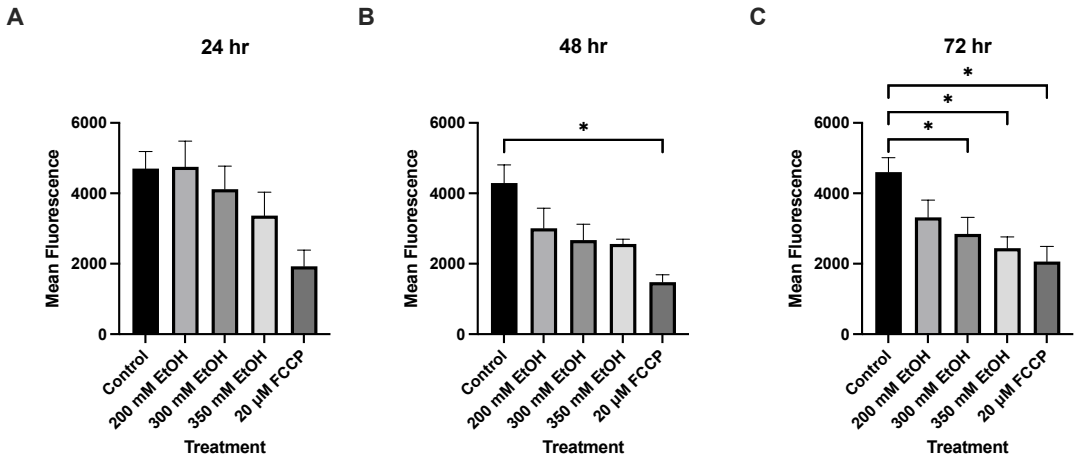

Figure 3.9 The effect of ethanol on mitochondrial membrane potential over a 72-hr period. A) mitochondrial membrane potential at 24 hrs, B) mitochondrial membrane potential at 48 hrs and C) mitochondrial membrane potential at 72 hrs. Cells were seeded in 12-well plates and treated with 200 mM, 300 mM and 350 mM ethanol and mitochondrial membrane potential was measured by TMRE staining using flow cytometry. FCCP (20 μM) was used as a positive control. Data is presented as mean fluorescence values. Results presented as mean ± SEM (n = 3). * $P \leq 0.05$.

3.3.7 Effect of ethanol exposure on mitochondrial superoxide production

Levels of mitochondrial superoxide species (mtROS) were assessed using MitoSOX staining. At 24 hrs 300 mM ethanol led to a small increase (6%) in mtROS at 24 hrs and 350 mM ethanol increased mtROS by 40%, although this did not reach statistical significance. At 48 hrs, 350 mM ethanol also led to a 40% increase. At 72 hrs increases in mtROS were seen in all ethanol treatments whereby 200 mM ethanol led to a 13% increase, 300 mM led to a 47% increase and 350 mM produced a 75% increase in mtROS. Although these results did not produce statistical significance, they suggest mtROS production may increase after chronic ethanol exposure (**Figure 3.10**).

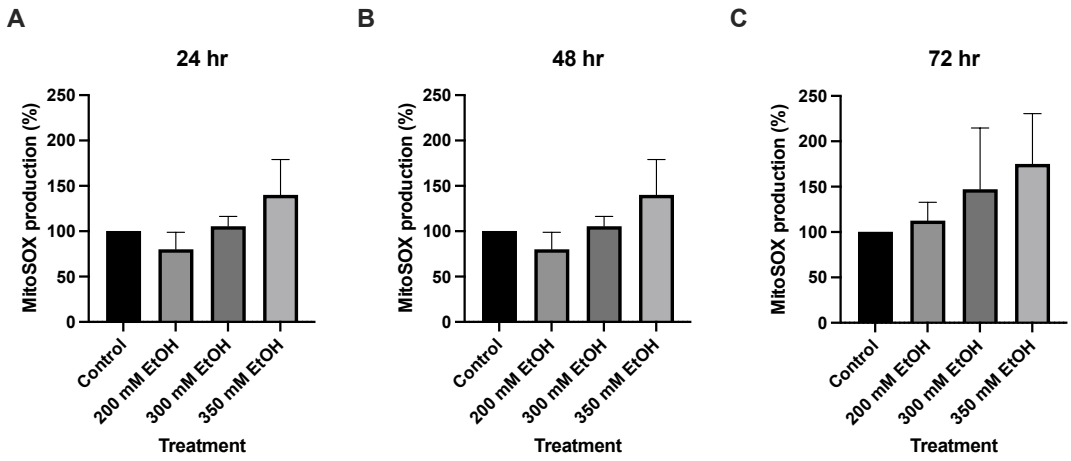

Figure 3.10 The effect of ethanol on mitochondrial superoxide production over a 72-hr period. A) mitochondrial superoxide production at 24 hrs, B) mitochondrial superoxide production at 48 hrs and C) mitochondrial superoxide production at 72 hrs. Cells were seeded in 96-well plates and treated with 200 mM, 300 mM and 350 mM ethanol and mitochondrial superoxide production was measured by using MitoSOX red dye. Data is presented as percentage difference from the control. Results presented as mean ± SEM (n = 3).

3.3.8 Effect of ethanol exposure on measures of chromosomal instability and DNA damage

Levels of chromosomal instability were measured after ethanol treatment including number of micronuclei, number of nucleoplasmic bridges (data not shown for brevity) and number of nuclear buds. Representative images are shown in **Figure 3.11**. Nucleoplasmic bridges were not observed in any treatment across all time points. Interestingly, control cells showed no measured of chromosomal instability across all time points and no micronuclei or nuclear buds were seen. However, preliminary data suggests treatment with ethanol increases measures of chromosomal instability across all time points. Particularly at both 48 hrs and 72 hrs the number of nuclear buds were significantly increased. At 48 hrs, treatment with 300 mM ethanol increased nuclear bud number from 0 to 13 ($p=0.0205$) and treatment with 350 mM ethanol increased from 0 to 16 ($p=0.0097$). Similarly, at 72 hrs, treatment with 300 mM ethanol increased nuclear budding from 0 to 10 ($p=0.0383$) and treatment with 350 mM ethanol increased from 0 to 14 ($p= 0.0136$) (**Figure 3.12**).

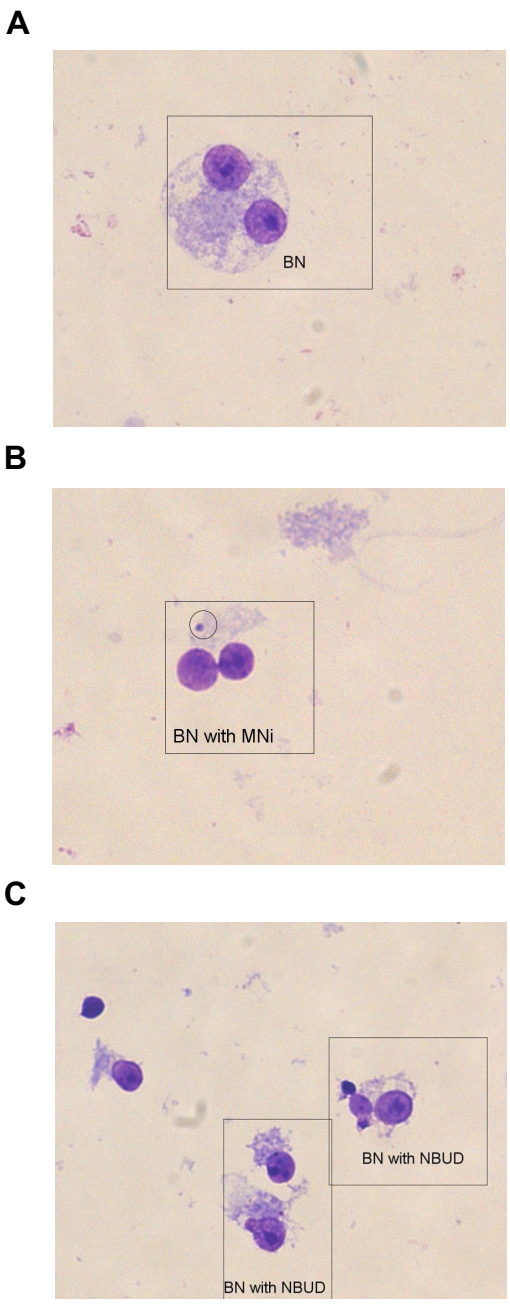

Figure 3.11 Representative analysis of genome damage. A) representative image of binucleated cells, B) representative image of micronuclei and C) representative image of nuclear budding. Cells were seeded in T75 flasks and treated with 200 mM, 300 mM, and 350 mM ethanol. Cells were then fixed and stained on slides using Gimsea. BN: binucleated cell, MNi: micronuclei, NBUD: nuclear budding.

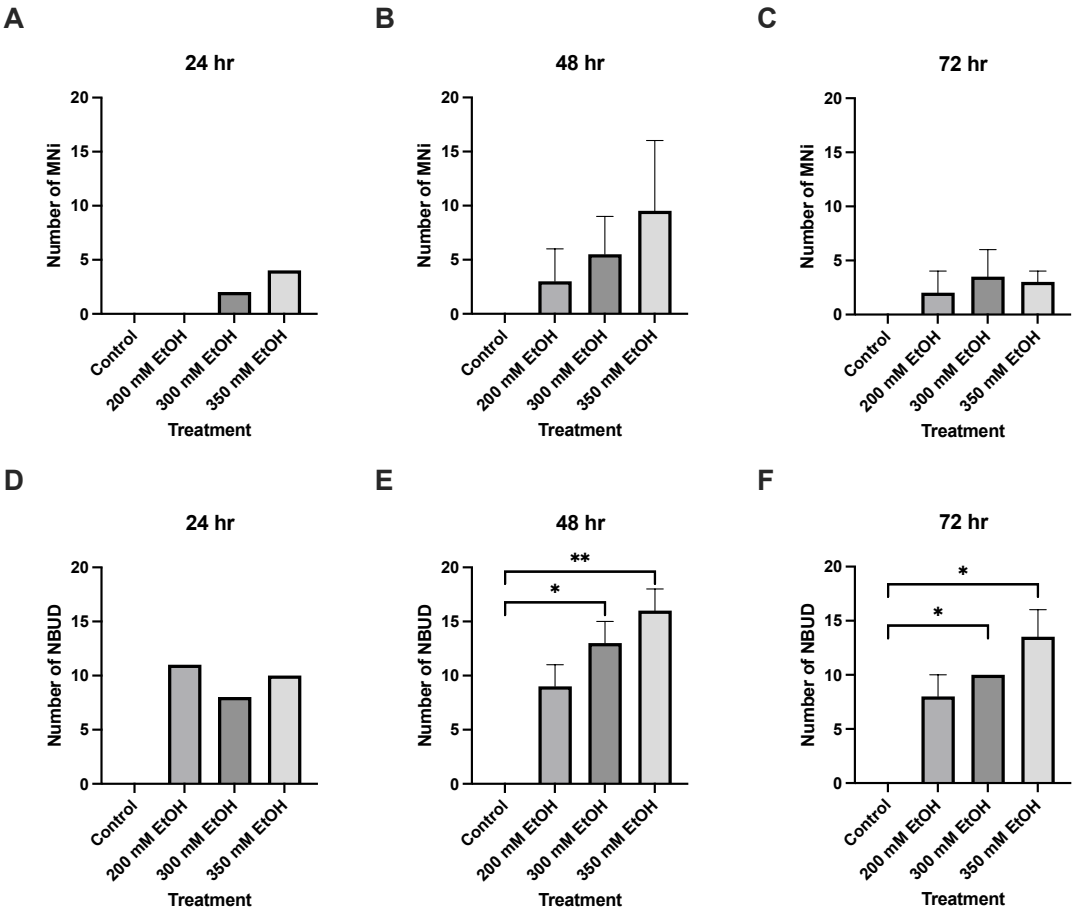

Figure 3.12 Preliminary data showing the effect of ethanol on measures of chromosomal instability over a 72-hr period. A) number of micronuclei at 24 hrs, B) number of micronuclei at 48 hrs, C) number of micronuclei at 72 hrs, D) number of nuclear buds at 24 hrs, E) number of nuclear buds at 48 hrs and F) number of nuclear buds at 72 hrs. Cells were seeded in T75 flasks and treated with 200 mM, 300 mM, and 350 mM ethanol. Cells were then fixed and stained on slides using Gimsea. Data is presented as percentage difference from the control. Results presented as mean ± SEM (n = 1-2). BN: binucleated cell, MNi: micronuclei, NBUD: nuclear budding. * $P \leq 0.05$, ** $P \leq 0.01$.

3.4 Discussion

In this study, VL-17A cells which over-express both alcohol metabolising enzymes CYP2E1 and ADH were used to model ALD. To establish a model of alcohol toxicity and damage in VL-17A cells, varying concentrations of alcohol were studied at different time points. To generate a model of alcohol toxicity a dose response with various concentrations of alcohol treatment was utilised (100 mM - 400 mM). For further experimentation, the concentrations of ethanol for cell treatments were 200 mM, 300 mM, and 350 mM ethanol.

In this study, it was hypothesised ethanol exposure to VL-17A cells will cause high cell toxicity as well as increase ROS production. Although no changes in cell viability were observed at 24 hrs with ethanol alone, at both 48 hrs and 72 hrs ethanol produced significant changes in cell viability with reductions of up to 63% were observed at 72 hrs with 400 mM ethanol exposure. Previous research has shown ethanol administration decreased cell viability dose-dependently, and studies observed 600 mM ethanol treatment reduced cell viability by 51% after 24 hrs (Zhang et al., 2018). In this study, some slight increases were observed at lower concentrations of ethanol, however, at 250 mM ethanol was found to decrease cell viability dose-dependently at 48 hrs and 72 hrs, as determined by MTT assay.

Research has suggested excessive alcohol can impair both the structure and function of mitochondria causing an increase in the production of ROS and cell toxicity. CYP2E1 is induced in response to alcohol consumption which oxidises alcohol to acetaldehyde causing endoplasmic reticulum. In the mitochondria, when ALDH2 further oxidises acetaldehyde into acetate forming NADH again

which later becomes oxidised in the electron transport chain (Osna, Donohue and Kharbanda, 2017). The increase in the conversion of NAD^+ to NADH can also alter the cellular redox status and plays a role in mitochondrial permeability transition. This can cause a leakage of electrons producing ROS and exacerbating disease state and oxidative damage (Zhao et al., 2019; Petagine, Zariwala and Patel, 2021). This study showed at 30 mins there was an increase in ROS production after ethanol treatment with 300 mM and 350 mM ethanol, as well as at 72 hrs with 300 mM ethanol. Although ROS production did not increase with 350 mM ethanol at 72 hrs this may be due to the reduction in viability also observed at this concentration and timepoint.

Apoptosis has been implicated in the pathogenesis of ALD. Research in both *in vitro* and in animal models has shown that alcohol metabolism can induce mitochondrial and endoplasmic reticulum stress, which leads to apoptosis (Petagine, Zariwala and Patel, 2021). Low concentrations of ethanol have been shown to induce apoptosis in HepG2 via activation of the Fas receptor (Castaneda and Rosin-Steiner, 2006). Therefore, the aim was to determine the effect of ethanol exposure on apoptosis in VL-17A cells. In this study, although there were no changes in apoptosis at 24 hrs, at 48 hrs, the percentage of cells in early apoptosis increased significantly. This continued to increase at 72 hrs, whereby, significant increases in late apoptosis were observed. Overproduction of ROS in HepG2 which express CYP2E1 has been shown increase lipid peroxidation and apoptosis (Wu and Cederbaum, 1999). Research suggests chronic alcohol exposure leaves cells more susceptible to apoptosis which has been commonly associated with increased ROS (Rodriguez et al., 2015). This study observed elevated percentages of cells in

apoptosis, suggesting chronic alcohol exposure renders cells more likely to go into apoptosis, however, this may not be associated with increases in ROS. On the other hand, this indicated that apoptosis may also be triggered by other stimuli other than ROS alone as well as cellular stress. For example, *in vivo*, alcohol increases gut permeability and increases levels of endotoxin such as lipopolysaccharide in the liver which activates Kupffer cells producing pro-inflammatory mediators such as TNF-α, and IL-8 which can induce apoptosis (Wang, 2014; Petagine, Zariwala and Patel, 2021). Protein adduct formation in the liver can also activate the immune response inducing IFN-γ and TNF-α which both contribute to activation of the apoptotic pathway and liver injury (Wang, 2014). These results indicate that at 48 hrs, ethanol treatment causes cells to enter early apoptosis whereby their membrane integrity is retained and at 72 hrs, cells enter late apoptosis, suggesting more chronic damage as these cells act like necrotic cells releasing proinflammatory intracellular contents as well as TNF-α, IL-1β, IL-6, and monocyte chemoattractant protein-1, serving as “danger signals” which stimulate inflammation.

Metabolism of ethanol in the liver is known to deplete oxygen, leading to a hypoxic environment and further ROS production in liver cells. The mechanisms behind apoptosis induction after ethanol treatment could be due to antioxidant levels as it is known that ethanol can reduce mitochondrial glutathione (Viña et al., 1980), releasing cytochrome c and other apoptotic proteins leading to downstream activation of the signalling cascade.

Ethanol can cause damage to mitochondria, causing leakage of electrons at complexes I and III in the electron transport chain (Hoek, Cahill and Pastorino, 2002). Oxidative damage and ROS accumulation can occur as complexes I

and III are considered as major sites of superoxide producers (Hoek, Cahill and Pastorino, 2002). Electron transport chain reactions include the generation of superoxide anion radical, which dismutates to form hydrogen peroxide, which can further react to ultimately form the hydroxyl radical (Cadenas and Davies, 2000), a harmful by-product of oxidative metabolism. Preliminary data suggests overall mitochondrial hydroxyl radicals may be higher at 48 hrs and 72 hrs after ethanol treatment, although this did not reach statistical significance.

It is well known that mitochondria play an essential role in hepatic alcohol metabolism. During the metabolism of alcohol oxidative damage may occur in the mitochondria causing mitochondrial dysfunction and damage to the electron transport chain. Hepatocyte mitochondrial dysfunction has both been previously reported in both cellular models on ALD and in human tissue. The metabolism of alcohol has been documented to causes increases in ROS production as well as damage and impaired function of complexes I–V of the electron transport chain as well as a reduction in mitochondrial polarisation ($\Delta\Psi m$) and ATP production. Animal studies have shown that mice fed a high fat diet have reportedly lower complex IV activity as well as dysfunctional mitochondrial membrane potential (Mantena et al., 2009). In this study, VL-17A cells treated with alcohol have displayed a dose dependent decrease in mitochondrial membrane potential following exposure with ethanol. This may be due to increases in hydroxyl radicals, particularly mitochondrial hydroxyl radicals which cause an increase in mitochondrial membrane permeability which leads to the loss of membrane potential and an induction in the opening of the mitochondrial permeability transition pore, which has also been linked

to oxidative stress and apoptosis. Chronic ethanol dosing has been shown to induce formation of megamitochondria, a key histological finding in ALD disease progression, and this may occur due to the increase in membrane permeability as well as loss of membrane potential (Manzo-Avalos and Saavedra-Molina, 2010). The loss of membrane potential may also provide an explanation to the differences in apoptosis. Loss of mitochondrial membrane potential is an indication of bioenergetic stress which in turn leads to induction of apoptotic factors resulting to programmed cell death. In this study, membrane potential decreased dose dependently after ethanol administration which was most significantly reduced at 72 hrs. The increases in early and late apoptosis at 48 hrs and 72 hrs after ethanol treatment may be induced by the reduction in membrane potential. Therefore, as the mitochondrial membrane potential is crucial for the maintenance of mitochondrial function and generation of ATP, ethanol administration causes mitochondrial permeability transition opening, and loss of membrane potential causing subsequent release of cytochrome C and may initiate other downstream signalling and cause a higher induction of apoptosis in VL-17A cells.

It is well known that excessive alcohol consumption causes many pathological factors which contribute to oxidative stress and DNA damage. Excessive alcohol has also been linked to an increased risk of various cancers. Dysfunctional DNA damage can increase chromosomal and genomic instability rendering cells more susceptible to the effects of oxidative stress caused by alcohol and inflammation (Benassi-Evans and Fenech, 2011). Alcohol is thought to induce chromosomal instability including a variety of morphological changes including micronuclei, nuclear budding, anaphase

bridging, and multipolar mitoses (Fenech et al., 2020). Preliminary data in this study shows that treatment with various concentrations of ethanol causes increased numbers of micronuclei and nuclear buds, which were not observed in the control groups. These preliminary results indicate that excessive alcohol treatment may be a probable cause of cancer initiation via the induction of both chromosomal instability and genome damage, which may occur through mechanisms of DNA damage (Benassi-Evans and Fenech, 2011). This may occur due to the toxic by-products of alcohol metabolism such as acetaldehyde, which can bind directly to DNA and cause point mutations (Hyun et al., 2021). Research has shown that ethanol treatment of cells resulted in increases in acetaldehyde-DNA adducts and also activation of breast cancer susceptibility networks (Abraham et al., 2011), as well as observational studies indicating alcohol consumption shortens telomere length (Topiwala et al., 2022). Therefore, further research regarding markers of DNA damage and alcohol warrants further research.

3.5 Conclusion

In this study, VL-17A cells were used as a model to investigate the effects of alcohol exposure on liver cells, with a focus on alcohol-induced toxicity, oxidative stress, apoptosis, mitochondrial dysfunction, and DNA damage. Results show ethanol exposure led to significant cell toxicity, with a dose-dependent reduction in cell viability observed over time. This decrease in viability was particularly pronounced at higher ethanol concentrations, indicating a clear relationship between alcohol dosage and reduction of viability. Results show ethanol exposure led to significant cell toxicity, with a

dose-dependent reduction in cell viability observed over time. This study also presented a dose-dependent decrease in mitochondrial membrane potential, suggesting that alcohol-induced damage to mitochondria can disrupt cellular energy production and contribute to the activation of apoptotic pathways. Furthermore, the study provided preliminary evidence of chromosomal instability and genome damage in ALD as increased numbers of micronuclei and nuclear buds were observed in cells treated with ethanol. In conclusion, this study highlights the multifaceted impact of alcohol on liver cells. Further research in this area is warranted to enhance understanding of the mechanisms underlying these effects and to explore potential interventions to mitigate the detrimental consequences of alcohol consumption on cellular health.

CHAPTER 4 THE EFFECT OF ETHANOL AND IRON EXPOSURE ON LIVER INJURY, OXIDATIVE STRESS AND MITOCHONDRIAL FUNCTION

Description of Chapter

This chapter focuses on oxidative stress and mitochondrial function of HepG2 (VL-17A) cells treated with combinations of both ethanol and iron. Iron overload is a common feature of ALD causing liver damage, oxidative stress, and cell death, which can further exacerbate inflammation. Parameters of ethanol and iron induced damage have not been well characterised in the VL-17A cell line overexpressing CYP2E1 and ADH, the alcohol metabolising enzymes. This chapter aims to elucidate mitochondrial and inflammatory mechanisms involved in ALD and iron overload investigating mechanisms of oxidative stress and mitochondrial function in an *in vitro* model of ALD and iron overload.

4.1 Introduction

Development of ALD is complex and is thought to encompass a variety of factors including ROS, inflammatory cell activation, gut dysbiosis and iron overload. Iron is an essential element involved in various mechanisms such as metabolism, transport of oxygen, DNA synthesis and innate immunity. However, when iron becomes dysregulated and iron overload occurs, liver damage is induced, and oxidative stress and cell death occurs, which can further exacerbate inflammation.

Chronic liver disease, in particular ALD, is often associated with dysregulated iron homeostasis. Excessive alcohol consumption is directly linked to iron overload which causes an increased labile iron pool (LIP) in hepatocytes

(Zanninelli et al., 2002; Ioannou et al., 2004; Maras et al., 2015). The presence of excessive iron promotes the formation of oxygen radicals and ROS causing oxidative stress (Galaris, Barbouti and Pantopoulos, 2019). Additionally, elevated iron levels in the liver contribute to liver damage and apoptosis. Iron accumulation in macrophages has also been considered an indicator of secondary iron overload in chronic liver disease (Batts, 2007). In patients with cirrhosis, down-regulation of circulating transferrin and the transferrin receptor have been reported, as well as elevated transferrin saturation index (%SAT) (Kalantar-Zadeh, Rodriguez and Humphreys, 2004). Elevated serum ferritin levels has been reported to be significant in predicting early mortality in patients with decompensated chronic liver disease (Maiwall et al., 2014). High serum ferritin to alanine aminotransferase (ALT) ratio has also been identified as a prognostic marker in acute liver failure (Ozawa et al., 2011).

Increased liver iron content is a primary feature of ALD and research has shown that moderate alcohol consumption can lead to elevated levels of iron in the liver (Harrison-Findik, 2007). Previous research has found that liver iron content is negatively correlated with ALD survival (Ganne-Carrié et al., 2000). An excessive accumulation of iron can contribute to the progression of alcohol-induced liver injury through various mechanisms such as oxidative stress, inflammation, and DNA damage. Iron and alcohol alone can independently cause oxidative stress and lipid peroxidation, but alcohol-induced iron overload can exacerbate liver injury through free radical and inflammatory cytokine production such as NF-κB and TNF-α (Ali, Ferrao and Mehta, 2022). In animal models of ALD, Kupffer cells have been shown to contain elevated

levels of iron which activated NF-κB and TNF-α (She et al., 2002; Xiong et al., 2003; Harrison-Findik, 2007).

Alcohol can play a role in the regulation and expression of hepcidin in the liver. Studies have shown that alcohol can decrease hepcidin expression in alcohol metabolising hepatoma cells as well as in animal models whereby mice were exposed to short-term alcohol consumption (Harrison-Findik et al., 2006). Animal models have also shown that alcohol reduces expression of hepcidin 1 mRNA, however, iron up-regulates hepcidin 1 gene expression (Lou et al., 2004; Harrison-Findik et al., 2006). This down regulation of hepcidin in response to alcohol leads to elevated expression of iron transporter proteins DMT1 and ferroportin (Harrison-Findik et al., 2006). As hepcidin functions to inhibit iron absorption in the small intestine and is proposed to be a negative inhibitor of iron absorption, downregulation of hepcidin can lead to enhanced intestinal iron absorption. Increased expression of the iron storage protein ferritin has also been documented. Therefore down-regulation of hepcidin in response to alcohol may be one of the primary mechanisms involved in iron overload during ALD.

4.2 Aims and Objectives

The primary aim of this chapter was to investigate and characterise the effect of ethanol and iron overload on liver injury, oxidative stress, mitochondrial function, and apoptosis. Specific research objectives were to:

1. Characterise the effect of iron with or without ethanol combination treatment on liver injury by measurement of cell viability and oxidative stress.

2. Assess the effect of iron alone and combinations of iron and ethanol on apoptosis.
3. Characterise the effect of both iron treatment with and without ethanol on mitochondrial function measured by oxygen consumption and mitochondrial ROS, and mitochondrial membrane potential.

4.3 Results

4.3.1 Effect of ethanol and iron exposure on cell viability

To further model chronic liver injury and induce possible further damage to VL-17A cells, both ethanol and iron were added to cells. After optimisation of ethanol doses, concentrations of 200 mM, 300 mM and 350 mM ethanol were used for further experimentation. The concentration of iron was optimised and 50 μM iron was assessed using the MTT assay over a 72-hr period to model chronic liver injury.

At 24 hrs no changes were observed after iron treatment only (**Figure 4.1**). However, ethanol and iron treatment in combination led to a 55% decrease ($p=0.0023$) in cell viability at 300 mM ethanol/50 μM iron, and a 63% decrease ($p=0.0008$) when treated with 350 mM ethanol/50 μM iron. At 24 hrs, treatment with ethanol and iron also produced significant differences when compared to the iron only treatment. 300 mM ethanol + 50 μM iron led to a 53% decrease ($p=0.0041$) and a 350 mM ethanol + 50 μM iron produced a 62% decrease ($p=0.0013$), when compared to iron treatment only (**Figure 4.1**).

At 48 hrs iron treatment only led to a 39% increase ($p=0.0022$) in cell viability (**Figure 4.1**). At 48 hrs, ethanol and iron treatment combined led to a 35% decrease in cell viability at 200 mM ethanol + 50 μM iron ($p=0.0044$), a 42% decrease ($p=0.0012$) when treated with 300 mM ethanol + 50 μM iron, and a 64% decrease ($p<0.0001$) when treated with 350 mM ethanol + 50 μM iron, when compared to the control (**Figure 4.1**). Also, treatment with ethanol and iron produced significant differences when compared to the iron only treatment

whereby 200 mM ethanol + 50 μM iron produced a 53% decrease ($p<0.0001$), 300 mM ethanol + 50 μM iron, and a 58% decrease ($p<0.0001$) and 350 mM ethanol + 50 μM iron produced a 74% decrease ($p<0.0001$), when compared to iron treatment only (**Figure 4.1**).

At 72 hrs, iron only treatment led to a 31% increase in cell viability. However, ethanol and iron treatment produced statistically significant changes when compared to the control. Treatment with 300 mM ethanol + 50 μM iron produced a 56% decrease ($p=0.0279$) and 350 mM ethanol + 50 μM iron produced a 51% decrease ($p=0.0448$) when compared to the control. All ethanol and iron combination treatments also produced significant changes when compared to the iron only treatment and 200 mM ethanol + 50 μM iron produced a 53% decrease ($p=0.0077$), 300 mM ethanol + 50 μM iron produced a 66% decrease ($p=0.0015$), and 350 mM ethanol + 50 μM iron produced a 63% decrease ($p=0.0023$), respectively (**Figure 4.1**).

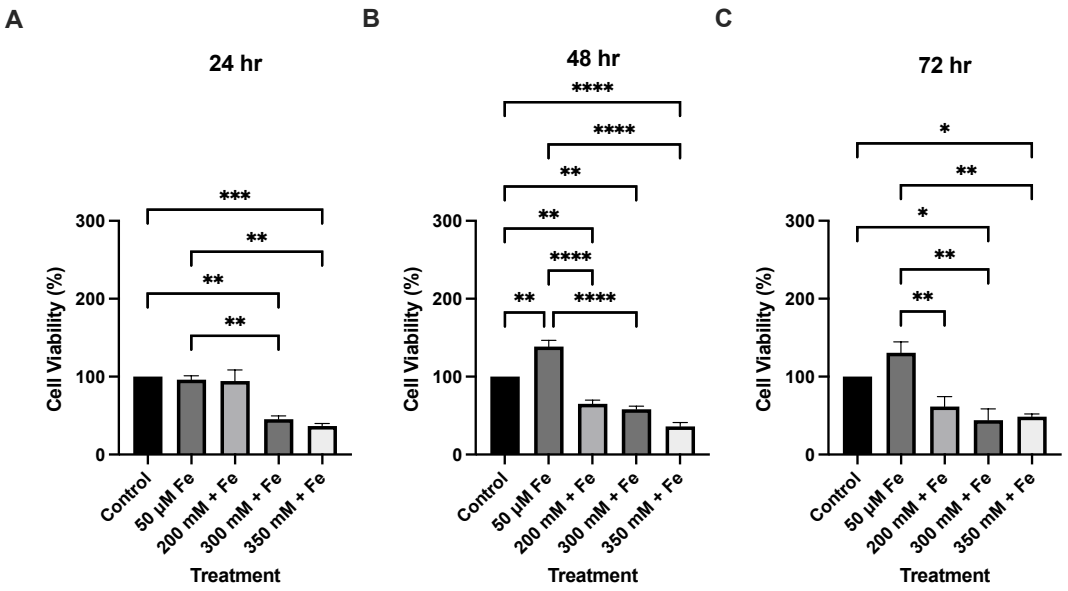

Figure 4.1 The effect of ethanol and iron exposure on cell viability over a 72-hr period. A) percentage of cell viability at 24 hrs, B) percentage of cell viability at 48 hrs and C) percentage of cell viability at 72 hrs. Cells were seeded in 96-well plates and treated with 200 mM, 300 mM, and 350 mM ethanol as well as 50 μM iron. Viability of cells was determined by the MTT assay and measured at 24 hrs, 48 hrs and 72 hrs. Data is presented as percentage from the control. Results presented as mean ± SEM (n = 3). * $P \leq 0.05$, ** $P \leq 0.01$, *** $P \leq 0.001$, **** $P \leq 0.0001$.

4.3.2 Effect of ethanol and iron exposure on ROS production

Increased ROS production and oxidative stress is a common feature of ALD. After optimisation, intracellular ROS production in VL-17A cells was measured using the DCFDA assay. Ethanol exposure at different time points was analysed to quantify the accumulation of ROS at different concentrations.

After 30 mins, iron treatment only also led to a significant increase (68%) in ROS ($p=0.0149$), however, no changes were observed with ethanol and iron treatment combined. After 1 hr, no changes were observed across all treatment groups. At 2 hrs, iron treatment alone led to a 92% increase ($p=0.0122$) in ROS. Also at 2 hrs, ethanol and iron treatment combined led to an 89% increase ($p=0.0154$) in ROS with 200 mM ethanol + 50 μM iron; a 108% increase ($p=0.0043$) when treated with 300 mM ethanol + 50 μM iron; and a 125% increase ($p=0.0014$) when treated with 350 mM ethanol + 50 μM iron (when compared to the DMEM only control) (**Figure 4.2**).

Iron treatment only led to a 60% increase ($p=0.0007$) at 24 hrs and a 115% increase at 48 hrs ($p<0.0001$). At 24 hrs, ethanol and iron treatment combined led to an 52% increase ($p=0.0020$) in ROS when treated with 200 mM ethanol + 50 μM iron, a 66% increase ($p=0.0003$) when treated with 300 mM ethanol + 50 μM iron, and a 63% increase ($p=0.0004$) when treated with 350 mM ethanol + 50 μM iron, when compared to the control (**Figure 4.2**). At 48 hrs ethanol and iron treatment combined led to an 118% increase ($p<0.0001$) in ROS at 200 mM ethanol + 50 μM iron, a 97% increase ($p<0.0001$) when treated with 300 mM ethanol + 50 μM iron, and an 89% increase ($p<0.0001$)

when treated with 350 mM ethanol + 50 μM iron, when compared to the control (**Figure 4.2**).

At 72 hrs, iron only increased ROS by 71% (p=0.0044) and 200 mM ethanol + 50 μM iron caused a 69% increase (p=0.0137) when compared to the control. No significant changes were observed when comparing ethanol and iron combination treatments to the iron only treatment across all time points.

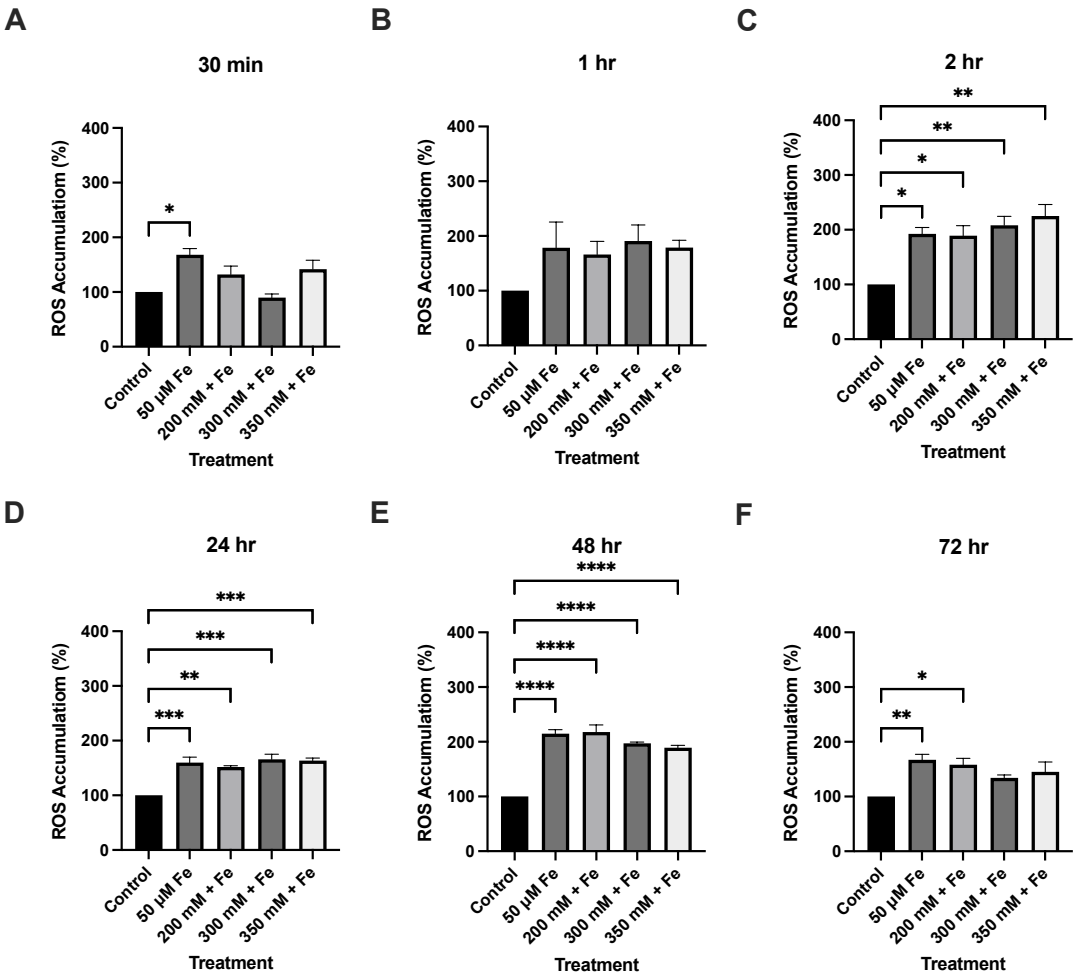

Figure 4.2 The effect of ethanol and iron exposure on ROS accumulation over a 72-hr period. A) percentage of ROS accumulation at 30 mins, B) percentage of ROS accumulation at 1 hr, C) percentage of ROS accumulation at 2 hrs and D) percentage of ROS accumulation at 24 hrs. Cells were seeded in 96-well plates and treated with 200 mM, 300 mM, and 350 mM ethanol as well as 50 μM iron. ROS accumulation was determined by the DCFDA assay and measured using fluorescence at 30 mins, 1 hr, 2 hrs, 24 hrs, 48 hrs and 72 hrs. Data is presented as percentage from the control. Results presented as mean ± SEM (n = 3). * P ≤ 0.05, ** * P ≤ 0.01, *** P ≤ 0.001, **** P ≤ 0.0001.

4.3.3 Effect of ethanol and iron exposure on apoptosis

At 24 hrs, percentage of cells in early apoptosis increased dose-dependently with ethanol and iron concentrations, although significance was not met. Cells in late apoptosis remained low with no significant differences (**Figure 4.3**). At 48 hrs, a similar pattern occurred in early apoptosis, however, the percentage of cells in late apoptosis increased from 24 hrs to 48 hrs. At 72 hrs, significant changes were observed in both early and late apoptosis. Treatment with 350 mM ethanol + 50 μM iron caused 39% of cells to undergo early apoptosis compared to 12% in the control group ($p=0.0057$) and 15% in the iron treatment ($p=0.0267$). Treatment with 350 mM ethanol + 50 μM also led to a total of 22% of cells in late apoptosis, also reaching statistical significance ($p=0.0478$).

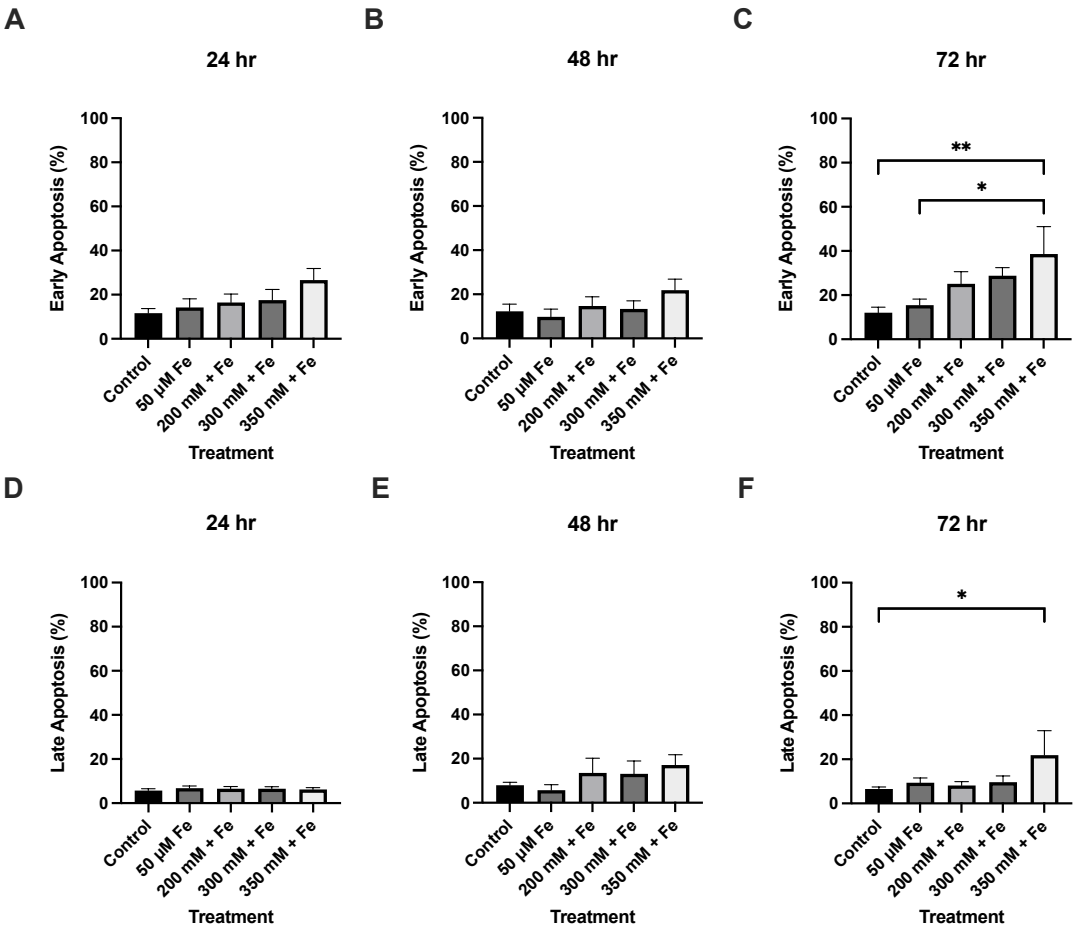

Figure 4.3 The effect of ethanol and iron exposure on apoptosis over a 72-hr period. A) percentage of cells in early apoptosis at 24 hrs, B) percentage of cells in early apoptosis at 48 hrs, C) percentage of cells in early apoptosis at 72 hrs, D) percentage of cells in late apoptosis at 24 hrs, D) percentage of cells in late apoptosis at 48 hrs and E) percentage of cells in late apoptosis at 72 hrs. Cells were seeded in 12-well plates and treated with 200 mM, 300 mM and 350 mM ethanol as well as 50 µM iron. Apoptosis was assessed at 24 hrs, 48 hrs and 72-hrs using the Annexin VI kit and measured using flow cytometry. Data is presented as percentage of positive cells. Results presented as mean ± SEM (n = 3). * $P \leq 0.05$, ** $P \leq 0.01$.

4.3.4 Effect of ethanol and iron exposure on mitochondrial hydroxyl radical production

The mitochondrial HO· detection assay was used to detect intracellular hydroxyl radicals. Preliminary data shows at 24 hrs (n=2) there are no changes in HO· production. However, at 48 hrs, preliminary data shows 50 μM iron increased HO· production by 108% (n=1), although treatment with ethanol and iron reduced HO· production. At 72 hrs, HO· production was also decreased across all treatment groups (n=2) (**Figure 4.4**).

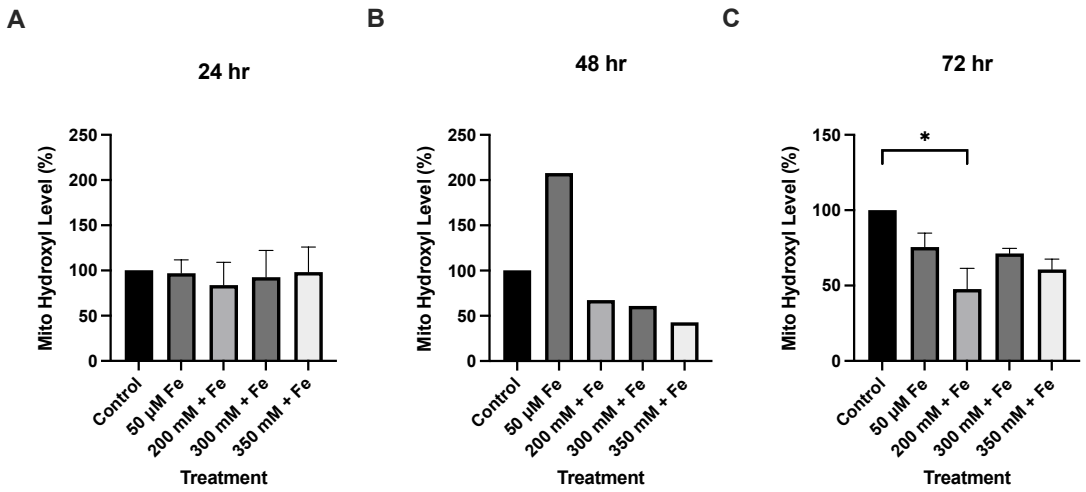

Figure 4.4 Preliminary data assessing the effect of ethanol and iron on mitochondrial hydroxyl levels over a 72-hr period. A) mitochondrial hydroxyl levels at 24 hrs, B) mitochondrial hydroxyl levels at 48 hrs and C) mitochondrial hydroxyl levels at 72 hrs. Cells were seeded in 96-well plates and treated with 200 mM, 300 mM, and 350 mM ethanol as well as 50 μM iron. Mitochondrial hydroxyl levels were assessed at 24 hrs, 48 hrs and 72-hrs using the Mitochondrial Hydroxyl Radical Detection Assay Kit (ab219931). Data is presented as percentage from control. Results presented as mean ± SEM (n = 1-2). * $P \leq 0.05$.

4.3.5 Effect of ethanol and iron exposure on mitochondrial oxygen consumption rate

The respiratory function of mitochondria was evaluated by measuring the oxygen consumption rate of ethanol and iron treatment on VL-17A cells (**Figure 4.5**). Significant decreases were observed in basal respiration at 24 hrs ($p=0.0433$) and maximal respiration at 48 hrs ($p=0.0326$) in the 350 mM ethanol + 50 μM iron treated cells. No significant changes were observed in any other parameters.

At 24 hrs (**Figure 4.6**), 50 μM iron alone caused a non-significant 11% reduction in basal respiration when compared to control DMEM. Basal respiration was decreased by 57% by 200 mM ethanol + 50 μM iron, 51% by 300 mM ethanol + 50 μM iron and 81% by 350 mM ethanol + 50 μM iron ($p=0.0433$) when compared to the control. When compared to 50 μM iron, basal respiration was decreased by 51% at 200 mM ethanol + 50 μM iron, 45% at 300 mM ethanol + 50 μM iron and 78% at 350 mM ethanol + 50 μM iron. Proton leak was decreased by 15% by 50 μM iron alone, 50% with 200 mM ethanol + 50 μM iron, 47% with 300 mM ethanol + 50 μM iron and 66% with 350 mM ethanol + 50 μM iron, when compared to the control (**Figure 4.6**). When compared to 50 μM iron, proton leak was decreased by 46% with 200 mM ethanol + 50 μM iron, 42% with 300 mM ethanol + 50 μM iron and 63% with 350 mM ethanol + 50 μM iron. Maximal respiration was also decreased by 15% following 50 μM iron treatment, and 200 mM ethanol + 50 μM iron caused a decrease of 54% following 200 mM ethanol + 50 μM iron, 42% with

300 mM ethanol + 50 μM iron and 76% with 350 mM ethanol + 50 μM iron, respectively, when compared to the control. Similar decreases of 46%, 32% and 72% were observed when compared to 50 μM iron treatment. Spare respiratory capacity was also decreased by 31% following 50 μM iron treatment. Treatment with 200 mM ethanol + 50 μM iron decreased spare respiratory capacity by 44% following 200 mM ethanol + 50 μM iron, 7% with 300 mM ethanol + 50 μM iron and 61% with 350 mM ethanol + 50 μM iron respectively, when compared to control DMEM. Data shows 50 μM iron alone caused a 12% increase in non-mitochondrial oxygen consumption. However, non-mitochondrial oxygen consumption was also decreased dose dependently with combinations of ethanol and iron treatment, by 49% with 200 mM ethanol + 50 μM iron, 50% with 300 mM ethanol + 50 μM iron and 68% with 350 mM ethanol + 50 μM iron when compared to the control. When compared to 50 μM iron, non-mitochondrial oxygen consumption also decreased dose dependently, 54% by 200 mM ethanol + 50 μM iron, 55% by 300 mM ethanol + 50 μM iron and 71% by 350 mM ethanol + 50 μM iron. ATP production was also decreased by 50 μM iron (13%) alone and by 59% with 200 mM ethanol + 50 μM iron, 52% with 300 mM ethanol + 50 μM iron and 71% with 350 mM ethanol + 50 μM iron, when compared to DMEM only. These decreases were also observed when compared to 50 μM iron treatment.

At 48 hrs (**Figure 4.7**), 50 μM iron alone caused a 23% increase in basal respiration when compared to control DMEM. However, basal respiration was decreased by 33% with 200 mM ethanol + 50 μM iron, 38% with 300 mM ethanol + 50 μM iron and 35% with 350 mM + 50 μM iron ethanol when

compared to control DMEM (**Figure 4.7**). When compared to 50 μM iron, decreases of 45%, 49% and 48% were observed. Proton leak was decreased by 18% with 50 μM iron alone, 47% with 200 mM ethanol + 50 μM iron, 52% with 300 mM ethanol + 50 μM iron and 38% with 350 mM ethanol + 50 μM iron when compared to the control. When compared to 50 μM iron, similar decreases of 35% (200 mM ethanol + 50 μM iron), 40% (300 mM ethanol + 50 μM iron) and 24% (350 mM ethanol + 50 μM iron) were found. Maximal respiration was also decreased by 7% following 50 μM iron treatment. Treatment with 200 mM ethanol + 50 μM iron caused a decrease of 50% following 200 mM ethanol + 50 μM iron, 36% with 300 mM ethanol + 50 μM iron and 79% with 350 mM ethanol + 50 μM iron ($p=0.0326$), when compared to the control. Similar decreases of 46%, 31% and 77% were observed when compared to 50 μM iron treatment. Spare respiratory capacity was also decreased by 16% following 50 μM iron treatment and 200 mM ethanol + 50 μM iron decreased spare respiratory capacity by 53% following 200 mM ethanol + 50 μM iron, 13% following 300 mM ethanol + 50 μM iron and 57% following 350 mM ethanol + 50 μM iron, when compared to control DMEM. Treatment with 50 μM iron alone caused a 63% increase in non-mitochondrial oxygen consumption; however, non-mitochondrial oxygen consumption was decreased by 20% following 350 mM ethanol + 50 μM iron, compared to the control. When compared to 50 μM iron, non-mitochondrial oxygen consumption decreased by 41% with 200 mM ethanol + 50 μM iron, 29% with 300 mM ethanol + 50 μM iron and 51% with 350 mM ethanol + 50 μM iron. No significant changes were observed in ATP production. However, ATP

production was decreased by 39% with 200 mM ethanol + 50 μM iron, 44% with 300 mM ethanol + 50 μM iron and 87% with 350 mM ethanol + 50 μM iron when compared to the control.

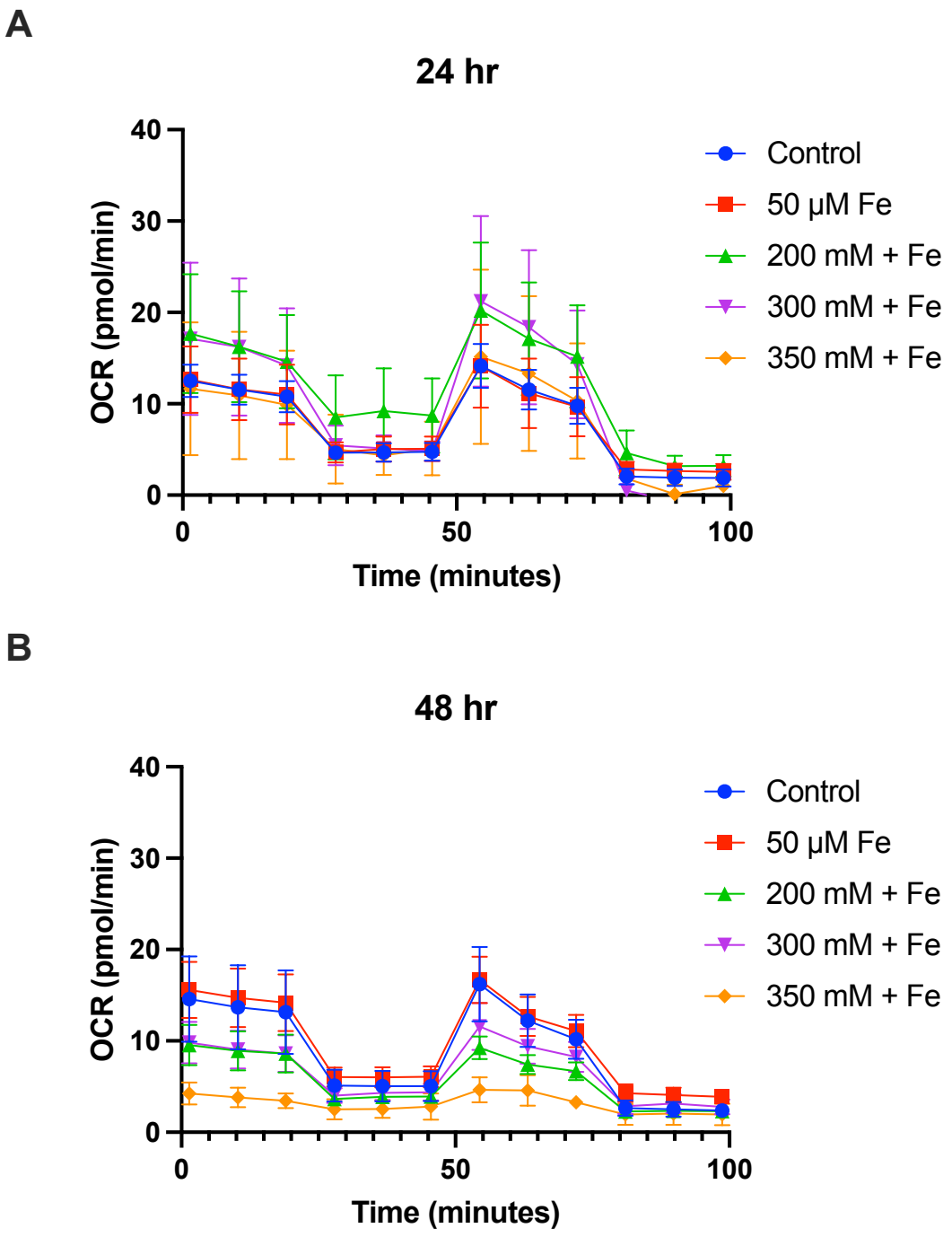

Figure 4.5 Mitochondrial oxygen consumption rate after ethanol and iron exposure at 24 hrs and 48 hrs. A) oxygen consumption rate at 24 hrs and B) oxygen consumption rate at 48 hrs. Cells were seeded in 24-well plates and treated with 200 mM, 300 mM, and 350 mM ethanol as well as 50 µM iron. Oxygen consumption rate was assessed over 48 hrs using the Seahorse XF24 analyser. Results presented as mean of replicates ± SEM (n = 3). OCR: oxygen consumption rate.

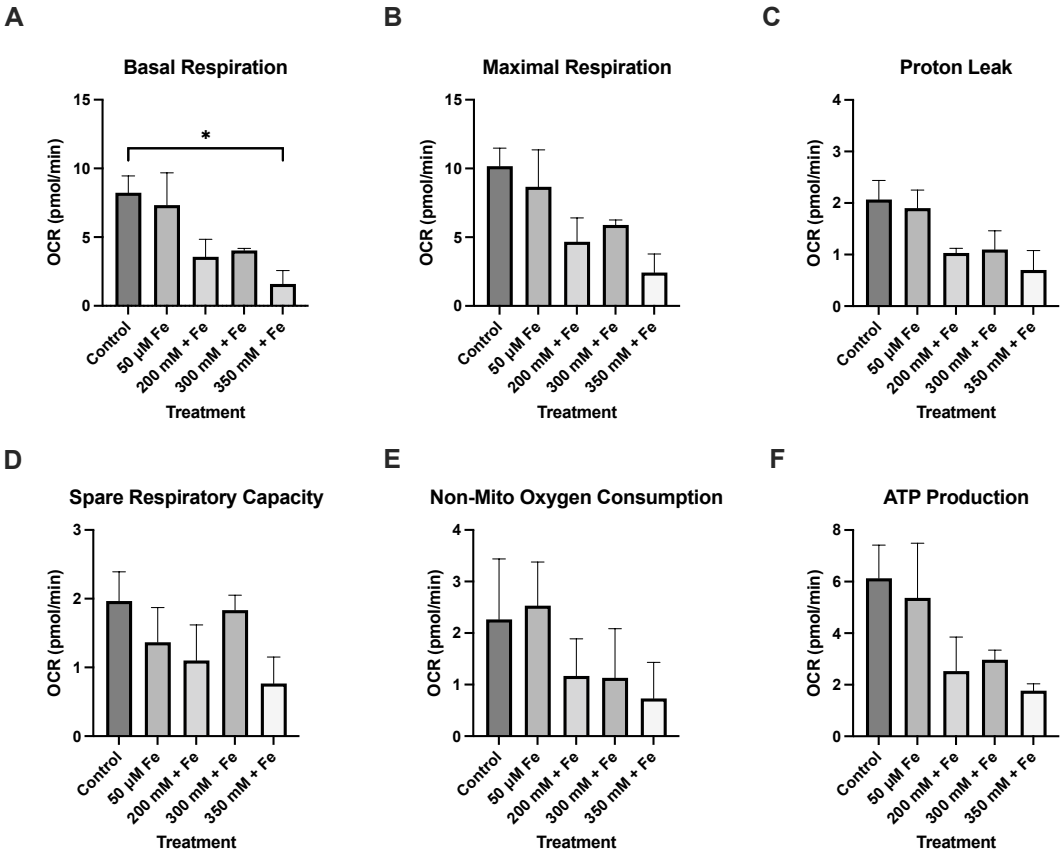

Figure 4.6 The effect of ethanol and iron on mitochondrial oxidative phosphorylation parameters at 24 hrs. A) Basal respiration, B) maximal respiration, C) proton leakage, D) spare respiratory capacity, E) non-mitochondrial oxygen consumption and F) ATP production. Cells were seeded in 24-well plates and treated with 200 mM, 300 mM, and 350 mM with 50 μM iron. Oxygen consumption rate was assessed at 24-hrs using the Seahorse XF24 analyser. Results presented as mean of replicates ± SEM (n = 3). OCR: oxygen consumption rate. * $P \leq 0.05$.

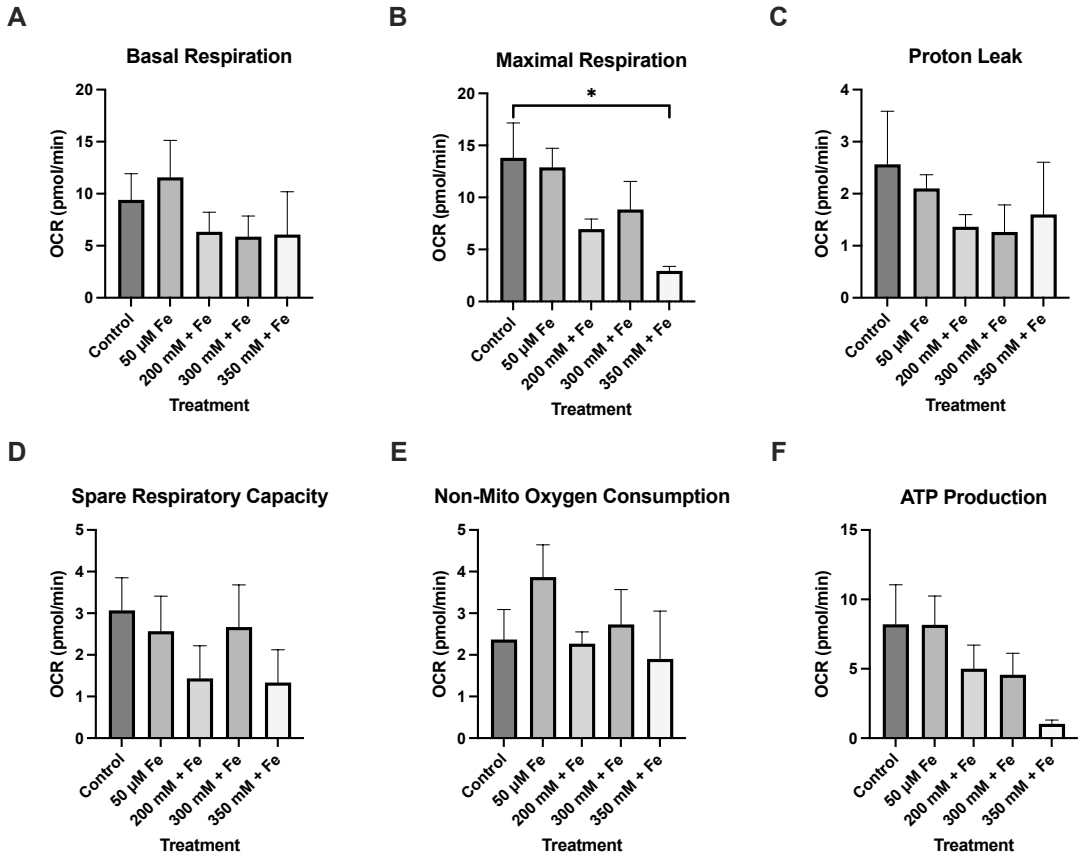

Figure 4.7 The effect of ethanol and iron on mitochondrial oxidative phosphorylation parameters at 48 hrs. A) Basal respiration, B) maximal respiration, C) proton leakage, D) spare respiratory capacity, E) non-mitochondrial oxygen consumption and F) ATP production. Cells were seeded in 24-well plates and treated with 200 mM, 300 mM, and 350 mM with 50 µM iron. Oxygen consumption rate was assessed at 48-hrs using the Seahorse XF24 analyser. Results presented as mean of replicates ± SEM (n = 3). OCR: oxygen consumption rate. * $P \leq 0.05$.

4.3.6 Effect of ethanol and iron exposure on mitochondrial membrane potential

To further model chronic liver injury and induce greater damage to VL-17A cells, combinations of ethanol and iron treatment were added to cells and mitochondrial membrane potential was assessed using TMRE staining. Although preliminary data suggests that ethanol and iron in combination may produce changes in some concentrations assessed, statistical significance was not reached in any of the treatment groups. Mitochondrial membrane potential was reduced at 24 hrs (n=2) by 34% with 50 μM iron, 10% with 200 mM ethanol + 50 μM iron and 36% with both 300 mM ethanol + 50 μM iron and 350 mM ethanol + 50 μM iron when compared to the control. At 48 hrs (n=3), treatment with 200 mM ethanol + 50 μM iron reduced mitochondrial membrane potential by 18% with 50 μM iron, 27% with 200 mM ethanol + 50 μM iron, 9% with 300 mM ethanol + 50 μM iron and 19% with 350 mM ethanol + 50 μM iron. At 72 hrs (n=3), mitochondrial membrane potential appeared to increase in all treatment groups (**Figure 4.8**).

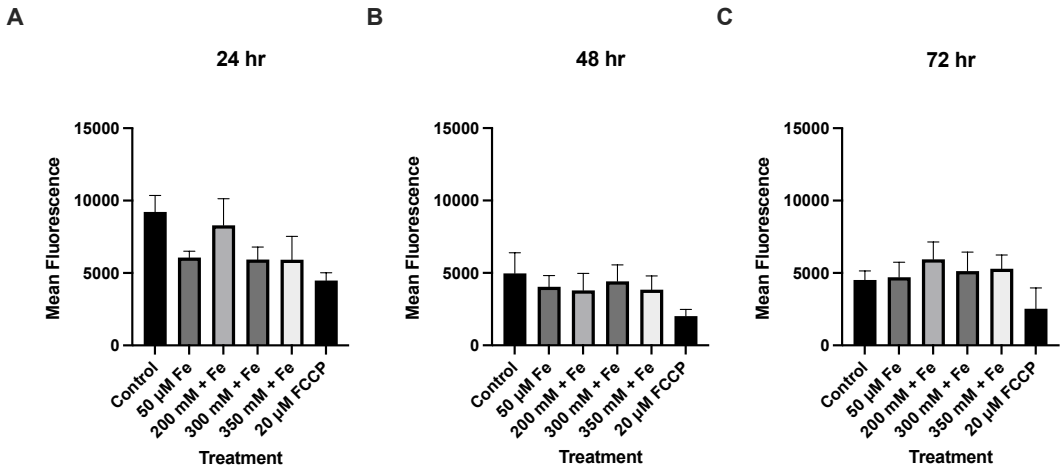

Figure 4.8 Preliminary data assessing the effect of ethanol and iron mitochondrial membrane potential over a 72-hr period. A) mitochondrial membrane potential at 24 hrs, B) mitochondrial membrane potential at 48 hrs and C) mitochondrial membrane potential at 72 hrs. Cells were seeded in 12-well plates and treated with 200 mM, 300 mM, and 350 mM ethanol as well as 50 μM iron and mitochondrial membrane potential was measured by TMRE staining using flow cytometry. FCCP (20 μM) was used as a positive control. Data is presented as mean fluoresce values. Results presented as mean ± SEM (n = 2-3).

4.3.7 Effect of ethanol and iron exposure on mitochondrial superoxide production

Levels of mtROS were assessed as previously described using MitoSOX staining. At 24 hrs, all treatments showed small decreases. However, at 48 hrs, 50 μM iron caused a 31% increase, 200 mM ethanol + 50 μM iron caused a 25% increase, 300 mM ethanol + 50 μM iron caused a 24% increase and 350 mM ethanol + 50 μM iron caused a 97% increase in mtROS when compared to the control. When compared to the iron only treatment, 200 mM ethanol + 50 μM iron and 300 mM ethanol + 50 μM iron did not show any effect, however, and 350 mM ethanol + 50 μM iron caused a 50% increase (**Figure 4.9**).

At 72 hrs, 50 μM iron caused a 116% increase, 200 mM ethanol + 50 μM iron caused a 13% increase, 300 mM ethanol + 50 μM iron caused a 16% increase and 350 mM ethanol + 50 μM iron caused a 72% increase in mtROS when compared to control DMEM. When compared to the iron only treatment, all treatments caused decreases in mtROS (**Figure 4.9**).

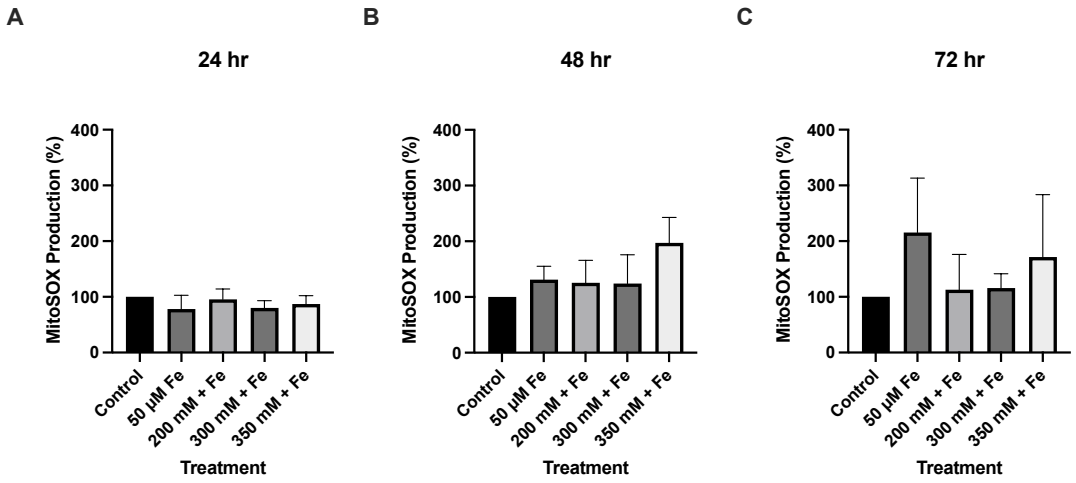

Figure 4.9 The effect of ethanol and iron on mitochondrial superoxide production over a 72-hr period. A) mitochondrial superoxide production at 24 hrs, B) mitochondrial superoxide production at 48 hrs and C) mitochondrial superoxide production at 72 hrs. Cells were seeded in 96-well plates and treated with 200 mM, 300 mM, and 350 mM ethanol as well as 50 μM iron and mitochondrial superoxide production was measured by using MitoSOX red dye. Data is presented as percentage difference from the control. Results presented as mean ± SEM (n = 3-4).

4.4 Discussion

To further model chronic liver injury and mimic the iron overload, which is prevalent in ALD patients, VL-17A cells were exposed to both ethanol and iron. Ethanol and iron combined led to a further reduction in viability suggesting both alcohol and iron furthers the detrimental effect on the liver. The effect of ethanol and iron on ROS production was assessed as it is known that iron can cause both increases in hydroxyl radicals and ROS during iron overload, which has been well documented in ALD patients (Milic et al., 2016). This study shows that iron causes further damage to VL-17A cells via the increase in ROS production. ROS production was significantly increased at 30 mins, 2 hrs and 24 hrs when treated with iron, and combined treatment with ethanol and iron also causes increases in ROS production. This shows that iron overload is linked to the production of ROS, and this may be due to the Fenton reaction. It has been demonstrated even mild alcohol consumption can elevate iron stores and >2 alcoholic drinks per day has been associated with an increased risk of iron overload (Ioannou et al., 2004). There is significant evidence to suggest that both iron and alcohol alone can cause oxidative stress and lipid peroxidation and therefore, a combination of both alcohol and iron can exacerbate disease via an increased production of proinflammatory cytokines and free radicals. Increased iron in Kupffer cells in animal studies has also shown downstream activation of NF-κB causing increase in proinflammatory cytokines such as TNF-α (She et al., 2002; Xiong et al., 2003). This pro-inflammatory effect has been completely eliminated in a model using iron chelation therapy (Xiong et al., 2003), suggesting there is a significant importance for iron signalling and metabolism in the progression and

inflammatory response during ALD. This evidence along with the toxic effects of iron demonstrated in this study such as and increased reduction in cell viability and elevated ROS production shows iron has a pathogenic effect.

Iron toxicity occurs due to an excess of iron catalysing the Fenton and Haber-Weiss reactions, increasing ROS production. ROS can undergo conversion into superoxide radicals which are then reduced to H_2O_2 by superoxide dismutase. H_2O_2 can then either be transformed into water by glutathione peroxidase or react with iron-sulphur proteins or heme, generating ferrous ions (Fe^{2+}) (Ying et al., 2021). Generation of Fe^{2+} and an increased LIP produce ROS via the Fenton reaction, which lead to generation of highly reactive hydroxyl peroxyl radicals. Hydroxyl peroxyl radicals can then cause DNA breaks as well as protein and lipid peroxidation, as can form lipid ROS or lipid peroxyl radicals (Ying et al., 2021), causing apoptosis and cellular damage. The increased availability of water soluble Fe^{2+} then saturates the antioxidant system due to excessive ROS (Mehta, Farnaud and Sharp, 2019). Therefore, excessive ROS caused by iron overload can result in cellular damage resulting in mitochondrial dysfunction, lipid peroxidation, cell membrane damage, and disruption of the electron transport chain, ultimately leading to apoptosis. This is evidenced in this study which demonstrates a significant increase in ROS production as well a substantial number of cells in apoptosis and dysregulation of mitochondrial oxygen consumption.

Mitochondrial dysfunction and ROS can also occur due to elevated iron and increased hepatic iron can also contribute to liver injury due to alcohol (Kohgo et al., 2005; Thomas et al., 2013), which contributes to hydroxyl radical

formation (Wu and Cederbaum, 2003). Therefore, as iron overload occurs during ALD and levels of iron increase during chronic ethanol intake, elevated mitochondrial hydroxyl radicals observed during ALD may be due to the increased iron. As iron exists in both $Fe2^{+}$ and $Fe3^{+}$ forms, which can both provide and accept electrons, this can act as a major catalyst for generation of free radicals. Therefore, iron can interact with hydrogen peroxide causing hydroxyl radical formation through the Fenton reaction (Galaris, Barbouti and Pantopoulos, 2019). Labile iron can also modulate activation of transcription factors such as NF-κB and STAT3 leafing to activation of proinflammatory genes and cytokines (Galaris, Barbouti and Pantopoulos, 2019).

High iron diet has been shown to promote iron accumulation in tissues which impaired mitochondrial function (Fischer et al., 2021). High liver iron levels correlated with a reduction in mitochondrial respiration capacity, increased ROS and reduced mitochondrial aconitase activity (Fischer et al., 2021). This may be due to the fact in mitochondria, iron is required for heme synthesis, iron sulphur and oxidative phosphorylation and iron overload may affect these pathways (Stehling and Lill, 2013). Previous data has also shown that the availability of iron may also affect the function of mitochondria (Paul, D H Manz, et al., 2017; Kelly et al., 2023). Therefore, iron overload in the liver, which is prevalent in ALD patients, can affect mitochondrial metabolic pathways and increase superoxide production due to electron leakage in the electron transport chain, exacerbating disease state.

Significant increases were observed in both early and late apoptosis at 72 hrs after treatment with ethanol and iron as well as increasing ROS production.

Extracellular iron can cause mitochondrial outer membrane permeabilisation leading to elevated intracellular iron and ROS production (Ying et al., 2021). Iron mediated ROS can therefore induce intrinsic apoptosis via different mechanisms. For example, ROS oxidises cardiolipin, a phospholipid present in mitochondrial membranes (Dudek, 2017; Cooper et al., 2023). Cardiolipin is required during mitochondrial processes including cellular respiration (Dudek, 2017). When iron oxidises cardiolipin, cytochrome c is released leading to downstream signalling and caspase activation leading to apoptosis, cardiolipin peroxidation and cytochrome c release (Sousa et al., 2020).

The interplay between both cardiolipin and ROS is complex and has not been fully investigated in ALD, however, its role in mitochondrial bioenergetics has been researched. Mitochondria deficient in cardiolipin exhibit decreased activity of respiratory complexes and carrier proteins increasing ROS. mtROS, which can be produced due to excessive ethanol and iron, are a significant trigger for ferroptosis. Induction of ferroptosis has been connected to decreases in NADPH levels (Wang et al., 2017), which is important for the synthesis glutathione. Therefore, glutathione and cardiolipin levels may be a contributing factor to levels of increased apoptosis observed in this study. This suggests that glutathione and cardiolipin may play a significant role in the development of liver disease. However, further research is required to fully understand the exact impact of mitochondrial cardiolipin alterations on the pathogenesis of alcohol-related liver damage.

4.5 Conclusion

In this study, VL-17A cells were used as a model to investigate the effects of alcohol exposure and iron overload in the liver by assessing measures of oxidative damage and mitochondrial function. Results show that iron treatment caused significant cell toxicity when combined with ethanol, with a dose-dependent reduction in cell viability observed over time, producing more profound effects than ethanol treatment alone. Ethanol and iron exposure as well as iron alone, was also associated with an increase in the production of ROS, indicating iron causes further oxidative damage to the liver. The percentage of apoptotic cells was also increased by ethanol and iron treatment. This study also presented a decrease in mitochondrial basal and maximal respiration when treated with ethanol and iron, suggesting that alcohol-induced damage to mitochondria can disrupt oxygen consumption. In conclusion, this study highlights the effects of both ethanol and iron toxicity in liver cell, causing further ROS and oxidative stress. Continued research in both iron overload and ALD is required to fully understand the mechanisms of oxidative damage including mitochondrial dysfunction and chromosomal instability. Research to mitigate the effects of alcohol as well as iron overload should also be explored to benefit cellular health.

CHAPTER 5 PROTECTIVE EFFECTS OF ANTIOXIDANTS AND NANOFORMULATIONS IN THE TREATMENT OF ALCOHOL-ASSOCIATED LIVER DISEASE

Description of Chapter

This chapter focuses on the use of nanoformulated antioxidant compounds in the treatment of oxidative stress in HepG2 (VL-17A) cells treated with both ethanol and iron. Although there are several clinical trials underway, therapeutics for ALD remain limited and abstinence is still regarded as the most important therapy. The use of antioxidant compounds such as curcumin and silibinin, as either free drugs (carrier free) or nanoformulations, were assessed in their ability to protect against ethanol and iron induced damage. Cell viability and ROS parameters were assessed after either pre-treatment or co-treatment of the compounds.

5.1 Introduction

Excessive alcohol consumption is known to cause significant morbidity and mortality worldwide. During chronic liver disease, disruptions to iron homeostasis including iron metabolism, iron regulation and iron absorption and iron can increase the labile iron pool in hepatocytes, causing further oxidative stress and damage (Zanninelli et al., 2002; Ioannou et al., 2004; Maras et al., 2015). Treatments for ALD have not advanced for many years and a lack of therapeutic options are currently available. Despite recent clinical studies and trials, abstinence is still regarded as the most important treatment for ALD with other treatments focussing on nutritional therapy, pharmacological therapy, and liver transplantation. Recent advances for treatment have demonstrated limited therapeutic efficiency and significant side

effects including mortality and infection (Petagine, Zariwala and Patel, 2021). Therefore, there is a need to develop novel approaches able to enhance therapeutic efficiency and limit disease progression.

Antioxidant therapy has been considered a beneficial treatment for ALD due to oxidative stress contributing to the pathogenesis of disease. Antioxidant compounds which can mediate ROS including those such as vitamins E and C, N-acetylcysteine, S-adenosyl methionine, and betaine. Glutathione is the main cellular antioxidant particularly found in the liver which functions in cellular redox buffer and major defence against oxidative stress. N-acetylcysteine is an antioxidant with glutamatergic modulating and anti-inflammatory properties. N-acetylcysteine has the benefit of being low-cost and well-tolerated which makes it a promising treatment for ALD. Although N-acetylcysteine has been shown to increase 1-month survival in alcoholic hepatitis, long term survival was not improved (Nguyen-Khac et al., 2011). Therefore, although natural compounds may be beneficial in the treatment of ALD they face some limitations such as low bioavailability, limited uptake, and low specificity (Yan et al., 2021).

Curcumin, the main active component in turmeric, has been shown to possess antioxidant properties. In mice, curcumin has been shown to reduce oxidative stress via a reduction in ROS production as well as reduce lipid accumulation in hepatocytes (Yan et al., 2021). Curcumin has low bioavailability and stability issues due to it low solubility in aqueous environments as well as its low stability in neutral and alkaline environments. Therefore, the ability to achieve targeted therapeutic doses becomes limited. However, novel nanocarrier delivery systems encapsulating the antioxidant curcumin has been shown to

protect against oxidative stress via improving cell viability and lipid peroxidation in a Parkinson's disease model (Mursaleen, Somavarapu and Zariwala, 2020).

Silymarin, derived from the milk thistle plant, has frequently been used as a medicinal herb. It contains various flavonolignans, with the main component as silibinin (also called silybin), which is known for its potent antioxidant, antifibrotic properties, anti-inflammatory effects and hepatoprotective nature, which make it a potential treatment option for chronic liver diseases (Gillessen and Schmidt, 2020). Silymarin functions as an antioxidant by scavenging free radicals, thereby reducing oxidative stress (Gillessen and Schmidt, 2020). It exerts its effects by modulating the activity of liver enzymes involved in various liver functions. Additionally, silymarin inhibits the activation of fibrogenic stellate cells and decrease the release of proinflammatory mediators (Surai, 2015; Federico, Dallio and Loguercio, 2017). Although flavonoids are quickly absorbed after oral intake, their concentrations in the bloodstream are low (Thilakarathna and Rupasinghe, 2013). Therefore, the low oral bioavailability of flavonoids possesses a limitation for their therapeutic potential.

Nanoformulations may overcome some of the difficulties faced with traditional drugs, allowing specific cell delivery, increasing its concentration at the target cell (Bartneck, Warzecha and Tacke, 2014). The ability for nanoformulation production to have various compositions, and controllable sizes provides an advantage, including controlled drug release, specific cell penetration, improved pharmacokinetics, and reduced side effects (Bai, Su and Zhai, 2020). Nanocarriers prepared by a modified thin film method formulated with ascorbyl palmitate and 1,2-distearoyl-sn-glycero-3-phosphoethanolamine

polyethylene glycol (DSPE-PEG) have been successfully researched in their antioxidant capacity, as well in their ability to significantly augment iron absorption, and are a potential delivery vehicle for nutritional applications (Zariwala et al., 2014). Therefore, their potential benefits for ALD should be assessed in relevant models. Consequently, this study aimed to develop a nanocarrier-based delivery system for potential antioxidant therapeutics with the objective of evaluating their efficacy in protecting against alcohol and iron induced damage in a liver cell model.

5.2 Aims and Objectives

The primary aim of this chapter was to investigate the potential of novel nanoformulations encapsulating antioxidants, as well as free drug (carrier free) antioxidants, in their ability to protect against ethanol and iron overload in VL-17A cells. Specific research objectives were to:

1. Assess the therapeutic potential of free drug antioxidant compounds to improve cell viability.
2. Assess the therapeutic potential of nanoformulations, encapsulating curcumin, against ethanol induced liver injury measured by cell viability and ROS production.
3. Assess the therapeutic potential of nanoformulations, encapsulating curcumin, against ethanol and ethanol and iron induced liver injury measured by cell viability and ROS production.

5.3 Results

5.3.1 Nanoformulation characteristics

All curcumin DSPE-PEG nanoformulations demonstrated high encapsulation efficiency (74-78%) (**Table 5.1**). 100% curcumin DSPE-PEG nanocarriers had the highest mean encapsulation efficiency (78.25%), and 90% curcumin, 10% AP-loaded DSPE-PEG nanocarriers had a mean encapsulation efficiency 74.15%. 100% curcumin DSPE-PEG showed a higher drug loading and encapsulation efficiency percentage. 100% curcumin DSPE-PEG had a mean drug loading of 7.11% and 90% curcumin, 10% AP-loaded DSPE-PEG had a mean drug loading of 6.74%.

The mean nanoformulation particle sizes as measured by diameter were <10 nm for both formulations with 100% curcumin DSPE-PEG nanocarriers mean diameter as 8.40 nm, and 90% curcumin, 10% AP-loaded DSPE-PEG nanocarriers had a mean diameter of 8.50 nm (**Table 5.1**). The polydispersity index was then assessed to measure the heterogenicity of nanocarrier solutions. Results indicated low polydispersity index values <0.5 for both DSPE-PEG nanoformulations.

Zeta Potential (mV) was then used to assess surface charge of nanoformultions. Both 100% curcumin DSPE-PEG nanocarriers and 90% curcumin, 10% AP-loaded DSPE-PEG nanocarriers had had similar low negative surface charges (-15.20 and -15.10 mV, respectively).

Table 5.1 Nanoformulation characteristics. Hydrodynamic Diameter (d), Polydispersity Index (PDI), Surface Charge, Drug Loading (DL) and Encapsulation Efficiency (EE) of curcumin and curcumin and ascorbyl palmitate (AP) DSPE-PEG nanoformulations prepared at 80°C (mean ± SEM n=3).

Active Ingredient (10 mg)	Polymer (100 mg)	Hydrodynamic Diameter (nm)	Polydispersity Index	Zeta Potential (mV)	Drug Loading (%)	Encapsulation Efficiency (%)
Curcumin	100% DSPE-PEG	8.40 ± 0.67	0.43 ± 0.03	-15.20 ± 0.95	7.11 ± 0.00	78.25 ± 0.02
Curcumin	90% DSPE-PEG, 10% ascorbyl palmitate (AP)	8.50 ± 0.64	0.43 ± 0.03	-15.10 ± 0.90	6.74 ± 0.00	74.17 ± 0.03

5.3.2 Effect of curcumin free drug on ethanol induced changes in cell viability

Free drug curcumin was tested in its ability to prevent cellular injury due to alcohol. 5 μM and 10 μM curcumin were assessed and data shows that curcumin provided protection against ethanol induced damage to the liver (**Figure 5.1**).

At 48 hrs, 200 mM ethanol led to a 22% reduction in viability, 300 mM led to a 53% reduction and 350 mM led to a 75% reduction in viability. At 72 hrs, a greater effect was observed, and 200 mM ethanol led to a 52% reduction in viability and 300 mM and 350 mM both led to a 95% reduction in viability.

Treatment with curcumin free drug was added to treatments with ethanol and reduced the effects of ethanol induced loss of viability at both 48 hrs and 72 hrs, when compared to corresponding ethanol only treatments. At 48 hrs, 5 μM free curcumin + 300 mM ethanol showed increased viability of 237% ($p=0.0030$) and 5 μM free curcumin + 350 mM ethanol showed increased viability of 369% ($p=0.0141$), when compared to the corresponding ethanol only treatment. At 72 hrs, significant increases in viability were observed after treatment with both 5 μM and 10 μM curcumin in all ethanol treated conditions. Treatment with 5 μM free curcumin + 200 mM ethanol showed increased viability of 88% ($p=0.0335$), 5 μM free curcumin + 300 mM ethanol showed a 1650% increase ($p=0.0002$) and 5 μM free curcumin + 350 mM ethanol showed increased viability of 1933% ($p<0.0001$), when compared to the corresponding ethanol only treated controls. Treatment with 10 μM free

curcumin + 200 mM ethanol showed increased viability of 139% ($p=0.0008$), 10 μM free curcumin + 300 mM ethanol showed a 2014% increase ($p<0.0001$) and 10 μM free curcumin + 350 mM ethanol showed increased viability of 1100% ($p= 0.0052$), when compared to the corresponding ethanol treatment. There was also a significant difference between 5 μM free curcumin + 350 mM ethanol and 10 μM free curcumin + 350 mM ($p=0.0367$).

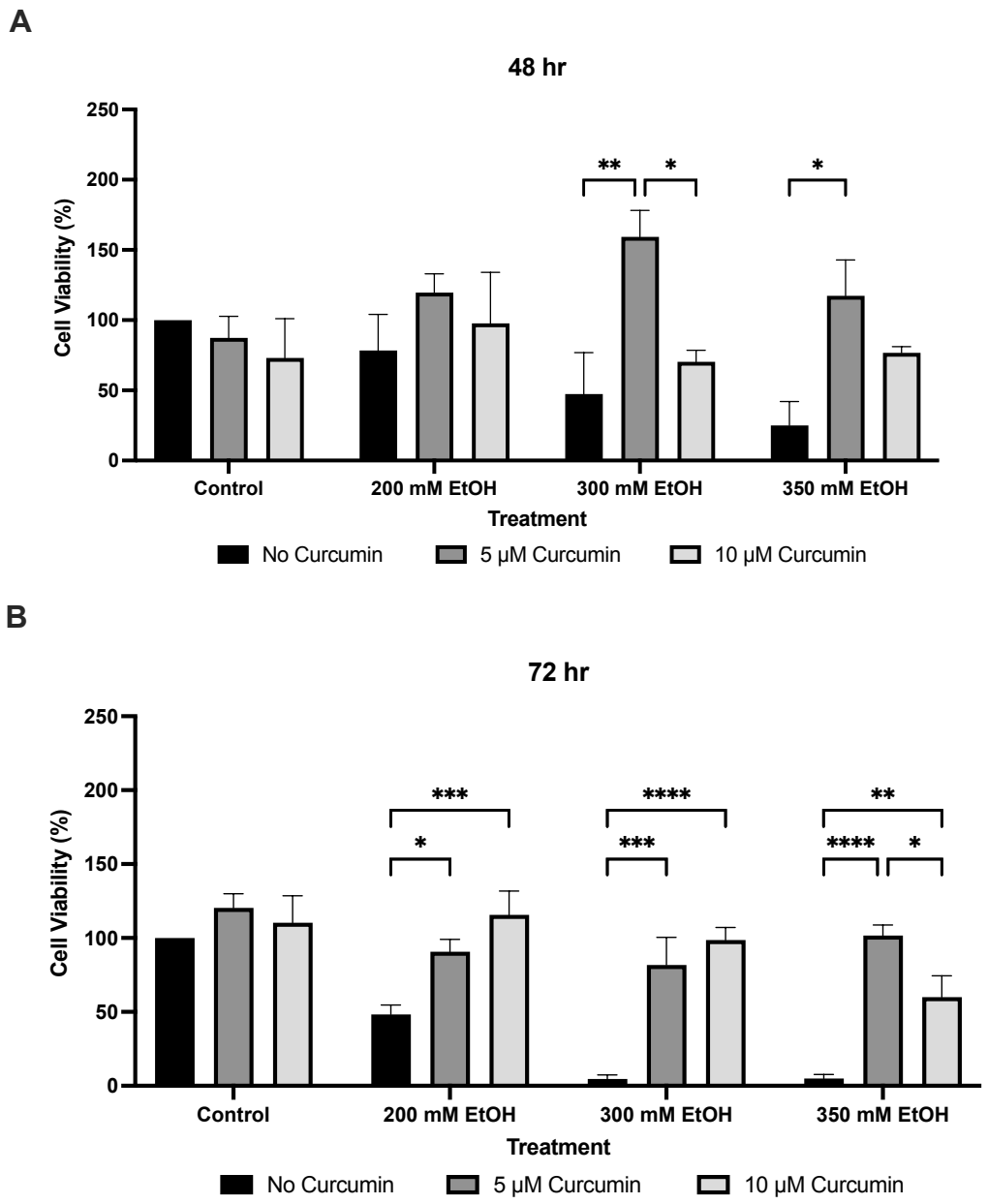

Figure 5.1 The effect of curcumin free drug and ethanol co-treatment on cell viability over a 72-hour period. A) percentage of cell viability at 48 hrs and B) percentage of cell viability at 72 hrs. Cells were seeded in 96-well plates and co-treated with 200 mM, 300 mM and 350 mM ethanol as well as 5 μM and 10 μM curcumin. Viability of cells was determined by the MTT assay and measured at 48 hrs and 72 hrs. Data is presented as percentage from the control. Results presented as mean ± SEM (n = 3) * P ≤ 0.05, ** P ≤ 0.01, *** P ≤ 0.001, **** P ≤ 0.0001.

5.3.3 Effect of curcumin DSPE-PEG nanoformulations on ethanol induced changes in cell viability

Novel nanocarrier delivery systems for the antioxidant curcumin were used to assess their ability in the protection against ethanol induced changed in VL-17A cells and changes in cell viability were measured. Curcumin was formulated in DSPE-PEG carriers with and without ascorbyl palmitate (AP) and cell viability was assessed using MTT assay.

At 48 hrs, 350 mM ethanol caused a reduction in cell viability by 45% when compared to the control. Blank formulations also reduced viability by 40%, free curcumin by 15% and nanoformualted curcumin by 20% without AP and 14% with AP. Despite the blank formulations causing reductions in viability when compared to DMEM control, 10 μM curcumin DSPE-PEG + AP increased viability by 78% ($p=0.0405$) and 10 μM curcumin DSPE-PEG increased viability by 24% when compared to 350 mM ethanol treatment alone, showing protection against ethanol induced loss of cell viability (**Figure 5.2**).

At 72 hrs, 350 mM ethanol caused a reduction in cell viability by 50% when compared to the control DMEM. Similarly, to 48 hrs, blank formulations also reduced viability by 40%, free curcumin by 10% and nanoformulated curcumin by 17% without AP. Curcumin DSPE-PEG + AP alone, increased viability by 3% compared to DMEM control. Despite the blank formulations causing reductions in viability at 72 hrs when compared to DMEM control, 10 μM curcumin DSPE-PEG + AP increased viability by 22% and 10 μM curcumin DSPE-PEG increased viability by 27% when compared to 350 mM ethanol treatment alone. This indicates nanoformulation curcumin has capacity to

reduce the effects of ethanol induced loss of viability at 48 hrs and 72 hrs in VL-17A cells (**Figure 5.2**).

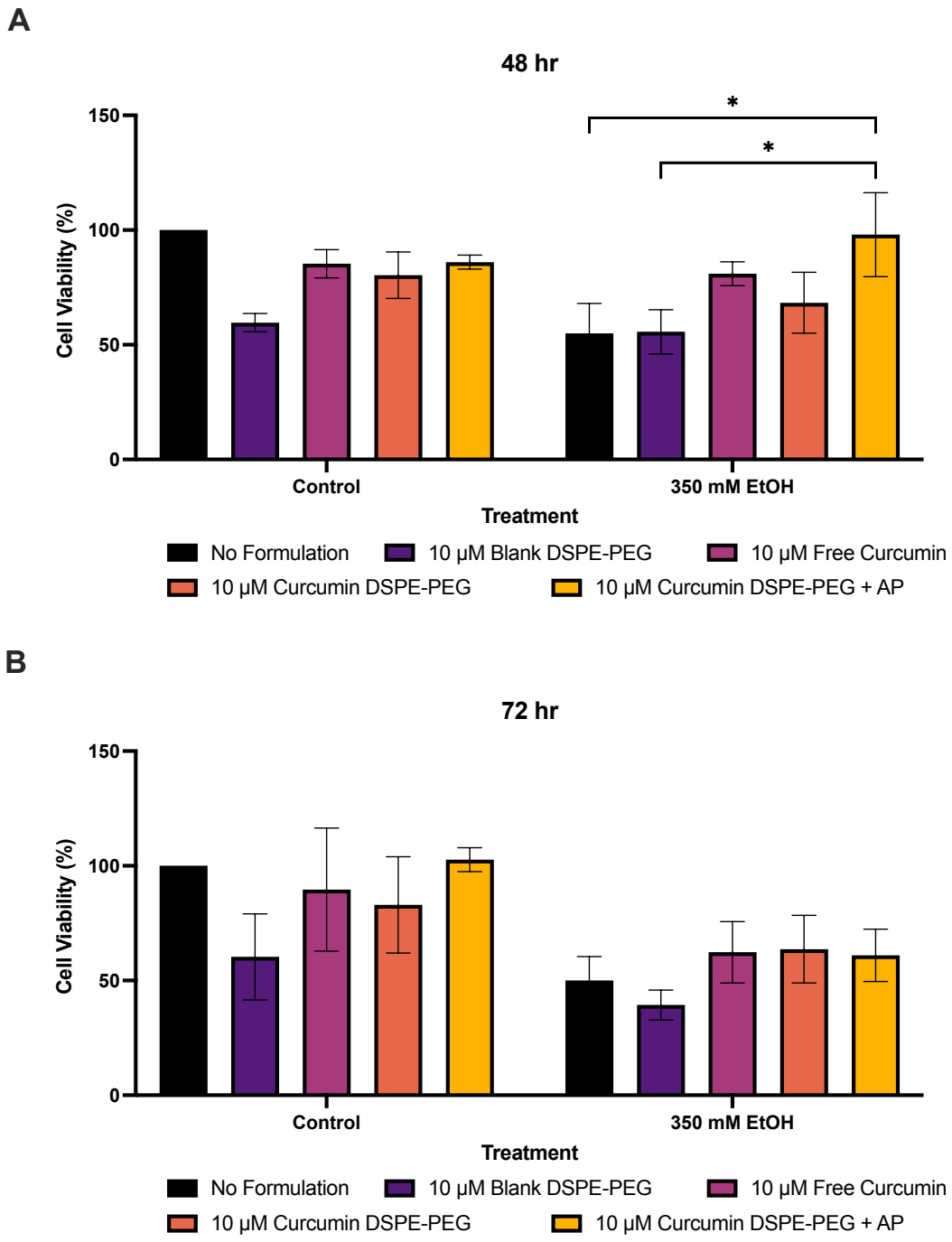

Figure 5.2 The effect of a 3-hr pre-treatment of nanoformulated curcumin on ethanol induced cell damage. A) percentage of cell viability at 48 hrs and B) percentage of cell viability at 72 hrs. Cells were seeded in 96-well plates and co-treated with 350 mM ethanol as well as 3 hr pre-treatment of formulations. Viability of cells was determined by the MTT assay and measured at 48 and 72 hrs. Data is presented as percentage from the control. Results presented as mean $\pm$ SEM (n = 3). * $P \leq 0.05$.

5.3.4 Effect of curcumin DSPE-PEG nanoformulations on ethanol induced changes in ROS accumulation

Novel nanocarrier delivery were also used to assess their ability to protect against ethanol induced changes in VL-17A cells. Curcumin was formulated in DSPE-PEG carriers with and without AP and ROS production was assessed using DCFDA.

Across the time points tested 350 mM ethanol did not increase ROS production compared to DMEM only control. Curcumin DSPE-PEG nanoformulations were shown to protect VL-17A cells against ROS production. At 30 mins, pre-treatment with 10 μM curcumin DSPE-PEG reduced ROS by 26% and 10 μM curcumin DSPE-PEG + AP reduced ROS by 33% and at 1 hr 10 μM curcumin DSPE-PEG a 20% reduction was observed, compared to corresponding ethanol only treatment. At 2 hrs, pre-treatment with 10 μM curcumin DSPE-PEG reduced ROS by 29% and 10 μM curcumin DSPE-PEG + AP significantly reduced ROS by 44% ($p=0.0326$) (**Figure 5.3**). Increases in ROS were observed at 24 hrs despite treatment with nanoformulations. At 48 hrs, pre-treatment with 10 μM curcumin DSPE-PEG reduced ROS by 36% ($p=0.0226$) and 10 μM curcumin DSPE-PEG + AP reduced ROS by 31%. At 72 hrs, pre-treatment with 10 μM curcumin DSPE-PEG significantly reduced ROS by 51% ($p=0.0013$) and 10 μM curcumin DSPE-PEG + AP significantly reduced ROS by 48% ($p=0.0024$) (**Figure 5.4**). At 72 hrs, blank formulation ($p=0.0029$) and free curcumin ($p=0.0116$) also significantly reduced ROS.

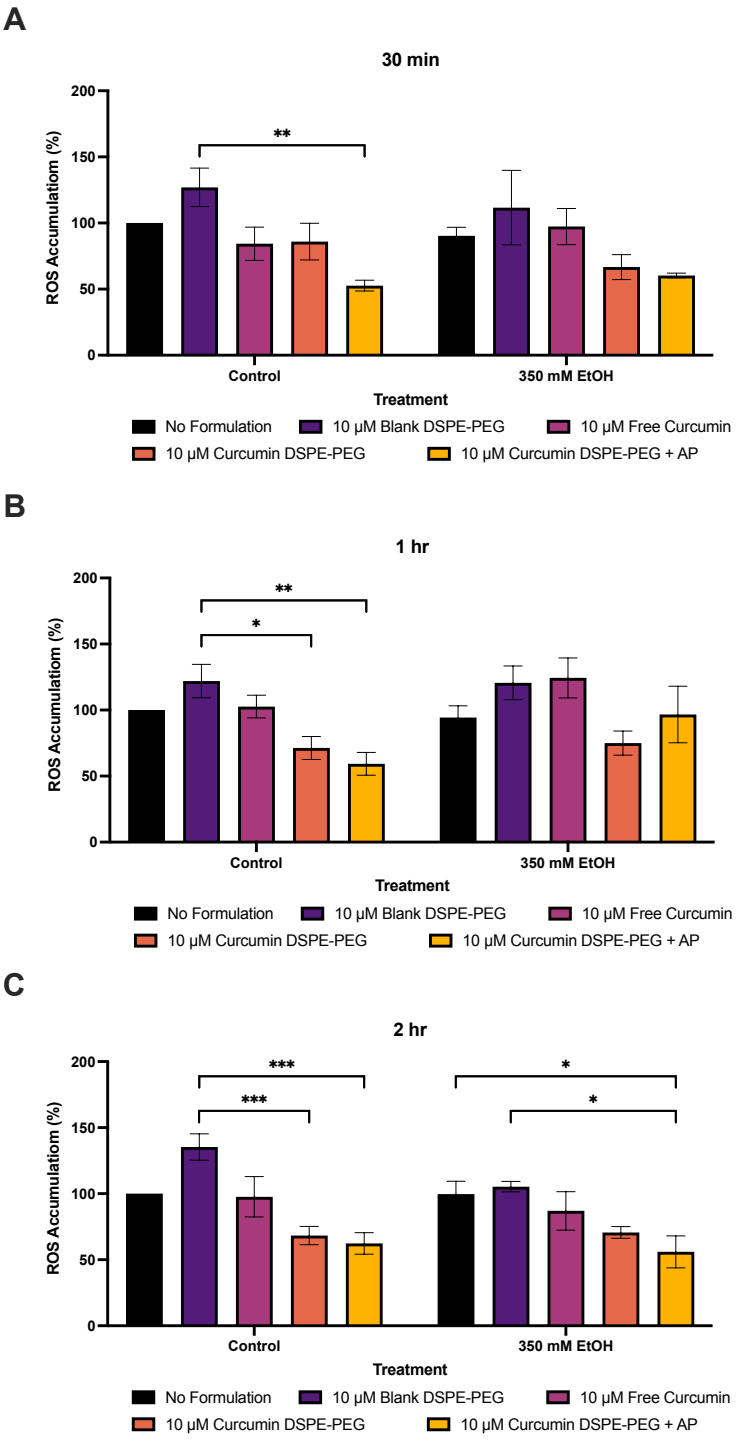

Figure 5.3 The effect of a 3-hr pre-treatment of nanoformulated curcumin on ethanol induced ROS production. A) ROS production at 30 mins, B) ROS production at 1 hr and C) ROS production at 2 hrs. Cells were seeded in 96-well plates and co-treated with 350 mM ethanol as well as 3 hr pre-treatment of formulations. ROS production was determined by an DCFDA assay. Data is presented as percentage from the control. Results presented as mean ± SEM (n = 3). * P ≤ 0.05, ** P ≤ 0.01, *** P ≤ 0.001.

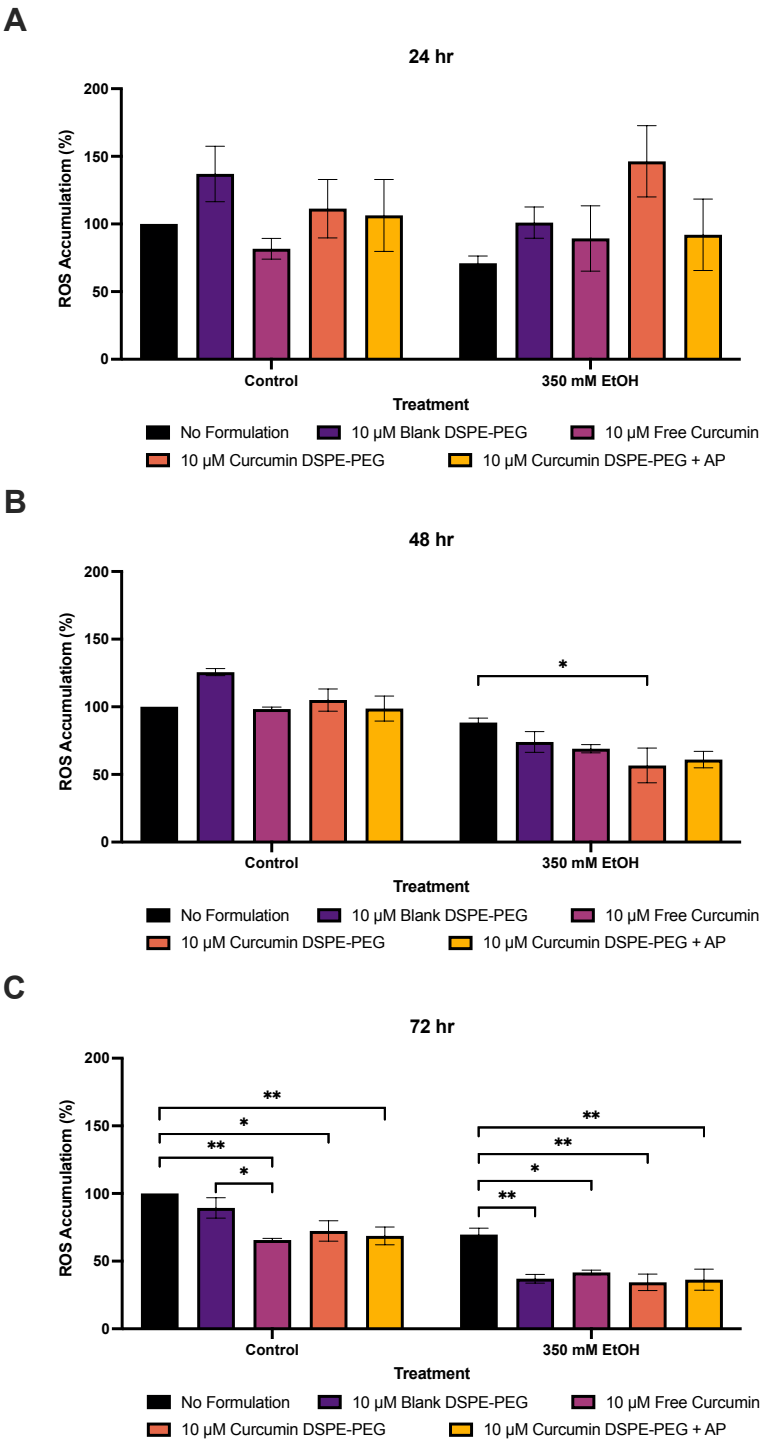

Figure 5.4 The effect of a 3-hr pre-treatment of nanoformulated curcumin on ethanol induced ROS production. A) ROS production at 24 hrs, B) ROS production at 48 hrs and C) ROS production at 72 hrs. Cells were seeded in 96-well plates and treated with 350 mM ethanol as well as 3 hr pre-treatment of formulations. ROS production was determined by an DCFDA assay. Data is presented as percentage from the control. Results presented as mean ± SEM (n = 3). * $P \leq 0.05$, ** $P \leq 0.01$.

5.3.5 Effect of curcumin DSPE-PEG nanoformulations on ethanol and iron induced changes in cell viability

To assess the novel nanocarrier delivery system in the protection against ethanol damage and iron overload in the liver, antioxidant curcumin was nanoforumalted in the carrier system DSPE-PEG with and without AP and used to assess changes in cell viability by the MTT assay. Both 350 mM ethanol and 50 μM iron were assessed in combination as well as 50 μM iron alone.

At 48 hrs, 50 μM iron caused a 25% reduction in viability and 350 mM ethanol + 50 μM iron also caused a reduction in cell viability by 52% when compared to the control DMEM. As described previously, blank formulations also reduced viability by 40%, free curcumin by 15% and nanoformualted curcumin by 20% without AP and 14% with AP. Despite the blank formulations causing reductions in viability, 350 mM ethanol + 50 μM iron as well as pre-treatment with 10 μM curcumin DSPE-PEG increased viability by 17% and pre-treatment with 10 μM curcumin DSPE-PEG + AP increased viability by 31% when compared to 50 μM iron treatment alone, showing protection against iron induced damage. Pre-treatment with 10 μM curcumin DSPE-PEG + AP also increased viability by 28% when compared to 350 mM ethanol + 50 μM iron treatment. This indicates nanoformulations of curcumin have the capacity to reduce the effects of ethanol and iron overload in in VL-17A cells (**Figure 5.5**). free curcumin was also shown to increase viability in the 50 μM iron group ($p=0.0464$).

At 72 hrs, 350 mM ethanol + 50 μM iron caused a reduction in cell viability by 36% when compared to the control DMEM. Similarly, to 48 hrs, blank formulations also reduced viability by 40%, free curcumin by 10% and nanoformulated curcumin by 17% without AP. Curcumin DSPE-PEG + AP alone, increased viability by 3% compared to DMEM control. Along with 350 mM ethanol + 50 μM iron, pre-treatment with 10 μM curcumin DSPE-PEG increased viability by 41% and 10 μM curcumin DSPE-PEG + AP increased viability by 40% when compared to 50 μM iron treatment alone. Nanoformulations were unable to provide protection against 350 mM ethanol + 50 μM iron treatment combined (**Figure 5.5**).

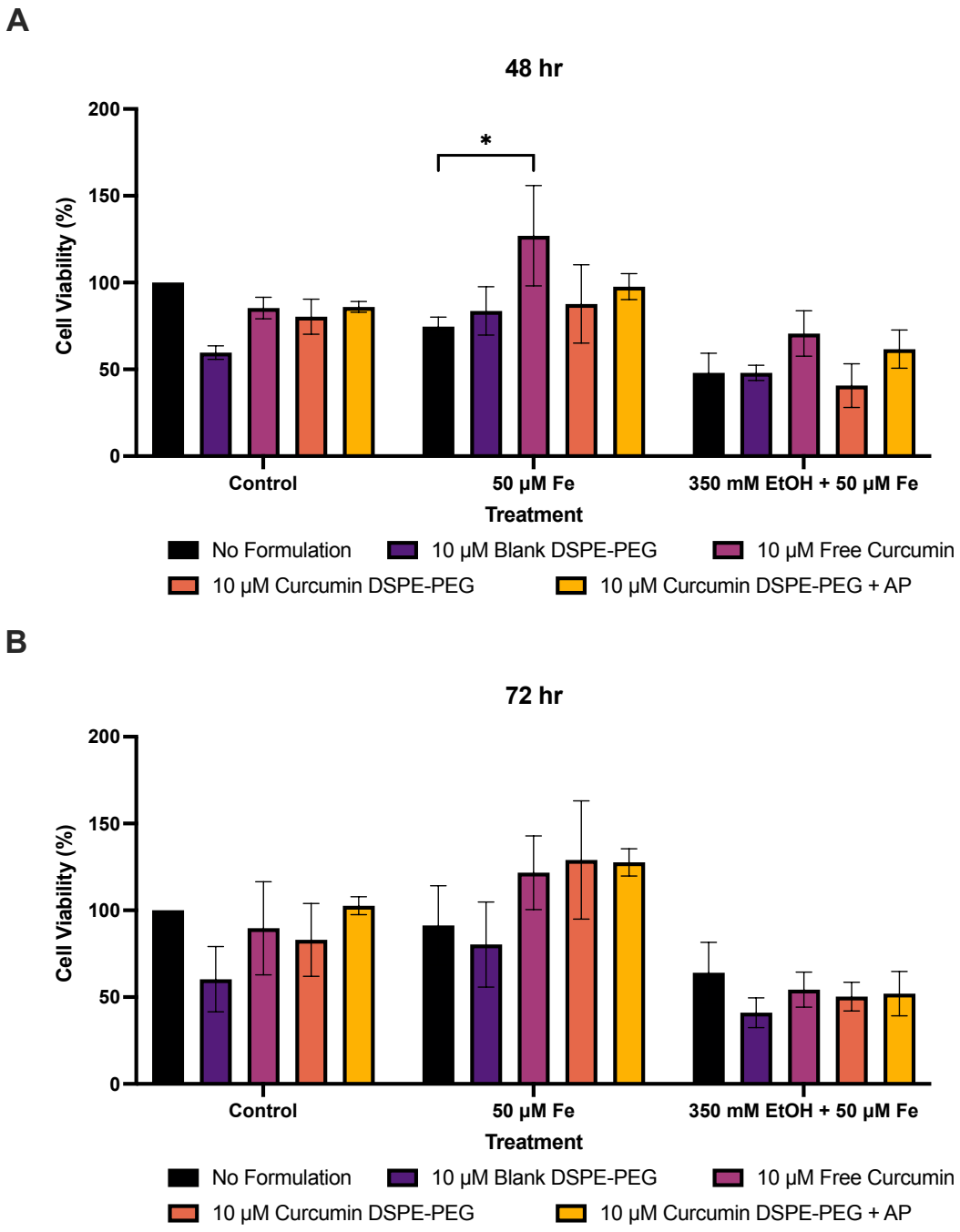

Figure 5.5 The effect of a 3-hr pre-treatment of nanoformulated curcumin on ethanol and iron induced cell damage. A) percentage of cell viability at 48 hrs and B) percentage of cell viability at 72 hrs. Cells were seeded in 96-well plates and co-treated with 350 mM ethanol and 50 µM iron as well as 3 hr pre-treatment of formulations. Viability of cells was determined by the MTT assay and measured at 48 and 72 hrs. Data is presented as percentage from the control. Results presented as mean ± SEM (n = 3). * $P \leq 0.05$.

5.3.6 Effect of curcumin DSPE-PEG nanoformulations on ethanol and iron induced changes in ROS accumulation

ROS production was assessed using DCFDA from 30 mins to 72 hrs to assess the ability of curcumin formulated in DSPE-PEG carriers with and without AP in the protection against ethanol and iron induced changes in VL-17A cells. ROS production was increased by the blank formulation; 27% at 30 mins, 22% at 1 hr, 35% at 2 hrs, 37% at 24 hrs and 26% at 48 hrs. Overall, curcumin DSPE-PEG nanoformulations showed some protection of VL-17A cells against ROS production caused by ethanol and iron overload.

At 30 mins, pre-treatment with 10 μM curcumin DSPE-PEG reduced ROS by 39% ($p=0.0070$) and pre-treatment with 10 μM curcumin DSPE-PEG + AP reduced ROS by 30%, in the 350 mM ethanol + 50 μM iron group, when compared to ethanol and iron combined treatment, respectively. In the 50 μM iron treated groups, 10 μM curcumin DSPE-PEG reduced ROS by 41% ($p=0.0005$) and 10 μM curcumin DSPE-PEG + AP reduced ROS by 36% ($p=0.0029$), when compared to 50 μM iron (**Figure 5.6**).

At 1 hr, 10 μM curcumin DSPE-PEG prior to 350 mM ethanol + 50 μM iron treatment also reduced ROS by 35% ($p=0.0122$), compared to corresponding ethanol and iron combined treatment (**Figure 5.6**). In the 50 μM iron treated groups, 10 μM curcumin DSPE-PEG reduced ROS by 34% ($p=0.0050$) and 10 μM curcumin DSPE-PEG + AP reduced ROS by 28% ($p= 0.0312$), when compared to 50 μM iron.

At 2 hrs, in the 350 mM ethanol + 50 μM iron groups, pre-treatment with 10 μM curcumin DSPE-PEG reduced ROS by 33% and 10 μM curcumin DSPE-PEG + AP reduced ROS by 21% (**Figure 5.6**). In the 50 μM iron treated groups, 10 μM curcumin DSPE-PEG reduced ROS by 33% and 10 μM curcumin DSPE-PEG + AP reduced ROS by 34% (p=0.0397), when compared to 50 μM iron.

No significant changes were observed at 24 hrs. However, at 48hrs, in the 350 mM ethanol + 50 μM iron groups, pre-treatment with 10 μM curcumin DSPE-PEG reduced ROS by 29% (p=0.0468). At 72 hrs, in the 350 mM ethanol + 50 μM iron groups, pre-treatment with 10 μM curcumin DSPE-PEG reduced ROS by 45% and 10 μM curcumin DSPE-PEG + AP reduced ROS by 21%, when compared to the 350 mM ethanol + 50 μM iron treatment (**Figure 5.7**). In the 50 μM iron treated groups, 10 μM curcumin DSPE-PEG reduced ROS by 36% (p=0.0015), and 10 μM curcumin DSPE-PEG + AP reduced ROS by 18% when compared to 50 μM iron.

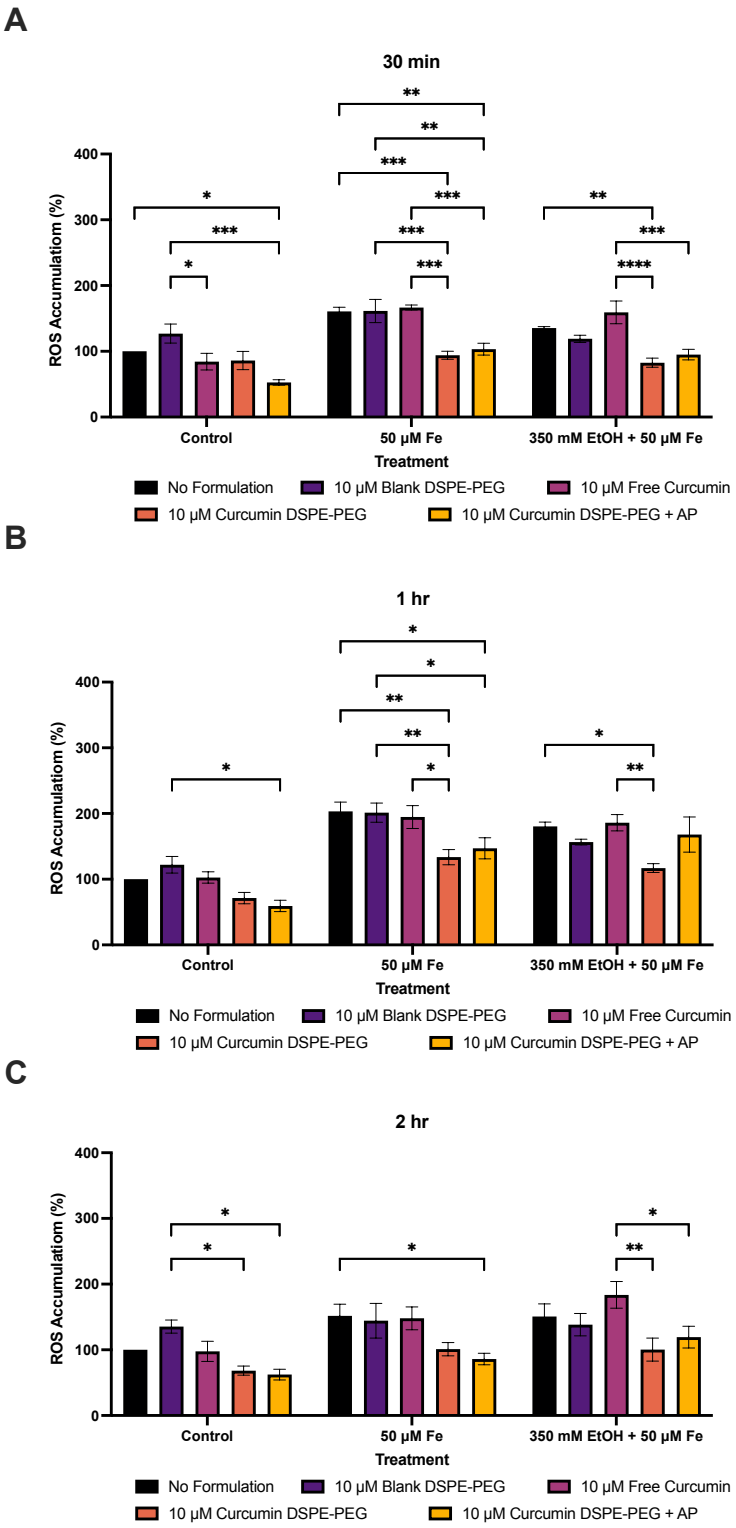

Figure 5.6 The effect of a 3-hr pre-treatment of nanoformulated curcumin on ethanol and iron induced ROS production. A) ROS production at 30 mins, B) ROS production at 1 hr and C) ROS production 72 hrs. ROS production was determined by the DCFDA assay. Data is presented as percentage from the control. Results presented as mean ± SEM (n = 3). * P ≤ 0.05, ** P ≤ 0.01, *** P ≤ 0.001, **** P ≤ 0.0001.

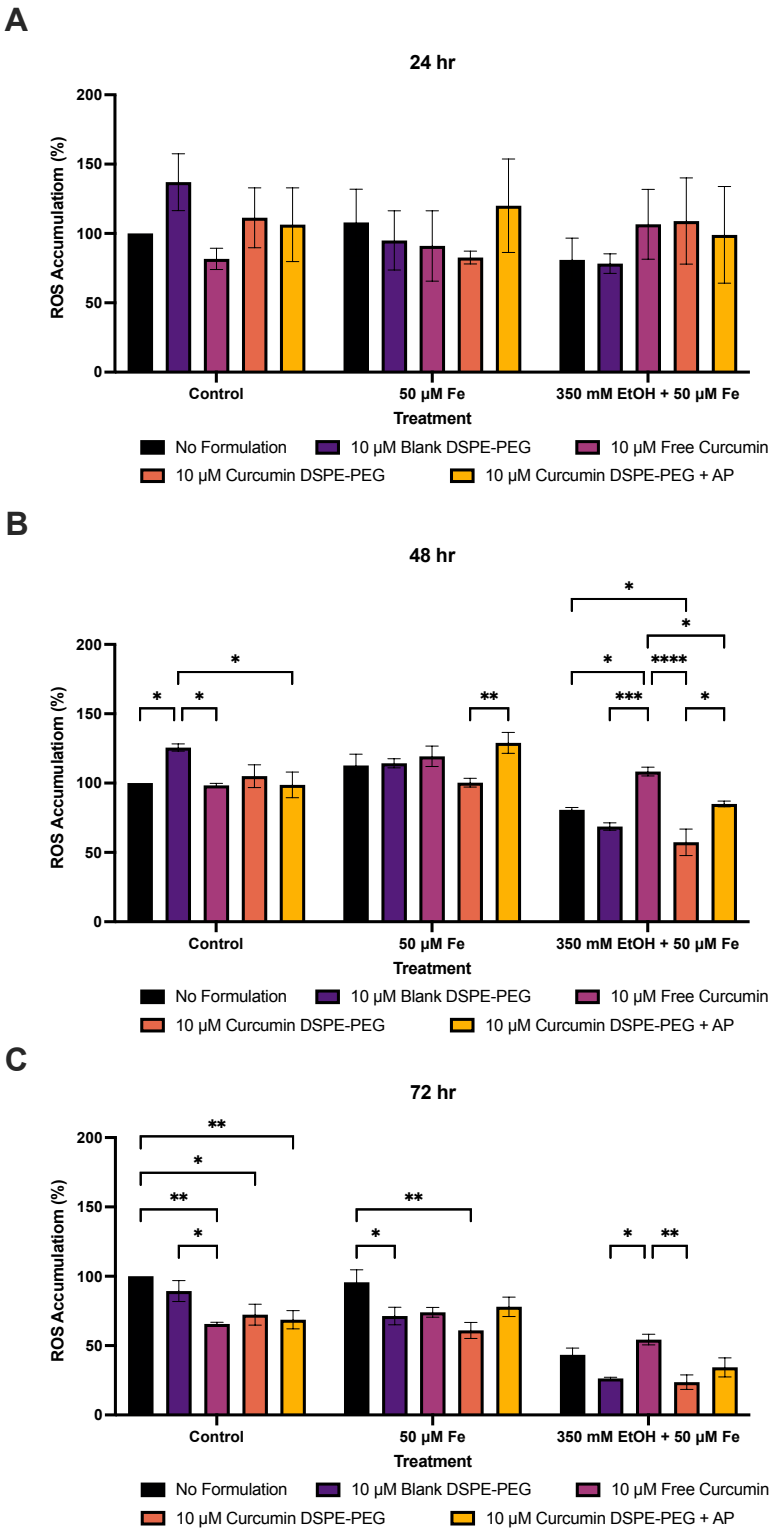

Figure 5.7 The effect of a 3-hr pre-treatment of nanoformulated curcumin on ethanol and iron induced ROS production. A) ROS production at 24 hrs, B) ROS production at 48 hrs and C) ROS production 72 hrs. ROS production was determined by the DCFDA assay. Data is presented as percentage from the control. Results presented as mean ± SEM (n = 3). * P ≤ 0.05, ** P ≤ 0.01, *** P ≤ 0.001, **** P ≤ 0.0001.

5.3.7 Effect of silibinin free drug on ethanol induced changes in cell viability

Silibinin at concentrations of 5 μM and 10 μM were tested in their ability to improve cellular viability in combination with ethanol and assess whether the antioxidant compound can provide protection against ethanol and induced damage to the liver. Silibinin was added as co-treatments alongside ethanol.

As described previously, at 48hrs, 200 mM ethanol led to a 22% reduction in viability, 300 mM led to a 53% reduction and 350 mM led to a 75% reduction in viability and at 72 hrs mM ethanol led to a 52% reduction in viability and 300 mM and 350 mM both led to a 95% reduction in viability. After the addition of silibinin to the ethanol treatments, it reduced the effects of ethanol induced loss of viability at both 48 hrs and 72 hrs when compared to corresponding ethanol only treatments.

At 48 hrs, no significant differences were observed. However, 5 μM silibinin + 200 mM ethanol increased viability by 57% and 10 μM silibinin + 200 mM ethanol increased viability by 1% when compared to 200 mM ethanol only treatment. 5 μM silibinin + 300 mM ethanol increased viability by 138% and 10 μM silibinin + 300 mM ethanol increased by 87% as well as 5 μM silibinin + 350 mM ethanol increasing by 441% and 10 μM silibinin + 350 mM increasing by 113%, when compared to corresponding ethanol only controls (**Figure 5.8**).

Significant changes were observed at 72 hrs and treatment with 5 μM silibinin + 200 mM increased viability by 55% and 10 μM silibinin + 200 mM increased viability by 59% when compared to 200 mM ethanol only treatment. 5 μM

silibinin + 300 mM increased viability by 986% (p=0.0059) and 10 μM silibinin + 300 mM increased by 1450% (p=0.0001) as well as 5 μM silibinin + 350 mM increasing by 1320% (p=0.0001) and 10 μM silibinin + 350 mM increasing viability by 400%, when compared to corresponding ethanol only controls (**Figure 5.8**).

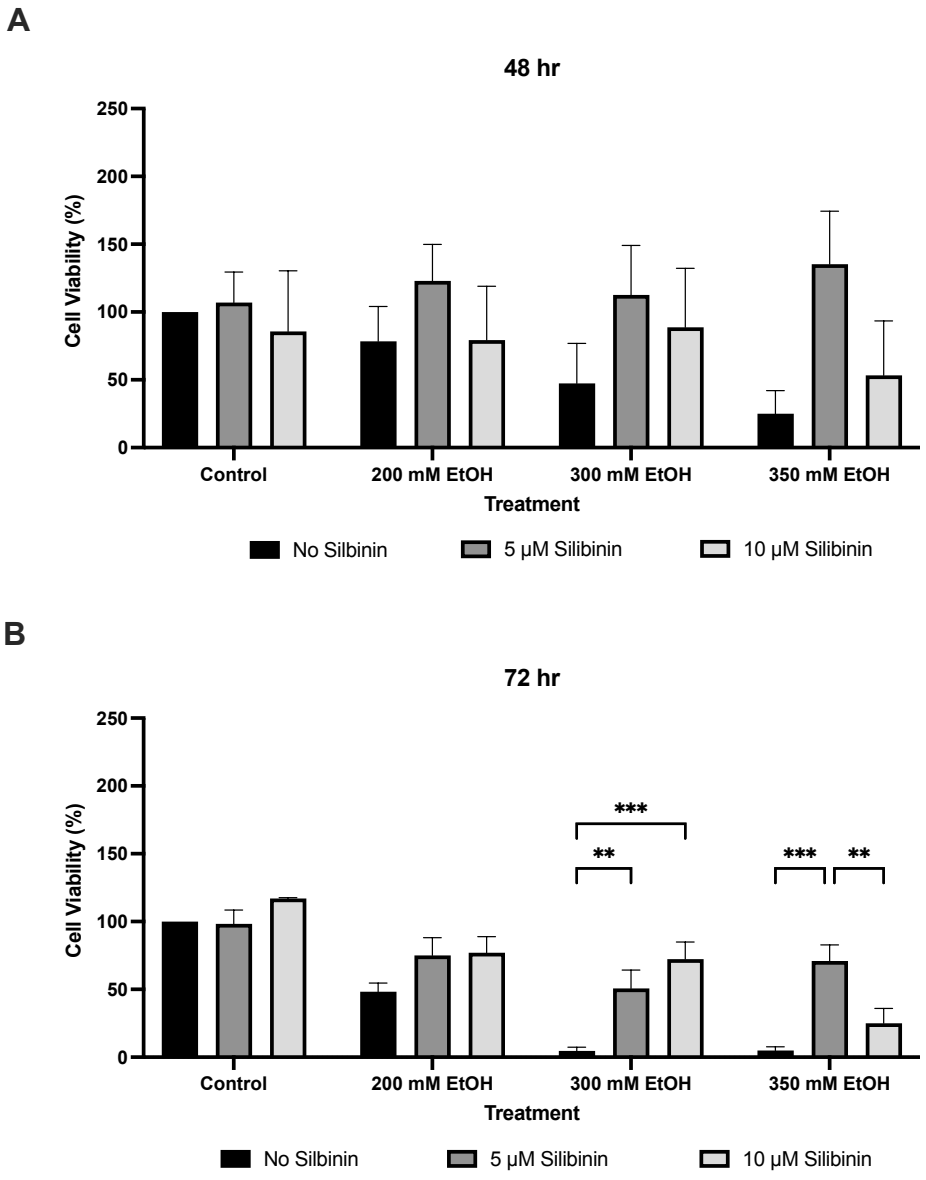

Figure 5.8 The effect of silibinin free drug and ethanol co-treatment on cell viability over a 72-hour period. A) percentage of cell viability at 48 hrs and B) percentage of cell viability at 72 hrs. Cells were seeded in 96-well plates and co-treated with 200 mM, 300 mM and 350 mM ethanol as well as 5 μM and 10 μM silibinin. Viability of cells was determined by an MTT assay and measured at 48 hrs and 72 hrs. Data is presented as percentage from the control. Results presented as mean ± SEM (n = 3). ** $P \leq 0.01$, *** $P \leq 0.001$.

5.3.8 Effect of silibinin free drug on ethanol and iron induced changes in cell viability

Silibinin, an extract of milk thistle, were then used to assess their ability in the protection against ethanol induced damage in VL-17A cells and changes in cell viability by the MTT assay were measured.

At 48 hrs, 350 mM ethanol led to a 79% reduction in viability, 50 μM iron led to a 53% reduction in viability and 350 mM ethanol + 50 μM iron led to a 92% reduction in cell viability. Treatment with 10 μM silibinin alone also reduced viability by 18%. However, when compared to corresponding treatments, 350 mM ethanol + 10 μM silibinin led to a 219% increase ($p=0.0266$) in viability when compared to ethanol alone, 50 μM iron + 10 μM silibinin led to a 84% increase in viability when compared to iron alone and 350 mM ethanol + 50 μM iron + 10 μM silibinin led to a 612% increase ($p=0.0131$) in cell viability when compared to 350 mM ethanol + 50 μM iron treatment.

At 72 hrs, 350 mM ethanol led to a 40% reduction in viability, 50 μM iron led to a 22% reduction in viability and 350 mM ethanol + 50 μM iron led to a 77% reduction in cell viability. Treatment with 10 μM silibinin alone also reduced viability by 16%, when compared to control DMEM only. However, when compared to corresponding treatments, 350 mM ethanol + 50 μM iron + 10 μM silibinin led to a 125% increase in cell viability when compared to 350 mM ethanol + 50 μM iron treatment.

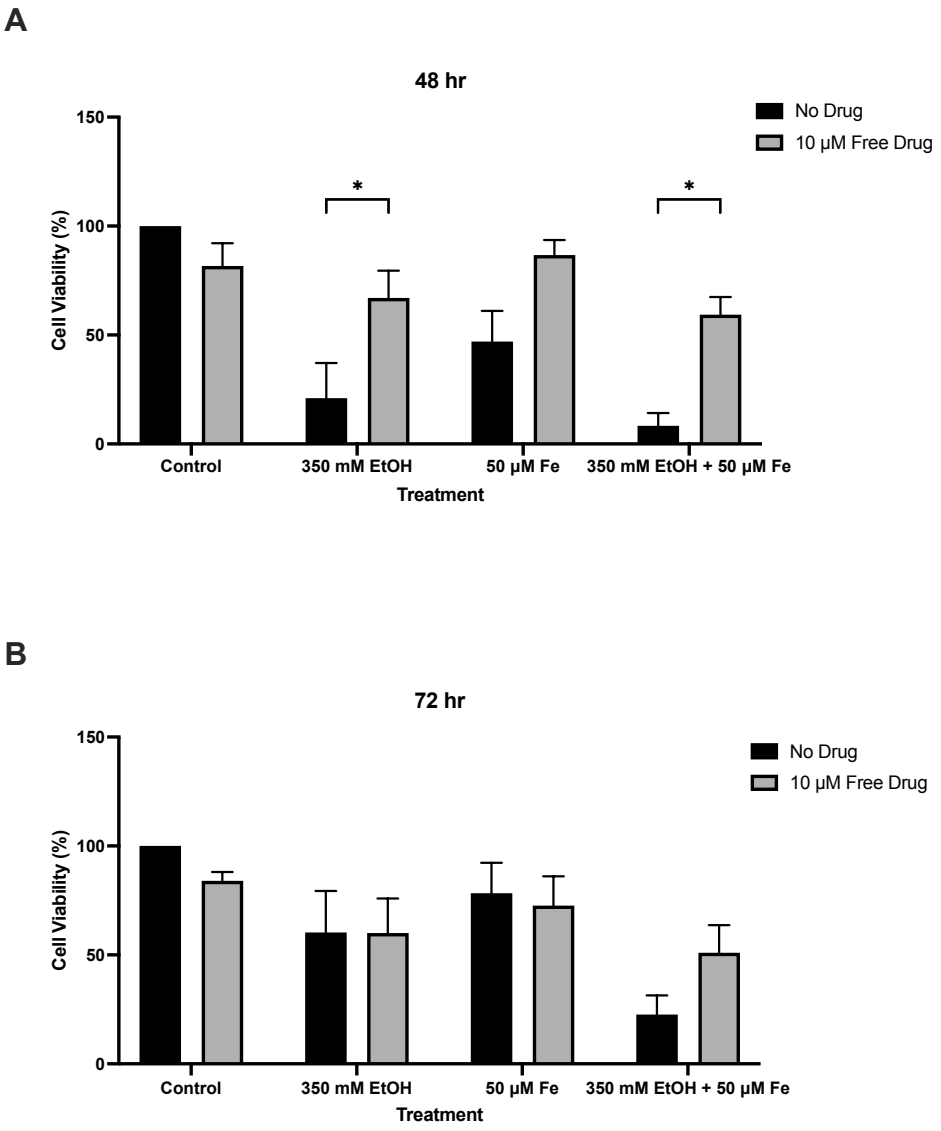

Figure 5.9 The effect of silibinin free drug and ethanol and iron co-treatment on cell viability over a 72-hour period. A) percentage of cell viability at 48 hrs and B) percentage of cell viability at 72 hrs. Cells were seeded in 96-well plates and co-treated 350 mM ethanol, 50 μM iron and 350 mM ethanol + 50 μM iron in combination as well as 10 μM silibinin. Viability of cells was determined by an MTT assay and measured at 48 hrs and 72 hrs. Data is presented as percentage from the control. Results presented as mean ± SEM (n = 3). * $P \leq 0.05$.

5.4 Discussion

There is increasing evidence that antioxidant therapy provides protection against ALD and may provide some promise in their therapeutic potential to treat ALD, however, their lack of targeted delivery and low bioavailability causes limitations to its full potential. Antioxidant compounds such as curcumin and silibinin (milk thistle) were investigated in this study.

Curcumin, the main active component in turmeric, has been shown to produce antioxidant properties as well as anti-inflammatory and anticarcinogenic properties. HepG2 cells treated with hydrogen peroxide (to induce oxidative stress) have been shown when also treated with curcumin, levels of ROS and malondialdehyde accumulation were reduced as well as increasing antioxidant enzyme capacity such as superoxide dismutase and catalase (Machado et al., 2023). Silibinin, a main component in the milk thistle plant is known to be a potent antioxidant, as well as containing antifibrotic, anti-inflammatory and hepatoprotective properties and treatment with milk thistle has been shown to lower liver enzymes in patients with ALD as well as improver overall 4-year survival. Similarly, to curcumin, silymarin has also been shown to increase by superoxide dismutase and glutathione peroxidase as well as reduce malondialdehyde levels.

Although natural compounds such as curcumin are quickly absorbed after oral ingestion, their concentrations in the bloodstream are limited due to low oral bioavailability. Novel nanocarrier delivery systems have become of interest due to the ability to enhance the stability, bioavailability, and delivery to targeted cells as well as their ability to cross biological membranes and co-

deliver treatments to the desired location. Formulations have also been developed to increase solubility as well as protecting it from being inactivated via hydrolysis (Jabczyk et al., 2021). The aim of this study was to use DSPE-PEG nanocarrier systems to encapsulate curcumin to assess their ability in protecting against reduced cell viability and increased ROS production observed in ALD and iron overload.

Curcumin alone or in combination with AP were successfully encapsulated into DSPE-PEG nanocarriers. All curcumin DSPE-PEG nanoformulations demonstrated high encapsulation efficiency (74-78%) although drug loading was approximately 7% for both nanoformulations. The mean nanoformulation particle sizes were <9 nm for both formulations and the polydispersity index measurements indicated low polydispersity index values <0.45 for both DSPE-PEG nanoformulations. As higher polydispersity index values are indicative of a broader size distribution within the particle sample, this data confirms overall uniformity of the particle solutions below 0.7, which indicates broad particle size distribution (Danaei et al., 2018). The surface charge of nanoformultions was -15.20 and -15.10 mV, and can be considered neutral, as solutions of ± 30 mV are considered strongly cationic and strongly anionic (Clogston and Patri, 2011).

Experiments were carried out on VL-17A cell lines due to their overexpression of both the alcohol metabolising enzymes, CYP2E1 and ADH. Concentrations of nanocarriers were used at theoretical doses of 10 μM in accordance with previously published data (Mursaleen et al., 2020, 2023; Mursaleen, Somavarapu and Zariwala, 2020).

Across all concentrations and time points free curcumin was shown to significantly increase viability of cells treated with varying concentrations of ethanol, and treatment with both concentrations of curcumin completely mitigating loss of viability back to control levels in some cases. Studies have suggested that curcumin both *in vitro* and *in vivo* may act on pathways associated with liver disease such as TGF-β1/Smad, JNK1/2-ROS, NF-κB as well as antioxidant signalling (Lukkunaprasit et al., 2023).

Despite blank formulations causing cytotoxicity to cells, all curcumin DSPE-PEG nanocarriers were able to protect to at least the same extent as the free curcumin against the ethanol induced loss of cell viability at both 48 hrs and 72 hrs, suggesting that these 3 hr pre-treatments could be protective against cell death and damage in ALD. However, curcumin DSPE-PEG + AP was the only curcumin nanocarrier able to protect against both ethanol and iron combination treatment, suggesting that AP may increase the protective effects of curcumin. Curcumin DSPE-PEG nanocarriers were also able to protect against ethanol-induced oxidative stress as measured by DCFDA assay and ROS production was significantly reduced by both curcumin DSPE-PEG nanocarriers and curcumin DSPE-PEG + AP nanocarriers, showing protection against the cellular antioxidant activity against 350 mM ethanol. Both curcumin DSPE-PEG with and without AP were also able to reduce ROS production, however, curcumin DSPE-PEG had more protection than curcumin DSPE-PEG + AP at reducing ROS production due to both excessive ethanol and iron overload.

The ability of curcumin DSPE-PEG + AP nanocarriers to match or exceed the antioxidant capability of curcumin DSPE-PEG alone may be due to the

pentose-phosphate pathway. The pentose-phosphate pathway is an important part of glucose metabolism which does not provide ATP, but instead supplies NADPH. NADPH is also then required for conversion of oxidised glutathione to reduced glutathione via glutathione reductase, which is essential for antioxidant defence mechanisms. Studies have shown that glutathione is involved in the maintenance of reduced vitamin C *in vitro*. *In vivo* studies have shown that supplementation with vitamin C maintains levels of reduced glutathione, and improves antioxidant capacity (Sitohang et al., 2021), therefore, these antioxidants may be interlinked. Pre-treatment with vitamin C in T cell lines (Jurkat and H9 human T lymphocytes) has also been shown to stimulate activity of the pentose-phosphate pathway, increasing intracellular glutathione levels and inhibiting cell death (Puskas et al., 2000). The antioxidant capacity of vitamin C has also been shown to inhibit hydrogen peroxide induced changes in mitochondrial membrane potential as well as inhibit cell death pathways and increase glutathione (Puskas et al., 2000). Vitamin C's effectiveness is due to its abundant presence and its rapid reaction rate with free radicals (Puskas et al., 2000). Therefore, the ability of curcumin nanocarrier to protect against ethanol mediated loss of viability and increases in ROS may be due to their potential in increasing intracellular glutathione, thus improving antioxidant capacity. The use of AP in curcumin encapsulation may therefore heighten its antioxidant capacity and free radical scavenging ability. This data supports the concept of curcumin and AP use in antioxidant therapy for ALD, since ethanol is implicated in the loss of antioxidant capacity and increases in oxidative stress.

Similarly, across all time points and concentrations free silibinin was shown to significantly increase viability of cells treated with ethanol, and treatment with both 5 μM and 10 μM concentrations of silibinin was able to ameliorate the ethanol induced loss of viability observed, and in some cases, even beyond control levels. Free silibinin was also able to significantly protect against loss of viability caused by a combination of both ethanol and iron at 48 hrs. The mechanisms of action of silibinin are complex but highly beneficial to hepatocytes. Silibinin is able to block toxins from entering hepatocytes as well as preventing against apoptosis and intracellular free radicals (Kostek et al., 2012). Antioxidant enzyme functions can also be modified by silibinin and concentrations of by superoxide dismutase, glutathione and glutathione peroxidase are increased (Kostek et al., 2012). Silibinin also functions to stabilise and strengthens cell membranes as well regenerate the liver.

The mechanism behind the beneficial properties of silibinin are most likely due to its ability to directly scavenge ROS and nitric oxide and increase levels of glutathione. Its hepatoprotective properties against ethanol have been previously well established. Milk thistle compounds primarily enhances the levels of glutathione via enhanced expression of transcription factor Nrf2, as well as by increasing the availability of cysteine (Giustarini et al., 2023). This is achieved by promoting cysteine synthesis and inhibiting its conversion to taurine. It is also thought that the protective properties of milk thistle and its compound silibinin are due to its ability to directly scavenge ROS and free radicals as well as maintain the redox balance in cells. In HepG2 cells, silibinin has also been shown to regulate metabolic enzymes of liver inflammation by increasing NAD+ and SIRT2 levels (Zhang et al., 2021). Both *in vitro* and *in*

vivo silibinin has been shown to modulate mitochondrial function via upregulated SIRT3 expression (Y Li et al., 2017). Together, these actions synergistically lead to heightened glutathione levels within cells.

5.5 Conclusion

In this study, potent antioxidant compounds were encapsulated into nanocarriers to assess their potential in protecting against ethanol and iron induced damage to VL-17A cells. Results show both free curcumin and silibinin were able to significantly increase viability of cells treated with ethanol, mitigating loss of viability, demonstrating their antioxidant capacity and beneficial effects to hepatocytes. Overall, this study demonstrates for the first time that successful encapsulation of curcumin DSPE-PEG carriers provides protection against oxidative stress in a cellular model of ALD. The results show that ethanol alone as well as in combination with iron causes significant reduction in cell viability and increase ROS production and treatment with encapsulated antioxidants was able to enhance or match the protective effects of the free drugs. Curcumin DSPE-PEG nanocarriers were observed to have a higher antioxidant capacity providing protection against oxidative stress in a cellular model of ALD and iron overload. Treatment for ALD is limited and has not progressed for many years. This study demonstrates evidence for the use of nanoformulated antioxidants in the treatment of ALD and iron overload. However, further investigations are required to assess the ability of these formulations to protect against other parameters of ALD such as mitochondrial function.

CHAPTER 6 ALCOHOL CONSUMPTION AND LIVER IRON UK BIOBANK STUDY

Description of Chapter

This chapter focuses on analysis of UK BioBank data. Iron overload is commonly associated with chronic liver disease due to alcohol consumption and causes further oxidative stress and damage to the liver. Magnetic resonance imaging (MRI) has emerged as a reliable method for detecting iron overload in the liver, however, limited studies exist exploring liver iron measured by MRI in relation to alcohol use. This study assessed liver iron content and self-reported frequency of drinking in a population of 25,781 individuals within the UK Biobank Cohort and assessed differences in relation to sex, body composition (BMI), age, concentration of liver iron, percentage of liver fat and frequency of drinking.

6.1 Introduction

Iron overload disorders encompass a range of conditions characterised by an excessive accumulation of iron throughout the body, leading to damage in various organs. When assessing elevated liver enzymes, it is frequently observed that the levels of ferritin and transferrin-bound iron saturation are elevated.

Iron is a key player in the human body necessary for enzyme function, oxygen transport and oxidative phosphorylation (Milic et al., 2016). Cells are also able to store iron within ferritin, which is thought to be bioavailable. Hepatocytes are a major producer of ferritin controlled by the iron response element/iron regulatory protein network (Milic et al., 2016) and therefore play an essential role in mobilisation of iron. The liver synthesises most of the proteins required

for the metabolism of iron, most importantly this includes including hepcidin and transferrin. Transferrin can bind iron reversibly and therefore is important due to its ability as an iron donor or acceptor. Hepcidin is a protein which functions as a key regulator in the metabolism of iron ad its expression is regulated by the bone morphogenetic protein and JAK2/STAT3 signalling pathways (Nemeth and Ganz, 2009). Hepcidin synthesis is determined by the amount of iron in the blood and regulated iron delivery by ferroportin.

During chronic liver disease, iron regulation may be disrupted as the liver plays an essential role in iron homeostasis and regulation. Elevated serum ferritin has been documented in chronic alcohol users which leads to an increase in hepatic iron stores. In chronic liver disease hepcidin is also decreased (Nemeth and Ganz, 2009). When hepcidin levels are decreased, iron overload occurs leading to iron deposits in the liver (Milic et al., 2016). As well as hepcidin, iron can cause an increase in hydroxyl radicals when combined with ROS can lead to phospholipid peroxidation as well as DNA strand breaks. Liver injury may also be increased due to elevated intestinal absorption causing oxidative stress and lipid peroxidation, and iron overload in patients with ALD may be a factor for disease progression (Milic et al., 2016).

Due to the relationship between ALD and iron overload, it is crucial to identify individuals with iron overload as well as determine its prevalence in the population, enabling early identification and disease severity. Approximately 50% of ALD patients exhibit iron overload in the liver (Mueller and Rausch, 2015; Ali, Ferrao and Mehta, 2022). Unfortunately, liver biopsies are considered the gold standard for diagnosis and evaluation of liver iron levels, and due to their invasive procedure, liver biopsy is not recommended for

routine clinical use. Magnetic resonance imaging (MRI) has become a well-established and reliable method for detecting iron overload in the liver. MRI-based measurements of liver iron follow the principle MR signal decay is affected by the iron levels in the tissue, therefore, higher iron levels lead to faster signal decay (McKay et al., 2018). Although liver iron content measured by MRI has previously been studied in large cohorts of the general population, limited studies exist exploring the liver iron and alcohol use. This study assessed liver iron content and alcohol use in a population of over 25,000 individuals within the UK Biobank Cohort to research examine differences in relation to gender, body composition liver iron, liver fat and alcohol use.

6.2 Aims and Objectives

The primary aim of this chapter was to investigate the association between frequency of drinking and liver iron content and percentage of liver fat. Specific research objectives were to:

1. Determine if there is a correlation between alcohol consumption (frequency of drinking) and levels of iron in the liver?
2. Determine if there is a correlation between vitamin intake and levels of iron in the liver?

6.3 Patients and Methods

Biobank Participants

The UK Biobank has recruited over 500,000 individuals aged between 40-69 years in 2006-2010 from across the UK. This research has been conducted using data accessed via the UK Biobank. This study assessed 25,781

participants to determine how the frequency of alcohol intake affects liver iron according to sex, age, and liver fat.

Statistical Analysis

Summary data is presented as median values with interquartile range. Statistical analyses were undertaken using GraphPad Prism (Version 9.5.1) and R 4.1.2 and RStudio 2022.02.0+443 "Prairie Trillium" Release. Normality and distribution were assessed using Kolmogorov-Smirnov test. Liner regression model analysis was completed and post hoc analyses using Tukey's honest significant difference test were performed using the R package multicomp (Hothorn, Bretz and Westfall, 2008).

6.4 Results

Liver iron and liver fat content (PDFF) was measured in 25781 participants from the UK BioBank. Participants were 54.23% male and 45.77% female, aged between 45 and 82 (during assessment centre visit at time of MRI). The majority of patients are White (97.54%), and no significant differences were seen between iron content between ethnicities. However, significant differences were observed in liver fat between White (median; 3.082%) and Asian (median; 3.353%) participants (p=0.0270). Differences in vitamin and mineral supplementation were also measured. The participant demographics are documented in **Table 6.1**.

Frequency distribution analysis of alcohol consumption is summarised in **Table 6.2.** Data has shown that 21.70% of male participants drank daily or almost daily compared to 14.12% female participants. 33.51% men drank three to four times a week, 27.47% drank one to two times a week, 9.96% drank one to three times a month and 7.35% drank special occasions only. 27.35% females drank three to four times a week, 29.53% drank one to two times a week, 14.63% drank one to three times a month and 14.37% drank special occasions only. Most men drank three to four times a week whereas most females drank one to two times a week.

When analysing age and frequency of drinking, 13.61% participants aged 40-49, 12.96% aged 50-59, 18.59% aged 60-69, 23.26% ages 70-79 and 30.53% 80-89 reported to consume alcohol daily or almost daily with 80-89 years having highest frequency of drinking. The highest frequency of drinking was

one to two times a week in 40-49 years and 50-59 years, three to four times a week in both 60-69 years and 70-79 years.

When analysing BMI and frequency of drinking, 18.16% participants BMI <20 kg/m^2, 18.88% BMI 20-24.9 kg/m^2, 19.94% BMI 25-29.9 kg/m^2, 16.40% BMI 30-34.9 kg/m^2 and 11.76% BMI >35 kg/m^2 reported to consume alcohol daily or almost daily with BMI 25-29.9 kg/m^2 having the highest frequency of drinking. The highest frequency of drinking was three to four times a week for BMI ranges <20 kg/m^2, 20-24.9 kg/m^2 and 25-29.9 kg/m^2 and one to two times a week in 30-34.9 kg/m^2 and >35 kg/m^2 ranges.

Frequency of drinking in participant ethnicities was also analysed and presented in **Table 6.2**. Daily or almost daily drinking was reported in 18.40% White participants, 12.26% mixed participants, 11.54% Asian participants and 7.75% Black participants.

Table 6.1 Demographics of participant analysed data in a UK BioBank cohort of alcohol consumers. Data shown as number of participants and percentage of participants.

	Participants (n)	Participants (%)
Total	25781	
Sex		
Male	13980	54.23%
Female	11801	45.77%
Age (Years)		
40–49 years	551	2.14%
50–59 years	7317	28.38%
60–69 years	10772	41.78%
70–79 years	6951	26.96%
80-89 years	190	0.74%
BMI (kg/m^2)		
<20 kg/m^2	716	2.78%
20–24.9 kg/m^2	9445	36.64%
25–29.9 kg/m^2	10887	42.23%
30–34.9 kg/m^2	3629	14.08%
>35 kg/m^2	1104	4.28%
Ethnicity		
White	25147	97.54%
Mixed	106	0.41%
Asian	234	0.91%
Black	129	0.50%
Other ethnicity	103	0.40%
Do not know/preferred not to answer	62	0.24%

Table 6.2 Frequency analysis and participant demographics for frequency of drinking in a UK BioBank cohort. Data shown as number of participants and percentage of participants.

	Daily or almost daily		3 – 4 times a week		1 – 2 times a week		1 – 3 times a month		Special occasions only	
	n	**%**	**n**	**%**	**n**	**%**	**n**	**%**	**n**	**%**
Total	4700	18.23	7912	30.69	7325	28.41	3120	12.10	2724	10.57
Sex										
Male	3034	21.70	4685	33.51	3840	27.47	1393	9.96	1028	7.35
Female	1666	14.12	3227	27.35	3485	29.53	1727	14.63	1696	14.37
Age (Years)										
40–49 years	752	13.61	124	22.50	185	33.58	106	19.24	61	11.07
50–59 years	948	12.96	2129	29.10	2383	32.57	1053	14.39	804	10.99
60–69 years	2002	18.59	3541	32.87	2973	27.60	1214	11.27	1042	9.67
70–79 years	1617	23.26	2082	29.95	1745	25.10	720	10.36	787	11.32
80-89 years	58	30.53	36	18.95	39	20.53	27	14.21	30	15.79
BMI (kg/m^2)										
<20 kg/m^2	130	18.16	221	30.87	198	27.65	74	10.34	93	12.99
20–24.9 kg/m^2	1783	18.88	3092	32.73	2659	28.15	1054	11.16	858	9.08
25–29.9 kg/m^2	2062	19.94	3393	31.17	3116	28.62	1263	11.60	1052	9.66
30–34.9 kg/m^2	595	16.40	996	27.45	1033	28.47	518	14.28	486	13.40
>35 kg/m^2	130	11.76	210	19.00	319	28.87	211	19.10	235	21.27
Ethnicity										
White	4267	18.40	7803	31.03	7158	28.46	3003	11.94	2556	10.16
Mixed	13	12.26	24	22.64	27	25.47	24	22.64	18	16.98
Asian	27	11.54	27	11.54	58	24.79	45	19.23	77	32.91
Black	10	7.75	27	20.93	29	22.48	24	18.60	39	30.23
Other ethnicity	13	12.62	15	14.56	34	33.01	15	14.56	26	25.24
Do not know/no answer	10	16.13	16	25.81	19	30.65	9	14.51	8	12.90

6.4.1 Demographics

There were 13980 male participants and 11801 female participants. The median liver iron concentration in both males and females was 1.15 mg/g. Liver iron was significantly higher in males than in females (p=0.0280) (**Figure 6.1**). The median liver fat was 3.56% in males compared to 2.63% in females. Liver fat was also significantly higher in males than in females (p<0.0001) (**Figure 6.1**). Age was also positively correlated with liver iron (p<0.0001, r = 0.1263, Spearman's) and liver fat (p<0.0001, r = 0.04146, Spearman's) (**Figure 6.2**). There were no differences in liver iron concentrations between ethnicities, however, liver fat percentage was statistically significant between mixed and Asian ethnicities (p=0.0270) (**Figure 6.3**).

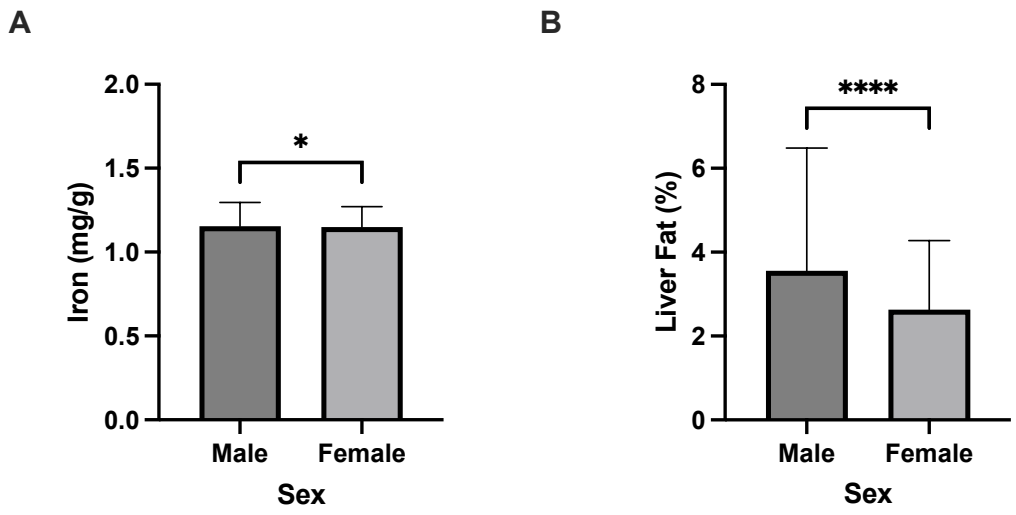

Figure 6.1 Liver iron concentration and liver fat percentages in male and female alcohol consumers in the UK BioBank. A) Iron concentration and B) Liver fat content (PDFF). Iron content is expressed as mg/g dry weight. Data was analysed using Mann-Whitney test and are presented as median with interquartile range. * $P \leq 0.05$, **** $P \leq 0.0001$.

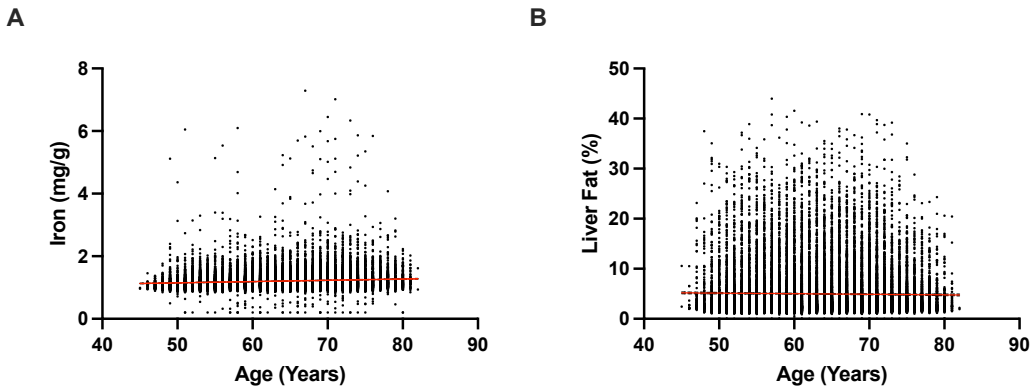

Figure 6.2 Graph showing distribution of liver iron and liver fat against age. A) Distribution of iron concentration (mg/g) against age and B) Distribution of liver fat content (PDFF) against age. Data was measured using Spearman's correlation.

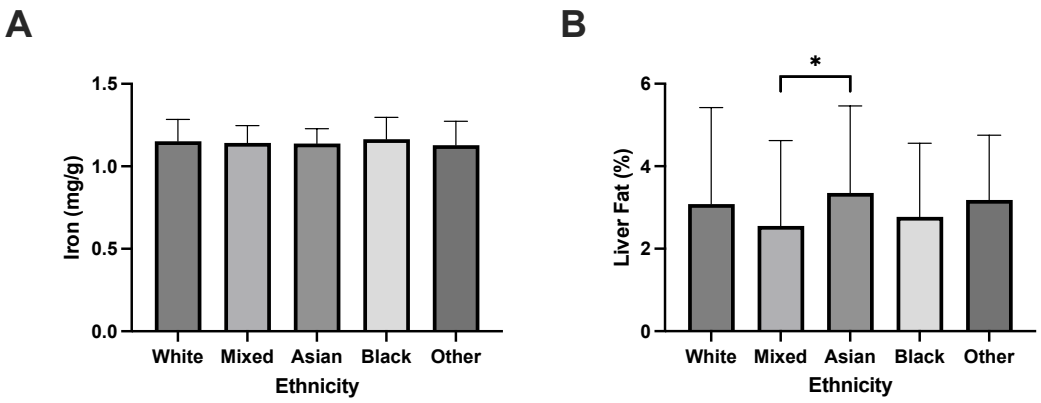

Figure 6.3 Liver iron concentration and liver fat percentages across different ethnicity groups in alcohol consumers from the UK BioBank. A) Distribution of iron concentration (mg/g) and B) Distribution of liver fat content (PDFF). Data was measured using Spearman's correlation. Data was measured using Kruskal-Wallis test and data is presented as median with interquartile range. * $P \leq 0.05$

6.4.2 Alcohol Intake

Alcohol intake as measured by frequency of drinking as well as 10-year previous frequency of drinking was measured to assess differences in liver iron concentration and liver fat. Frequency of drinking was reported as 'daily or almost daily' in 4700 participants, 'three to four times a week' in 7912 participants, 'once or twice a week' in 7325 participants, 'one to three times a month' in 3120 participants and 'special occasions only' in 2724 participants. The median concentration of liver iron in those who reported 'daily or almost daily' was 1.19 mg/g, 'three to four times a week' was 1.16 mg/g, 'once or twice a week' was 1.13 mg/g, 'one to three times a month' was 1.13 mg/g and 'special occasions only' was 1.12 mg/g. Data showed statistical significance ($p<0.0001$), and 'daily or almost daily drinking' showed the higher liver iron concentration and was significant between all other groups. 'Three to four times a week' was also statistically significant ($p<0.0001$) across all groups. The median liver fat percentage in those who reported 'daily or almost daily' was 3.47%, 'three to four times a week' was 3.01%, 'once or twice a week' 2.94%, 'one to three times a month' was 3.08% and 'special occasions only' was 3.13%. Data showed statistical significance ($p<0.0001$), with higher liver fat percentages in those who drank daily and was statistically significant across all other groups. Statistical significance was also reported between those who drank once or twice a week vs one to three times a month ($p=0.0021$) and once or twice a week and special occasions only ($p=0.0005$) (**Figure 6.4**).

10-year previous frequency of drinking was also analysed. 9948 participants reported as 'about the same', 12762 reported as 'less nowadays', 2947 reported as 'more nowadays', 118 reported as 'do not know' and 6 reported

‘prefer not to answer’. The median concentration of liver iron in those who reported as ‘about the same’ was 1.15 mg/g, ‘less nowadays’ was 1.15 mg/g participants, ‘more nowadays’ was 1.17 mg/g. Data showed statistical significance between ‘about the same’ and ‘less nowadays’ ($p=0.0007$), ‘about the same’ and ‘more nowadays’ ($p=0.0089$) as well as between ‘less nowadays’ and ‘more nowadays’ ($p<0.0001$). The median liver fat percentage in those who reported as ‘about the same’ was 3.02%, ‘less nowadays’ was 3.10% participants, ‘more nowadays’ was 3.26%. Data showed statistical significance between ‘about the same’ and ‘less nowadays’ ($p=0.0041$), ‘about the same’ and ‘more nowadays’ ($p<0.0001$), as well as between ‘less nowadays’ and ‘more nowadays’ ($p=0.0147$) (**Figure 6.4**).

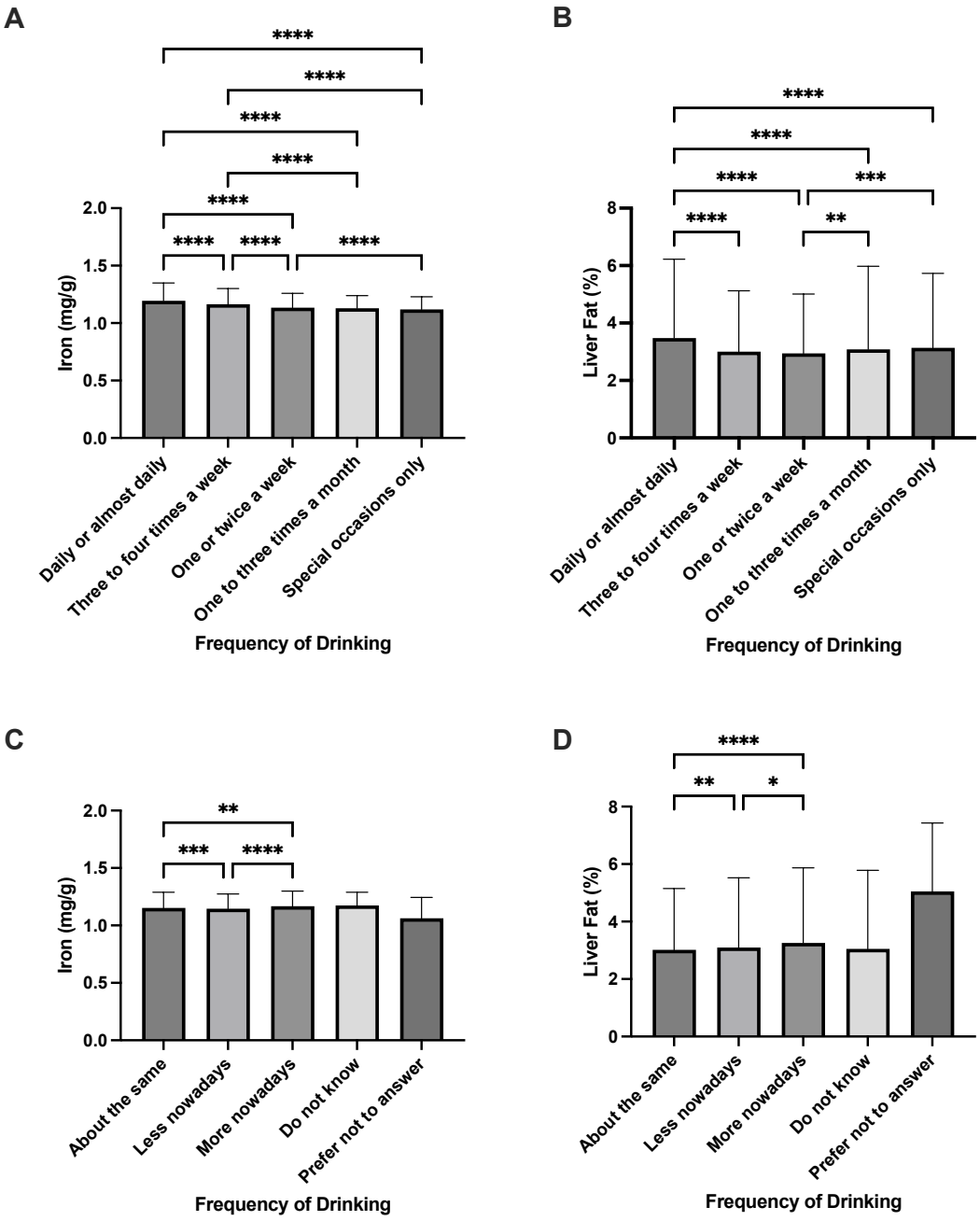

Figure 6.4 Alcohol frequency intake, liver iron concentration and percentage of liver fat in the UK BioBank. A) Iron concentration and frequency of drinking, B) liver fat content (PDFF) and frequency of drinking, C) alcohol intake vs 10 year previously and iron concentration and D) alcohol intake vs 10 year previously and liver fat. Iron content is expressed as mg/g dry weight. Data was measured using Kruskal-Wallis test and data is presented as median with interquartile range. * $P \leq 0.05$, ** $P \leq 0.01$, *** $P \leq 0.001$, **** $P \leq 0.0001$.

6.4.3 Vitamin Supplementation

The impact of vitamin supplementation on levels of iron in the liver and liver fat was also investigated. Vitamin supplementation was reported as folate in 194 participants, multi-vitamins in 3541 participants, vitamin A in 343 participants, vitamin B in 966 participants, vitamin C in 1308 participants, vitamin D in 2935 participants, vitamin E in 76 participants, none in 16355 and 62 preferred not to answer. The median concentration of liver iron in those who reported folate supplementation was 1.13 mg/g, multi-vitamin supplementation was 1.15 mg/g, vitamin A supplementation was 1.12 mg/g, vitamin B supplementation was 1.14 mg/g, vitamin C supplementation was 1.16 mg/g, vitamin D supplementation was 1.15 mg/g, vitamin E supplementation was 1.14 mg/g and no supplementation was 1.15 mg/g. Statistical significance was observed between vitamin A and vitamin D ($p=0.0208$) and vitamin A and none ($p=0.0213$) (**Figure 6.5**).

The median liver fat percentage in those who reported folate supplementation was 3.15%, multi-vitamin supplementation was 3.01%, vitamin A supplementation was 2.95%, vitamin B supplementation was 2.90%, vitamin C supplementation was 3.12%, vitamin D supplementation was 2.74%, vitamin E supplementation was 2.73% and no supplementation was 3.18%. Statistical significance was observed between folate and vitamin D ($p=0.0310$), multi-vitamin and vitamin D ($p<0.0001$), multi-vitamin and none ($p=0.0500$), vitamin B and none ($p=0.0009$), vitamin C and vitamin D ($p<0.0001$) and vitamin D vs none ($p<0.0001$) (**Figure 6.5**).

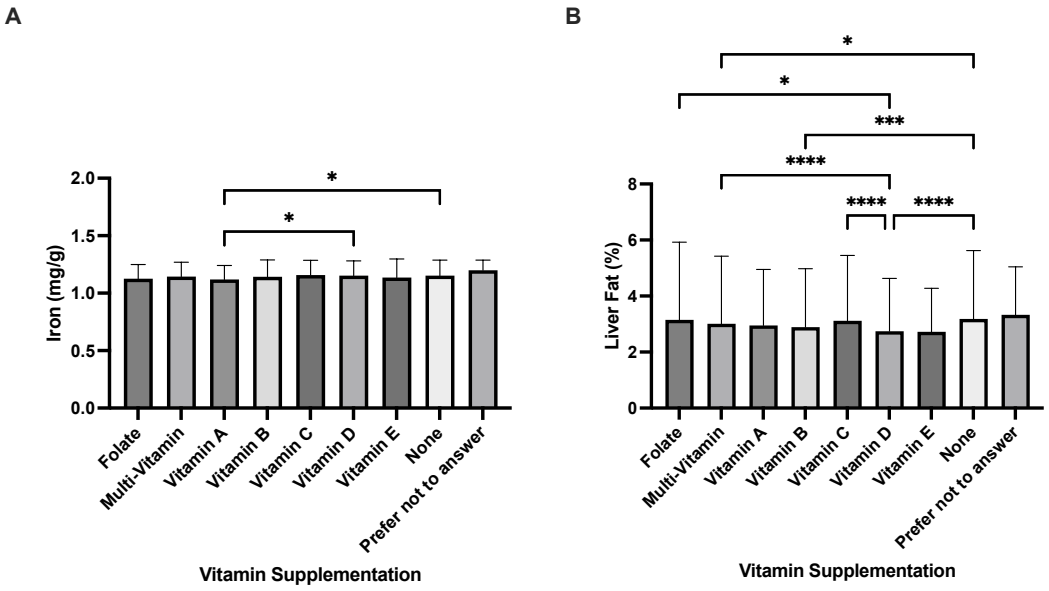

Figure 6.5 Vitamin and mineral supplementation, liver iron concentration and liver fat percentage in alcohol consumers in the UK BioBank. A) Iron concentration and vitamin and mineral supplementation and B) liver fat content (PDFF) and vitamin and mineral supplementation. Iron content is expressed as mg/g dry weight. Data was measured using Kruskal-Wallis test and data is presented as median with interquartile range. ** $P \leq 0.01$, *** $P \leq 0.001$, **** $P \leq 0.0001$.

6.4.4 Body Mass Index

The impact of BMI on both liver iron and liver fat was also analysed. In the participants analysed, 39.41% had a normal BMI, 42.23% were overweight and 18.36% were obese. There was a significant correlation between BMI and liver iron ($r=-0.01768$, $p=0.0045$). There was also a significant correlation between BMI and liver fat ($r=0.5996$, $p<0.0001$) (**Figure 6.6**).

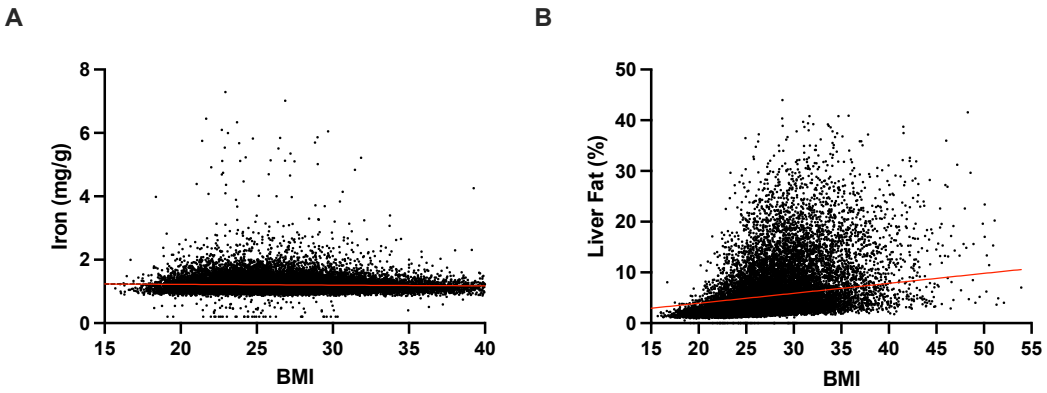

Figure 6.6 Distribution of liver iron concentration and liver fat percentage against body mass index in alcohol consumers in the UK BioBank. A) Iron concentration and B) Liver fat content (PDFF). Iron content is expressed as mg/g dry weight. Data was measured using Spearman's correlation.

6.4.5 Multivariate Model

To determine how changes in liver iron and liver fat are associated with frequency of alcohol intake, adjusting for age, sex and BMI liner regression model analysis was completed. Correlation coefficients and p values for variables can be found in Supplementary data, **Table 9.1**. For all the hypotheses tested (in **Section 6.4.5**), the Bonferroni-corrected threshold for statistical significance was 0.05/20=0.0025.

The linear regression model revealed liver iron levels (mg/g) was positively associated with alcohol intake frequency (coefficient = 0.0221, $p<0.0001$). Age was also found to be positively associated with levels of liver iron (coefficient=0.0038, $p<0.0001$). BMI was found to be negatively associated with liver iron content (coefficient = -0.0016, $p<0.0001$). Sex was found not to be statistically significant.

The linear regression model revealed liver fat percentage was positively associated with alcohol intake frequency (coefficient = 0.1200, $p<0.0001$). BMI was found to be positively associated with percentage liver fat (coefficient=0.5412, $p<0.0001$). Males also had higher liver fat percentage (coefficient=0.8435, $p<0.0001$). Age was found to be negatively associated with liver fat percentage (coefficient=-0.0126, $p=0.0003$).

Post-hoc analyses using Tukey's honest significant difference test were performed to investigate pairwise differences between the following alcohol intake frequency groups: 'Special occasions only' – 'Daily or almost daily', 'Special occasions only' – 'Three or four times a week', 'Special occasions

only' – 'Once or twice a week', 'Special occasions only' – 'One to three times a month', using the R package multicomp (Hothorn, Bretz and Westfall, 2008).

Multiple comparisons for liver iron content revealed significant differences between 'Special occasions only' – 'Daily or almost daily' ($p=0.0001$), 'Special occasions only' – 'Three or four times a week' ($p<0.0001$), and 'Special occasions only' – 'Once or twice a week' ($p<0.0001$). Self-reported frequency of drinking showed that daily or almost daily consumption of alcohol increased liver iron by 0.0865 mg/g. On the other hand, multiple comparisons for liver fat percentage revealed significant differences between 'Special occasions only' – 'Daily or almost daily' ($p<0.0001$). Self-reported frequency of drinking showed that daily or almost daily consumption of alcohol increased liver fat percentage by 0.6014%.

6.5 Discussion

Iron overload disorders encompass a range of conditions characterised by an excessive accumulation of iron throughout the body, leading to damage in various organs. The role of iron, liver fat, frequency of drinking, vitamin supplementation, age at assessment and BMI were investigated.

Currently, MRI is considered the most reliable non-invasive method for detecting and quantifying iron overload in the liver iron overload. Liver iron overload is characterised by a liver iron concentration exceeding 36 μmol Fe/g as well as elevated liver iron >1.8 mg/g (Obrzut et al., 2020; Alustiza et al., 2023), which can ultimately lead to liver-related disorders. In this present study, liver iron concentration in the UK Biobank participants showed 2.54% of the subjects had liver iron levels greater than 1.8 mg/g. Of those who has elevated liver iron levels 31.30% reported as drinking 'daily or almost daily', 34.66% reported as drinking 'three to four times a week' and 22.41% reported as drinking 'once or twice a week'. Similar patient cohort studies have documented elevated liver iron in 4.82% of 9108 subjects (McKay et al., 2018) as well as 17.40% of 2581 subjects (Kühn et al., 2017).

In this study, liver iron levels were found to be significantly higher in men than women, although the difference in absolute mean values was 0.018 mg/g and the difference in the median was 0.0006 mg/g. These differences between men and women has also been documented in previous studies (McKay et al., 2018; Wilman et al., 2019; Obrzut et al., 2020). These findings were anticipated due to premenopausal women experiencing iron loss through menstruation. The mean liver fat was also significantly higher in men, with a

1.31% compared to females, which has also been previously documented. Age was also positively correlated with liver iron but not liver fat which may be explained by increasing iron levels in women after the menopause as well as iron associated with ageing disorders, due to increases in oxidative stress. The process of ageing has also been linked to the accumulation of non-heme iron in various tissues (Chen, Kung and Gnana-Prakasam, 2022). This accumulation of iron with age as well as its retention is also exacerbated by other factors such as diet (Milman et al., 2003).

As iron overload is common in ALD, alcohol intake was measured to assess differences in liver iron concentration and liver fat. The highest liver concentration was documented in those who reported a higher frequency of drinking and data showed statistical significance in liver iron and frequency of alcohol intake, with higher liver fat percentages in those who drank ‘daily’ and ‘one to three times a month’, although high liver fat was also documented in those who drank on ‘special occasions only’. As described previously, the median liver fat percentage in those drank ‘daily or almost daily’ was 3.47%, ‘three to four times a week’ was 3.01%, ‘once or twice a week’ 2.94%, ‘one to three times a month’ was 3.08% and ‘special occasions only’ was 3.13%. This suggests there is a link between liver iron and alcohol consumption, whereby the lowest levels of liver fat are in the middle ranges (once or twice a week), with high liver fat in both the low frequency (special occasions only) and high frequency drinking (daily or almost daily), suggesting liver fat may be highest in binge drinkers and alcoholics. 10-year previous frequency of drinking was also analysed, and the highest mean of iron concentration and percentage of

liver fat was documented in those who reported to drink more nowadays, when compared to 10 years previously.

The impact of vitamin supplementation on levels of iron in the liver and percentage of liver fat was also investigated, due to their antioxidant capacities. It was observed that ‘prefer not to answer’ had the highest median liver iron concentration, followed by vitamin C supplementation. Liver fat was also highest in those who reported ‘prefer not to answer’ followed by folate. Studies have shown that serum folate levels may play a role in the progression of fatty liver disease (L Li et al., 2022) and therefore, provide an explanation for higher liver fat during folate supplementation. However, this remains controversial, and other results have shown higher serum folate level was associated with lower risk of MASLD (Chen et al., 2023). These conflicting findings demonstrate the need for future prospective studies. Statistical significance was observed between vitamin A and vitamin D and vitamin A and none, with vitamin A supplementation showing lowest liver iron median values. The median liver fat percentage was highest in those who reported folate supplementation and no supplementation. Higher levels of iron and liver fat in those who reported no supplementation may be due to the antioxidant capacity of vitamins. Previous research has shown that high dietary iron is associated with low vitamin A as well as a high intake of vitamin A being associated with low liver iron (Staab et al., 1984). Antioxidants play a crucial role in the liver via prevention of the oxidation of biomolecules. These counteract the detrimental effects caused by free radicals and therefore the use of supplementation may counteract some of the oxidative damage caused by iron overload in the liver. For example, *in vivo* studies show vitamin C

supplementation maintains levels of reduced glutathione, improving antioxidant capacity (Sitohang et al., 2021), although in this study vitamin C was associated with higher median iron levels. However, as the results reported in this study are preliminary, further investigations are required for understanding the relationship between vitamin supplementation, iron overload and alcohol use in large cohorts.

Ethnicity did not appear to show any difference in the concentration of liver iron, however, in percentage of liver fat, Asian ethnicities has the highest liver fat. However, there is very little ethnic diversity within participants as 97.54% of participants were white, and therefore differences were limited. BioBank participants were also from a healthy UK population, whereas fatty liver disease has been documented to have different prevalence between ethnicities. A recent meta-analysis has shown that 23% of Hispanics, 14% of Caucasians, and 13% of African Americans have fatty liver disease (Bonacini et al., 2021). Another study also assessing liver fat by MRI found prevalence rates of MASLD different between ethnic groups, with the highest prevalence in Caucasians (Tricò et al., 2018). Differences in distribution of body fat have been explored in different ethnicities and central adiposity and visceral fat deposition has been document in individuals of Asian ethnicity and also have higher body fat percentages at lower BMI (Wong and Ahmed, 2014; Agbim et al., 2019). Therefore, the impact of ethnicity on liver iron and liver fat levels in alcohol consumers may warrant further investigation.

This study found a negative correlation between liver iron and BMI. A study from Nelson et al also reported lower BMI and increased liver iron (Nelson et

al., 2011). These findings are also conflicting, as previous data has reported positive associations between liver iron and BMI (Zheng et al., 2011; McKay et al., 2018). As expected, BMI and liver fat percentage was found to be strongly correlated. This is consistent with previous findings in males which found a higher percentage of body fat was linked to disruptions in iron regulation. This is manifested by elevated levels of serum hepcidin and serum ferritin, leading to an increased likelihood of individuals being at severe risk of iron overload (Moore Heslin et al., 2021).

The multivariate linear regression model also showed alcohol intake frequency produced a significant effect on liver iron levels as well as liver fat, revealing liver iron levels (mg/g) and liver fat percentage were positively associated with alcohol intake frequency. Self-reported frequency of drinking showed that ‘daily or almost daily’ consumption of alcohol increased liver iron by 0.0865 mg/g and liver fat percentage by 0.6014%. As expected, BMI was also found to be positively associated with percentage liver fat. It is well known that BMI is a risk factor for fatty liver risk, as fatty liver disease is prevalent in obesity, and incidence of fatty liver has been reported as much as 14-fold higher with increased BMI (Fan, Wang and Du, 2018). Obesity has also been documented as a risk factor for progression of ALD. An overweight BMI for 10 years is associated steatosis, acute alcoholic hepatitis, and cirrhosis. Therefore, taken together, this finding corroborates association of both iron overload in the liver during excessive alcohol consumption.

In this study, although the variables assessed had some effect on liver iron and liver fat there are many other variables which affect both liver iron and fat

in the general population. The adjusted r^2 values are 0.02 for liver iron and 0.24 for liver fat, and therefore, more variables may be required in this model. For example, variables such as diet and supplementation, including iron supplements and levels of iron in red meat including beef may affect levels of liver iron. Previous research has documented a relationship between the consumption of red meat and serum ferritin levels (Quintana Pacheco et al., 2018), as well as hyperglycaemia and high triglyceride levels (Esfandiar et al., 2019). Other dietary factors including consumption of carbohydrate rich diet. Excess glucose is converted into fatty acids through lipogenesis, which are integrated into very-low-density lipoprotein for transport and storage in white adipose tissue (Petagine, Zariwala and Patel, 2023). Accumulation of lipids in adipocytes triggers JNK signalling pathways promoting development of fatty liver (Petagine, Zariwala and Patel, 2023). Although the results reported in this study are preliminary, the vast dataset available from the UK Biobank offers a promising avenue for conducting more in-depth investigations into the influence of various dietary factors on iron overload and fatty liver in both healthy individuals and ALD. It is plausible that the variables assessed in this study may have some interaction with pathways of iron homeostasis in the liver. However, further comprehensive studies are required to understand the effects.

6.6 Conclusion

This study showed that levels of iron and liver fat percentages were positively associated with self-reported frequency of drinking in a UK BioBank cohort. Although these findings present preliminary data associating alcohol

consumption and liver iron, considering variables such as age, sex and BMI, future studies should assess liver iron and liver fat with more in-depth investigations, including the impact of various lifestyle factors. This study has shown that 2.54% of participants had elevated liver iron levels, and 88.09% of these high iron levels were reported from participants who drank daily or weekly. This study also suggested a link between 10-year previous frequency of drinking as the highest mean of iron concentration and percentage of liver fat was documented in those who reported to drink more nowadays, when compared to 10 years previously. Due to the increasing health burden of ALD, both levels of iron in the liver as well as percentages of liver fat should represent risk factors for the general population.

CHAPTER 7 GENERAL DISCUSSION

7.1 Results and Main Findings

ALD is one of the most prevalent chronic liver diseases which causes significant worldwide disease burden. The histological spectrum of ALD is widely recognised and ranges from simple liver steatosis, progresses to alcoholic hepatitis, and then ultimately to fibrosis and hepatocellular carcinoma (Petagine, Zariwala and Patel, 2021). Although the spectrum of disease is widely accepted, the precise molecular and biochemical mechanisms contributing to the pathogenesis and progression of disease are not fully understood. It is thought that disease progression may involve various mechanisms including mitochondrial dysfunction, oxidative stress, iron dysregulation, gut dysbiosis, activation of inflammatory pathways and decreased synthesis of antioxidants (Petagine, Zariwala and Patel, 2021). Iron overload is also commonly associated with ALD. Excess iron can accelerate the Fenton reaction, leading to the production of ROS causing oxidative damage.

In **Chapter 3**, VL-17A cells were used as a model to investigate the effects of alcohol exposure on liver cells, due to their over-expression of two alcohol metabolising enzymes (CYP2E1 and ADH). A clear model of alcohol toxicity and chronic disease model of ALD was established, whereby ethanol exposure led to significant cell toxicity, with a dose-dependent reduction in cell viability which decreased further over time. The toxic effect was more pronounced at high ethanol concentrations, as well as at longer time-points. The model of

alcohol toxicity also showed ROS production was increased at 30 mins, possibly reflecting immediate alcohol metabolism, whereas at 72 hrs impaired/damaged mitochondria causing leakage of electrons. Ethanol exposure was also associated with a higher percentage of cells in late apoptosis, suggesting more chronic damage. The mechanisms behind apoptosis induction are thought to be due to oxidative stress and mitochondrial damage. The latter occurred via reductions in mitochondrial membrane potential. Lastly, preliminary data shows increased micronuclei and nuclear buds after ethanol treatment, highlighting involvement of oxidative DNA damage in ALD.

Excessive alcohol consumption is directly linked to hepatic iron overload and in **Chapter 4**, VL-17A cells were used as a model to characterise the effect of iron overload and excessive alcohol on liver injury, oxidative stress, mitochondrial function, and apoptosis. Features of iron overload and ALD was established, whereby a combination of iron and ethanol exposure caused further damage to cells compared to ethanol alone, leading to additional reductions in cell viability as well as increased ROS production. Both ethanol and iron cause oxidative stress and lipid peroxidation, and the combination of both exacerbates hepatic injury through increased production of proinflammatory cytokines and ROS. Iron overload causes free radical generation through the Fenton reaction causing tissue damage and fibrosis, accelerating disease progression. A higher percentage of cells in early apoptosis at 48 hrs were documented when treated with ethanol and iron in comparison to ethanol alone (**Chapter 3**) as well as reductions in basal and maximal respiration. Taken together, this suggests a combination of excessive

ethanol and iron overload causes impaired mitochondrial function, decreased mitochondrial respiration capacity and increased ROS, and renders cells into apoptosis at an earlier time-point. Therefore, the alterations of mitochondrial metabolic pathways in iron overload in ALD may cause electron leakage in the electron transport chain, increasing superoxide production, exacerbating disease processes.

At present there are no effective treatments for ALD due to the incomplete understanding of hepatic biochemical alterations and pathogenic mechanisms involved in ALD progression (Petagine, Zariwala and Patel, 2021). Although abstinence remains the most important treatment there is a need to develop an effective treatment for ALD associated with the excessive prolonged misuse of alcohol (Petagine, Zariwala and Patel, 2021). In **Chapter 5**, novel nanoformulations encapsulating antioxidants were assessed in their ability to protect against ethanol and iron in VL-17A cells. Although both curcumin and silibinin in their free drug form were shown to significantly increase the viability of cells, curcumin DSPE-PEG nanocarriers were also able to protect against ethanol-induced oxidative stress via increases in cell viability and a reduction in ROS. Curcumin DSPE-PEG + AP nanocarriers were also able to protect against both ethanol and iron combination treatment, suggesting that AP may increase the protective effects of curcumin in iron overload conditions. The antioxidant curcumin, is thought to alter inflammatory signalling pathways such as TGF-β1/Smad, JNK1/2-ROS, NF-κB, which may improve liver injury through the attenuation of inflammation and oxidative stress (Lukkunaprasit et al., 2023). The addition of AP into nanocarriers may improve antioxidant levels through the pentose-phosphate pathway, which produces NADPH, which is

required for the conversion of oxidised glutathione to reduced glutathione via glutathione reductase, and essential for antioxidant defence; this may increase intracellular glutathione levels and inhibit cell death (Puskas et al., 2000). Combinations of curcumin with AP may improve oxidative damage by increasing free radical scavenging. These results show curcumin nanoformulations are beneficial in protecting against both ethanol and iron and have the potential for future clinical translation for nanocarrier systems in the therapy of ALD and iron overload. Free drug antioxidant compounds, such as silibinin and curcumin, as well as curcumin nanoformulations were shown in **Chapter 5**, to protect against both ethanol and iron induced damage. Antioxidant supplementation may therefore have the capacity to prevent ethanol and iron mediated damage in ALD, however, future studies are required to confirm this association *in vivo*.

To investigate associations of frequency of drinking, in **Chapter 6**, liver iron content and percentage of liver fat 25,781 participants data was analysed from the UK Biobank. In this cohort, 2.54% had liver iron levels greater than 1.8 mg/g, a value associated with iron overload. Of those who has elevated liver iron levels many participants had reported higher frequencies of drinking. Higher frequency of drinking was also associated with higher liver fat percentage suggesting a link between liver iron and alcohol consumption. These results were also corroborated by results of 10-year previous frequency of drinking, with highest liver iron and liver fat documented in those who reported to ‘drink more nowadays’. The multivariate linear regression model also showed self-reported alcohol intake frequency produced a significant effect on liver iron levels as well as liver fat, revealing liver iron levels (mg/g)

and liver fat percentage were positively associated with alcohol intake frequency.

7.2 Future Direction

Based on the outcomes of results from this thesis, future research should assess mitochondrial morphology, bioenergetics and mitophagy markers in response to ethanol and iron, to fully characterise the VL-17A cell model.

Firstly, to further investigate mitochondrial function it would be interesting to assess other parameters including levels of mitochondrial calcium and cardiolipin, due to its importance as a phospholipid in cellular respiration and ROS oxidisation. Calcium ions play crucial roles in cellular functions, and the dynamics of calcium concentration, are critical for cellular signalling and mitochondrial function (Duchen, 2000). Disruptions in mitochondrial calcium levels can lead to various pathologies and oxidative stress, and evidence suggests calcium overload occurs during ALD (Thoudam et al., 2023), however, the pathways and factors which drive its accumulation warrant further research. Future research should include mitochondrial calcium investigation in cellular models of ALD using Rhod-2, AM. As described earlier, the relationship between both cardiolipin and ROS has not been fully investigated in ALD, and therefore, it would be interesting to assess the levels of cardiolipin in both a chronic ethanol and iron overload model. It would also be interesting to measure markers of mitophagy and mitochondrial morphology. For example, Western blotting to quantify mitophagy proteins such as PINK1 and Parkin and use of MitoTracker probes to further

understand mitochondrial biogenesis and mitophagy due to iron overload in ALD.

Finally, additional studies would be required to establish the therapeutic potential of nanocarrier systems encapsulating potent antioxidants. Curcumin was successfully encapsulated into DSPE-PEG nanocarriers demonstrating a high encapsulation efficiency. The therapeutic potential of these nanocarriers should be further tested at different doses as well as assessing pre-treatment, co-treatment, and post-treatment protocols. As free drug silibinin showed protection against both ethanol toxicity as well as ethanol and iron damage, nanoformulations encapsulating silibinin should be prepared, characterised and their therapeutic potential assessed on a cellular model of ALD and iron overload. The ability of nanocarriers to prevent the effects of alcohol and iron on markers of oxidative damage should be assessed as well as changes to apoptosis and mitophagy. As mitochondrial dysfunction is a common feature of ALD it would also be useful to assess the ability of the nanocarrier systems to specifically target the mitochondria and protect against mitochondrial dysfunction in ALD, using methods described in **Chapter 3** as well as imaging techniques and Western blotting mentioned above. Due to the lack of treatment options available for ALD the long-term aim of this study would be to clinically translate nanocarrier systems for therapy as these antioxidant compounds have already been extensively studied and are approved as dietary supplements. However, it is important to note curcumins recent controversy in the media and the possibility of *in vitro* interference characteristics of curcumin, which may present limitations in scientific research (Nelson et al., 2017).

There are also several limitations which should be considered when analysing data from the UK BioBank. Limitations of this study include the use of self-reported data as well as the possibility of a healthier than normal study population. Also, the age range of participants measured was between 45-85 and therefore data does not account for all ages in the general population. The dataset also has little ethnic diversity, with over 97% of the participants in this study White Caucasian. Although the variables assessed produced significant effects on liver iron and liver fat, r^2 values suggest future analysis should include more variables in this model. As this cohort all reported a frequency of drinking to some level, the assessment in people who report never drinking would also be valuable. These results reported are preliminary and further investigations are required for understanding the relationship between vitamin supplementation, iron overload and alcohol use in large cohorts as well as including other variables such as impact of various lifestyle factors including red meat intake. Future analysis in this cohort should also include investigations into the type of alcohol consumed by UK BioBank participants and iron content in each alcohol type, as well as antioxidant properties of alcoholic type consumed.

7.3 Final Conclusions

ALD is a global public health issue and characterised by a spectrum of liver stages, ranging from steatosis to fibrosis. Despite its well-recognised clinical manifestations and spectrum of disease, the exact molecular and biochemical mechanisms underlying pathogenesis and progression of disease remain incompletely understood. It is thought ALD involves a multitude of mechanisms, including mitochondrial dysfunction, oxidative stress, iron dysregulation, gut dysbiosis, inflammatory pathway activation, and diminished antioxidant production. Iron overload, a common condition associated with ALD, further exacerbates liver damage through the Fenton reaction, generating free radicals and ROS, and accelerating disease progression and onset of fibrosis.

In this thesis, results showed ethanol exposure led to significant cell toxicity, which was especially evident at higher ethanol concentrations, as well as increases in ROS production and apoptosis, indicating a clear relationship between alcohol and oxidative stress. This study also found mitochondrial dysregulation after alcohol treatment such as reductions in mitochondrial membrane potential. Therefore alcohol-induced damage to mitochondria can disrupt cellular energy production and contribute to apoptosis.

Results also show that iron treatment caused further toxicity, producing more profound effects than ethanol treatment alone as well as iron exposure increasing the production of ROS, indicating iron causes further oxidative damage to the liver. Mitochondrial damage was also evident due to increased intrinsic apoptosis, as well as decreases in basal and maximum respiration.

Associations between drinking frequency, liver iron content, and liver fat percentages in a large dataset from the UK Biobank showed elevated liver iron levels, indicative of iron overload, which were linked to higher drinking frequencies. These results were consistent with the relationship between high liver iron concentration and liver fat content.

While abstinence remains the primary treatment for ALD, the need for effective therapeutic interventions persists. This study assessed the potential of antioxidant nanoformulations to protect against ethanol and iron overload in liver cells and demonstrated their ability to increase cell viability and reduce ROS production. Nanoformulations encapsulating curcumin exhibited promise in mitigating oxidative damage caused by ethanol and iron overload.

In conclusion, this research describes the effects of both ethanol and iron toxicity, causing liver damage via oxidative stress. While this study contributes valuable insights into ALD's multifaceted nature and the potential of antioxidant nanoformulations, continued research in both iron overload and ALD is required to fully understand the mechanisms of oxidative damage including mitochondrial dysfunction and chromosomal instability. Research into the use of antioxidant compounds as well as nanoformulations to mitigate the effects of alcohol as well as iron overload should also be explored to benefit cellular health. In summary, ALD remains a significant health challenge, demanding continued research to unravel its complexities and identify effective treatments. The exploration of antioxidant novel nanoformulations offers a promising avenue for mitigating the oxidative damage central to ALD pathogenesis and iron overload, with the potential for innovative therapeutic approaches for clinical translation.

REFERENCES

Abdallah, M.A. and Singal, A.K. (2020). Mitochondrial dysfunction and alcohol-associated liver disease: a novel pathway and therapeutic target. *Signal Transduction and Targeted Therapy 2020 5:1*, 5 (1), 1–2. Available from https://doi.org/10.1038/s41392-020-0128-8 [Accessed 29 September 2021].

Abdelmegeed, M.A. et al. (2013). CYP2E1 potentiates binge alcohol-induced gut leakiness, steatohepatitis, and apoptosis. *Free Radical Biology and Medicine*, 65, 1238–1245. Available from https://doi.org/10.1016/j.freeradbiomed.2013.09.009.

Abraham, J. et al. (2011). Alcohol metabolism in human cells causes DNA damage and activates the Fanconi anemia-breast cancer susceptibility (FA-BRCA) DNA damage response network. *Alcoholism, clinical and experimental research*, 35 (12), 2113–2120. Available from https://doi.org/10.1111/j.1530-0277.2011.01563.x.

Adams, L.A. (2005). Nonalcoholic fatty liver disease. *Canadian Medical Association Journal*, 172 (7), 899–905. Available from https://doi.org/10.1503/cmaj.045232 [Accessed 4 October 2019].

Adrain, C., Creagh, E.M. and Martin, S.J. (2001). Apoptosis-associated release of Smac/DIABLO from mitochondria requires active caspases and is blocked by Bcl-2. *EMBO Journal*, 20 (23), 6627–6636. Available from https://doi.org/10.1093/emboj/20.23.6627.

Agbim, U. et al. (2019). Ethnic Disparities in Adiposity: Focus on Non-alcoholic Fatty Liver Disease, Visceral, and Generalized Obesity. *Current obesity reports*, 8 (3), 243–254. Available from https://doi.org/10.1007/s13679-019-00349-x.

Ali, N., Ferrao, K. and Mehta, K.J. (2022). Liver Iron Loading in Alcohol-Associated Liver Disease. *The American Journal of Pathology*. Available from https://doi.org/https://doi.org/10.1016/j.ajpath.2022.08.010.

Alirezaei, M. et al. (2011). Betaine prevents ethanol-induced oxidative stress and reduces total homocysteine in the rat cerebellum. *Journal of Physiology and Biochemistry*, 67 (4), 605–612. Available from https://doi.org/10.1007/s13105-011-0107-1 [Accessed 2 June 2020].

Alustiza, J.M. et al. (2023). Non-invasive measurement of liver iron concentration by magnetic resonance imaging and its clinical usefulness. *Archives of medical science : AMS*, 19 (3), 784–791. Available from https://doi.org/10.5114/aoms/119118.

Alvarez, M.A. et al. (2004). Combining steroids with enteral nutrition: a better therapeutic strategy for severe alcoholic hepatitis? Results of a pilot study. *European journal of gastroenterology & hepatology*, 16 (12), 1375–80. Available from https://doi.org/10.1097/00042737-200412000-00023 [Accessed 10 December 2019].

An International Group. (1981). Alcoholic Liver Disease: Morphological Manifestations. *The Lancet*, 317 (8222), 707–711. Available from https://doi.org/10.1016/S0140-6736(81)91984-X.

An, L., Wang, X. and Cederbaum, A.I. (2012). Cytokines in alcoholic liver disease. *Archives of Toxicology*, 86 (9), 1337–1348. Available from https://doi.org/10.1007/s00204-012-0814-6.

Anderson, G.J. and Frazer, D.M. (2005). Hepatic iron metabolism. *Seminars in Liver Disease*, 25 (4), 420–432. Available from https://doi.org/10.1055/S-2005-923314/ID/48 [Accessed 4 May 2022].

Anderson, G.J. and Frazer, D.M. (2017). Current understanding of iron homeostasis. *The American Journal of Clinical Nutrition*, 106 (suppl_6), 1559S-1566S. Available from https://doi.org/10.3945/ajcn.117.155804.

Angermayr, B. et al. (2003). Child-Pugh versus MELD score in predicting survival in patients undergoing transjugular intrahepatic portosystemic shunt. *Gut*, 52 (6), 879–885. Available from https://doi.org/10.1136/gut.52.6.879 [Accessed 18 January 2021].

Aragon, C.M.G., Rogan, F. and Amit, Z. (1992). Ethanol metabolism in rat

brain homogenates by a catalase-H2O2 system. *Biochemical Pharmacology*, 44 (1), 93–98. Available from https://doi.org/10.1016/0006-2952(92)90042-H.

Arrese, M. et al. (2016). Innate Immunity and Inflammation in NAFLD/NASH. *Digestive diseases and sciences*, 61 (5), 1294–303. Available from https://doi.org/10.1007/s10620-016-4049-x [Accessed 11 October 2019].

Ashkenazi, A. and Dixit, V.M. (1998). Death receptors: Signaling and modulation. *Science*, 281 (5381), 1305–1308. Available from https://doi.org/10.1126/science.281.5381.1305.

Ayala, A., Muñoz, M.F. and Argüelles, S. (2014). Lipid Peroxidation: Production, Metabolism, and Signaling Mechanisms of Malondialdehyde and 4-Hydroxy-2-Nonenal. *Oxidative Medicine and Cellular Longevity*, 2014. Available from https://doi.org/10.1155/2014/360438.

Bai, X., Su, G. and Zhai, S. (2020). Recent advances in nanomedicine for the diagnosis and therapy of liver fibrosis. *Nanomaterials*, 10 (10), 1–18. Available from https://doi.org/10.3390/nano10101945 [Accessed 27 April 2021].

Bajaj, J.S. et al. (2014). Altered profile of human gut microbiome is associated with cirrhosis and its complications. *Journal of Hepatology*, 60 (5), 940–947. Available from https://doi.org/10.1016/j.jhep.2013.12.019 [Accessed 17 February 2021].

Barnes, M.A., Roychowdhury, S. and Nagy, L.E. (2014). Innate immunity and cell death in alcoholic liver disease: Role of cytochrome P4502E1. *Redox Biology*, 2 (1), 929–935. Available from https://doi.org/10.1016/j.redox.2014.07.007.

Bartneck, M., Warzecha, K.T. and Tacke, F. (2014). Therapeutic targeting of liver inflammation and fibrosis by nanomedicine. *Hepatobiliary surgery and nutrition*, 3 (6), 364–36476. Available from https://doi.org/10.3978/j.issn.2304-3881.2014.11.02.

Batts, K.P. (2007). Iron overload syndromes and the liver. *Modern pathology :*

an official journal of the United States and Canadian Academy of Pathology, Inc, 20 Suppl 1, S31-9. Available from https://doi.org/10.1038/modpathol.3800715.

Bayly, G.R. (2014). Lipids and disorders of lipoprotein metabolism. *Clinical Biochemistry: Metabolic and Clinical Aspects: Third Edition*. Elsevier Inc., 702–736. Available from https://doi.org/10.1016/B978-0-7020-5140-1.00037-7.

Beckemeier, M.E. and Bora, P.S. (1998). Fatty acid ethyl esters: Potentially toxic products of myocardial ethanol metabolism. *Journal of Molecular and Cellular Cardiology*, 30 (11), 2487–2494. Available from https://doi.org/10.1006/jmcc.1998.0812.

Benassi-Evans, B. and Fenech, M. (2011). Chronic alcohol exposure induces genome damage measured using the cytokinesis-block micronucleus cytome assay and aneuploidy in human B lymphoblastoid cell lines. *Mutagenesis*, 26 (3), 421–429. Available from https://doi.org/10.1093/mutage/geq110.

Bersuker, K. et al. (2019). The CoQ oxidoreductase FSP1 acts parallel to GPX4 to inhibit ferroptosis. *Nature*, 575 (7784), 688–692. Available from https://doi.org/10.1038/s41586-019-1705-2.

Bonacini, M. et al. (2021). Racial differences in prevalence and severity of non-alcoholic fatty liver disease. *World journal of hepatology*, 13 (7), 763–773. Available from https://doi.org/10.4254/wjh.v13.i7.763.

Bradford, M.M. (1976). A rapid and sensitive method for the quantitation of microgram quantities of protein utilizing the principle of protein-dye binding. *Analytical biochemistry*, 72, 248–54. Available from https://doi.org/10.1006/abio.1976.9999.

Brooks, P.J. and Zakhari, S. (2014). Acetaldehyde and the genome: Beyond nuclear DNA adducts and carcinogenesis. *Environmental and Molecular Mutagenesis*, 55 (2), 77–91. Available from https://doi.org/10.1002/em.21824.

Brunt, E.M. (2001). Nonalcoholic steatohepatitis: Definition and pathology. *Seminars in Liver Disease*, 21 (1), 3–16. Available from https://doi.org/10.1055/s-2001-12925.

Brunt, P.W. et al. (1974). Studies in alcoholic liver disease in Britain: 1 Clinical and pathological patterns related to natural history. *Gut*, 15 (1), 52–58. Available from https://doi.org/10.1136/gut.15.1.52 [Accessed 30 April 2020].

Burra, P. and Lucey, M.R. (2005). Liver transplantation in alcoholic patients. *Transplant International*, 18 (5), 491–498. Available from https://doi.org/10.1111/j.1432-2277.2005.00079.x [Accessed 10 December 2019].

Cadenas, E. and Davies, K.J. (2000). Mitochondrial free radical generation, oxidative stress, and aging. *Free radical biology & medicine*, 29 (3–4), 222–30. Available from https://doi.org/10.1016/s0891-5849(00)00317-8 [Accessed 28 October 2021].

Castaneda, F. and Rosin-Steiner, S. (2006). Low concentration of ethanol induce apoptosis in HepG2 cells: role of various signal transduction pathways. *International Journal of Medical Sciences*, 3 (4), 160. Available from https://doi.org/10.7150/IJMS.3.160 [Accessed 12 October 2021].

Caulin, C. et al. (2000). Keratin-dependent, epithelial resistance to tumor necrosis factor- induced apoptosis. *Journal of Cell Biology*, 149 (1), 17–22. Available from https://doi.org/10.1083/jcb.149.1.17.

Cederbaum, A.I. (2010). Hepatoprotective effects of S-adenosyl-L-methionine against alcohol- and cytochrome P450 2E1-induced liver injury. *World Journal of Gastroenterology*, 16 (11), 1366–1376. Available from https://doi.org/10.3748/wjg.v16.i11.1366.

Cederbaum, A.I. (2012). Alcohol Metabolism. *Clinics in Liver Disease*, 16 (4), 667–685. Available from https://doi.org/10.1016/j.cld.2012.08.002 [Accessed 24 April 2020].

Celli, R. and Zhang, X. (2014). Pathology of Alcoholic Liver Disease. *Journal of clinical and translational hepatology*, 2 (2), 103–109. Available from https://doi.org/10.14218/JCTH.2014.00010 [Accessed 10 October 2019].

Chan, S.H.Y. et al. (2023). Dry powder formulation of azithromycin for COVID-19 therapeutics. *Journal of microencapsulation*, 40 (4), 217–232. Available from https://doi.org/10.1080/02652048.2023.2175924.

Chang, B. et al. (2015). Short- or long-term high-fat diet feeding plus acute ethanol binge synergistically induce acute liver injury in mice: An important role for CXCL1. *Hepatology*, 62 (4), 1070–1085. Available from https://doi.org/10.1002/hep.27921 [Accessed 16 October 2019].

Chelikani, P., Fita, I. and Loewen, P.C. (2004). Diversity of structures and properties among catalases. *Cellular and Molecular Life Sciences*, 61 (2), 192–208. Available from https://doi.org/10.1007/s00018-003-3206-5.

Chen, G. et al. (2012). Autophagy is a protective response to ethanol neurotoxicity. *Autophagy*, 8 (11), 1577–1589. Available from https://doi.org/10.4161/auto.21376.

Chen, H.-K. et al. (2023). Serum folate associated with nonalcoholic fatty liver disease and advanced hepatic fibrosis. *Scientific Reports*, 13 (1), 12933. Available from https://doi.org/10.1038/s41598-023-39641-1.

Chen, J. et al. (2022). The multifaceted role of ferroptosis in liver disease. *Cell Death & Differentiation*, 29 (3), 467–480. Available from https://doi.org/10.1038/s41418-022-00941-0.

Chen, W.J., Kung, G.P. and Gnana-Prakasam, J.P. (2022). Role of Iron in Aging Related Diseases. *Antioxidants (Basel, Switzerland)*, 11 (5). Available from https://doi.org/10.3390/antiox11050865.

Cichoz-Lach, H. and Michalak, A. (2014). Oxidative stress as a crucial factor in liver diseases. *World Journal of Gastroenterology*, 20 (25), 8082–8091. Available from https://doi.org/10.3748/wjg.v20.i25.8082.

Clogston, J.D. and Patri, A.K. (2011). Zeta potential measurement. *Methods*

in molecular biology (Clifton, N.J.), 697, 63–70. Available from https://doi.org/10.1007/978-1-60327-198-1_6.

Cooper, I.D. et al. (2023). Bio-Hacking Better Health - Leveraging Metabolic Biochemistry to Maximise Healthspan. *Antioxidants*, 12 (9). Available from https://doi.org/10.3390/antiox12091749.

Crawford, J.M. (2012). Histologic Findings in Alcoholic Liver Disease. *Clinics in Liver Disease*, 16 (4), 699–716. Available from https://doi.org/10.1016/j.cld.2012.08.004.

Cubero, F.J. and Nieto, N. (2008). Ethanol and arachidonic acid synergize to activate Kupffer cells and modulate the fibrogenic response via tumor necrosis factor α, reduced glutathione, and transforming growth factor β-dependent mechanisms. *Hepatology*, 48 (6), 2027–2039. Available from https://doi.org/10.1002/hep.22592.

Cunningham, C.C., Coleman, W.B. and Spach, P.I. (1990). The effects of chronic ethanol consumption on hepatic mitochondrial energy metabolism. *Alcohol and Alcoholism*, 25 (2–3), 127–136. Available from https://doi.org/10.1093/oxfordjournals.alcalc.a044987 [Accessed 28 August 2020].

Danaei, M. et al. (2018). Impact of Particle Size and Polydispersity Index on the Clinical Applications of Lipidic Nanocarrier Systems. *Pharmaceutics*, 10 (2). Available from https://doi.org/10.3390/pharmaceutics10020057.

Dancygier, H. (2010). Cellular Adaptation, Intracellular Inclusions and Deposits. *Clinical Hepatology: Principles and Practice of Hepatobiliary Diseases*. Springer New York LLC, 226–227. Available from https://books.google.co.uk/books?id=ZfJN6NS0ZY4C&pg=PA226&lpg=PA226&dq=MDBs+in+the+liver+cytokeratins&source=bl&ots=VHhUnbdeYb&sig=ACfU3U3T7WgU_jrVzZsbBGzP0npY1_XZxA&hl=en&sa=X&ved=2ahUKEwiIy6P6iJ7lAhUSEVAKHaJfB8YQ6AEwBHoECAkQAQ#v=onepage&q=MDBs in the li [Accessed 15 October 2019].

Dang, K. et al. (2020). Alcoholic Liver Disease Epidemiology in the United

States: A Retrospective Analysis of 3 US Databases. *American Journal of Gastroenterology*, 115 (1), 96–104. Available from https://doi.org/10.14309/ajg.0000000000000380 [Accessed 4 January 2021].

Dao, A. and Rangnekar, A.S. (2018). Steroids for Severe Alcoholic Hepatitis: More Risk Than Reward? *Clinical Liver Disease*, 12 (6), 151–153. Available from https://doi.org/10.1002/cld.736 [Accessed 27 March 2020].

Dara, L., Ji, C. and Kaplowitz, N. (2011). The contribution of endoplasmic reticulum stress to liver diseases. *Hepatology*, 53 (5), 1752–1763. Available from https://doi.org/10.1002/hep.24279.

Degterev, A. et al. (2005). Chemical inhibitor of nonapoptotic cell death with therapeutic potential for ischemic brain injury. *Nature Chemical Biology*, 1 (2), 112–119. Available from https://doi.org/10.1038/nchembio711.

Degterev, A. et al. (2008). Identification of RIP1 kinase as a specific cellular target of necrostatins. *Nature Chemical Biology*, 4 (5), 313–321. Available from https://doi.org/10.1038/nchembio.83.

Dhuriya, Y.K. and Sharma, D. (2018). Necroptosis: A regulated inflammatory mode of cell death. *Journal of Neuroinflammation*, 15 (1). Available from https://doi.org/10.1186/s12974-018-1235-0.

Dilger, K. et al. (1997). CYP2E1 activity in patients with alcoholic liver disease. *Journal of Hepatology*, 27 (6), 1009–1014. Available from https://doi.org/10.1016/S0168-8278(97)80144-4 [Accessed 10 October 2019].

Ding, R.B., Bao, J.L. and Deng, C.X. (2017). Emerging roles of SIRT1 in fatty liver diseases. *International Journal of Biological Sciences*, 13 (7), 852–867. Available from https://doi.org/10.7150/ijbs.19370.

Ding, W.-X. and Yin, X.-M. (2004). Dissection of the multiple mechanisms of TNF-a-induced apoptosis in liver injury. *Journal of Cellular and Molecular Medicine*, 8 (4), 445–454. Available from

https://doi.org/10.1111/j.1582-4934.2004.tb00469.x [Accessed 19 November 2019].

Ding, W.X. and Yin, X.M. (2012). Mitophagy: mechanisms, pathophysiological roles, and analysis. *Biological Chemistry*, 393 (7), 547–564. Available from https://doi.org/10.1515/hsz-2012-0119.

Ding, W.X., Li, M. and Yin, X.M. (2011). Selective taste of ethanol-induced autophagy for mitochondria and lipid droplets. *Autophagy*, 7 (2), 248–249. Available from https://doi.org/10.4161/auto.7.2.14347.

Ding, W.X. et al. (2012). Parkin and mitofusins reciprocally regulate mitophagy and mitochondrial spheroid formation. *Journal of Biological Chemistry*, 287 (50), 42379–42388. Available from https://doi.org/10.1074/jbc.M112.413682.

Dixon, S.J. et al. (2012). Ferroptosis: an iron-dependent form of nonapoptotic cell death. *Cell*, 149 (5), 1060–1072. Available from https://doi.org/10.1016/j.cell.2012.03.042.

Donnadieu-Rigole, H. et al. (2017). Follow-Up of Alcohol Consumption After Liver Transplantation: Interest of an Addiction Team? *Alcoholism: Clinical and Experimental Research*, 41 (1), 165–170. Available from https://doi.org/10.1111/acer.13276 [Accessed 12 December 2019].

Donohue, T.M. (2007). Alcohol-induced steatosis in liver cells. *World Journal of Gastroenterology*, 13 (37), 4974. Available from https://doi.org/10.3748/wjg.v13.i37.4974 [Accessed 10 October 2019].

Donohue, T.M., Tuma, D.J. and Sorrell, M.F. (1983). Acetaldehyde adducts with proteins: Binding of [14C]acetaldehyde to serum albumin. *Archives of Biochemistry and Biophysics*, 220 (1), 239–246. Available from https://doi.org/10.1016/0003-9861(83)90406-X.

Duchen, M.R. (2000). Mitochondria and calcium: from cell signalling to cell death. *The Journal of physiology*, 529 Pt 1 (Pt 1), 57–68. Available from https://doi.org/10.1111/j.1469-7793.2000.00057.x.

Dudek, J. (2017). Role of Cardiolipin in Mitochondrial Signaling Pathways. *Frontiers in Cell and Developmental Biology*, 5. Available from https://doi.org/10.3389/fcell.2017.00090.

Dunn, W. and Shah, V.H. (2016). Pathogenesis of Alcoholic Liver Disease. *Clinics in Liver Disease*, 20 (3), 445–456. Available from https://doi.org/10.1016/j.cld.2016.02.004 [Accessed 11 October 2019].

Eid, N. et al. (2013). Elevated autophagic sequestration of mitochondria and lipid droplets in steatotic hepatocytes of chronic ethanol-treated rats: An immunohistochemical and electron microscopic study. *Journal of Molecular Histology*, 44 (3), 311–326. Available from https://doi.org/10.1007/s10735-013-9483-x.

Eid, N. et al. (2016). Ethanol-induced mitophagy in liver is associated with activation of the PINK1-Parkin pathway triggered by oxidative DNA damage. *Histology and Histopathology*, 31 (10), 1143–1159. Available from https://doi.org/10.14670/HH-11-747.

Esfandiar, Z. et al. (2019). Red meat and dietary iron intakes are associated with some components of metabolic syndrome: Tehran Lipid and Glucose Study. *Journal of Translational Medicine*, 17 (1), 313. Available from https://doi.org/10.1186/s12967-019-2059-0.

Fan, R., Wang, J. and Du, J. (2018). Association between body mass index and fatty liver risk: A dose-response analysis. *Scientific Reports*, 8 (1), 15273. Available from https://doi.org/10.1038/s41598-018-33419-6.

Federico, A., Dallio, M. and Loguercio, C. (2017). Silymarin/Silybin and Chronic Liver Disease: A Marriage of Many Years. *Molecules*, 22 (2). Available from https://doi.org/10.3390/molecules22020191.

Fenech, M. et al. (2020). Micronuclei as biomarkers of DNA damage, aneuploidy, inducers of chromosomal hypermutation and as sources of pro-inflammatory DNA in humans. *Mutation Research/Reviews in Mutation Research*, 786, 108342. Available from https://doi.org/https://doi.org/10.1016/j.mrrev.2020.108342.

Fischer, C. et al. (2021). Dietary Iron Overload and Hfe−/− Related Hemochromatosis Alter Hepatic Mitochondrial Function. *Antioxidants*, 10 (11), 1818. Available from https://doi.org/10.3390/antiox10111818.

Forrest, E. et al. (2007). The Glasgow alcoholic hepatitis score identifies patients who may benefit from corticosteroids. *Gut*, 56 (12), 1743–1746. Available from https://doi.org/10.1136/gut.2006.099226 [Accessed 18 January 2021].

Forrest, E. et al. (2013). Steroids or pentoxifylline for alcoholic hepatitis (STOPAH): study protocol for a randomised controlled trial. *Trials*, 14 (1), 262. Available from https://doi.org/10.1186/1745-6215-14-262 [Accessed 27 March 2020].

Forrest, E.H. et al. (2018). Application of prognostic scores in the STOPAH trial: Discriminant function is no longer the optimal scoring system in alcoholic hepatitis. *Journal of Hepatology*, 68 (3), 511–518. Available from https://doi.org/10.1016/j.jhep.2017.11.017.

Frazier, T.H. et al. (2011). Treatment of alcoholic liver disease. *Therapeutic advances in gastroenterology*, 4 (1), 63–81. Available from https://doi.org/10.1177/1756283X10378925 [Accessed 6 October 2019].

Friedman, S.L. (2008). Hepatic stellate cells: Protean, multifunctional, and enigmatic cells of the liver. *Physiological Reviews*, 88 (1), 125–172. Available from https://doi.org/10.1152/physrev.00013.2007.

Galaris, D., Barbouti, A. and Pantopoulos, K. (2019). Iron homeostasis and oxidative stress: An intimate relationship. *Biochimica et Biophysica Acta (BBA) - Molecular Cell Research*, 1866 (12), 118535. Available from https://doi.org/https://doi.org/10.1016/j.bbamcr.2019.118535.

Ganne-Carrié, N. et al. (2000). Liver iron is predictive of death in alcoholic cirrhosis: a multivariate study of 229 consecutive patients with alcoholic and/or hepatitis C virus cirrhosis: a prospective follow up study. *Gut*, 46 (2), 277–282. Available from https://doi.org/10.1136/GUT.46.2.277 [Accessed 4 May 2022].

Gao, B. (2012). Hepatoprotective and anti-inflammatory cytokines in alcoholic liver disease. *Journal of Gastroenterology and Hepatology (Australia)*, 27 (SUPPL.2), 89–93. Available from https://doi.org/10.1111/j.1440-1746.2011.07003.x.

Gao, B. and Bataller, R. (2011). Alcoholic liver disease: pathogenesis and new therapeutic targets. *Gastroenterology*, 141 (5), 1572–85. Available from https://doi.org/10.1053/j.gastro.2011.09.002 [Accessed 4 October 2019].

Gao, B. and Tsukamoto, H. (2016). Inflammation in Alcoholic and Nonalcoholic Fatty Liver Disease: Friend or Foe? *Gastroenterology*, 150 (8), 1704–1709. Available from https://doi.org/10.1053/j.gastro.2016.01.025 [Accessed 16 October 2019].

Gao, B., Ma, J. and Xiang, X. (2018). MAIT cells: A novel therapeutic target for alcoholic liver disease? *Gut*, 67 (5), 784–786. Available from https://doi.org/10.1136/gutjnl-2017-315284 [Accessed 28 April 2021].

Gao, B. et al. (2019). Inflammatory pathways in alcoholic steatohepatitis. *Journal of Hepatology*, 70 (2), 249–259. Available from https://doi.org/10.1016/j.jhep.2018.10.023 [Accessed 1 November 2019].

García-Ruiz, C., Kaplowitz, N. and Fernandez-Checa, J.C. (2013). Role of Mitochondria in Alcoholic Liver Disease. *Current Pathobiology Reports*, 1 (3), 159–168. Available from https://doi.org/10.1007/s40139-013-0021-z.

Gentile, C.L. and Pagliassotti, M.J. (2008). The role of fatty acids in the development and progression of nonalcoholic fatty liver disease. *Journal of Nutritional Biochemistry*, 19 (9), 567–576. Available from https://doi.org/10.1016/j.jnutbio.2007.10.001.

Ghazali, R. et al. (2020). High omega arachidonic acid/docosahexaenoic acid ratio induces mitochondrial dysfunction and altered lipid metabolism in human hepatoma cells. *World Journal of Hepatology*, 12 (3), 84–98.

Available from https://doi.org/10.4254/wjh.v12.i3.84.

Gillessen, A. and Schmidt, H.H.J. (2020). Silymarin as Supportive Treatment in Liver Diseases: A Narrative Review. *Advances in Therapy*, 37 (4), 1279. Available from https://doi.org/10.1007/s12325-020-01251-y [Accessed 1 February 2021].

Giustarini, D. et al. (2023). How to Increase Cellular Glutathione. *Antioxidants*, 12 (5). Available from https://doi.org/10.3390/antiox12051094.

Goedde, H.E. et al. (1983). Population genetic studies on aldehyde dehydrogenase isozyme deficiency and alcohol sensitivity. *American Journal of Human Genetics*, 35 (4), 769–772.

Gordon, E.R. (1984). Alcohol-induced mitochondrial changes in the liver. *Recent developments in alcoholism : an official publication of the American Medical Society on Alcoholism, the Research Society on Alcoholism, and the National Council on Alcoholism*, 2, 143–158. Available from https://doi.org/10.1007/978-1-4684-4661-6_9.

Gottlieb, Y. et al. (2012). Endoplasmic reticulum anchored heme-oxygenase 1 faces the cytosol. *Haematologica*, 97 (10), 1489–1493. Available from https://doi.org/10.3324/haematol.2012.063651.

Groebner, J.L. and Tuma, P.L. (2015). The altered hepatic tubulin code in alcoholic liver disease. *Biomolecules*, 5 (3), 2140–2159. Available from https://doi.org/10.3390/biom5032140.

Groschwitz, K.R. and Hogan, S.P. (2009). Intestinal barrier function: Molecular regulation and disease pathogenesis. *Journal of Allergy and Clinical Immunology*, 124 (1), 3–20. Available from https://doi.org/10.1016/j.jaci.2009.05.038.

Guicciardi, M.E. (2005). Apoptosis: a mechanism of acute and chronic liver injury. *Gut*, 54 (7), 1024–1033. Available from https://doi.org/10.1136/gut.2004.053850 [Accessed 25 March 2020].

Guo, S. et al. (2013). Lipopolysaccharide causes an increase in intestinal tight junction permeability in vitro and in vivo by inducing enterocyte membrane expression and localization of TLR-4 and CD14. *American Journal of Pathology*, 182 (2), 375–387. Available from https://doi.org/10.1016/j.ajpath.2012.10.014.

Gyamfi, D. et al. (2012). Hepatic mitochondrial dysfunction induced by fatty acids and ethanol. *Free Radical Biology and Medicine*, 53 (11), 2131–2145. Available from https://doi.org/10.1016/j.freeradbiomed.2012.09.024.

Gyamfi, M.A. and Wan, Y.J.Y. (2010). Pathogenesis of alcoholic liver disease: The role of nuclear receptors. *Experimental Biology and Medicine*, 235 (5), 547–560. Available from https://doi.org/10.1258/ebm.2009.009249.

Halsted, C.H. (2004). Nutrition and Alcoholic Liver Disease. *Seminars in Liver Disease*, 24 (3), 289–304. Available from https://doi.org/10.1055/s-2004-832941 [Accessed 10 December 2019].

Han, D. et al. (2012). Dynamic adaptation of liver mitochondria to chronic alcohol feeding in mice: Biogenesis, remodeling, and functional alterations. *Journal of Biological Chemistry*, 287 (50), 42165–42179. Available from https://doi.org/10.1074/jbc.M112.377374.

Han, M.K. et al. (2008). SIRT1 Regulates Apoptosis and Nanog Expression in Mouse Embryonic Stem Cells by Controlling p53 Subcellular Localization. *Cell Stem Cell*, 2 (3), 241–251. Available from https://doi.org/10.1016/j.stem.2008.01.002.

Hancock, J.T. (2016). Life, Death and Apoptosis. *Cell Signalling*. OUP Oxford, 387–394.

Handa, P. et al. (2019). Iron alters macrophage polarization status and leads to steatohepatitis and fibrogenesis. *Journal of leukocyte biology*, 105 (5), 1015–1026. Available from https://doi.org/10.1002/JLB.3A0318-108R.

Harrison-Findik, D.D. (2007). Role of alcohol in the regulation of iron metabolism. *World journal of gastroenterology*, 13 (37), 4925–4930. Available from https://doi.org/10.3748/wjg.v13.i37.4925.

Harrison-Findik, D.D. et al. (2006). Alcohol metabolism-mediated oxidative stress down-regulates hepcidin transcription and leads to increased duodenal iron transporter expression. *The Journal of biological chemistry*, 281 (32), 22974–22982. Available from https://doi.org/10.1074/jbc.M602098200.

Hartmann, P., Seebauer, C.T. and Schnabl, B. (2015). Alcoholic liver disease: The gut microbiome and liver cross talk. *Alcoholism: Clinical and Experimental Research*, 39 (5), 763–775. Available from https://doi.org/10.1111/acer.12704.

Heymann, H.M., Gardner, A.M. and Gross, E.R. (2018). Aldehyde-Induced DNA and Protein Adducts as Biomarker Tools for Alcohol Use Disorder. *Trends in Molecular Medicine*, 24 (2), 144–155. Available from https://doi.org/10.1016/j.molmed.2017.12.003.

Higuchi, H. (2001). The mitochondrial permeability transition contributes to acute ethanol-induced apoptosis in rat hepatocytes. *Hepatology*, 34 (2), 320–328. Available from https://doi.org/10.1053/jhep.2001.26380 [Accessed 19 November 2019].

Hirschey, M.D. et al. (2011). SIRT3 deficiency and mitochondrial protein hyperacetylation accelerate the development of the metabolic syndrome. *Molecular Cell*, 44 (2), 177–190. Available from https://doi.org/10.1016/j.molcel.2011.07.019.

Hoeft, K. et al. (2017). Iron Loading Exaggerates the Inflammatory Response to the Toll-like Receptor 4 Ligand Lipopolysaccharide by Altering Mitochondrial Homeostasis. *Anesthesiology*, 127 (1), 121–135. Available from https://doi.org/10.1097/ALN.0000000000001653.

Hoek, J.B., Cahill, A. and Pastorino, J.G. (2002). Alcohol and mitochondria: A dysfunctional relationship. *Gastroenterology*, 122 (7), 2049–2063.

Available from https://doi.org/10.1053/gast.2002.33613.

Hothorn, T., Bretz, F. and Westfall, P. (2008). Simultaneous inference in general parametric models. *Biometrical journal. Biometrische Zeitschrift*, 50 (3), 346–363. Available from https://doi.org/10.1002/bimj.200810425.

Houglum, K., Bedossa, P. and Chojkier, M. (1994). TGF-beta and collagen-alpha 1 (I) gene expression are increased in hepatic acinar zone 1 of rats with iron overload. *The American journal of physiology*, 267 (5 Pt 1), G908-13. Available from https://doi.org/10.1152/ajpgi.1994.267.5.G908.

Huang, C.K. et al. (2015). Restoration of Wnt/β-catenin signaling attenuates alcoholic liver disease progression in a rat model. *Journal of Hepatology*, 63 (1), 191–198. Available from https://doi.org/10.1016/j.jhep.2015.02.030.

Hyun, J. et al. (2021). Pathophysiological Aspects of Alcohol Metabolism in the Liver. *International journal of molecular sciences*, 22 (11). Available from https://doi.org/10.3390/ijms22115717.

Ibusuki, R. et al. (2017). Human neutrophil peptide-1 promotes alcohol-induced hepatic fibrosis and hepatocyte apoptosis. *PLOS ONE*, 12 (4), e0174913. Available from https://doi.org/10.1371/journal.pone.0174913 [Accessed 4 November 2019].

Ioannou, G.N. et al. (2004). The effect of alcohol consumption on the prevalence of iron overload, iron deficiency, and iron deficiency anemia. *Gastroenterology*, 126 (5), 1293–301. Available from https://doi.org/10.1053/j.gastro.2004.01.020.

Jabczyk, M. et al. (2021). Curcumin in Metabolic Health and Disease. *Nutrients*, 13 (12). Available from https://doi.org/10.3390/nu13124440.

Ji, C., Chan, C. and Kaplowitz, N. (2006). Predominant role of sterol response element binding proteins (SREBP) lipogenic pathways in hepatic steatosis in the murine intragastric ethanol feeding model. *Journal of Hepatology*, 45 (5), 717–724. Available from https://doi.org/10.1016/j.jhep.2006.05.009.

John, M. et al. (1998). Inhaled Corticosteroids Increase Interleukin-10 but Reduce Macrophage Inflammatory Protein-1 α , Granulocyte-Macrophage Colony-stimulating Factor, and Interferon- γ Release from Alveolar Macrophages in Asthma. *American Journal of Respiratory and Critical Care Medicine*, 157 (1), 256–262. Available from https://doi.org/10.1164/ajrccm.157.1.9703079 [Accessed 10 December 2019].

Julien, J. et al. (2020). Projected prevalence and mortality associated with alcohol-related liver disease in the USA, 2019–40: a modelling study. *The Lancet Public Health*, 5 (6), e316–e323. Available from https://doi.org/10.1016/S2468-2667(20)30062-1 [Accessed 11 March 2021].

Kalantar-Zadeh, K., Rodriguez, R.A. and Humphreys, M.H. (2004). Association between serum ferritin and measures of inflammation, nutrition and iron in haemodialysis patients. *Nephrology, dialysis, transplantation : official publication of the European Dialysis and Transplant Association - European Renal Association*, 19 (1), 141–149. Available from https://doi.org/10.1093/ndt/gfg493.

Kawaratani, H. et al. (2013). The effect of inflammatory cytokines in alcoholic liver disease. *Mediators of Inflammation*, 2013. Available from https://doi.org/10.1155/2013/495156.

Kelley, N. et al. (2019). The NLRP3 inflammasome: An overview of mechanisms of activation and regulation. *International Journal of Molecular Sciences*, 20 (13). Available from https://doi.org/10.3390/ijms20133328 [Accessed 11 May 2021].

Kelly, C.J. et al. (2023). Iron status influences mitochondrial disease progression in Complex I-deficient mice. *eLife*, 12, e75825. Available from https://doi.org/10.7554/eLife.75825.

Kenney, W.C. (1982). Acetaldehyde Adducts of Phospholipids. *Alcoholism: Clinical and Experimental Research*, 6 (3), 412–416. Available from https://doi.org/10.1111/j.1530-0277.1982.tb05000.x.

Keshavarzian, A. et al. (2009). Evidence that chronic alcohol exposure promotes intestinal oxidative stress, intestinal hyperpermeability and endotoxemia prior to development of alcoholic steatohepatitis in rats. *Journal of Hepatology*, 50 (3), 538–547. Available from https://doi.org/10.1016/j.jhep.2008.10.028.

Kharbanda, K.K. et al. (2005). A Comparison of the Effects of Betaine and S-Adenosylmethionine on Ethanol-Induced Changes in Methionine Metabolism and Steatosis in Rat Hepatocytes. *The Journal of Nutrition*, 135 (3), 519–524. Available from https://doi.org/10.1093/jn/135.3.519.

Khodja, Y. and Samuels, M.E. (2020). Ethanol-mediated upregulation of APOA1 gene expression in HepG2 cells is independent of de novo lipid biosynthesis. *Lipids in Health and Disease 2020 19:1*, 19 (1), 1–13. Available from https://doi.org/10.1186/S12944-020-01309-4 [Accessed 23 September 2021].

Kim, M.S., Ong, M. and Qu, X. (2016). Optimal management for alcoholic liver disease: Conventional medications, natural therapy or combination? *World Journal of Gastroenterology*, 22 (1), 8–23. Available from https://doi.org/10.3748/wjg.v22.i1.8.

Kim, S.J. et al. (2008). Alleviation of acute ethanol-induced liver injury and impaired metabolomics of S-containing substances by betaine supplementation. *Biochemical and Biophysical Research Communications*, 368 (4), 893–898. Available from https://doi.org/10.1016/j.bbrc.2008.02.003 [Accessed 2 June 2020].

Kischkel, F.C. et al. (1995). Cytotoxicity-dependent APO-1 (Fas/CD95)-associated proteins form a death-inducing signaling complex (DISC) with the receptor. *The EMBO Journal*, 14 (22), 5579–5588. Available from https://doi.org/10.1002/j.1460-2075.1995.tb00245.x.

Kobyliak, N., Dynnyk, O. and Abenavoli, L. (2016). The Role of Liver Biopsy to Assess Alcoholic Liver Disease. *Reviews on Recent Clinical Trials*, 11 (3), 175–179. Available from https://doi.org/10.2174/1574887111666160724184103.

Kohgo, Y. et al. (2005). Iron Accumulation in Alcoholic Liver Diseases. *Alcoholism: Clinical & Experimental Research*, 29 (Supplement), 189S-193S. Available from https://doi.org/10.1097/01.alc.0000189274.00479.62 [Accessed 28 October 2021].

Kong, L.Z. et al. (2019). Pathogenesis, early diagnosis, and therapeutic management of alcoholic liver disease. *International Journal of Molecular Sciences*, 20 (11). Available from https://doi.org/10.3390/ijms20112712 [Accessed 11 October 2019].

Kostek, H. et al. (2012). Silibinin and its hepatoprotective action from the perspective of a toxicologist. *Przeglad lekarski*, 69 (8), 541–3. Available from http://www.ncbi.nlm.nih.gov/pubmed/23243923.

Krishnamurthy, P., Xie, T. and Schuetz, J.D. (2007). The role of transporters in cellular heme and porphyrin homeostasis. *Pharmacology & therapeutics*, 114 (3), 345–358. Available from https://doi.org/10.1016/j.pharmthera.2007.02.001.

Kühn, J.-P. et al. (2017). Prevalence of Fatty Liver Disease and Hepatic Iron Overload in a Northeastern German Population by Using Quantitative MR Imaging. *Radiology*, 284 (3), 706–716. Available from https://doi.org/10.1148/radiol.2017161228.

Lackner, C. and Tiniakos, D. (2019). Fibrosis and alcohol-related liver disease. *Journal of Hepatology*, 70 (2), 294–304. Available from https://doi.org/10.1016/j.jhep.2018.12.003.

Lackner, C. et al. (2008). Ballooned hepatocytes in steatohepatitis: The value of keratin immunohistochemistry for diagnosis. *Journal of Hepatology*, 48 (5), 821–828. Available from https://doi.org/10.1016/j.jhep.2008.01.026.

Lambert, J.C., Zhou, Z. and Kang, Y.J. (2003). Suppression of Fas-Mediated Signaling Pathway is Involved in Zinc Inhibition of Ethanol-Induced Liver Apoptosis. *Experimental Biology and Medicine*, 228 (4), 406–412.

Available from https://doi.org/10.1177/153537020322800411 [Accessed 19 November 2019].

Lange, L.G. and Sobel, B.E. (1983). Mitochondrial dysfunction induced by fatty acid ethyl esters, myocardial metabolites of ethanol. *Journal of Clinical Investigation*, 72 (2), 724–731. Available from https://doi.org/10.1172/JCI111022.

Lebourgeois, S. et al. (2018). Effect of N-acetylcysteine on motivation, seeking and relapse to ethanol self-administration. *Addiction Biology*, 23 (2), 643–652. Available from https://doi.org/10.1111/adb.12521 [Accessed 13 January 2021].

Lebrec, D. et al. (2010). Pentoxifylline Does Not Decrease Short-term Mortality but Does Reduce Complications in Patients With Advanced Cirrhosis. *Gastroenterology*, 138 (5). Available from https://doi.org/10.1053/j.gastro.2010.01.040.

Lee, J.H. et al. (2009). OverexpressionofSIRT1ProtectsPancreaticβ-CellsAgainstCytokineToxicitybySuppressingtheNuclearFactor-κBSignalingPathway. *Diabetes*, 58 (2), 344–351. Available from http://www.ncbi.nlm.nih.gov/entrez/query.fcgi?cmd=Retrieve&db=PubMed&dopt=Citation&list_uids=19008341 [Accessed 3 January 2020].

Lee, J.Y. et al. (2001). Saturated Fatty Acids, but Not Unsaturated Fatty Acids, Induce the Expression of Cyclooxygenase-2 Mediated through Toll-like Receptor 4. *Journal of Biological Chemistry*, 276 (20), 16683–16689. Available from https://doi.org/10.1074/jbc.M011695200.

Lee, T.D. et al. (2004). Abnormal Hepatic Methionine and Glutathione Metabolism in Patients with Alcoholic Hepatitis. *Alcoholism: Clinical and Experimental Research*, 28 (1), 173–181. Available from https://doi.org/10.1097/01.ALC.0000108654.77178.03 [Accessed 13 January 2021].

Lee, Y.J. and Shukla, S.D. (2007). Histone H3 phosphorylation at serine 10 and serine 28 is mediated by p38 MAPK in rat hepatocytes exposed to

ethanol and acetaldehyde⁎. *European Journal of Pharmacology*, 573 (1–3), 29–38. Available from https://doi.org/10.1016/j.ejphar.2007.06.049 [Accessed 4 November 2019].

Lefkowitch, J.H. (2005). Morphology of Alcoholic Liver Disease. *Clinics in Liver Disease*, 9 (1), 37–53. Available from https://doi.org/10.1016/j.cld.2004.11.001 [Accessed 15 October 2019].

Lemasters, J.J. (2014). Variants of mitochondrial autophagy: Types 1 and 2 mitophagy and micromitophagy (Type 3). *Redox Biology*, 2 (1), 749–754. Available from https://doi.org/10.1016/j.redox.2014.06.004.

Lemasters, J.J. and Zhong, Z. (2018). Mitophagy in hepatocytes: Types, initiators and role in adaptive ethanol metabolism. *Liver Research*, 2 (3), 125–132. Available from https://doi.org/10.1016/j.livres.2018.09.005 [Accessed 26 March 2020].

Lemmers, A. et al. (2009). The interleukin-17 pathway is involved in human alcoholic liver disease. *Hepatology*, 49 (2), 646–657. Available from https://doi.org/10.1002/hep.22680.

Lenz, K. et al. (2015). Treatment and management of ascites and hepatorenal syndrome: an update. *Therapeutic Advances in Gastroenterology*, 8 (2), 83–100. Available from https://doi.org/10.1177/1756283X14564673 [Accessed 10 December 2019].

Li, F. et al. (2016). Probiotics and alcoholic liver disease: Treatment and potential mechanisms. *Gastroenterology Research and Practice*, 2016. Available from https://doi.org/10.1155/2016/5491465 [Accessed 28 April 2021].

Li, L.-X. et al. (2022). Iron overload in alcoholic liver disease: underlying mechanisms, detrimental effects, and potential therapeutic targets. *Cellular and molecular life sciences : CMLS*, 79 (4), 201. Available from https://doi.org/10.1007/s00018-022-04239-9.

Li, L. et al. (2017). The spleen in liver cirrhosis: revisiting an old enemy with

novel targets. *Journal of Translational Medicine*, 15 (1), 111. Available from https://doi.org/10.1186/s12967-017-1214-8 [Accessed 11 February 2020].

Li, L. et al. (2022). The Association between Non-Alcoholic Fatty Liver Disease (NAFLD) and Advanced Fibrosis with Serological Vitamin B12 Markers: Results from the NHANES 1999-2004. *Nutrients*, 14 (6). Available from https://doi.org/10.3390/nu14061224.

Li, P. et al. (1997). Cytochrome c and dATP-dependent formation of Apaf-1/caspase-9 complex initiates an apoptotic protease cascade. *Cell*, 91 (4), 479–489. Available from https://doi.org/10.1016/S0092-8674(00)80434-1.

Li, S. et al. (2019). Recent Insights Into the Role of Immune Cells in Alcoholic Liver Disease. *Frontiers in immunology*, 10, 1328. Available from https://doi.org/10.3389/fimmu.2019.01328.

Li, Y. et al. (2017). Activation of Sirtuin 3 by Silybin Attenuates Mitochondrial Dysfunction in Cisplatin-induced Acute Kidney Injury. *Frontiers in Pharmacology*, 8, 178. Available from https://doi.org/10.3389/fphar.2017.00178.

Li, Y. et al. (2020). Regulation of Iron Homeostasis and Related Diseases. *Mediators of Inflammation*, 2020, 6062094. Available from https://doi.org/10.1155/2020/6062094.

Lieber, C.S. (2002). S-Adenosyl-l-methionine and alcoholic liver disease in animal models. *Alcohol*, 27 (3), 173–177. Available from https://doi.org/10.1016/S0741-8329(02)00230-6 [Accessed 13 January 2021].

Lieber, C.S. (2004). New concepts of the pathogenesis of alcoholic liver disease lead to novel treatments. *Current Gastroenterology Reports*, 6 (1), 60–65. Available from https://doi.org/10.1007/s11894-004-0027-0.

Lieber, C.S. and DeCarli, L.M. (1968). Ethanol oxidation by hepatic microsomes: Adaptive increase after ethanol feeding. *Science*, 162

(3856), 917–918. Available from https://doi.org/10.1126/science.162.3856.917.

Lin, C.J. et al. (2018). Complements are involved in alcoholic fatty liver disease, hepatitis and fibrosis. *World Journal of Hepatology*, 27 (10), 662–669. Available from https://doi.org/10.4254/wjh.v10.i10.662.

Lobo, V. et al. (2010). Free radicals, antioxidants and functional foods: Impact on human health. *Pharmacognosy Reviews*, 4 (8), 118–126. Available from https://doi.org/10.4103/0973-7847.70902.

Locksley, R.M., Killeen, N. and Lenardo, M.J. (2001). The TNF and TNF receptor superfamilies: Integrating mammalian biology. *Cell*, 104 (4), 487–501. Available from https://doi.org/10.1016/S0092-8674(01)00237-9.

Lombard, D.B. et al. (2007). Mammalian Sir2 homolog SIRT3 regulates global mitochondrial lysine acetylation. *Molecular and cellular biology*, 27 (24), 8807–14. Available from https://doi.org/10.1128/MCB.01636-07 [Accessed 3 January 2020].

Lou, D.-Q. et al. (2004). Functional differences between hepcidin 1 and 2 in transgenic mice. *Blood*, 103 (7), 2816–2821. Available from https://doi.org/10.1182/blood-2003-07-2524.

Louvet, A. et al. (2007). The Lille model: A new tool for therapeutic strategy in patients with severe alcoholic hepatitis treated with steroids. *Hepatology*, 45 (6), 1348–1354. Available from https://doi.org/10.1002/hep.21607 [Accessed 10 December 2019].

Lu, S.C. and Mato, J.M. (2012). S -adenosylmethionine in Liver Health, Injury, and Cancer. *Physiological Reviews*, 92 (4), 1515–1542. Available from https://doi.org/10.1152/physrev.00047.2011 [Accessed 4 December 2019].

Lu, Y. and Cederbaum, A.I. (2008). CYP2E1 and oxidative liver injury by alcohol. *Free Radical Biology and Medicine*, 44 (5), 723–738. Available from https://doi.org/10.1016/j.freeradbiomed.2007.11.004.

Lu, Y. and Cederbaum, A.I. (2015). Autophagy Protects against CYP2E1/Chronic Ethanol-Induced Hepatotoxicity. *Biomolecules*, 5 (4), 2659–74. Available from https://doi.org/10.3390/biom5042659 [Accessed 4 November 2019].

Luan, J. and Ju, D. (2018). Inflammasome: A Double-Edged Sword in Liver Diseases. *Frontiers in Immunology*, 9 (SEP). Available from https://doi.org/10.3389/fimmu.2018.02201 [Accessed 11 October 2019].

Lucey, M.R. (2014). Liver transplantation for alcoholic liver disease. *Nature Reviews Gastroenterology & Hepatology*, 11 (5), 300–307. Available from https://doi.org/10.1038/nrgastro.2013.247 [Accessed 10 December 2019].

Lucey, M.R. et al. (1997). Minimal criteria for placement of adults on the liver transplant waiting list: A report of a national conference organized by the American Society of Transplant Physicians and the American Association for the Study of Liver Diseases. *Liver Transplantation and Surgery*, 3 (6), 628–637. Available from https://doi.org/10.1002/lt.500030613 [Accessed 10 December 2019].

Lucey, M.R., Mathurin, P. and Morgan, T.R. (2009). Alcoholic hepatitis. *New England Journal of Medicine*, 360 (26), 2758. Available from https://doi.org/10.1056/NEJMra0805786 [Accessed 2 April 2020].

Lukkunaprasit, T. et al. (2023). An updated meta-analysis of effects of curcumin on metabolic dysfunction-associated fatty liver disease based on available evidence from Iran and Thailand. *Scientific Reports*, 13 (1), 5824. Available from https://doi.org/10.1038/s41598-023-33023-3.

Ma, G.D. et al. (2014). Pre-endurance training prevents acute alcoholic liver injury in rats through the regulation of damaged mitochondria accumulation and mitophagy balance. *Hepatology International*, 8 (3), 425–435. Available from https://doi.org/10.1007/s12072-014-9529-5 [Accessed 21 April 2020].

Ma, X. et al. (2020). Role and Mechanisms of Mitophagy in Liver Diseases.

Cells, 9 (4), 837. Available from https://doi.org/10.3390/cells9040837 [Accessed 21 April 2020].

Machado, I.F. et al. (2023). Targeting Oxidative Stress with Polyphenols to Fight Liver Diseases. *Antioxidants*, 12 (6). Available from https://doi.org/10.3390/antiox12061212.

Madushani Herath, K.H.I.N. et al. (2018). Sasa quelpaertensis leaves ameliorate alcohol-induced liver injury by attenuating oxidative stress in HepG2 cells and mice. *Acta Histochemica*, 120 (5), 477–489. Available from https://doi.org/10.1016/J.ACTHIS.2018.05.011.

Maiwall, R. et al. (2014). Serum ferritin predicts early mortality in patients with decompensated cirrhosis. *Journal of hepatology*, 61 (1), 43–50. Available from https://doi.org/10.1016/j.jhep.2014.03.027.

Malesza, I.J. et al. (2022). The Dark Side of Iron: The Relationship between Iron, Inflammation and Gut Microbiota in Selected Diseases Associated with Iron Deficiency Anaemia-A Narrative Review. *Nutrients*, 14 (17). Available from https://doi.org/10.3390/nu14173478.

Malhi, H., Guicciardi, M.E. and Gores, G.J. (2010). Hepatocyte death: A clear and present danger. *Physiological Reviews*, 90 (3), 1165–1194. Available from https://doi.org/10.1152/physrev.00061.2009.

Mansouri, A. et al. (1999). An alcoholic binge causes massive degradation of hepatic mitochondrial DNA in mice. *Gastroenterology*, 117 (1), 181–190. Available from https://doi.org/10.1016/S0016-5085(99)70566-4.

Mantena, S.K. et al. (2008). Mitochondrial dysfunction and oxidative stress in the pathogenesis of alcohol- and obesity-induced fatty liver diseases. *Free Radical Biology and Medicine*, 44 (7), 1259–1272. Available from https://doi.org/10.1016/j.freeradbiomed.2007.12.029.

Mantena, S.K. et al. (2009). High fat diet induces dysregulation of hepatic oxygen gradients and mitochondrial function in vivo. *The Biochemical journal*, 417 (1), 183–193. Available from https://doi.org/10.1042/BJ20080868.

Manzo-Avalos, S. and Saavedra-Molina, A. (2010). Cellular and mitochondrial effects of alcohol consumption. *International Journal of Environmental Research and Public Health*, 7 (12), 4281–4304. Available from https://doi.org/10.3390/ijerph7124281.

Maras, J.S. et al. (2015). Dysregulated iron homeostasis is strongly associated with multiorgan failure and early mortality in acute-on-chronic liver failure. *Hepatology*, 61 (4), 1306–1320. Available from https://doi.org/https://doi.org/10.1002/hep.27636.

Markwick, L.J.L. et al. (2015). Blockade of PD1 and TIM3 restores innate and adaptive immunity in patients with acute alcoholic hepatitis. *Gastroenterology*, 148 (3), 590-602.e10. Available from https://doi.org/10.1053/j.gastro.2014.11.041.

Mathurin, P. et al. (2011). Corticosteroids improve short-term survival in patients with severe alcoholic hepatitis: meta-analysis of individual patient data. *Gut*, 60 (2), 255–260. Available from https://doi.org/10.1136/gut.2010.224097 [Accessed 20 November 2019].

Mathurin, P. et al. (2012). EASL Clinical Practical Guidelines: Management of Alcoholic Liver Disease. *Journal of Hepatology*, 57 (2), 399–420. Available from https://doi.org/10.1016/j.jhep.2012.04.004 [Accessed 4 October 2019].

Mathurin, P. et al. (2013). Prednisolone with vs without pentoxifylline and survival of patients with severe alcoholic hepatitis: A randomized clinical trial. *JAMA - Journal of the American Medical Association*, 310 (10), 1033–1041. Available from https://doi.org/10.1001/jama.2013.276300.

Mauch, T.J. et al. (1986). Covalent binding of acetaldehyde selectively inhibits the catalytic activity of lysine-dependent enzymes. *Hepatology*, 6 (2), 263–269. Available from https://doi.org/10.1002/hep.1840060218.

Mavrelis, P.G. et al. (2007). Hepatic Free Fatty Acids in Alcoholic Liver Disease and Morbid Obesity. *Hepatology*, 3 (2), 226–231. Available from https://doi.org/10.1002/hep.1840030215 [Accessed 14 October 2019].

McCullough, A.J., O'Shea, R.S. and Dasarathy, S. (2011). Diagnosis and management of alcoholic liver disease. *Journal of Digestive Diseases*, 12 (4), 257–262. Available from https://doi.org/10.1111/j.1751-2980.2010.00470.x [Accessed 14 October 2019].

McKay, A. et al. (2018). Measurement of liver iron by magnetic resonance imaging in the UK Biobank population. *PloS one*, 13 (12), e0209340. Available from https://doi.org/10.1371/journal.pone.0209340.

Mehta, K.J., Farnaud, S.J. and Sharp, P.A. (2019). Iron and liver fibrosis: Mechanistic and clinical aspects. *World journal of gastroenterology*, 25 (5), 521–538. Available from https://doi.org/10.3748/wjg.v25.i5.521.

Menachery, J. and Duseja, A. (2011). Treatment of Decompensated Alcoholic Liver Disease. *International Journal of Hepatology*, 2011, 1–7. Available from https://doi.org/10.4061/2011/219238 [Accessed 21 November 2019].

Menon, K.V.N. et al. (2004). A pilot study of the safety and tolerability of etanercept in patients with alcoholic hepatitis. *The American journal of gastroenterology*, 99 (2), 255–60. Available from https://doi.org/10.1111/j.1572-0241.2004.04034.x [Accessed 10 December 2019].

Merksamer, P.I. et al. (2013). The sirtuins, oxidative stress and aging: An emerging link. *Aging*, 5 (3), 144–150. Available from https://doi.org/10.18632/aging.100544.

Milic, S. et al. (2016). The Role of Iron and Iron Overload in Chronic Liver Disease. *Medical Science Monitor : International Medical Journal of Experimental and Clinical Research*, 22, 2144. Available from https://doi.org/10.12659/MSM.896494 [Accessed 13 October 2021].

Milman, N. et al. (2003). Iron status in Danish women, 1984-1994: a cohort comparison of changes in iron stores and the prevalence of iron deficiency and iron overload. *European journal of haematology*, 71 (1), 51–61. Available from https://doi.org/10.1034/j.1600-0609.2003.00090.x.

Mohammad, M.K. et al. (2012). Zinc and Liver Disease. *Nutrition in Clinical Practice*, 27 (1), 8–20. Available from https://doi.org/10.1177/0884533611433534 [Accessed 10 December 2019].

Moniot, S., You, W. and Steegborn, C. (2018). Structural and Mechanistic Insights in Sirtuin Catalysis and Pharmacological Modulation. *Introductory Review on Sirtuins in Biology, Aging, and Disease*. Elsevier, 63–70. Available from https://doi.org/10.1016/b978-0-12-813499-3.00005-8.

Mookerjee, R.P. et al. (2004). Infliximab and alcoholic hepatitis. *Hepatology*, 40 (2), 499–500. Available from https://doi.org/10.1002/hep.20344 [Accessed 10 December 2019].

Moore Heslin, A. et al. (2021). Risk of Iron Overload in Obesity and Implications in Metabolic Health. *Nutrients*, 13 (5). Available from https://doi.org/10.3390/nu13051539.

Morgan, B.P. and Gasque, P. (1997). Extrahepatic complement biosynthesis: Where, when and why? *Clinical and Experimental Immunology*, 107 (1), 1–7. Available from https://doi.org/10.1046/j.1365-2249.1997.d01-890.x.

Mueller, S. and Rausch, V. (2015). The role of iron in alcohol-mediated hepatocarcinogenesis. *Advances in experimental medicine and biology*, 815, 89–112. Available from https://doi.org/10.1007/978-3-319-09614-8_6.

Mursaleen, L., Somavarapu, S. and Zariwala, M.G. (2020). Deferoxamine and Curcumin Loaded Nanocarriers Protect Against Rotenone-Induced Neurotoxicity. *Journal of Parkinson's Disease*, 10 (1), 99–111. Available from https://doi.org/10.3233/JPD-191754 [Accessed 9 April 2020].

Mursaleen, L. et al. (2020). N-Acetylcysteine Nanocarriers Protect against Oxidative Stress in a Cellular Model of Parkinson's Disease. *Antioxidants 2020, Vol. 9, Page 600*, 9 (7), 600. Available from https://doi.org/10.3390/ANTIOX9070600 [Accessed 1 November 2021].

Mursaleen, L. et al. (2023). Curcumin and N-Acetylcysteine Nanocarriers Alone or Combined with Deferoxamine Target the Mitochondria and Protect against Neurotoxicity and Oxidative Stress in a Co-Culture Model of Parkinson's Disease. *Antioxidants (Basel, Switzerland)*, 12 (1). Available from https://doi.org/10.3390/antiox12010130.

Nace, G.W. et al. (2013). Cellular-specific role of toll-like receptor 4 in hepatic ischemia-reperfusion injury in mice. *Hepatology*, 58 (1), 374–387. Available from https://doi.org/10.1002/hep.26346.

Nagura, H. et al. (1985). THE THIRD (C3) AND FOURTH (C4) COMPONENTS OF COMPLEMENT IN HUMAN LIVER: Immunocytochemical Evidence for Hepatocytes as the Site of Synthesis. *Pathology International*, 35 (1), 71–78. Available from https://doi.org/10.1111/j.1440-1827.1985.tb02206.x.

Nagy, L.E. (2015). The Role of Innate Immunity in Alcoholic Liver Disease. *Alcohol research : current reviews*, 37 (2), 237–50. Available from https://doi.org/.

Nagy, L.E. et al. (2016). Linking Pathogenic Mechanisms of Alcoholic Liver Disease with Clinical Phenotypes. *Gastroenterology*, 150 (8), 1756–1768. Available from https://doi.org/10.1053/j.gastro.2016.02.035.

Nanji, A.A. and French, S.W. (1989). Dietary linoleic acid is required for development of experimentally induced alcoholic liver injury. *Life Sciences*, 44 (3), 223–227. Available from https://doi.org/10.1016/0024-3205(89)90599-7.

Nanji, A.A. and Hiller-Sturmhöfel, S. (1997). Apoptosis and necrosis: Two types of cell death in alcoholic liver disease. *Alcohol Research and Health*, 21 (4), 325–330.

Narendra, D. et al. (2008). Parkin is recruited selectively to impaired mitochondria and promotes their autophagy. *Journal of Cell Biology*, 183 (5), 795–803. Available from https://doi.org/10.1083/jcb.200809125.

Nassir, F. (2014). Role of mitochondria in alcoholic liver disease. *World*

Journal of Gastroenterology, 20 (9), 2136. Available from https://doi.org/10.3748/wjg.v20.i9.2136 [Accessed 8 November 2019].

Naveau, S. et al. (2004). A double-blind randomized controlled trial of infliximab associated with prednisolone in acute alcoholic hepatitis. *Hepatology*, 39 (5), 1390–1397. Available from https://doi.org/10.1002/hep.20206 [Accessed 10 December 2019].

Nelson, J.E. et al. (2011). Relationship between the pattern of hepatic iron deposition and histological severity in nonalcoholic fatty liver disease. *Hepatology (Baltimore, Md.)*, 53 (2), 448–457. Available from https://doi.org/10.1002/hep.24038.

Nelson, K.M. et al. (2017). The Essential Medicinal Chemistry of Curcumin. *Journal of Medicinal Chemistry*, 60 (5), 1620–1637. Available from https://doi.org/10.1021/acs.jmedchem.6b00975.

Nemeth, E. and Ganz, T. (2009). The Role of Hepcidin in Iron Metabolism. *Acta Haematologica*, 122 (2–3), 78. Available from https://doi.org/10.1159/000243791 [Accessed 3 April 2022].

Neuman, M.G. et al. (2015). Alcoholic liver disease: Role of cytokines. *Biomolecules*, 5 (3), 2023–2034. Available from https://doi.org/10.3390/biom5032023.

Nguyen-Khac, E. et al. (2011). Glucocorticoids plus N -Acetylcysteine in Severe Alcoholic Hepatitis . *New England Journal of Medicine*, 365 (19), 1781–1789. Available from https://doi.org/10.1056/nejmoa1101214 [Accessed 13 January 2021].

Ni, H.M., Williams, J.A. and Ding, W.X. (2015). Mitochondrial dynamics and mitochondrial quality control. *Redox Biology*, 4, 6–13. Available from https://doi.org/10.1016/j.redox.2014.11.006.

Nicoletti, A. et al. (2019). Intestinal permeability in the pathogenesis of liver damage: From non-alcoholic fatty liver disease to liver transplantation. *World Journal of Gastroenterology*, 25 (33), 4814–4834. Available from https://doi.org/10.3748/wjg.v25.i33.4814.

O'Grady, J.G. (2006). Liver transplantation alcohol related liver disease: (Deliberately) stirring a hornet's nest! *Gut*, 55 (11), 1529–1531. Available from https://doi.org/10.1136/gut.2005.090506.

O'Shea, R.S., Dasarathy, S. and McCullough, A.J. (2010). AASLD Practice Guidelines: Alcoholic Liver Disease. *Hepatology*, 51 (1), 307–328. Available from https://doi.org/10.1002/hep.23258 [Accessed 10 October 2019].

Obrzut, M. et al. (2020). Value of liver iron concentration in healthy volunteers assessed by MRI. *Scientific Reports*, 10 (1), 17887. Available from https://doi.org/10.1038/s41598-020-74968-z.

Ohgami, R.S. et al. (2005). Identification of a ferrireductase required for efficient transferrin-dependent iron uptake in erythroid cells. *Nature genetics*, 37 (11), 1264–1269. Available from https://doi.org/10.1038/ng1658.

ONS. (2021). Quarterly alcohol-specific deaths in England and Wales - Office for National Statistics. Available from https://www.ons.gov.uk/peoplepopulationandcommunity/birthsdeathsandmarriages/deaths/datasets/quarterlyalcoholspecificdeathsinenglandandwales [Accessed 11 May 2021].

Osna, N.A., Donohue, T.M. and Kharbanda, K.K. (2017). Alcoholic Liver Disease: Pathogenesis and Current Management. *Alcohol research : current reviews*, 38 (2), 147–161. Available from https://doi.org/.

Ozawa, E. et al. (2011). Ferritin/alanine aminotransferase ratio as a possible marker for predicting the prognosis of acute liver injury. *Journal of gastroenterology and hepatology*, 26 (8), 1326–1332. Available from https://doi.org/10.1111/j.1440-1746.2011.06743.x.

Pani, G. et al. (2004). Abrogation of hepatocyte apoptosis and early appearance of liver dysplasia in ethanol-fed p53-deficient mice. *Biochemical and Biophysical Research Communications*, 325 (1), 97–100. Available from https://doi.org/10.1016/j.bbrc.2004.09.213.

Parker, R. and Holt, A. (2018). Transplanting Patients with Alcohol-related Liver Disease in the National Health System: New Rules and Decisions. *Alcohol and alcoholism (Oxford, Oxfordshire)*, 53 (2), 145–150. Available from https://doi.org/10.1093/alcalc/agx103 [Accessed 1 November 2019].

Pasala, S., Barr, T. and Messaoudi, I. (2015). Impact of Alcohol Abuse on the Adaptive Immune System. *Alcohol research : current reviews*, 37 (2), 185–97. Available from https://doi.org/.

Paul, B., Manz, D.H., et al. (2017). Mitochondria and Iron: current questions. *Expert review of hematology*, 10 (1), 65–79. Available from https://doi.org/10.1080/17474086.2016.1268047.

Paul, B., Manz, D., et al. (2017). Mitochondria and Iron: Current Questions. *Expert review of hematology*, 10 (1), 65. Available from https://doi.org/10.1080/17474086.2016.1268047 [Accessed 22 April 2022].

Pessione, F. et al. (2003). Five-year survival predictive factors in patients with excessive alcohol intake and cirrhosis. Effect of alcoholic hepatitis, smoking and abstinence. *Liver International*, 23 (1), 45–53. Available from https://doi.org/10.1034/j.1600-0676.2003.01804.x.

Petagine, L. et al. (2021). Acute Alcohol Tissue Damage: Protective Properties of Betaine. *Journal of Renal and Hepatic Disorders*, 5 (1), 19–29. Available from https://doi.org/10.15586/jrenhep.v5i1.96 [Accessed 28 April 2021].

Petagine, L., Zariwala, M.G. and Patel, V.B. (2021). Alcoholic liver disease: Current insights into cellular mechanisms. *World J Biol Chem.*, 12 (5), 87–103. Available from https://doi.org/10.4331/WJBC.V12.I5.87 [Accessed 22 September 2021].

Petagine, L., Zariwala, M.G. and Patel, V.B. (2023). Non-alcoholic fatty liver disease: Immunological mechanisms and current treatments. *World Journal of Gastroenterology*, 29 (32), 4831–4850. Available from

https://doi.org/10.3748/wjg.v29.i32.4831.

Petrasek, J. et al. (2013). STING-IRF3 pathway links endoplasmic reticulum stress with hepatocyte apoptosis in early alcoholic liver disease. *Proceedings of the National Academy of Sciences of the United States of America*, 110 (41), 16544–16549. Available from https://doi.org/10.1073/pnas.1308331110.

Pietrangelo, A. (2003). Iron-induced oxidant stress in alcoholic liver fibrogenesis. *Alcohol (Fayetteville, N.Y.)*, 30 (2), 121–129. Available from https://doi.org/10.1016/s0741-8329(03)00126-5.

Pimpin, L. et al. (2018). Burden of liver disease in Europe: Epidemiology and analysis of risk factors to identify prevention policies. *Journal of Hepatology*, 69 (3), 718–735. Available from https://doi.org/10.1016/j.jhep.2018.05.011 [Accessed 10 October 2019].

Piskin, E. et al. (2022). Iron Absorption: Factors, Limitations, and Improvement Methods. *ACS Omega*, 7 (24), 20441–20456. Available from https://doi.org/10.1021/acsomega.2c01833.

Pritchard, M.T. et al. (2007). Differential Contributions of C3, C5, and Decay-Accelerating Factor to Ethanol-Induced Fatty Liver in Mice. *Gastroenterology*, 132 (3), 1117–1126. Available from https://doi.org/10.1053/j.gastro.2007.01.053.

Puskas, F. et al. (2000). Stimulation of the pentose phosphate pathway and glutathione levels by dehydroascorbate, the oxidized form of vitamin C. *FASEB journal : official publication of the Federation of American Societies for Experimental Biology*, 14 (10), 1352–1361. Available from https://doi.org/10.1096/fj.14.10.1352.

Qin, X. and Gao, B. (2006). The Complement System in Liver Diseases. 3.

Quintana Pacheco, D.A. et al. (2018). Red meat consumption and risk of cardiovascular diseases-is increased iron load a possible link? *The American journal of clinical nutrition*, 107 (1), 113–119. Available from https://doi.org/10.1093/ajcn/nqx014.

Quintanilla, M.E. et al. (2016). Beyond the 'First Hit': Marked Inhibition by N-Acetyl Cysteine of Chronic Ethanol Intake But Not of Early Ethanol Intake. Parallel Effects on Ethanol-Induced Saccharin Motivation. *Alcoholism: Clinical and Experimental Research*, 40 (5), 1044–1051. Available from https://doi.org/10.1111/acer.13031 [Accessed 13 January 2021].

Rahimi, E. and Pan, J.-J. (2015). Prognostic models for alcoholic hepatitis. *Biomarker Research*, 3 (1), 20. Available from https://doi.org/10.1186/s40364-015-0046-z [Accessed 22 February 2021].

Ramaiah, S.K. and Jaeschke, H. (2007). Role of Neutrophils in the Pathogenesis of Acute Inflammatory Liver Injury. *Toxicologic Pathology*, 35 (6), 757–766. Available from https://doi.org/10.1080/01926230701584163.

Riva, A. et al. (2018). Mucosa-associated invariant T cells link intestinal immunity with antibacterial immune defects in alcoholic liver disease. *Gut*, 67 (5), 918–930. Available from https://doi.org/10.1136/gutjnl-2017-314458 [Accessed 25 March 2020].

Roberts, B.J. (1995). Ethanol Induces CYP2E1 by Protein Stabilization. *Journal of Biological Chemistry*, 270 (50), 29632–29635. Available from https://doi.org/10.1074/jbc.270.50.29632 [Accessed 10 October 2019].

Rodriguez, A. et al. (2015). Alcohol and Apoptosis: Friends or Foes? *Biomolecules*, 5 (4), 3193. Available from https://doi.org/10.3390/BIOM5043193 [Accessed 12 October 2021].

Roychowdhury, S. et al. (2013). Absence of receptor interacting protein kinase 3 prevents ethanol-induced liver injury. *Hepatology*, 57 (5), 1773–1783. Available from https://doi.org/10.1002/hep.26200.

Schieber, M. and Chandel, N.S. (2014). ROS function in redox signaling and oxidative stress. *Current Biology*, 24 (10), R453. Available from https://doi.org/10.1016/j.cub.2014.03.034.

Schwabe, R.F. and Luedde, T. (2018). Apoptosis and necroptosis in the liver: a matter of life and death. *Nature Reviews Gastroenterology and Hepatology*, 15 (12), 738–752. Available from https://doi.org/10.1038/s41575-018-0065-y.

Schwenger, K.J., Clermont-Dejean, N. and Allard, J.P. (2019). The role of the gut microbiome in chronic liver disease: the clinical evidence revised. *JHEP Reports*, 1 (3), 214–226. Available from https://doi.org/10.1016/j.jhepr.2019.04.004 [Accessed 18 February 2021].

Seitz, H.K. and Stickel, F. (2010). Acetaldehyde as an underestimated risk factor for cancer development: Role of genetics in ethanol metabolism. *Genes and Nutrition*, 5 (2), 121–128. Available from https://doi.org/10.1007/s12263-009-0154-1.

Seitz, H.K. et al. (2018). Alcoholic liver disease. *Nature reviews. Disease primers*, 4 (1), 16. Available from https://doi.org/10.1038/s41572-018-0014-7 [Accessed 16 October 2019].

Senoo, H. (2004). Structure and function of hepatic stellate cells. *Medical Electron Microscopy*, 37 (1), 3–15. Available from https://doi.org/10.1007/s00795-003-0230-3.

Seo, W. and Jeong, W. Il. (2016). Hepatic non-parenchymal cells: Master regulators of alcoholic liver disease? *World journal of gastroenterology*, 22 (4), 1348–1356. Available from https://doi.org/10.3748/wjg.v22.i4.1348.

Shayeghi, M. et al. (2005). Identification of an intestinal heme transporter. *Cell*, 122 (5), 789–801. Available from https://doi.org/10.1016/j.cell.2005.06.025.

She, H. et al. (2002). Iron activates NF-kappaB in Kupffer cells. *American journal of physiology. Gastrointestinal and liver physiology*, 283 (3). Available from https://doi.org/10.1152/AJPGI.00108.2002 [Accessed 29 April 2022].

Shefa, U. et al. (2019). Mitophagy links oxidative stress conditions and neurodegenerative diseases. *Neural Regeneration Research*, 14 (5), 749–756. Available from https://doi.org/10.4103/1673-5374.249218.

Sheth, M., Riggs, M. and Patel, T. (2002). Utility of the Mayo End-Stage Liver Disease (MELD) score in assessing prognosis of patients with alcoholic hepatitis. *BMC Gastroenterology*, 2. Available from https://doi.org/10.1186/1471-230X-2-2 [Accessed 22 February 2021].

Shi, H. et al. (2006). TLR4 links innate immunity and fatty acid-induced insulin resistance. *Journal of Clinical Investigation*, 116 (11), 3015–3025. Available from https://doi.org/10.1172/JCI28898.

Singal, A.K. (2013). Liver transplantation in alcoholic liver disease current status and controversies. *World Journal of Gastroenterology*, 19 (36), 5953. Available from https://doi.org/10.3748/wjg.v19.i36.5953 [Accessed 12 December 2019].

Singal, A.K. et al. (2012). Outcomes after liver transplantation for alcoholic hepatitis are similar to alcoholic cirrhosis: Exploratory analysis from the UNOS database. *Hepatology*, 55 (5), 1398–1405. Available from https://doi.org/10.1002/hep.25544 [Accessed 12 December 2019].

Singh, C.K. et al. (2018). The Role of Sirtuins in Antioxidant and Redox Signaling. *Antioxidants and Redox Signaling*, 28 (8), 643–661. Available from https://doi.org/10.1089/ars.2017.7290.

Singh, S., Osna, N.A. and Kharbanda, K.K. (2017). Treatment options for alcoholic and non-alcoholic fatty liver disease: A review. *World Journal of Gastroenterology*, 23 (36), 6549–6570. Available from https://doi.org/10.3748/wjg.v23.i36.6549.

Sitohang, I.B.S. et al. (2021). Evaluating Oral Glutathione Plus Ascorbic Acid, Alpha-lipoic Acid, and Zinc Aspartate as a Skin-lightening Agent: An Indonesian Multicenter, Randomized, Controlled Trial. *The Journal of clinical and aesthetic dermatology*, 14 (7), E53–E58.

Song, K. et al. (2002). Chronic ethanol consumption by mice results in

activated splenic T cells. *Journal of leukocyte biology*, 72 (6), 1109–16. Available from https://doi.org/10.1189/jlb.72.6.1109 [Accessed 25 April 2020].

Song, X. et al. (2015). Glycycoumarin ameliorates alcohol-induced hepatotoxicity via activation of Nrf2 and autophagy. *Free radical biology & medicine*, 89, 135–46. Available from https://doi.org/10.1016/j.freeradbiomed.2015.07.006 [Accessed 4 November 2019].

Sousa, L. et al. (2020). Iron overload: Effects on cellular biochemistry. *Clinica Chimica Acta*, 504, 180–189. Available from https://doi.org/https://doi.org/10.1016/j.cca.2019.11.029.

Spahr, L. et al. (2002). Combination of steroids with infliximab or placebo in severe alcoholic hepatitis: a randomized controlled pilot study. *Journal of Hepatology*, 37 (4), 448–455. Available from https://doi.org/10.1016/S0168-8278(02)00230-1 [Accessed 10 December 2019].

Staab, D.B. et al. (1984). Relationship between Vitamin A and Iron in the Liver. *The Journal of Nutrition*, 114 (5), 840–844. Available from https://doi.org/https://doi.org/10.1093/jn/114.5.840.

Stehling, O. and Lill, R. (2013). The Role of Mitochondria in Cellular Iron–Sulfur Protein Biogenesis: Mechanisms, Connected Processes, and Diseases. *Cold Spring Harbor Perspectives in Biology*, 5 (8). Available from https://doi.org/10.1101/CSHPERSPECT.A011312 [Accessed 29 April 2022].

Strader, D.B. et al. (2002). Use of complementary and alternative medicine in patients with liver disease. *The American Journal of Gastroenterology*, 97 (9), 2391–2397. Available from https://doi.org/10.1111/j.1572-0241.2002.05993.x.

Sun, Y. et al. (2018). Glutathione depletion induces ferroptosis, autophagy, and premature cell senescence in retinal pigment epithelial cells. *Cell*

death & disease, 9 (7), 753. Available from https://doi.org/10.1038/s41419-018-0794-4.

Surai, P.F. (2015). Silymarin as a Natural Antioxidant: An Overview of the Current Evidence and Perspectives. *Antioxidants (Basel, Switzerland)*, 4 (1), 204–247. Available from https://doi.org/10.3390/antiox4010204.

Tan, H.K. et al. (2020). Oxidative stress in alcohol-related liver disease. *World Journal of Hepatology*, 12 (7), 332. Available from https://doi.org/10.4254/WJH.V12.I7.332 [Accessed 29 September 2021].

Tandra, S. et al. (2011). Presence and significance of microvesicular steatosis in nonalcoholic fatty liver disease. *Journal of Hepatology*, 55 (3), 654–659. Available from https://doi.org/10.1016/j.jhep.2010.11.021.

Teli, M.R. et al. (1995). Determinants of progression to cirrhosis or fibrosis in pure alcoholic fatty liver. *The Lancet*, 346 (8981), 987–990. Available from https://doi.org/10.1016/S0140-6736(95)91685-7.

Teschke, R. (2018). Alcoholic Liver Disease: Alcohol Metabolism, Cascade of Molecular Mechanisms, Cellular Targets, and Clinical Aspects. *Biomedicines*, 6 (4), 106. Available from https://doi.org/10.3390/biomedicines6040106 [Accessed 4 October 2019].

Theise, N.D. (2013). Histopathology of alcoholic liver disease. *Clinical Liver Disease*, 2 (2), 64–67. Available from https://doi.org/10.1002/cld.172 [Accessed 15 October 2019].

Thilakarathna, S.H. and Rupasinghe, H.P.V. (2013). Flavonoid bioavailability and attempts for bioavailability enhancement. *Nutrients*, 5 (9), 3367–3387. Available from https://doi.org/10.3390/nu5093367.

Thomas, C. et al. (2013). Hydroxyl radical is produced via the Fenton reaction in submitochondrial particles under oxidative stress: implications for diseases associated with iron accumulation. *http://dx.doi.org/10.1179/135100009X392566*, 14 (3), 102–108. Available from https://doi.org/10.1179/135100009X392566 [Accessed 28

October 2021].

Thoudam, T. et al. (2023). Enhanced Ca2+-channeling complex formation at the ER-mitochondria interface underlies the pathogenesis of alcohol-associated liver disease. *Nature Communications*, 14 (1), 1703. Available from https://doi.org/10.1038/s41467-023-37214-4.

Thursz, M.R. et al. (2015). Prednisolone or Pentoxifylline for Alcoholic Hepatitis. *New England Journal of Medicine*, 372 (17), 1619–1628. Available from https://doi.org/10.1056/NEJMoa1412278 [Accessed 27 March 2020].

Tilg, H., Moschen, A.R. and Szabo, G. (2016). Interleukin-1 and inflammasomes in alcoholic liver disease/acute alcoholic hepatitis and nonalcoholic fatty liver disease/nonalcoholic steatohepatitis. *Hepatology*, 64 (3), 955–965. Available from https://doi.org/10.1002/hep.28456.

Tilokani, L. et al. (2018). Mitochondrial dynamics: Overview of molecular mechanisms. *Essays in Biochemistry*, 62 (3), 341–360. Available from https://doi.org/10.1042/EBC20170104.

Tiniakos, D.G., Anstee, Q.M. and Burt, A.D. (2018). Fatty Liver Disease. *Macsween's Pathology of the Liver*. Philadelphia: Elsevier, 308–371. Available from https://doi.org/10.1016/B978-0-7020-6697-9.00005-4 [Accessed 10 October 2019].

Topiwala, A. et al. (2022). Alcohol consumption and telomere length: Mendelian randomization clarifies alcohol's effects. *Molecular psychiatry*, 27 (10), 4001–4008. Available from https://doi.org/10.1038/s41380-022-01690-9.

Torruellas, C., French, S.W. and Medici, V. (2014). Diagnosis of alcoholic liver disease. *World Journal of Gastroenterology*, 20 (33), 11684–11699. Available from https://doi.org/10.3748/wjg.v20.i33.11684.

Tricò, D. et al. (2018). Metabolic Features of Nonalcoholic Fatty Liver (NAFL) in Obese Adolescents: Findings From a Multiethnic Cohort. *Hepatology (Baltimore, Md.)*, 68 (4), 1376–1390. Available from

https://doi.org/10.1002/hep.30035.

Troadec, M.-B. et al. (2010). Induction of FPN1 transcription by MTF-1 reveals a role for ferroportin in transition metal efflux. *Blood*, 116 (22), 4657–4664. Available from https://doi.org/10.1182/blood-2010-04-278614.

Tsuchida, T. and Friedman, S.L. (2017). Mechanisms of hepatic stellate cell activation. *Nature Reviews Gastroenterology and Hepatology*, 14 (7), 397–411. Available from https://doi.org/10.1038/nrgastro.2017.38.

Tuma, D.J. (2002). Role of malondialdehyde-acetaldehyde adducts in liver injury. *Free Radical Biology and Medicine*, 32 (4), 303–308. Available from https://doi.org/10.1016/S0891-5849(01)00742-0.

Van Der Bliek, A.M., Shen, Q. and Kawajiri, S. (2013). Mechanisms of mitochondrial fission and fusion. *Cold Spring Harbor Perspectives in Biology*, 5 (6), a011072. Available from https://doi.org/10.1101/cshperspect.a011072.

Venkatraman, A. et al. (2004). Modification of the Mitochondrial Proteome in Response to the Stress of Ethanol-dependent Hepatotoxicity. *Journal of Biological Chemistry*, 279 (21), 22092–22101. Available from https://doi.org/10.1074/jbc.M402245200 [Accessed 29 September 2021].

Vidali, M. et al. (2003). Genetic and epigenetic factors in autoimmune reactions toward cytochrome P4502E1 in alcoholic liver disease. *Hepatology*, 37 (2), 410–419. Available from https://doi.org/10.1053/jhep.2003.50049 [Accessed 21 January 2021].

Viña, J. et al. (1980). Effect of ethanol on glutathione concentration in isolated hepatocytes. *The Biochemical journal*, 188 (2), 549–552. Available from https://doi.org/10.1042/bj1880549.

Voican, C.S. et al. (2015). Alcohol withdrawal alleviates adipose tissue inflammation in patients with alcoholic liver disease. *Liver International*, 35 (3), 967–978. Available from https://doi.org/10.1111/liv.12575.

Vucic, D., Dixit, V.M. and Wertz, I.E. (2011). Ubiquitylation in apoptosis: A post-translational modification at the edge of life and death. *Nature Reviews Molecular Cell Biology*, 12 (7), 439–452. Available from https://doi.org/10.1038/nrm3143.

Wajant, H. (2002). The Fas signaling pathway: More than a paradigm. *Science*, 296 (5573), 1635–1636. Available from https://doi.org/10.1126/science.1071553.

Walker, A.K. et al. (2011). A conserved SREBP-1/phosphatidylcholine feedback circuit regulates lipogenesis in metazoans. *Cell*, 147 (4), 840–852. Available from https://doi.org/10.1016/j.cell.2011.09.045.

Wallace, D.F. (2016). The Regulation of Iron Absorption and Homeostasis. *The Clinical biochemist. Reviews*, 37 (2), 51–62.

Wang, H. et al. (2011). Alcohol affects the late differentiation of progenitor B cells. *Alcohol and Alcoholism*, 46 (1), 26–32. Available from https://doi.org/10.1093/alcalc/agq076 [Accessed 26 March 2021].

Wang, H. et al. (2017). Characterization of ferroptosis in murine models of hemochromatosis. *Hepatology (Baltimore, Md.)*, 66 (2), 449–465. Available from https://doi.org/10.1002/hep.29117.

Wang, H.J. et al. (2012). Inflammation in Alcoholic Liver Disease. *Annual Review of Nutrition*, 32 (1), 343–368. Available from https://doi.org/10.1146/annurev-nutr-072610-145138 [Accessed 11 October 2019].

Wang, K. (2014). Molecular mechanisms of hepatic apoptosis. *Cell Death and Disease*, 5 (1), e996–e996. Available from https://doi.org/10.1038/cddis.2013.499.

Wang, S. et al. (2016). A Mechanistic Review of Cell Death in Alcohol-Induced Liver Injury. *Alcoholism: Clinical and Experimental Research*, 40 (6), 1215–1223. Available from https://doi.org/10.1111/acer.13078.

Werner, J. et al. (2002). Alcoholic pancreatitis in rats: injury from

nonoxidative metabolites of ethanol. *American Journal of Physiology-Gastrointestinal and Liver Physiology*, 283 (1), G65–G73. Available from https://doi.org/10.1152/ajpgi.00419.2001 [Accessed 19 November 2019].

WHO. (2018). *Global status report on alcohol and health 2018*. Available from https://apps.who.int/iris/bitstream/handle/10665/274603/9789241565639-eng.pdf?ua=1.

Williams, J.A. and Ding, W.X. (2015a). A mechanistic review of mitophagy and its role in protection against alcoholic liver disease. *Biomolecules*, 5 (4), 2619–2642. Available from https://doi.org/10.3390/biom5042619.

Williams, J.A. and Ding, W.X. (2015b). Targeting Pink1-Parkin-mediated mitophagy for treating liver injury. *Pharmacological Research*, 102, 264–269. Available from https://doi.org/10.1016/j.phrs.2015.09.020.

Williams, J.A. et al. (2015). Parkin regulates mitophagy and mitochondrial function to protect against alcohol-induced liver injury and steatosis in mice. *American Journal of Physiology - Gastrointestinal and Liver Physiology*, 309 (5), G324–G340. Available from https://doi.org/10.1152/ajpgi.00108.2015.

Wilman, H.R. et al. (2019). Genetic studies of abdominal MRI data identify genes regulating hepcidin as major determinants of liver iron concentration. *Journal of Hepatology*, 71 (3), 594–602. Available from https://doi.org/https://doi.org/10.1016/j.jhep.2019.05.032.

Wong, R.J. and Ahmed, A. (2014). Obesity and non-alcoholic fatty liver disease: Disparate associations among Asian populations. *World journal of hepatology*, 6 (5), 263–273. Available from https://doi.org/10.4254/wjh.v6.i5.263.

Wu, D. and Cederbaum, A.I. (1999). Ethanol-Induced Apoptosis to Stable HepG2 Cell Lines Expressing Human Cytochrome P-4502E1. *Alcoholism: Clinical and Experimental Research*, 23 (1), 67–76. Available from https://doi.org/10.1111/J.1530-0277.1999.TB04025.X

[Accessed 12 October 2021].

Wu, D. and Cederbaum, A.I. (2003). Alcohol, Oxidative Stress, and Free Radical Damage. *Alcohol Research & Health*, 27 (4), 277. Available from /pmc/articles/PMC6668865/ [Accessed 28 October 2021].

Wu, H. et al. (2006). Metabolic basis of ethanol-induced cytotoxicity in recombinant HepG2 cells: Role of nonoxidative metabolism. *Toxicology and Applied Pharmacology*, 216 (2), 238–247. Available from https://doi.org/10.1016/j.taap.2006.05.003.

Wu, H. et al. (2007). Ethanol-induced cytotoxicity in rat pancreatic acinar AR42J cells: Role of fatty acid ethyl esters. *Alcohol and Alcoholism*, 43 (1), 1–8. Available from https://doi.org/10.1093/alcalc/agm044 [Accessed 19 November 2019].

Xiong, S. et al. (2003). Iron-dependent activation of NF-kappaB in Kupffer cells: a priming mechanism for alcoholic liver disease. *Alcohol (Fayetteville, N.Y.)*, 30 (2), 107–113. Available from https://doi.org/10.1016/S0741-8329(03)00100-9 [Accessed 29 April 2022].

Yan, J. et al. (2021). Natural Compounds: A Potential Treatment for Alcoholic Liver Disease? *Frontiers in Pharmacology*, 12, 1695. Available from https://doi.org/10.3389/FPHAR.2021.694475/BIBTEX.

Yang, Y.M. and Seki, E. (2015). TNFα in Liver Fibrosis. *Current Pathobiology Reports*, 3 (4), 253–261. Available from https://doi.org/10.1007/s40139-015-0093-z.

Yin, C. et al. (2013). Hepatic stellate cells in liver development, regeneration, and cancer. *Journal of Clinical Investigation*, 123 (5), 1902–1910. Available from https://doi.org/10.1172/JCI66369.

Yin, H. et al. (2012). MicroRNA-217 promotes ethanol-induced fat accumulation in hepatocytes by down-regulating SIRT1. *Journal of Biological Chemistry*, 287 (13), 9817–9826. Available from https://doi.org/10.1074/jbc.M111.333534.

Yin, X.-M. and Ding, W.-X. (2003). Death Receptor Activation-Induced Hepatocyte Apoptosis and Liver Injury. *Current Molecular Medicine*, 3 (6), 491–508. Available from https://doi.org/10.2174/1566524033479555 [Accessed 12 November 2019].

Yin, X.-M. and Ding, W.-X. (2013). The reciprocal roles of PARK2 and mitofusins in mitophagy and mitochondrial spheroid formation. *Autophagy*, 9 (11), 1687–1692. Available from https://doi.org/10.4161/auto.24871 [Accessed 26 March 2020].

Yin, X.M. et al. (1999). Bid-deficient mice are resistant to Fas-induced hepatocellular apoptosis. *Nature*, 400 (6747), 886–891. Available from https://doi.org/10.1038/23730.

Ying, J.-F. et al. (2021). The role of iron homeostasis and iron-mediated ROS in cancer. *American journal of cancer research*, 11 (5), 1895–1912.

You, M. et al. (2015). Sirtuin 1 signaling and alcoholic fatty liver disease. *Hepatobiliary surgery and nutrition*, 4 (2), 88–100. Available from https://doi.org/10.3978/j.issn.2304-3881.2014.12.06.

Youle, R.J. and Van Der Bliek, A.M. (2012). Mitochondrial fission, fusion, and stress. *Science*, 337 (6098), 1062–1065. Available from https://doi.org/10.1126/science.1219855.

Zanninelli, G. et al. (2002). The labile iron pool of hepatocytes in chronic and acute iron overload and chelator-induced iron deprivation. *Journal of hepatology*, 36 (1), 39–46. Available from https://doi.org/10.1016/s0168-8278(01)00222-7.

Zariwala, M.G. et al. (2014). Ascorbyl palmitate/DSPE-PEG nanocarriers for oral iron delivery: Preparation, characterisation and in vitro evaluation. *Colloids and Surfaces B: Biointerfaces*, 115, 86–92. Available from https://doi.org/10.1016/J.COLSURFB.2013.11.028.

Zelickson, B.R. et al. (2011). Nitric oxide and hypoxia exacerbate alcohol-induced mitochondrial dysfunction in hepatocytes. *Biochimica et Biophysica Acta - Bioenergetics*, 1807 (12), 1573–1582. Available from

https://doi.org/10.1016/j.bbabio.2011.09.011.

Zelner, I. et al. (2013). Synthesis of fatty acid ethyl esters in mammalian tissues after ethanol exposure: a systematic review of the literature. *Drug Metabolism Reviews*, 45 (3), 277–299. Available from https://doi.org/10.3109/03602532.2013.795584 [Accessed 19 November 2019].

Zetterman, R.K. (2005). Liver transplantation for alcoholic liver disease. *Clinics in Liver Disease*, 9 (1), 171–181. Available from https://doi.org/10.1016/j.cld.2004.10.002.

Zhang, H. and Meadows, G.G. (2005). Chronic alcohol consumption in mice increases the proportion of peripheral memory T cells by homeostatic proliferation. *Journal of Leukocyte Biology*, 78 (5), 1070–1080. Available from https://doi.org/10.1189/jlb.0605317 [Accessed 25 April 2020].

Zhang, R. et al. (2021). Silybin Restored CYP3A Expression through the Sirtuin 2/Nuclear Factor κ-B Pathway in Mouse Nonalcoholic Fatty Liver Disease. *Drug Metabolism and Disposition*, 49 (9), 770 LP – 779. Available from https://doi.org/10.1124/dmd.121.000438.

Zhang, Y. et al. (2018). Gastrodin Protects against Ethanol-Induced Liver Injury and Apoptosis in HepG2 Cells and Animal Models of Alcoholic Liver Disease. *Biological and Pharmaceutical Bulletin*, 41 (5), 670–679. Available from https://doi.org/10.1248/BPB.B17-00825.

Zhao, R.Z. et al. (2019). Mitochondrial electron transport chain, ROS generation and uncoupling (Review). *International Journal of Molecular Medicine*, 44 (1), 3–15. Available from https://doi.org/10.3892/ijmm.2019.4188.

Zheng, J. and Conrad, M. (2020). The Metabolic Underpinnings of Ferroptosis. *Cell metabolism*, 32 (6), 920–937. Available from https://doi.org/10.1016/j.cmet.2020.10.011.

Zheng, X. et al. (2011). Hepatic iron stores are increased as assessed by magnetic resonance imaging in a Chinese population with altered

glucose homeostasis. *The American journal of clinical nutrition*, 94 (4), 1012–1019. Available from https://doi.org/10.3945/ajcn.111.015743.

Zhong, Z. et al. (2014). Acute Ethanol Causes Hepatic Mitochondrial Depolarization in Mice: Role of Ethanol Metabolism. *PLoS ONE*, 9 (3), e91308. Available from https://doi.org/10.1371/journal.pone.0091308 [Accessed 19 November 2019].

Zhou, Z., Han, V. and Han, J. (2012). New components of the necroptotic pathway. *Protein and Cell*, 3 (11), 811–817. Available from https://doi.org/10.1007/s13238-012-2083-9.

Zorov, D.B. et al. (2000). Reactive oxygen species (ROS)-induced ROS release: A new phenomenon accompanying induction of the mitochondrial permeability transition in cardiac myocytes. *Journal of Experimental Medicine*, 192 (7), 1001–1014. Available from https://doi.org/10.1084/jem.192.7.1001.

SUPPLEMENTARY DATA

Table 9.1 Correlation coefficients for variables in linear regression models of liver iron concentration and liver fat percentage.

Variable	Liver Iron (mg/g)		Liver Fat (%)	
	Effect estimate	**P value**	**Effect estimate**	**P value**
Age	0.0036	$<2x10^{-16}$	-0.0151	$1.27x10^{-5}$
Sex (Female)	0	(Reference)	0	(Reference)
Sex (Male)	0.0039	0.2786	0.8570	$<2x10^{-16}$
BMI	-0.0017	$4.09x10^{-5}$	0.5386	$<2x10^{-16}$
Alcohol intake – Special occasions only	0	(Reference)	0	(Reference)
Alcohol intake – One to three times a month	0.0105	0.154947	0.1350	0.2271
Alcohol intake – One to three times a week	0.0244	0.0001	-0.2639	0.0061
Alcohol intake – Three to four times a week	0.0503	$1.90x10^{-15}$	-0.0504	0.5988
Alcohol intake – Daily or almost daily	0.0865	$<2x10^{-16}$	0.6015	$7.33x10^{-50}$
Intercept	0.9799	$<2x10^{-16}$	-8.8787	$<2x10^{-16}$
r^2	0.0226		0.2415	

APPENDICES

Appendix A: Figure and Table Acknowledgements and Copyright

Table 1.1 Adapted from: Petagine, Zariwala and Patel (2021). This work is licensed under CC BY-NC 4.0. To view a copy of this license, visit http://creativecommons.org/licenses/by-nc/4.0/

Figure 1.1 Source: Petagine, Zariwala and Patel (2021). This work is licensed under CC BY-NC 4.0. To view a copy of this license, visit http://creativecommons.org/licenses/by-nc/4.0/

Figure 1.3 Source: Source: Ohashi, Pimienta and Seki (2018). This work is licensed under CC BY-NC-ND 4.0. To view a copy of this license, visit http://creativecommons.org/licenses/by-nc-nd/4.0/

Figure 1.4 Adapted from: Tsuchida and Friedman (2017). Reproduced with permission from Springer Nature. License Number: 5637700524272

Figure 1.5 Created with BioRender.com

Figure 1.6 Adapted from “Extrinsic and Intrinsic Apoptosis”, by BioRender.com (2023). Retrieved from https://app.biorender.com/biorender-templates

Figure 1.7 Created with BioRender.com

Figure 1.8 Source: Petagine, Zariwala and Patel (2021). This work is licensed under CC BY-NC 4.0. To view a copy of this license, visit http://creativecommons.org/licenses/by-nc/4.0/

Figure 1.9 Source: Petagine, Zariwala and Patel (2021). This work is licensed under CC BY-NC 4.0. To view a copy of this license, visit http://creativecommons.org/licenses/by-nc/4.0/

Figure 1.10 Adapted from “Ferroptosis Signaling Pathway”, by BioRender.com (2023). Retrieved from https://app.biorender.com/biorender-templates